Palaeo and In-Situ Stress Analysis of the Perth Basin: Implications for subsurface fluid flow

Thesis submitted in accordance with the requirements of the University of Adelaide for an Honours Degree in Geology/Geophysics

Alastair Beuzeville Taylor Stark

October 2017

THE UNIVERSITY of ADELAIDE

PALAEO AND IN-SITU STRESS ANALYSIS OF THE PERTH BASIN: IMPLICATIONS FOR SUBSURFACE FLUID FLOW.

STRESS ANALYSIS OF THE PERTH BASIN.

ABSTRACT

Understanding the orientation, stress conditions, and fluid-flow history of natural fracture networks can provide tighter constraints on the fracture genesis and tectonic evolution of the Perth Basin, Western Australia. To date, combined data from King et al. (2008) and Bailey et al. (2012) indicate a present-day transpressional stress regime, and a maximum horizontal stress orientation of 076°E. However, palaeo stress and the timing of fracture generation are poorly constrained. A comparison and analysis of present-day stress, and palaeo stress orientations and magnitudes, is integrated with an analysis of natural fracture network orientations, using data from wellbore image logs, well tests (leak-off tests) and sample analysis across eight petroleum drill holes in the Perth Basin. Stress indicators in wellbore image logs are analysed to further constrain present-day stress, and Etchecopar's (1984) computerised Calcite Stress Inversion Technique is used to constrain the palaeo stress conditions in the basin. This data is then used to establish a four-dimensional understanding of the tectonic history of the Perth Basin, and the potential structural permeability of its tectonic features. From analysis of stress indicators, the mean regional maximum horizontal stress orientation in the study area is 089.9°N. Through fracture analysis, orientations comply with past studies (Bailey et al., 2012; King et al., 2008), as defined by a clear set of resistive fractures dipping 157°-337° (NNE-SSW), reflecting palaeo-basinal stresses and present-day in-situ stresses. Magnitudes highlighted in the Perth Basin closely match previous works defining the basin as a transpressional ($\sigma_{Hmax} > \sigma_V \approx \sigma_{Hmin}$) stress regime. This includes a vertical stress profile established in seven wells at 22 MPa km^{-1}. The minimum horizontal stress was measured using two leak-off tests and formation integrity tests at 14 MPa km^{-1}. The maximum horizontal stress magnitude was measured using frictional limits (Kirsch, 1898) at 30 MPa km^{-1}. Calculated palaeo stress tensors indicate that polyphase deformation has occurred in the Perth Basin. These tensors include; a NNW-SSE compressional event attributed to Early to Middle Triassic N-S compression; Late Triassic to Earliest Jurassic E-W extensional phase; and a NW-SE extensional regime in the Jurassic concluding with Post-Neocomian, N-S compression.

KEYWORDS

Present-day stress, Perth Basin, Stress magnitudes, Calcite Stress Inversion Technique, Structural Permeability, Subsurface fluid flow

TABLE OF CONTENTS

LIST OF FIGURES AND TABLES

1.0 INTRODUCTION

Exploration for engineered geothermal systems, as well as unconventional hydrocarbon resources and water resources, relies increasingly on an understanding of the role that stress and structure play in determining the permeability of the subsurface. While previous exploration in the geothermal sector has primarily focused on temperature as a measure of success in the geothermal sector, structural permeability is increasingly becoming the focus for research and exploration.

Fractures are likely to reactivate when parallel, or up to 26° with respect to the *in-situ* horizontal maximum stress (σ_{Hmax}) orientation (Laubach et al., 2004). Rotation of the σ_{Hmax} orientation over time reflects the plate tectonic evolution of a region and/or local tectonics, often resulting in a complex system of cross cutting fractures (Sibson, 1996). These fracture networks may be open to fluid flow while others remain closed (Heffer & Lean, 1993; Laubach et al., 2004; Reynolds et al., 2006).

The controlling factor in circulating fluids at depth are the *in-situ* stresses, with fluid preferentially migrating parallel to the σ_{Hmax}. Fluid flow is assumed to flow in the aforementioned direction, due to assumptions made that σ_1 is considered to have the lowest normal stresses acting across the fluid pathway, and thus, encounter the least impedance to flow (Heffer & Lean, 1993; Laubach et al., 2004). When open fractures are optimally aligned within 26° of σ_{Hmax}, they are assumed open to fluid flow and thus hydraulically active (Healy et al., 2006). This however, is not the case for open fractures outside this range (Heffer & Lean, 1993; Heffer et al., 1997; Healy, Jones, & Holdsworth, 2006; Sibson, 1996). This case study of the Perth Basin has been initiated in order to

recognise the controls on structural permeability which have evolved due to the complex nature of the basin's history, and the applications it has for the water, geothermal and petroleum industries. The evolution of the basin has led to the systematic opening and closing of natural fractures, allowing for fluid migration through natural fracture networks. The complex structural evolution of the Perth Basin requires a four-dimensional knowledge so that permeability and potential subsurface fluid flow pathways may be predicted.

Through implementation of the Calcite Stress Inversion Technique (CSIT), palaeo stress in the Perth Basin will be established through the analysis of twinning shown in euhedral calcite crystals. In addition, interpretation of image logs to identify Drilling-Induced Tensile Fractures (DITF's) and borehole breakout (BO's) will provide the orientation of the horizontal stresses. Formation Integrity Tests (FIT's) and Leak Off Tests (LOT's) will assist in constraining present-day σ_{Hmin} magnitude in the Perth Basin, with subsequent σ_V and σ_{Hmax} magnitudes used in order to establish the present-day stress regime. The stress analysis for both palaeo and present-day regimes will then be applied to interpreted fractures in the Perth Basin to define which of these fractures may be open to fluid flow.

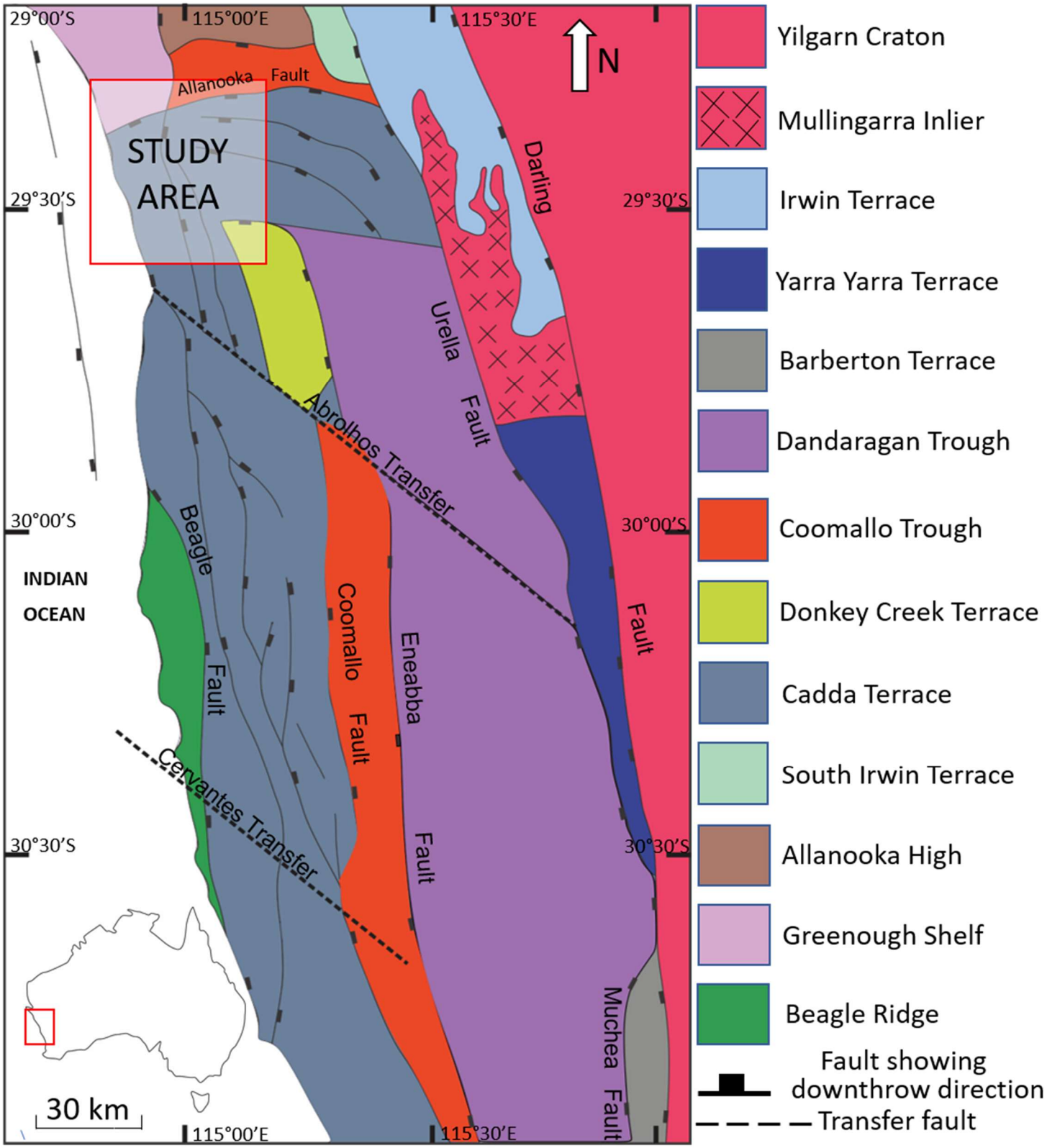

Figure 1: A regional map of the Perth Basin, showing tectonic elements as described by Iasky and Mory (1996) and study site; Adapted from Bailey et al., (2012).

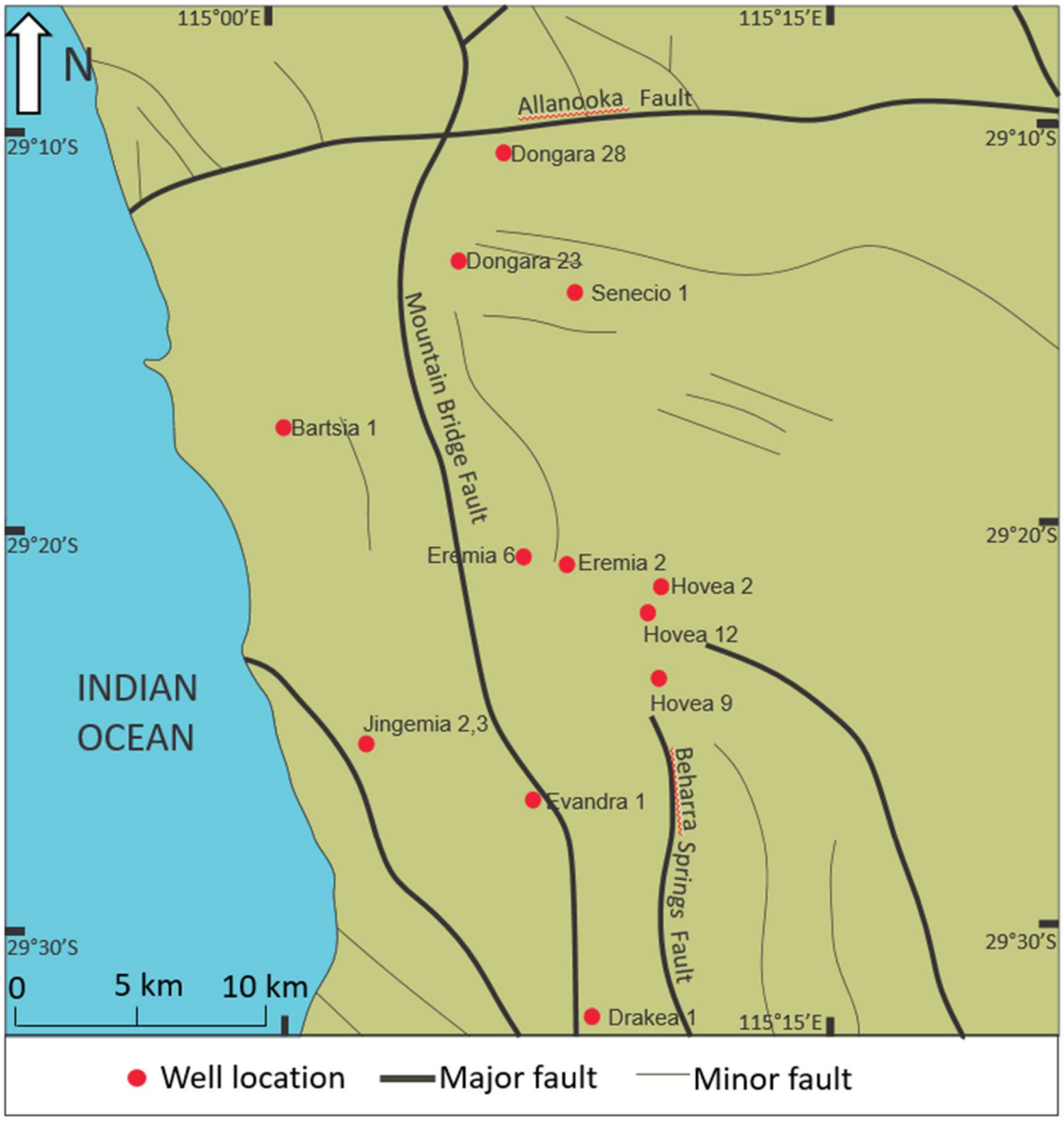

Figure 2: Study site complete with well locations and major geological features (adapted from Bailey et al., 2012).

2.0 GEOLOGICAL SETTING

The Perth Basin is an elongate intracontinental extensional basin which formed as a result of the tectonic breakup of Gondwana, and the subsequent rifting of Greater India into its present-day location (Harris, 1994; Marshall et al., 1989; Olierook et al., 2014). The Perth Basin covers ~172 000 km^2 of on and offshore area along the SW margin of Western Australia and is broken into three sub basins with a further fifteen troughs defined by gravity anomalies. This basin is structurally complex, resulting from repeated extensional

and compressional cycles recorded throughout the Phanerozoic (Clark, 2005; Hall, 1989; Harris, 1994; Marshall et al., 1989; Mory & Iasky, 1996; Playford et al., 1976)

The record of detrital deposition can be traced from the Permian to Present-Day, with fluvially dominated sedimentary sequences, showing evidence of past marine transgressions that correlate to the breakup of the supercontinent Gondwana (Crostella, 2000; Hall, 1989; Marshall et al., 1989; Playford et al., 1976). The development of the Perth Basin can be categorised into the following phases (Harris, 1994; Marshall et al., 1989; Mory & Iasky, 1996; Playford et al., 1976):

- Post-Neocomian to Holocene (post-rift stage)
- Upper Triassic to Lower Cretaceous (syn-rift) (multiple stages)
- Late Ordovician to Late Permian (pre-rift stage)

3.0 METHODS

3.1 Calcite Stress Inversion Technique (CSIT)

The Calcite Stress Inversion Technique (CSIT) (Etchecopar, 1984) utilisied calcite twin lamellae to determine the regional palaeo stress tensor orientations for the Perth Basin (Figure 3). For mechanical twinning to develop, the Resolved Shear Stress (RSS) must exceed the yield stress value of 10+/-4 MPa (Ferrill, 1998; Lacombe, 2010; Lacombe et al., 2007; Lacombe and Laurent, 1996; Laurent et al., 2000; Turner et al., 1954).

Etchecopar's (1984) method applies to small twinning strains that can be approximated though coaxial conditions, so orientation can be correlated with palaeo stress orientation (Amrouch et al., 2010a, 2011) [see details in Lacombe (2001, 2007)]. Data provided from the above step, allows for the calculation of the ellipsoid shape ratio $\Phi = (\sigma_2-\sigma_3) / (\sigma_1-\sigma_3)$ and peak differential stress $(\sigma_1-\sigma_3)$ (with $\sigma_1 \geq \sigma_2 \geq \sigma_3$ as a compressive stress, positive in

value). The tensor solution is calculated and normalised as a Reduced Stress Tensor (RST) and differential stress is scaled to $(\sigma_1-\sigma_3)^*=1$. Twinned planes observed must have sustained a τ_s value larger than any untwinned plane in the given direction of twinning. Best solutions ideally limit the function of f (ideally equalling 0); this process can be defined as the following:

$$f = \sum_{j=1}^{N}(\tau_{sj}-\tau_{a'}) \quad (1)$$

The $\tau_{a'}$ value is established from the inversion and relates to the critical RSS for the normalised tensor used for the initial calculation, with the best fitting tensor established when: (1) the maximum number of twinned planes is taken into account; (2) the maximum of untwinned planes is taken into account; and (3) the *f* value is minimal. In practice, one can authorize a weak percentage, 10%–15%, of untwinned planes receiving a RSS larger than $\tau_{a'}$ because of measurement uncertainties and local heterogeneities at the crystal scale (Kulikowski & Amrouch, 2017). This process leads to the establishment of the orientation of the principal stresses, as well as the stress ellipsoid shape ratio $\Phi=(\sigma_2-\sigma_3)/(\sigma_1-\sigma_3)$ being between 0 and 1 (Etchecopar, 1984; Laurent, 1984) (Figure 3). If polyphase deformation has occurred, this methodology provides an efficient way of deciphering the sets of twins, and thus, deformation events (Etchecopar, 1984; Laurent, 1984).

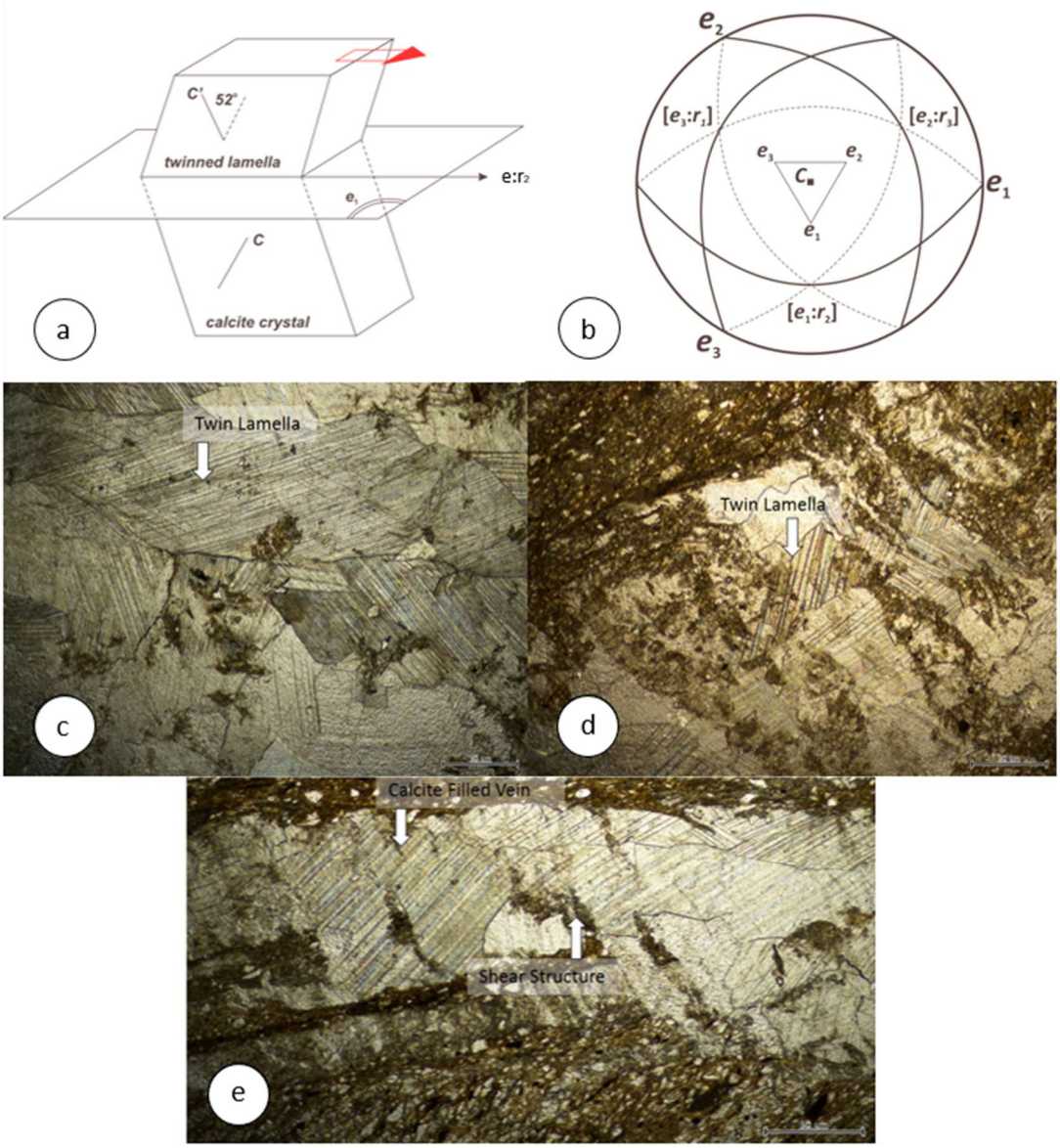

Figure 3: (a) A schematic sketch of a twin lamella in a calcite crystal (Arboit et al., 2015; Burkhard, 1993). The twinning direction (e1:r2) is the direction of atoms situated above the twin plane. The direction of shear is shown by the red arrow and is directed by the crystal geometry. (b) A stereographic projection of calcite twin planes, with a vertical optical axes C. The corresponding poles to planes of the three twin planes (e1, e2, e3) are separated by 26.5° from the C axis. The planes of twins are shown, giving the three directions of twinning (Evans & Groshong, 1994). (c-d) Examples of microscope images obtained from thin sections, prepared from Senecio 1 showing a calcite filled natural fracture and subsequent shear structure observed under cross polarised light; (c) Thin twin lamella exhibiting type I and II geometry (Burkhard, 1993). This describes a low temperature deformational environment (<200°C to 300°C) with varying deformation extremes, as shown by the percentage of calcite grain taken by twin lamella; (d) Thick twin lamella (> 1µm). (e) Vein filled with large euhedral calcite grains deformed by intense shear.

3.2 Calculation of stress magnitudes (σ_{Hmax}, σ_{Hmin} and σ_V)

3.2.1 VERTICAL STRESS (σ_v)

Vertical stress (σ_V) increases with growing depth because of the cumulative weight of the overburden (Bell, 1996a, 1996b). Vertical stress can be quantified through data collected from wireline density logs, run after drilling is completed. Wireline density logs were obtained from the Western Australian Petroleum and Geothermal Information Management System (WAPIMS). The σ_V was calculated using the following equation:

$$\sigma v = \int_0^z \rho(z) g \, dz \approx \bar{\rho} \, gz \qquad (2)$$

In the absence of a complete density log, checkshot or vertical seismic profile (VSP) data was used as a proxy to calculate areas where density logs were not run, providing an accurate calculation for σ_V. This calculation was conducted in order to establish a Top of Log value (TOL), so as to extrapolate density from the surface to the first density reading from the wireline log.

3.2.2 MINIMUM HORIZONTAL STRESS (σ_{Hmin})

Minimum horizontal stress (σ_{Hmin}) was quantified from leak-off pressures obtained from Leak-Off Tests (LOTs) and maximum reported pressures from Formation Integrity Tests (FITs) (White et al., 2002). Calculation of σ_{Hmin} from FITs led to an underestimation of stress values as down hole fracture formation never fully initiated. For fractures to from pressure increasing, fluid pressure must overcome the tensile strength of the rock, the pore pressure, the σ_{Hmin} and the σ_{Hmax} magnitudes. The ranking of data was dependent on the type of drilling test performed. A quality data is established from Fracture Closure Pressure (FCP) as determined from an Extended Leak-Off Test (XLOT). B quality

rankings are determined through FCPs; however, these are only established from one single LOT instead of multiple 'runs' as found in XLOTs. C quality data was ranked through taking the leak-off pressure established from a LOT graph in a Well Completion Report (WCR). If the well has no LOT graph, but a leak off value is included, this is determined to be D quality. An E quality ranking is confirmed through reports of an FIT undertaken in the well, with the maximum value reported in the WCR. F quality pertains to an FIT being reported in a WCR, but this value may not be the maximum pressure the test progressed to. F quality is not an accurate representation of σ_{Hmin} and thus should be considered a lower bound (Heidbach et al., 2008).

3.2.3 MAXIMUM HORIZONTAL STRESS (σ_{Hmax})

The frictional limit equation was used to quantify the upper bound for σ_{Hmax} (equation 3), which can be simplified to equation 4.

$$\frac{S_1 - P_P}{S_3 - P_P} \leq 3.12 \tag{3}$$

$$\therefore S_1 = 3.12(S_3 - P_P) + P_P \tag{4}$$

3.3 In-situ stress measurement

In-situ stress orientations were established using two techniques. Borehole breakouts (BOs) and Drilling-Induced Tensile Fractures (DITFs).

3.3.1 BOREHOLE BREAKOUTS

Borehole breakouts are stress-induced elongations across a wellbore cross section (Figure 4). This occurs when the maximum circumferential stress exceeds the compressive strength of the rock, resulting in the collapse of affected regions of the well and

subsequent infill of conductive drilling mud. This presents itself as dark shading on image logs (Bell, 1996a, 1996b; Bell and Gough, 1979; Kirsch, 1898). These stress indicators when observed in image logs have characteristic horizontal banding resulting in an "ovalised" or "elliptical" shape (Bell, 1996a) (Figure 4). Circumferential (hoop) stress is defined by:

$$\sigma_{\theta\theta} = \frac{F}{tl} \tag{5}$$

F is the force exerted circumferentially upon an area of the cylinder wall, t is the radial thickness of the cylinder, and l is the axial length of the section of wellbore. Stress concentration around a vertical borehole is greatest in the direction of the σ_{Hmin}; hence, BOs will form perpendicular to the σ_{Hmax} (Plumb and Hickman, 1985) (Figure 4).

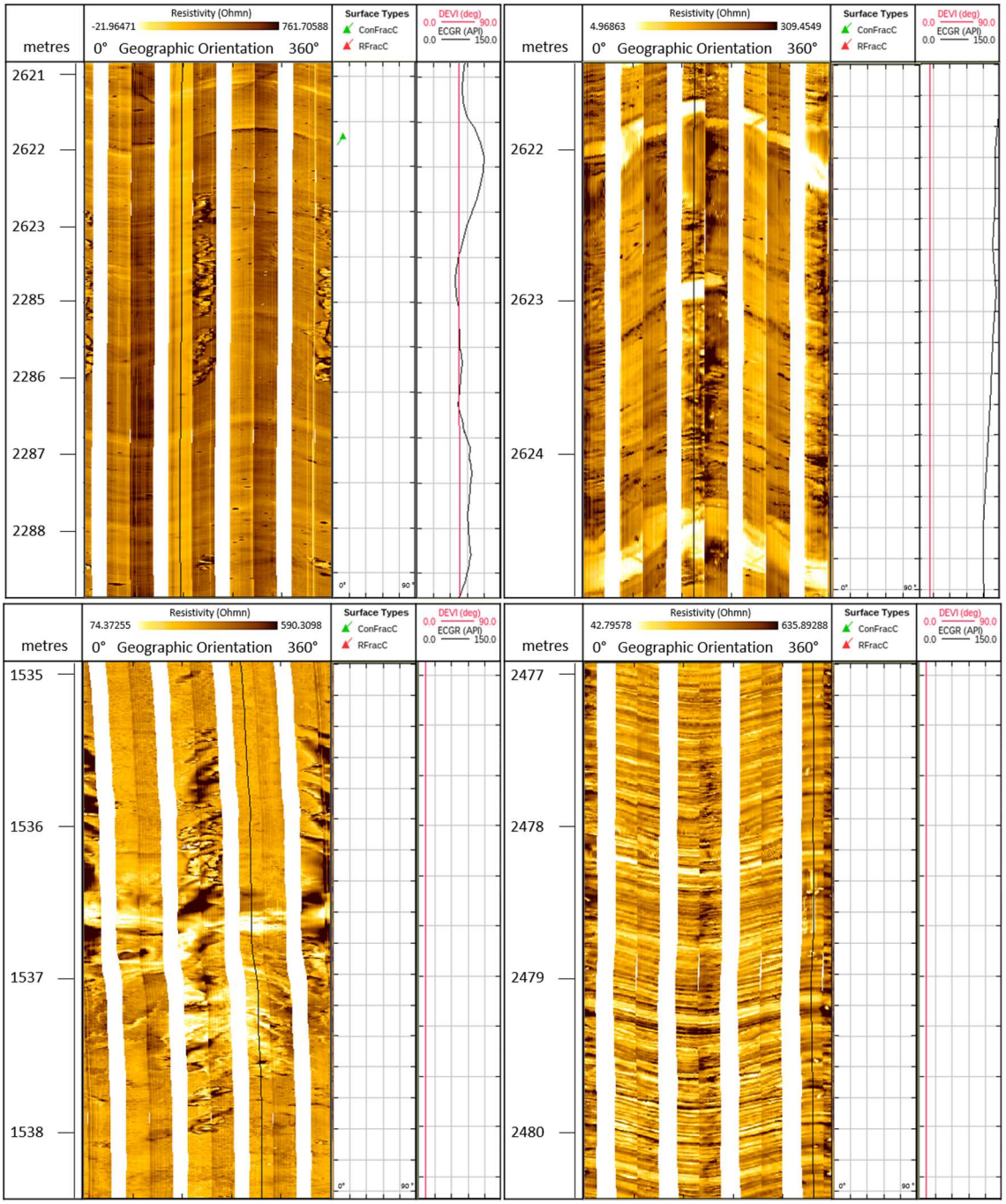

Figure 4: A range of borehole breakouts interpreted from a variety of wells: note the slight horizontal and discontinuous banding, indicative of a borehole break-out.

3.3.2 DRILLING-INDUCED TENSILE FRACTURES

Drilling-induced tensile fractures appear on an image log as a pair of dark vertical lines, separated by 180° (Bell, 1996a) (Figure 5). Drilling-induced tensile fractures are aligned with the present-day σ_{Hmax} direction in vertical wells (Bell, 1996a). Stress indicators occur when the minimum circumferential stress becomes tensile (negative) and exceeds the tensile strength of the wellbore wall (Brudy & Zoback, 1999; Peška & Zoback, 1995). They are distinguished in image logs through their discontinuous nature. The angle of deviation has a large impact (visually) upon the DITF (Figure 5). Although conditions and stress states, leading to DITF formation are ubiquitous, wells with substantial deviation from vertical, can present en echelon DITFs, where drilling induced fractures appear to form in a non-perpendicular manner (Bell, 1996a).

3.3.3 QUALITY RANKING STRESS ORIENTATIONS

Circular statistics were used to determine the orientation of σ_{Hmax} for each well. These were then ranked as per the World Stress Map quality ranking scheme (Heidbach et al., 2008). From the quantification of total number, total length and the standard deviation of stress indicators (Heidbach et al., 2008), where A quality is the highest and E quality is the lowest. Each well can provide two σ_{Hmax} orientations based on BOs and DITFs. Data ranking D or higher is widely accepted as a reliable record of σ_{Hmax} orientations with E quality seen to be unreliable (King et al., 2010; Tingay et al., 2005; Zoback et al., 1992).

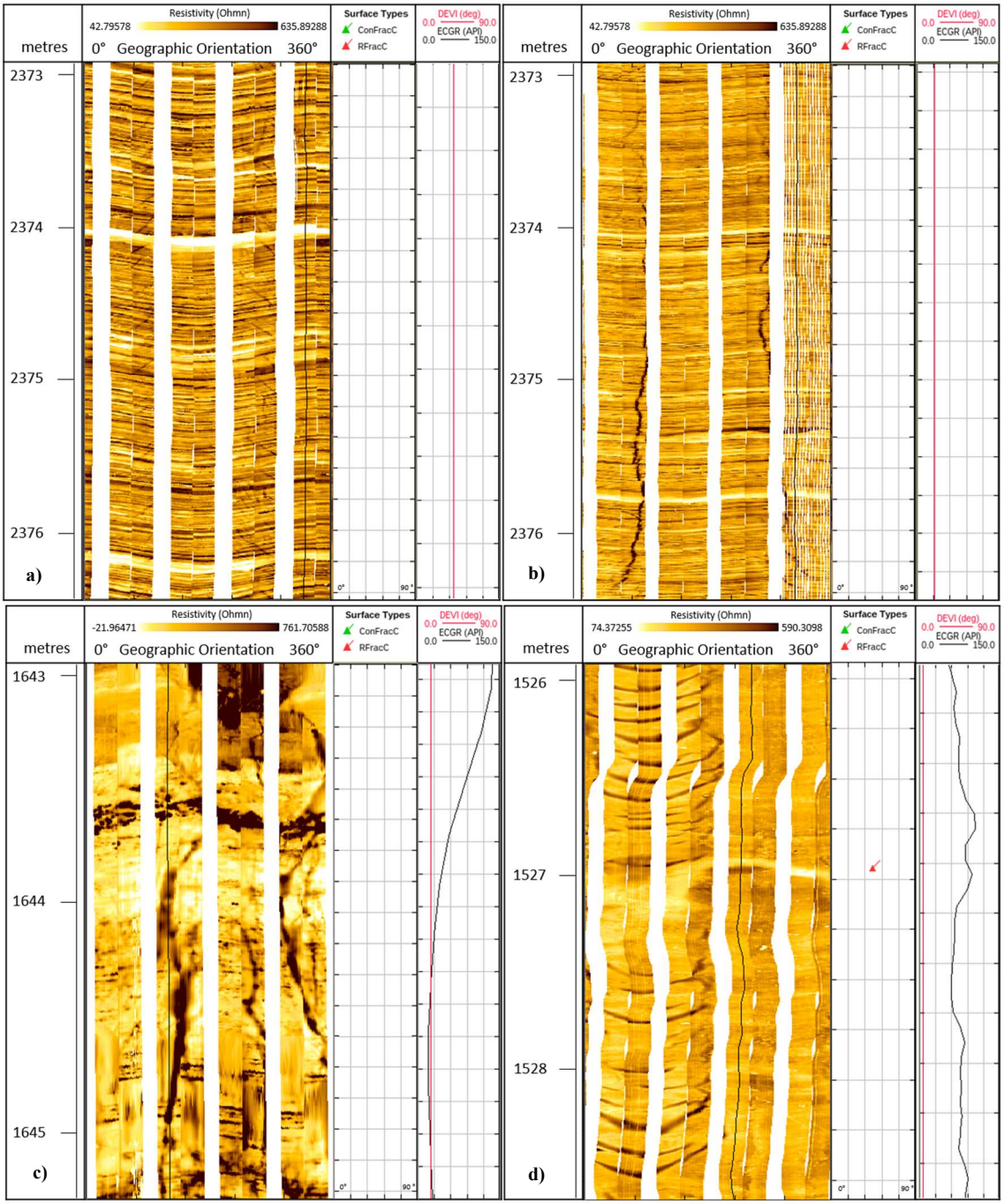

Figure 5: A range of drilling induced tensile fractures observed and interpreted. These range from common DITFs as seen in b) and c) through to en echelon and wing DITFs observed in c) and d). The change in form can be established through the deviation from vertical.

c)

3.4 Natural fracture analysis from image logs

Natural fractures were identified using Formation Micro Imager (FMI) logs. Electrically conductive fractures are identified through a dark sinusoid (Figure 6). These analogous, dark, cross-cutting fractures are assumed to have been shallowly filled with electrically conductive drilling mud, giving rise to the dark colour observed (Figure 6). Electrically resistive fractures as seen in Figure 6 are identified by cross-cutting, light in colour sinusoids, and are thus void of drilling muds, equating to the light brown/white colour observed. The shape of the sinusoid is a function of the dip of the fracture identified, with high dip angle fractures producing higher amplitude sinusoids than lower dip angle fractures (Zoback, 1992). Identification of structures was possible through analogous dip angles and dip directions with respect to the surrounding beds as seen in Figure 6. Identified fracture sets were categorised based on dip and dip direction and depth from surface, to determine any systematic patterns in their distribution with respect to mechanical stratigraphy.

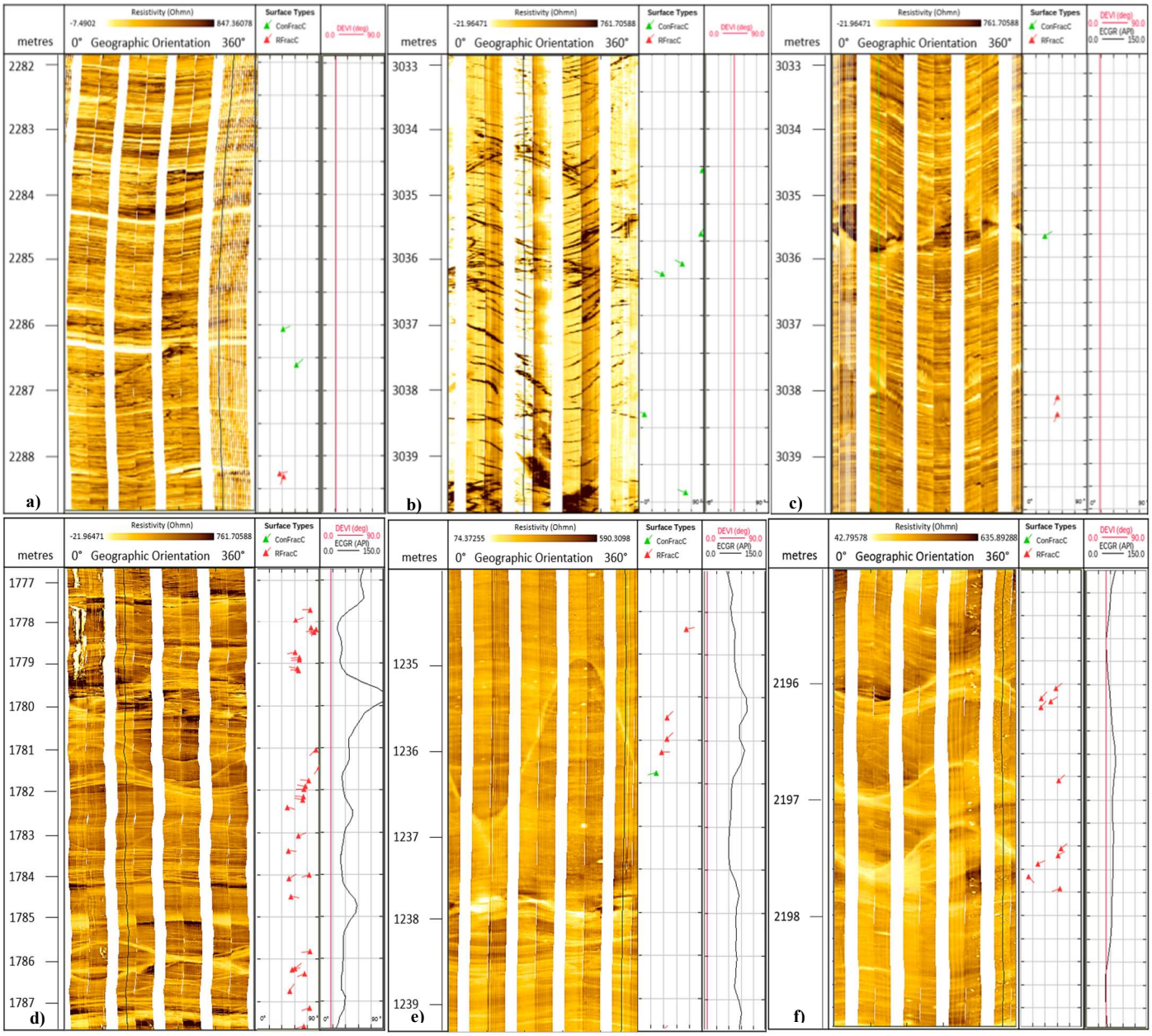

Figure 6: a) to c) illustrate interpreted conductive natural fractures as shown by the black/dark brown, cross cutting sinousoids indicating drilling mud has inprinted the natural fracture. d) to f) exemplify interpreted electrically resistive fracture as highlighted by the white/light brown cross cutting sinousoids.

4.0 RESULTS

4.1 Palaeo stress (Calcite Stress Inversion Technique)

Calcite stress inversion technique was undertaken on samples NPS1 and NPS2. Each sample had three perpendicular thin sections cut to encompass the three major faces of the sample (Appendix A). Both samples were obtained from Senecio 1, with NPS1 taken from a depth from 2714 m, while NPS2 was taken from a depth of 2718 m. (Figure 2). Samples NPS1 and NPS2 displayed low levels of coarse-grained euhedral calcitic matrix; therefore, cross-cutting veinlets were used for analysis (Appendix B). 300 calcite grains were analysed in sample NPS1 and 285 grains analysed in NPS 2. Samples were analysed using a universal stage microscope. In twins observed, the internal twinning deformation was concurrent with type I twinning, indicative of temperatures below ~150-200 °C, with internal strain not exceeding 3-4% (Burkhard, 1993) (Figure 3). Perpendicular thin sections were cut (Appendix A; Appendix B) and twinned calcite lamellae were measured along strike providing the azimuth of the twin. From analysis and calculation of the RST, samples provided a second tensor (Table 1) of lesser, but usable quality data. Orientation of the RST seen in Figure 10, 11, 12, and 13 has been calculated in both the present-day bed dip and dip direction as well as correcting for any tilt of the bedding plane to highlight shifts in data.

4.1.1 TILTED BEDDING RELATED STRESS TENSORS

The first calculated twinning event has characteristics in common with an extensional setting. This is demonstrated by the vertical σ_1 axis (Table 1) (Figure 12). Bedding was tilted at 18° uniformly across both samples. The ellipsoid shape ratio in NPS1 is 0.1, indicating the magnitudes of σ_2 and σ_3 are similar in value. This tensor accounts for 54%

of the available data collected. The σ_1 axis found in the second tensor for NPS1, incorporated 50% of the remaining data with a shape ratio value of 0.4 (Table 1). The strike and angle of plunge in σ_1 implied a NNW-SSE compression regime (Figure 10). A total of 187 calcite twin planes were used in this calculation; however, due to the high percentage of untwinned planes incorporated, care was taken when linking this tensor to palaeo structures (Table 1). The σ_1 axis in the first tensor calculated in NPS2 has a trend of 351°-171°, implying N-S compression, due to the relatively low plunge angle (Table 1) (Figure 13). This tensor accounted for 30% of the data set with a shape ratio of 0.1, suggesting magnitudes of σ_2 and σ_3 are similar in value. Two secondary tensors were calculated in NPS2, separated by the inclusion of 1% of the data set. The σ_1 axis in both tensors strikes SW-NE, with variations observed in the penalisation function (*f)* and shape ratio (ϕ) (Table 1) (Figure 12). A total 195 calcite twin planes were used in this calculation (Table 1).

4.1.2 CORRECTED BEDDING RELATED STRESS TENSORS

After the rotation of bedding to remove the effect of tilting, both samples observed very little change in stress regime compared to the unrotated readings. However, in NPS1 tensor 1, after rotation was conducted, σ_1 moved 18° closer to vertical. (Table 1) (Figure 11).

Table 5: Results of stress tensor determination based on calcite twin data. Corrections relate to the process of un-tilting tensors to account for bedding dip camouflaging potential tensors.

Sample	Bedding dip direction/dip	Trend of the principle stress axes			Ratio between differential stress (Φ)	Number of T/UT data	Number of data consistent with the tensor T/UT	Quality estimator function (*f*)
		σ_1	σ_2	σ_3				
NPS1	132/18	207/71	112/02	022/19	0.1	211/89	113/38	0.63
		179/19	272/11	030/68	0.4	98/89	49/81	0.61
NPS2*	132/18	171/32	296/42	059/31	0.1	195/90	58/41	1.01
		245/32	028/30	133/31	0.4	138/89	52/57	0.80
NPS1 (corrected)	132/00	150/84	298/05	029/03	0.1	211/89	113/38	0.63
		178/28	279/20	040/55	0.4	98/89	49/81	0.61
NPS2* (corrected)	132/00	165/41	317/45	063/14	0.1	195/90	58/41	1.01
		256/48	036/14	129/29	0.4	138/89	52/57	0.80

4.2 Present-Day stress magnitudes

4.2.1 VERTICLE STRESS(σ_V)

There was little variation in σ_V profiles with Jingemia 2, 3, Bartsia 1, Eremia 6 and Hovea 9, exhibiting a range of 0.7 MPa at 1 km depth. In Eremia 6 at 1 km, the σ_V profile is 22.69 MPa compared to 22.19 MPa at 1 km in Hovea 9. At 2.5 km (excluding the outlier Hovea 2) the spread is 0.8 MPa (with an s.d. of 0.60 MPa). Spread is exemplified by Bartsia 1 which possessed a σ_V of 58.08MPa (at 2.5 km depth) compared to 57.64 MPa as seen in Hovea 12 at the same depth. By including Hovea 2 (61.71 MPa at 2.5 km depth) the range of σ_V increased significantly to 4.53 MPa (with an s.d. of 2.41 MPa) (Figure 7).

4.2.2 MINIMUM HORIZONTAL STRESS (σ_{Hmin})

Values of σ_{Hmin} were quantified in eight wells, with two D quality readings (Dongara 28 & Eremia 2) coming from LOTs, conducted at 800 m and 1525 m. From D quality rankings, σ_{Hmin} ranged from 13.01 MPa at 800 m in Eremia 2, to 26.60 MPa at 1525 m in Dongara 28. From the sole E quality ranking (Jingemia 2), the σ_{Hmin} was established as 11.58 MPa at 533 m. This was calculated from the maximum pressure from FIT, reported in the WCR. The remaining six wells contain F quality readings from reported FITs and these can provide a lower bound for σ_{Hmin}. F quality readings were not plotted in Figure 7 due to their low quality.

4.2.3 MAXIMUM HORIZONTAL STRESS (σ_{Hmax})

Due to the limited availability of LOT data and the pre-existing relationship between equations 2 and 3, σ_{Hmax} has been calculated for two wells; Eremia 2 and Dongara 28. The σ_{Hmax} magnitude in the two wells ranges from 23.97 MPa at 800 m in Eremia 2, to 51.30 MPa at 1525 m in Dongara 28. Although not presented in Figure 7, the hoop stress equation was utilised in Dongara 28 to provide a lower of bound of σ_{Hmax}. This lower bound equates to 22.48 MPa at 1525 m.

4.2.4 STRESS REGIME IN THE PERTH BASIN

Stress magnitudes calculated for this area of the Perth Basin broadly define a strike-slip fault stress regime ($\sigma_{Hmax} > \sigma_V > \sigma_{Hmin}$) at depth as seen in Figure 7. However, due to the relationship shown in Figure 7, some σ_{Hmin} and σ_V are roughly equal ($\sigma_{Hmax} > \sigma_V \approx \sigma_{Hmin}$) for depths <500 m leading to the conclusion that certain regions in the Perth Basin are in

reverse/transpressive fault stress regimes (Bailey et al., 2012; Hillis and Reynolds, 2000; King et al., 2008).

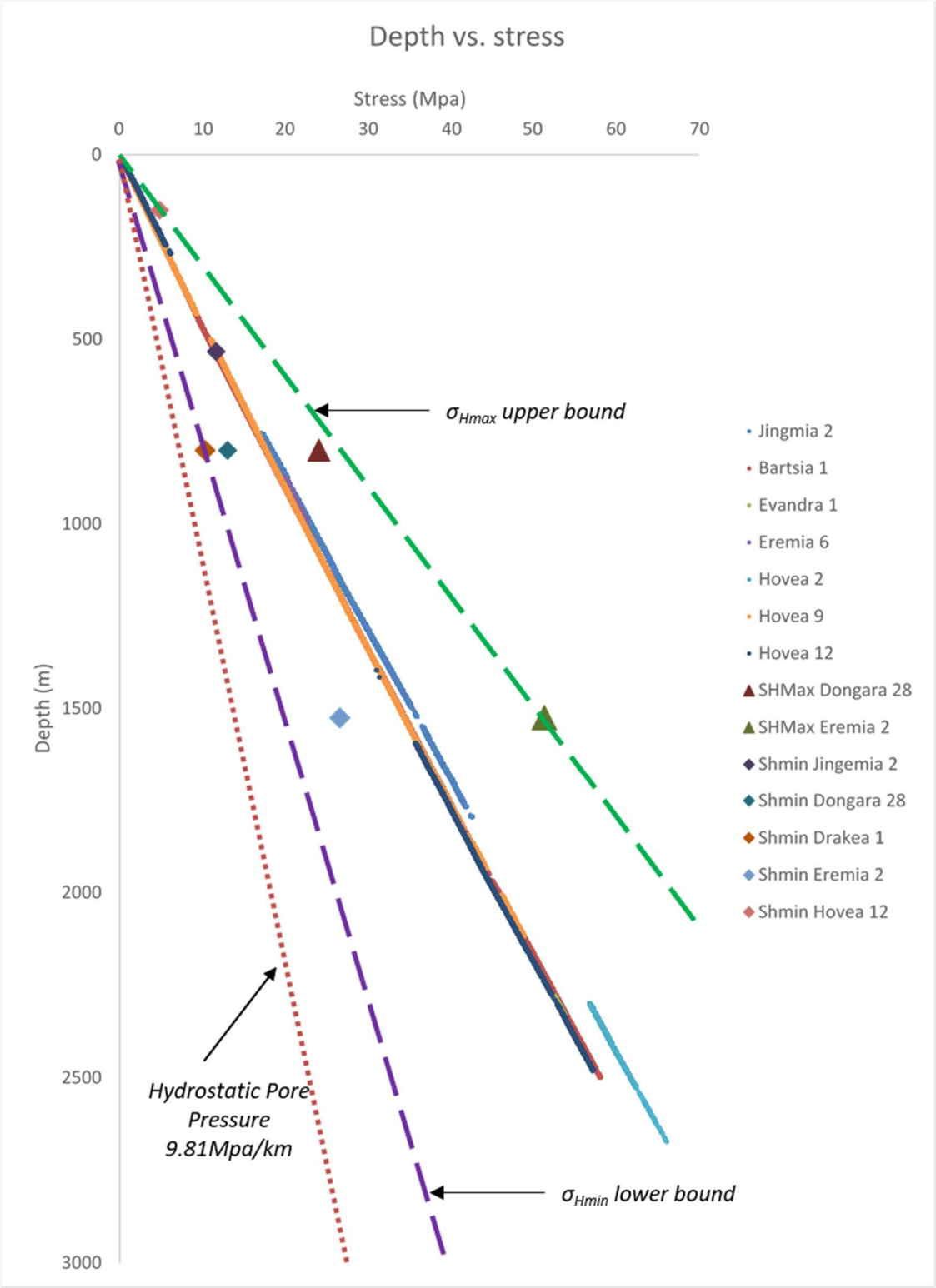

Figure 7: The three principle stress magnitudes as defined by this study. From density logs gathered in seven wells, a vertical stress profile could be constructed, thus defining the vertical stress magnitude for each well. From the implementation of data gathered from LOTs and FITs, equation two was used to constrain the minimum horizontal stress magnitude. Through the use of equation three, a relationship between the minimum and circumferential stress was used to quantify the maximum horizontal stress and thus define the Perth Basin as that of a transitional strike slip reverse fault stress regime.

4.3 Orientation of in-situ stresses

186 BOs and 45 DITFs were analysed from image logs in eight wells from the study area (Figure 2) (Table 1). BOs were observed in five of the seven wells (Drakea 1, Hovea 9, Hovea 12, Jingemia 2 and 3), with Jingemia 2, 3, Hovea 9 and Drakea 1 containing both stress indicators. Figure 2 and well cards (Appendix C) show the location of the wells in the Perth Basin and intervals where image logs were run (Table 2). All seven wells analysed were ranked at D quality or above, with Jingemia 2 and Hovea 9 having BO rankings of A quality (Table 1). Based on BO measurements, Jingemia 2 & Hovea 9 contained A quality ranking (±15°), Drakea 1 was B quality ranking (±15-20°), Jingemia 3 C quality ranking (±20-25°) and Hovea 12 D quality ranking (±25-40°) (Table 3). Wells containing D quality or higher were used in the calculation of the mean σ_{Hmax} orientation of 089.9°N (Table 3). A suite of characteristics was observed when picking DITFs in image logs, ranging from typical near vertical pairs of electrically conductive fractures, to en echelon DITFs observed in Drakea 1 and wing DITFs as seen in Jingemia 2 (Figure 5). Full picking sets of BOs and DITFs can be found in Appendix D.

Table 6: Location, depth interval over which the Formation Micro-Imager (FMI) tool was run and maximum deviation of the eight wells analysed in this study.

Well Name	Location		Depth Interval (m)		Tool Used	Well Deviation
	Latitude	Longitude	Top	Bottom	Image Log	Max deviation from vertical
Bartsia 1	29.288°S	114.974°E	1387	2487	FMI	19.30°
Drakea 1	29.403°S	115.061°E	773	3091	FMI	45.93°
Dongara 23	29.261°S	115.007°E	-	-	-	-
Dongara 28	29.244°S	115.015°E	-	-	-	-
Evandra 1	29.348°S	115.021°E	1841	2325	FMI	14.90°
Jingemia 2	29.339°S	114.990°E	500	2778	FMI	30.06°
Jingemia 3	29.339°S	114.990°E	500	2636.5	FMI	21.36°
Eremia 2	29.310°S	115.027°E	503	2290	FMI	28.42°
Eremia 6	29.309°S	115.019°E	-	-	-	-
Hovea 2*	29.314°S	115.045°E	820	2690	FMI	-
Hovea 9	29.329°S	115.044°E	498	2112.5	FMI	15.92°
Hovea 12	29.318°S	115.042°E	1600	2475	FMI	38.08°

*Although said Hovea 2 had an Image log run, none could be found, even when requesting from WAPIMS.

Table 7: Summary of maximum horizontal stress orientations from borehole breakout and Drilling-Induced Tensile Fracture across the thirteen wells featuring wellbore resistivity image logs in the Perth Basin. Quality ranking according the World Stress Map (Heidbach et al., 2008).

Well Name	Indicator type	σHmax orientation (°)	Number of indicators	Total cumulative length (m)	Standard deviation in orientation	Quality*
Bartsia 1	BO	-	-	-	-	E
	DITF	-	-	-	-	E
Drakea 1	BO	89	47	80.39	17	B
	DITF	78	13	20.11	15	D
Dongara 23	BO	-	-	-	-	E
	DITF	-	-	-	-	E
Dongara 28	BO	-	-	-	-	E
	DITF	-	-	-	-	E
Evandra 1	BO	-	-	-	-	E
	DITF	104	7	20.00	13	D
Jingemia 2	BO	94	24	101.53	6	A
	DITF	83	7	20.72	4	D
Jingemia 3	BO	93	8	24.01	2	C
	DITF	89	8	26.76	10	D
Eremia 2	BO	-	-	-	-	E
	DITF	-	-	-	-	E
Eremia 6	BO	-	-	-	-	E
	DITF	-	-	-	-	E
Hovea 2	BO	-	-	-	-	E
	DITF	-	-	-	-	E
Hovea 9	BO	94	87	195.87	10	A
	DITF	82	10	29.27	19	D
Hovea 12	BO	93	12	12.02	1	D
	DITF	-	-	-	-	E

4.4 Natural Fractures

4.4.1 RESISTIVE FRACTURE

Natural fractures were interpreted from eight wells containing image logs and appeared commonly throughout the length of the image log run. A total of 1283 resistive fractures were picked, ranging in angle of dip and dip direction. In Bartsia 1, Jingemia 2 and 3 resistive fractures formed tight sets striking NE-SW. A mean dip direction of 157°-337° (NNE-SSW) was observed for the primary set of resistive fractures. A second set of resistive fractures seen in Hovea 9, Evandra 1, and Drakea 1 was observed dipping NNE-SSW. Significant variations in dip direction were observed in Eremia 2, Hovea 12, where a mean dip direction of 037°-217° was established. Resistive fractures appear to have little association with lithologies or any type of formation in all eight wells where resistive fractures were interpreted.

4.4.2 CONDUCTIVE FRACTURE

Electrically conductive fractures were observed in the eight wells with a total of 480 conductive fractures identified (Table 4) (Figure 8). A clearly defined primary set of conductive fractures dipping ENE-WSW (076°-256°) were observed in seven of the eight wells, with only Hovea 9 showing no conductive fractures dipping ENE-WSW (Appendix C.5). Hovea 9, 12 and Drakea 1 (Appendix C.2, C.5 and C.6) present a secondary set of conductive fractures with a mean dip direction of 026°-206° (NNW-SSE). However, this was significantly smaller when compared to the primary set (Appendix C.1, C.2, C.3, C. 4, C.6, C.7 and C.8). Conductive fractures appeared to have minor associations with Woodada formation and Kockatea shale. Full picking sets of both resistive and conductive fractures can be found in Appendix E.

Table 8: Total fractures identified across eight wells, showing a large disparity between resistive and conductive fractures identified in the Perth Basin.

Well Name	Total number of fractures	Conductive fracture total	Resistive fracture total	Percentage split (%)
Bartsia 1	145	48	97	33/67
Drakea 1	729	171	558	24/76
Eremia 2	56	30	26	53/47
Evandra 1	60	15	45	25/75
Hovea 9	245	73	172	30/70
Hovea 12	119	41	78	35/65
Jingemia 2	129	41	88	32/68
Jingemia 3	281	61	220	21/79
Total	**1763**	**480**	**1283**	**27/73**

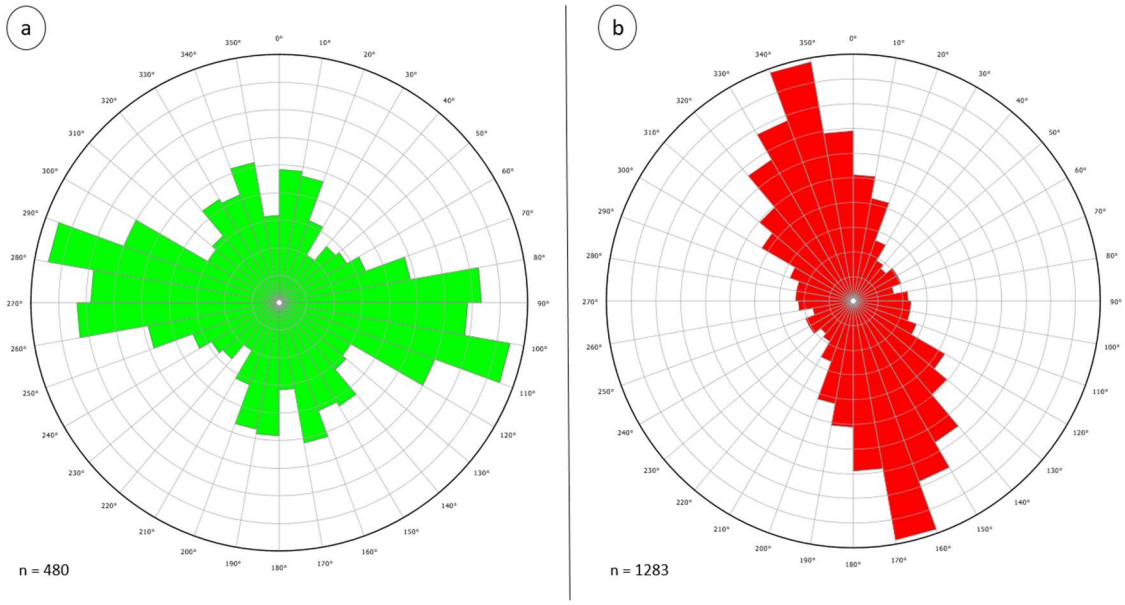

Figure 8: Rose diagrams, showing total fractures across eight wells. Rose diagram a) shows the total conductive fractures exhibiting a clear main set of fractures striking east-west with minor rotation observed and constrained to ±20° of the mean azimuth. Supplementary sets are shown striking NNW-SSE along with NNE-SSW. Rose diagram b) exhibits the total number of resistive fractures, displaying a clear tight set striking NNE-SSE with rotation limited to ± 15° of the mean azimuth.

4.5 Fracture reactivation in the Perth Basin

Fracture reactivation plots have been created for two settings, one indicative of a reverse fault stress regime at 500 m depth (Figure 9), with the other pertaining to a strike slip fault regime at a depth of 1 km as well (Figure 9).

Fracture plots were constructed with extrapolated magnitude data, with a rock tensile strength of zero and a coefficient of friction of 0.6 as per Byerlee (1978). Fracture reactivation plots work in a similar manner to a combination of a stereonet and a Mohr's circle. Fractures are plotted as poles to planes, with the subsequent position indicating the change in pore pressure (Pp) required for the fracture to become critically stressed (Means, 1976). Areas in red, represent fracture/fault orientations most optimally aligned in the stress field to reactivate and thus need the smallest change in Pp for this to occur. Blue regions are the least optimally orientated and thus require a large change in pressure.

4.5.1 REACTIVATION OF RESISTIVE FRACTURES

Figure 9 illustrates all the resistive fractures identified as per a reverse fault setting. This regime was observed in shallow depths in the Perth Basin and while extrapolated values are used in construction of this plot, a loosely constrained set is apparent. This set is comprised of a large number of approximate E-W fractures, dipping roughly between 10° and 60°. This set, however, is not clear; as Figure 9 shows, fractures fall into all regions of the reactivation plot. The majority of fractures plot in red areas, indicating they are most likely to reactivate (Figure 9). The cementation present may have resulted in these fractures becoming stress insensitive, thus requiring a higher Pp value than stated in fracture reactivation plots (Laubach et al., 2004).

As Figure 9 demonstrates, the trend above is completely reversed if the stress regime is that of pure strike slip. At 1 km depth, Figure 7 demonstrates this as being the most likely stress regime. The E-W trend of fracture remains; however, the majority of fractures now fall into blue regions, implying these fractures are less likely to reactivate. Bailey et al. (2012) conducted a similar fracture plot for a transpressional system and when comparing this study's results and Bailey's, a strong consensus is developed surrounding the present-day stress regime and resistive fracture reactivation.

4.5.2 REACTIVATION OF CONDUCTIVE FRACTURES

For a shallow reverse fault stress regime as observed in Figure 9, clear clustering of conductive fracture exists in an easterly direction with a dip ranging from 30° to 70° (Figure 9). Significant spatial variations exist in the remaining data set, with a minor set situated N-S in dip direction with shallow dip (<15°) (Figure 9). The majority of the total data plots are within regions of high reactivation potential, illustrating that given the current stress regime and orientation these fractures are optimally aligned for reactivation (Figure 9). Conductive fractures plotting in green/blue areas are likely to have formed as a result of palaeo stress regimes and contain partial conductive mineralisation, giving the appearance of being electrically conductive (Bailey et al., 2012).

When the total fracture set is plotted on a purely strike slip stress regime, no movement of fractures is observed, and one broad trend exists (Figure 9). This trend is composed of an unequal spread of data, favouring the eastern side of the reactivation plot. Little disparity appears between fractures that plot in the red regions or blue regions, with a visual estimation suggesting this number is close to equal (Figure 9).

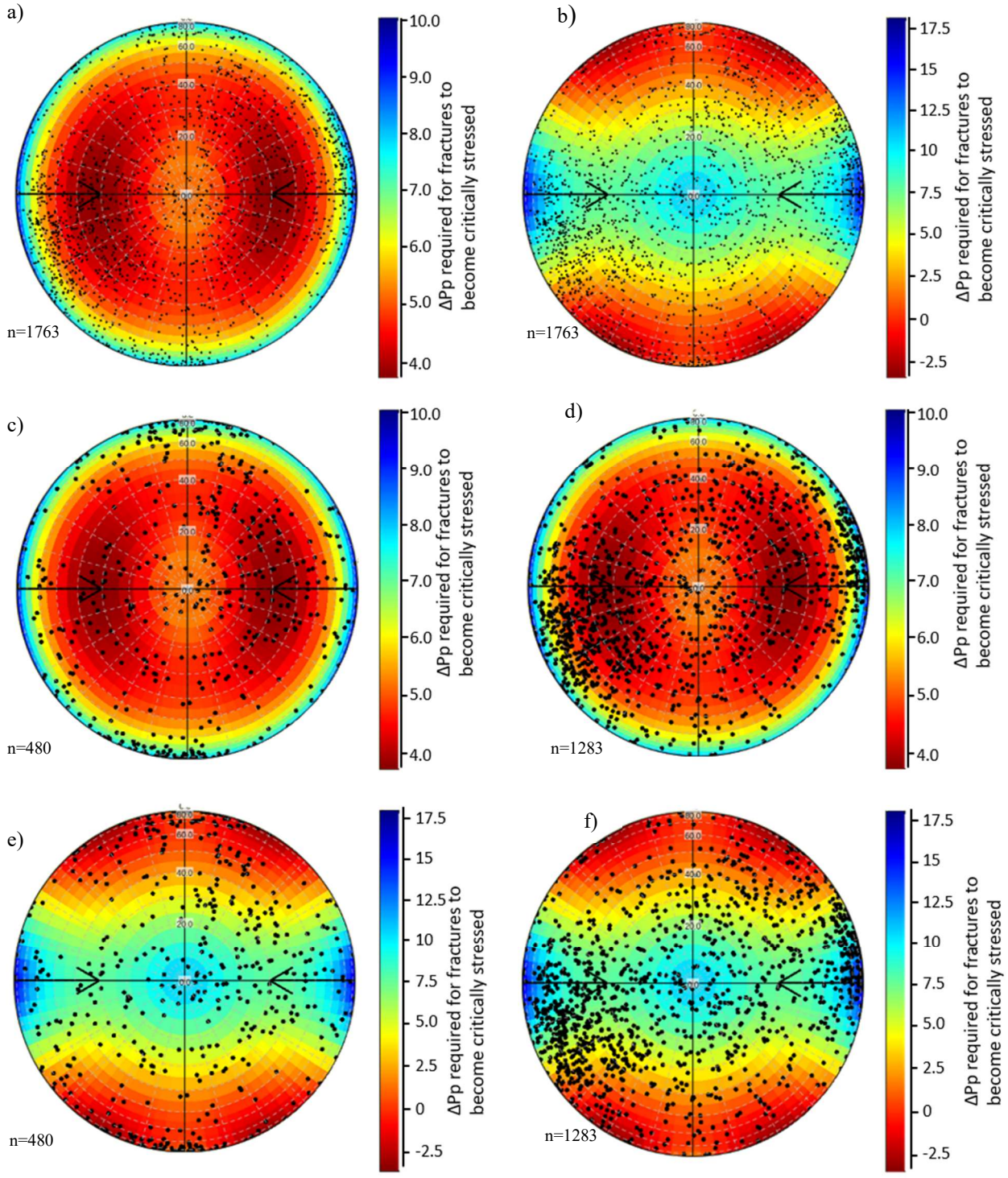

Figure 9: Fracture reactivation plots as per a strike slip stress regime (b, e, f) and reverse faulting stress regime (a, c, d). Fractures are plotted as poles to planes with ΔPp representing the change in pore pressure required to move the conditions to that of critical stress as per the Griffith-Coloumb failure envelope. Fracture susceptibility plots are for 1 km (strike-slip) and 500 m (reverse) depth and 0.6 coefficient of friction. a) All fractures (conductive & resistive) for a reverse fault stress regime. b) All fractures for a strike slip fault stress regime. c) Total conductive fractures as per a reverse fault stress regime. d) Total resistive fractures as per a reverse fault stress regime. e) Total conductive fractures as per a strike slip fault stress regime. f) Total resistive fractures as per a strike slip fault stress regime.

5.0 DISCUSSION

5.1 Tectonic evolution of the Perth Basin

5.1.1 COMPARISON OF MACRO AND MICROSCOPIC PALAEO STRESS ANALYSIS

A significant problem in the analysis of palaeo stress is finding the palaeo stress tensor that best fits the distribution and number of twinned and untwinned planes (Amrouch et al., 2010a). One solution for this is to implement the inversion process mentioned previously. The inversion process and its efficiency have been widely debated (Angelier, 1984, 1990; Lacombe, 2012), with standards needed to be established as to statistically justify results presented (Lacombe et al., 1990). The main cause of high error functions (*f*) (>1) in the inversion function can be traced through U-stage measurements, poor sample collection and preparation. Lacombe et al (1990) verified that a total of 90 twins per sample are required to remove any inversion associated errors (Lacombe et al., 1992). Therefore, data presented in Table 3 is determined to be reliable and is expected to highlight potential regionally consistent palaeo stress tensors (Amrouch et al., 2010a, 2010b; Lacombe et al., 1992, 2007). Sample NPS2 exhibits a high *f* function due to the large incorporation of untwinned planes into the inversion process and a low ratio consistent with the palaeo stress tensor (Table 3). Due to limited sampling horizons and uncertainties inherent in the inversion process to determine palaeo stress orientation, the deviation amounts to ~10-20° (Lacombe et al., 1992).

5.1.2 CORRELATION OF PALAEO STRESS TENSORS WITH TECTONIC ENVIRONMENTS

Previous work in the Perth Basin has generated several informed, well-established regional tectonic models (Bailey et al., 2012; Harris, 1994; Hillis and Reynolds., 2000; King et al., 2008; Marshall et al., 1989; Mory & Iasky, 1996; Playford et al., 1976); this study will discuss these interpretations of palaeo stress tensors established through calcite twin analysis.

Palaeo stress tensors seek to validate previous authors hypotheses regarding the formation of the basin and the evolution of structural trends. It is well established that Precambrian terranes of S-W Western Australia were dismembered during WNW-ESE crustal shortening/NNE-SSW extension in the Early Cambrian (Harris & Li, 1992); resulting in movement along the proto-Darling Fault because of local reactivations of mylonitic foliations (Harris, 1994). A process of "down-warping" in the proto-Perth Basin in the Carboniferous, was described by Falvey and Mutter (1981) and follows the local reactivations, however, this is predominantly conjectural (Balme, 1980). From Permian sedimentation, extensive faulting is evident, particularly through interbedded shalely units (Hall, 1989). Evidence for N-W striking faults contained to the lower Triassic through stress tensor analysis was compiled by Beeson (1992b). A compressional phase dominated the Mid Triassic with evidence of reactivation in the Northampton basement (Hall, 1989). Through the rotation of the σ_{Hmax} (from NW-SE to NE-SW), large volumes of poorly sorted alluvial sediments and coals were identified by Marshall et al (1989), marking an end of the Gondwana supercontinent in the Late Jurassic as compression turned to extension. (Harris, 1994; Marshall et al., 1989). This sedimentation was a result of large N-W dipping normal faults providing accommodation space (Marshall et al., 1989). Compartmentalization of strain potentially resulted in minor compressional events

as intra-cratonic rifting took place (Harris, 1994). Post-Neocomian compressional regimes are illustrated by east striking reverse faults in the Perth Basin and Yilgarn Craton (Beeson, 1992b) with rotation of the σ_{Hmax} through to E-W orientation appearing to have occurred over the space of millions of years. This may be due to the impact of large scale plate tectonics (Harris, 1994; Zoback, 1992). Highlighted in Post-Pleistocene N-S compression because of complex plate boundary interactions between the subducting Australian plate and overlying Pacific and Eurasian plates (Harris, 1994). With limited samples and horizons, these events are potentially representative of recorded stress indicators. Conversely, the observed tensors could also be the result of local stresses influenced by the localised effects of faults and thus, not representative of basin scale deformation.

5.1.2.1 Late Early to Middle Triassic compressional phase

The RST obtained from NPS1 tensor 2, is consistent with a NNW-SSE compressional event (Figure 10) with a near horizontal σ_1 (19°) and vertical σ_3 (68°) (Figure 10) (Table 1). This tensor may be attributed to Late-Early to Middle-Triassic N-S compression, through a reverse sense movement in basement structures (Hall, 1989). This evidence is supported by descriptions of regressional sedimentary formations including correlations of the Lesueur Sandstone as per Morey (1992). Compression established may be attributable to terminal collision on the Panthalassa margin and transfer of stresses intra-plate (Daly et al., 1989, 1991, 1992).

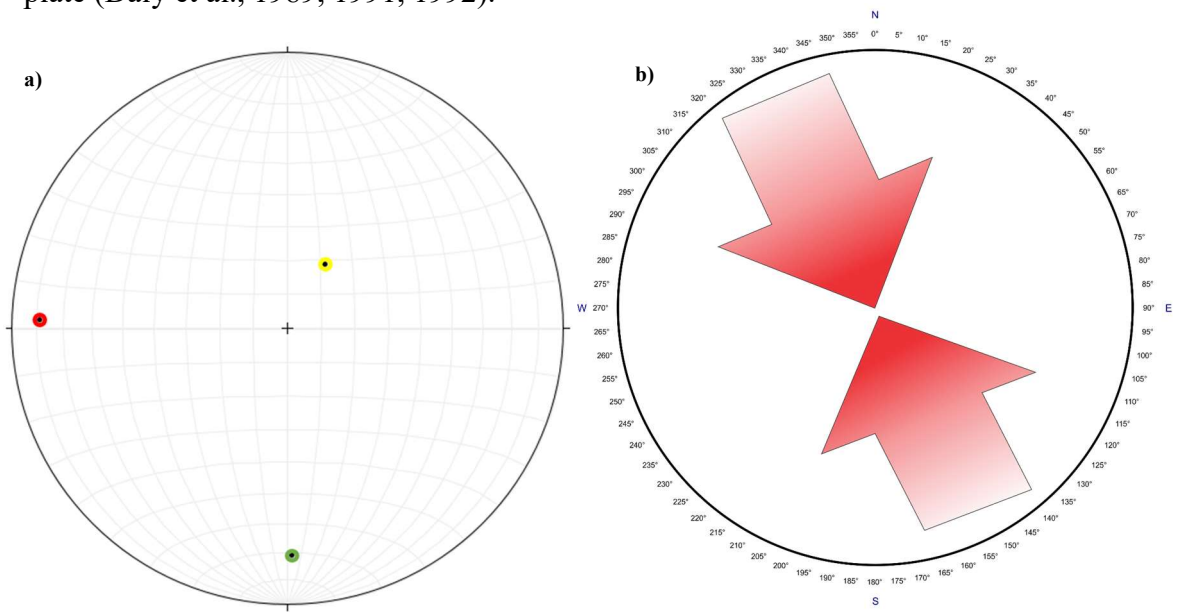

Figure 10: Palaeo stress tensor recorded in NPS1 tensor 2 from CSIT analysis relating to Late Early to Middle Triassic compression. a) illustrates the stereonet constructed from calcite stress inversion technique calculations with σ_1 highlighted in yellow, σ_2 in red and σ_3 in green. b) stress regime visualised from calcite stress inversion technique calculations.

5.1.2.2 Late Triassic to Earliest Jurassic extensional phase

Through analysis of NPS2 tensor 2, an E-W extensional regime can be deduced. After correction for bedding, σ_1 becomes increasingly vertical (32°→48°) with σ_3 adjusting to align with an Andersionsian system (Figure 11). This regime may comply with Late Triassic extension, highlighted through the formation of the Cattamarra Coal Measures during times of marine transgression (Harris, 1994). Paralic inputs of detritus material have been noted by Marshall et al (1989), with formation of marine shales and limestone lamellae indicative of the Cadda Formation (Marshall et al., 1989). Sediments observed locally, tend to lie unconformably upon Late Cretaceous to Early Triassic sediments (Hall and Kneale, 1992) providing further evidence of compression.

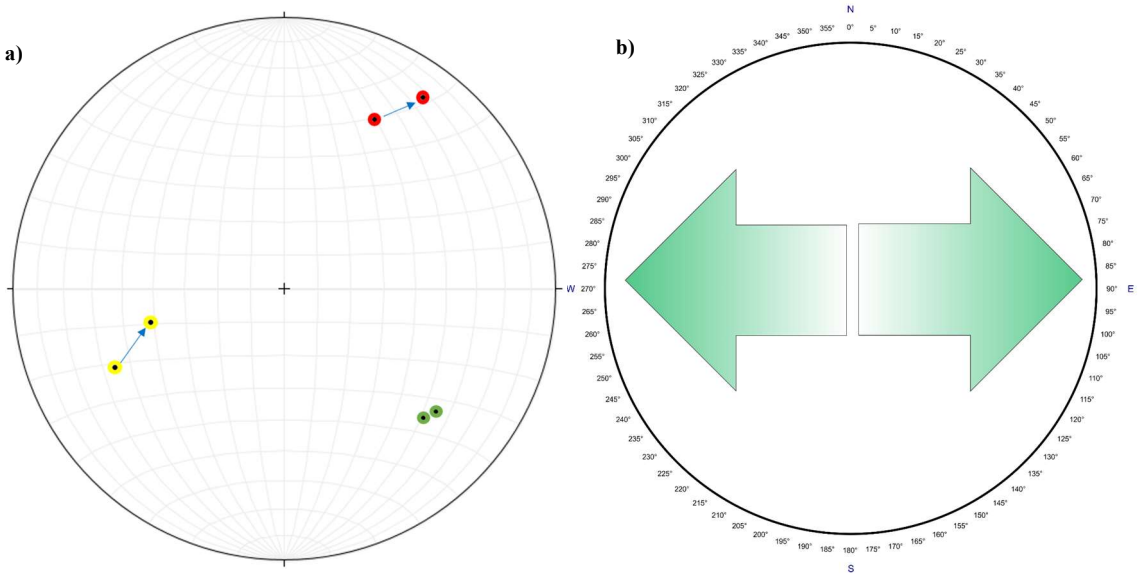

Figure 11: Palaeo stress tensor recorded in NPS2 tensor 2 from CSIT analysis relating to Late Triassic to Earliest Jurassic extension. a) illustrates the stereonet constructed from calcite stress inversion technique calculations with σ_1 highlighted in yellow, σ_2 in red and σ_3 in green. Blue arrows in a) signify pre-and post bedding corrections, with a shift to the right-hand side of the stereonet observed. b) stress regime visualised from calcite stress inversion technique calculations.

5.1.2.3 Early to Late Jurassic; principal rift stage

By performing rotations in NPS1 tensor 1, a NW-SE extensional regime is clearly observed. A near vertical σ_1 (84.4°) and horizontal σ_3 (03.2°) complete with most comparable twinned to untwinned planes result in the greatest confidence of calculated tensors (Figure 12) (Table 3). This rifting stage is observed through large NW dipping normal faults cutting through Jurassic strata (Harris, 1994; Mory & Iasky, 1996; Marshall et al., 1989; Playford et al., 1976). These primary structures are commonly recognised and subsequently linked to the breakup of Gondwana (Harris, 1994; Hillis and Reynolds., 2000; King et al., 2008; Marshall et al., 1989; Mory & Iasky, 1996; Playford et al., 1976). Significant displacement along visable present-day structures such as the Darling and Urella Fault (Hall and Kneale, 1992; Marshall et al., 1989), support interpretation from microscopic deformation (calcite twins) observed in calcite crystals. Palaeo stress calculations conducted by Beeson (1992b) from fault striations has furthermore concluded that, along with NW-SE extension, additional ENE-WSW of sub-horizontal extension pre-dates Early to Late Jurassic extension. These results do not support this hypothesis gathered from CSIT analysis. Due to the complex nature of the Perth Basin's history and lack of absolute age data, stress regimes established through the inversion process are not clear as multiple deformation events have occurred.

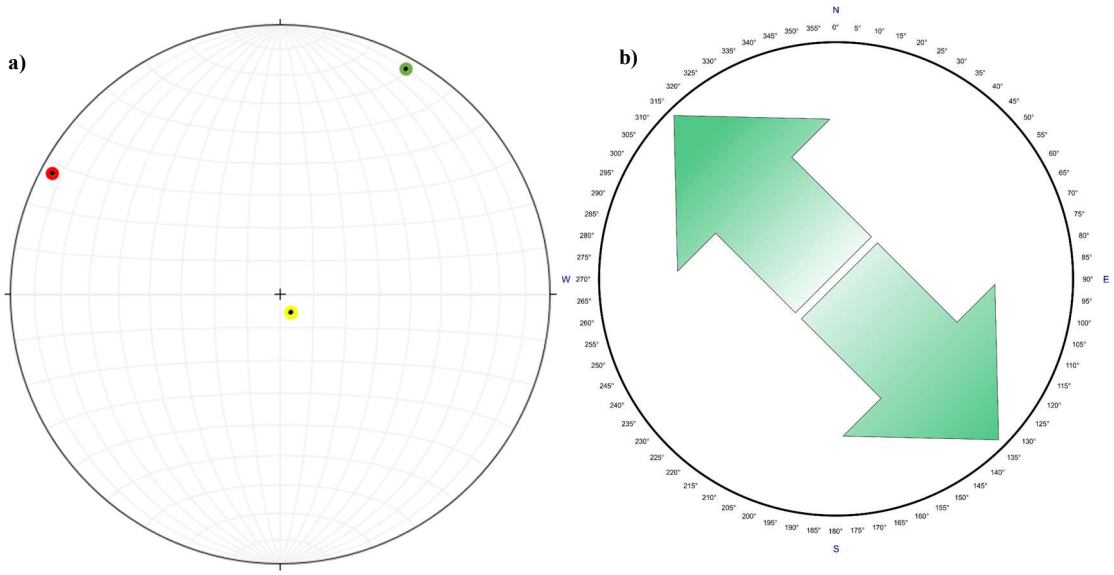

Figure 12: Palaeo stress tensor recorded in NPS1 tensor 1 from CSIT analysis relating to Early to Late Jurassic rifting. a) illustrates the stereonet constructed from calcite stress inversion technique calculations with σ_1 highlighted in yellow, σ_2 in red and σ_3 in green. b) stress regime visualised from calcite stress inversion technique calculations.

5.1.2.4 Post-Neocomian to Holocene

The Post-Neocomian Perth Basin is defined by an E-W σ_{Hmax} orientation and varying reverse/strike-slip stress regime through time (Audley-Charles et al., 1988; Veevers, 1984, 1991b). These cyclical shifts between reverse/strike-slip stress regimes, has been attributed to a new oblique spreading ridge developing in the Indian Ocean, as NNW-SSE contraction from ridge push forces would have occurred (Veevers, 1991b). In light of Richardson's (1992) paper ranking the orders of magnitude, ridge push contributes to plate driving forces, careful consideration should be placed around this. A more likely option is related to complex interactions at plate boundaries resulting in stresses developing intra plate (Hillis and Reynolds, 2000; Muller et al., 1992). The RST established from NPS2 tensor 1 (unrotated) is most applicable to this set of tensors. However, as NPS2 tensor 1 contains by far the highest error function (Table 3), it is

imperative that more data be collected in order to confirm this hypothesis. Raw data from calcite twin analysis is available in Appendix E.

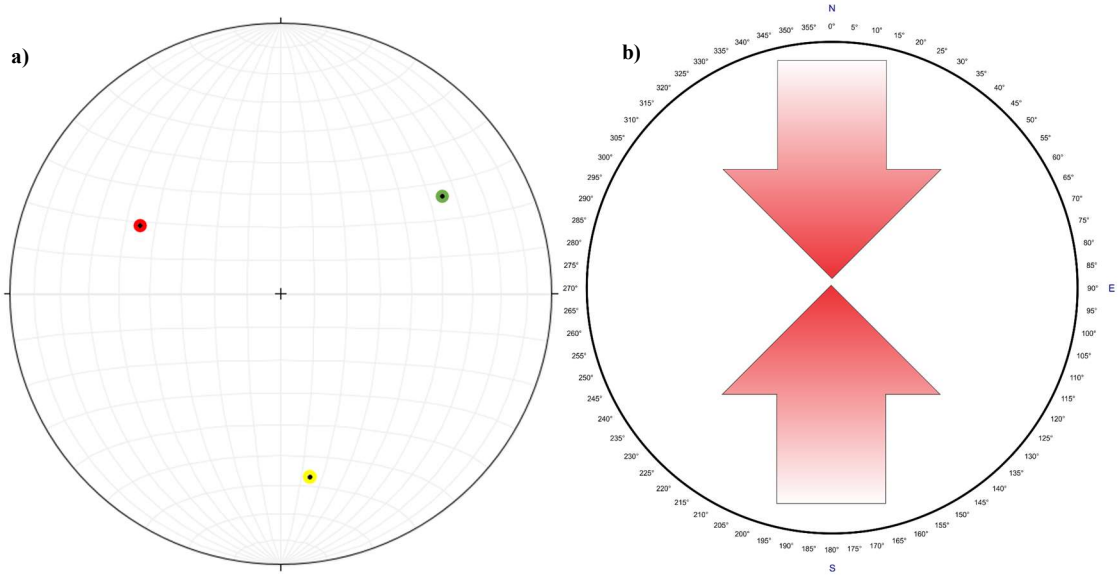

Figure 13:Palaeo stress tensor recorded in NPS2 tensor 1 from CSIT analysis relating to Post-Neocomian compression. a) illustrates the stereonet constructed from calcite stress inversion technique calculations with σ_1 highlighted in yellow, σ_2 in red and σ_3 in green. b) stress regime visualised from calcite stress inversion technique calculations.

5.2 Present-Day stress magnitudes in the Perth Basin

From density logs, the σ_V profile was calculated and compared to previous studies conducted in the Perth Basin (Bailey et al., 2012; King et al., 2008). When results in this study are compared to Bailey et al. (2012), a strong correlation is evident. This is highlighted at 1 km depth, where the average σ_V value for this study is 22.54 MPa, whereas Bailey et al. (2012) reports an average σ_V profile of 22.3 MPa, resulting in a spread of 0.24MPa. Although King et al. (2008) does not present an average σ_V profile at 1 km depth, values reported in two wells (21.1 MPa and 22.8 MPa) are close in nature to values found in this study. From collaboration of three different authors σ_V profiles, this further suggests σ_V is uniform across the Perth Basin. From LOTs performed in two wells (Eremia 2 and Dongara 28) two σ_{Hmin} values (13.01 MPa and 26.60 MPa) were calculated. Direct comparison of σ_{Hmin} values is difficult, as LOTs were conducted at different depths.

Bailey et al. (2012) calculated the σ_{Hmin} for eight wells, however, as no LOTs were undertaken in any of the wells, the σ_{Hmin} which Bailey et al. (2012) calculated (a range between 15.5 and 18 MPa/km) should be considered as a lower bound. King et al. (2008) calculated a σ_{Hmin} value for a depth which corresponds to this study. Although direct comparison is not available at depth (>1000 m), σ_{Hmin} values calculated from a LOT at 800 m in Eremia 2 (13.01 MPa) shows a parallel relationship when compared to King et al. (2008), whom calculated a σ_{Hmin} of 13.1 MPa also at 800 m in Dongara 28. The second σ_{Hmin} value King et al. (2008) calculated is significantly different (21.0 MPa at 822 m in Hovea 2) and should be considered erroneous. From the σ_{Hmax} quantified; 23.97 MPa at 800 m in Eremia 2 and 51.30 MPa at 1525 m in Dongara 28, comparison between previous authors proved difficult due to differing depths. From surplus data obtained from King et al. (2008), Bailey et al. (2012) calculated a σ_{Hmax} of 33 MPa at 1.2 km depth. While comparison between σ_{Hmax} values is difficult due to a range of depths, when comparing the two closest readings, a significant variation is observed. This variation is in the order of 18.3 MPa when comparing the σ_{Hmax} calculated in Dongara 28 (51.30 MPa at 1525 m) and Bailey et al. (2012) of 25.4 MPa at 1.2 km. This may be because of erroneous calculations, or due to both studies only having access to D or E quality data. The comparison in specific σ_{Hmax} values between this study and King et al. (2008) has not been undertaken, due to values not correlating with regards to depth. However, when extrapolated, σ_{Hmax} values follow an approximate regional trend of 25 MPa/km. In order to accurately compare studies, magnitude data must be calculated from alike quality ranked data, from similar depths, making accurate comparison of studies challenging. As no wells were over pressured (pore pressure > hydrostatic pressure (9.81 MPa/km)) no σ_{Hmax} values from calculations were disregarded (Brudy and Zoback, 1999).

5.3 Present-Day stress orientation in the Perth Basin

From observed stress indicators (BOs and DITFs), a mean σ_{Hmax} orientation of 089.9°N was determined (Table 1). This orientation of σ_{Hmax} correlates well with past studies (Bailey et al., 2012; Hillis and Reynolds, 2000; King et al., 2008), confirming the presence of a basin wide E-W oriented σ_{Hmax}. Bailey et al. (2012) conducted the most recent research, regarding the establishment of present-day stress magnitudes. They concluded a regional σ_{Hmax} orientation of 076°N exists. This 14° variation observed when comparing this study to that of Bailey et al. (2012), could be attributed to a larger sample size. While both studies were conducted in similar study areas, Bailey et al. (2012) interpreted 13 wells containing 365 BOs and 81 DITFs compared to this study containing five wells and 45 DITFs. Although the 14º variation may be attributed to their larger sample size, the D quality data of their study shows much less variation than the A-C quality data. From the analysis of the D quality data from Bailey at al. (2012), a regional σ_{Hmax} orientation of 084°N exists. This correlates well with results from King et al. (2008) and this study. Compared to King et al. (2008), a closer comparison is evident, from the regional σ_{Hmax} of 084ºN, King et al. (2008) deduced, a 6º variation is observed when all quality wells are included.

Through wide spread industry implementation of image logs instead of calliper logs, a significant increase in accuracy and precision can be observed when analysing and interpreting stress indicators and fractures, illustrated in the comparison of King et al. (2008) to Reynolds and Hillis (2000). There is a variation of 24º implicant of a new methodology (Heidbach et al., 2008). This in-part is due to the larger area of wellbore cover by image logs when compared to calliper logs (calliper logs have two pads

compared to image logs that have four pads in contact with the surrounding lithology). From the eight wells studied, five contain DITFs of D quality data, therefore, the measured σ_{Hmax} orientation accuracy is low (± 40°) (Zoback, 1992). While some conjecture surrounds the inclusion of D quality data into sets, King et al. (2008) and Tingay et al. (2005) have shown that this quality of data is reliable, due to providing estimates in which the regional σ_{Hmax} orientation can be contained. As the regional σ_{Hmax} orientation varies between wells, this approach to the inclusion of D quality data is supported by this study.

5.4 Natural fractures in the Perth Basin

5.4.1 RESISTIVE FRACTURES

Electrically resistive fractures were commonly identified in eight wells, containing image logs (73% resistive as opposed to 27% conductive). A total of 1283 fractures were identified, with one clear set dipping approximately NW-SE (Figure 8). From analysis, resistive fractures appear to be void of any lithological controlling factors upon fracture formation as observed through analysis of gamma ray logs (Appendix C). A wide variety of dip directions and dip angles were also observed. Resistive fractures appear to form with increasing depth, due to the likely effect of diagenesis and cementation at greater burial depths (Fruth et al., 1966; Dvorkin et al., 1994; Sibson, 1983). This is not considered a significant trend, as large quantities of resistive fractures at shallow depths can be observed in Drakea 1 and Hovea 9, inferring that other factors may control the open or closed nature of fractures in the Perth Basin (Appendix C). These factors include *in-situ* stresses and effects of pore pressure on fracture formation and reactivation. Large quantities of resistive fractures at shallow depths indicates high levels of shallow

permeability due to the closed and cementated nature of fractures, suggesting multiple hydraulically active pathways. Drakea 1, Bartsia 1, Evandra 1, Hovea 9 and Jingemia 2 & 3 all contained the primary set of resistive fractures observed dipping NW-SE (Appendix C.1, C.2, C.4, C.5, C.7 and C.8). The strike of these fractures is within 26° of large scale N-S striking faults, such as the Darling Fault to the east of the Perth Basin (Figure 1). The primary set incorporates the majority of the fracture data sets (conductive & resistive) associated with the Late Jurassic-Early Cretaceous continental break-up of Gondwana (Harris, 1994); indicating this fracture set is the youngest of the three sets (Harris, 1994, King et al., 2008).

N-S striking structures such the Mountain Bridge Fault, Darling Fault and Beharra Springs Fault (Figure 1) were active in the Early Permian through to Middle Triassic and again in the Jurassic (Marshall et al., 1989). Alternatively, it has been proposed that the Darling Fault has been active since the Neoproterozoic (Harris, 1993). Approximate NW-SE extension associated with one of the aforementioned stress regimes is considered the main cause of the dip direction observed in the resistive fracture set. This primary set of fractures from this study closely parallels data from past publications (Bailey et al., 2012; King et al., 2008), with a rotation in strike of 2° to the north when compared to electrically resistive fracture sets presented by Bailey et al (2012).

Minor secondary sets of resistive fractures striking NE-SW were observed in Eremia 2 and Hovea 12 (Appendix C.3, C.6). The minor sets are explained through their proximity to N-S striking faults and association with early basinal history. This fracture set is believed to be a result of N-S extension that commenced early in the Permian (Iasky et al., 1993; Mory & Iasky, 1996). These fractures strike perpendicular to the younger N-S

striking faults; which can be observed in the Allanooka transfer fault. Fault displacement along the Allanooka Fault varies, ranging from 100 m through to 2000 m (Song & Cawood, 1999). An increase in displacement when abutting or offsetting normal faults such as the Mountain Bridge Fault (Song, Cawood & Middleton, 2001). E-W transfer faults were active in the early Permian and Carboniferous, although no new large-scale E-W striking faults were created; only reactivation occurred (Song, Cawood & Middleton, 2001). It is possible that this fracture set was formed due to this N-S extension or simply rotated by a separate deformation event.

Eremia 2 presents the solitary tertiary set of resistive fractures from this study, striking approximately E-W. As there were such few fractures (<10), this data is not considered representative of a basin wide, tertiary set of resistive fractures (Appendix C.3).

5.4.2 CONDUCTIVE FRACTURES

169 conductive fractures encompass the primary set, with fracture distribution defined through a relationship with depth and specific lithologies. A noticeable increase of fractures at depths greater than 2400 m was apparent and minor clustering of fractures were observed in the Woodada Formation, Kockatea Shale, Dongara Sandstone and Limestone Marker (Appendix C). Clear mud losses were highlighted in the Limestone Marker with significant gas shows in the Kockatea Shale and Dongara Sandstone, the formations most targeted by the petroleum industry (Appendix C.2, C.3, C.4, C.6 and C.8). Evidence from industry reports highlight significant mud losses and gas shows when drilling through five (Drakea 1, Eremia 2, Hovea 12, Jingemia 2 and Jingemia 3) of the eight wells located in the Dongara Sandstone and Kockatea Shale.

As a result of the significant variation in dip direction of fractures observed (±20° from 175°-355°), numerous sets of conductive fractures potentially occurred throughout the Perth Basin's history. Large damage zones created through the formation of larger N-S striking faults (Darling Fault & Mountain Bridge Fault) may have also resulted in subsequent fracture formation, as implied by conductive fractures (Bailey et al., 2012; Harris, 1994).

The secondary set of 155 conductive fractures can be seen striking broadly E-W in seven of the eight wells (Appendix C.1, C.2, C.3, C.4, C.6, C.7 and C.8). When observed from the remainder of the data set, 155 fractures make up this set; their importance lies within their distribution in the majority of the wells. This set closely follows the orientation of σ_{Hmax} (089.9°). Due to the E-W dip direction of this fracture set, it is difficult to determine whether these fractures were a) a relic of Permian-Triassic rifting having remained open to fluid flow from formation to present-day or, b) due to the orientation of present-day σ_{Hmax} (089.9°N) where these fractures have been reactivated as a result of present-day *in-situ* stresses.

Works conducted by Bailey et al. (2012) and Olierook et al. (2014), indicate the iron bearing mineral precipitate siderite is a common infill in a large quantity of wells. The differentiasation of fractures filled with siderite and open natural fractures can only be conclusively undertaken with core samples that are limited in size and quantity. Siderite as fracture infill can cause difficulties when interpreting electrically conductive fractures from image logs, as it can cause what appear to be electrically conductive fractures on image logs (Olierook et al., 2014).

5.5 Structural permeability in the Perth Basin

Structural permeability is defined as the ability for a fluid to pass through fractures within strata (Sibson, 1996). From interpretation of fracture reactivation plots, with associated stress regimes including fractures contained within, the affect of a transpressional stress regime will significantly change what percentage of fractures are critically stressed.

Figure 9 and Figure 14, exemplifies large quantities of conductive and resistive fractures are optimally aligned for reactivation, implying if an increase in permeability were required by industry application, then a minimal pore pressure increase would be needed. 56 fractures out of a total 1763 (or <3%) would require a Pp change of >10 MPa to become critically stressed. From image log analysis, numerous conductive and resistive fractures were observed, suggesting that fractures of both characteristics were common throughout the area. As resistive fractures were the most frequent feature identified, these structures could impede the permeability of the basin. If cementation observed is concurrent with Bailey et als' (2012) descriptions regarding siderite cementation, this could lead to the misclassification of conductive fractures thus, further lowering the permeability of the Perth Basin.

Drilling mud losses were noted in the Dongara Sandstone and Kockatea Shale (ArcEnergy) (Appendix C.2, C.6, C.7 and C.8). Depths of the two permeable formations (Dongara Sandstone and Kockatea Shale) varied between the four wells, supporting the prediction made that these formations were active, hydraulic, open paths for fluid flow. The difference of the formation lies in the ability for the fracture to pass a fluid through the structure rather than drilling mud merely imprinting the fracture (Barton et al., 1995; Laubach, 2003). Studies conducted by Kempton et al (2011), potential late-Jurassic flow has been identified through highly permeable formations such as the Irwin River Coal

Measures and Dongara Sandstone. Kempton et al (2011), illustrates these palaeo migration pathways are only representative for the palaeo stress regimes and may not be active today. Analysis of daily drilling reports have determined permeable pathways do exist within the Dongara Sandstone even with the present-day stress regime. This is evident from drilling mud losses reported in Jingemia 2, Jingmeia 3 and Hovea 12, when drilling through the Dongara Sandstone. Further losses of drilling muds were also observed in Drakea 1 when drilling through the Irwin River Coal Measures (Appendix C.2, C.6, C.7 and C.8).

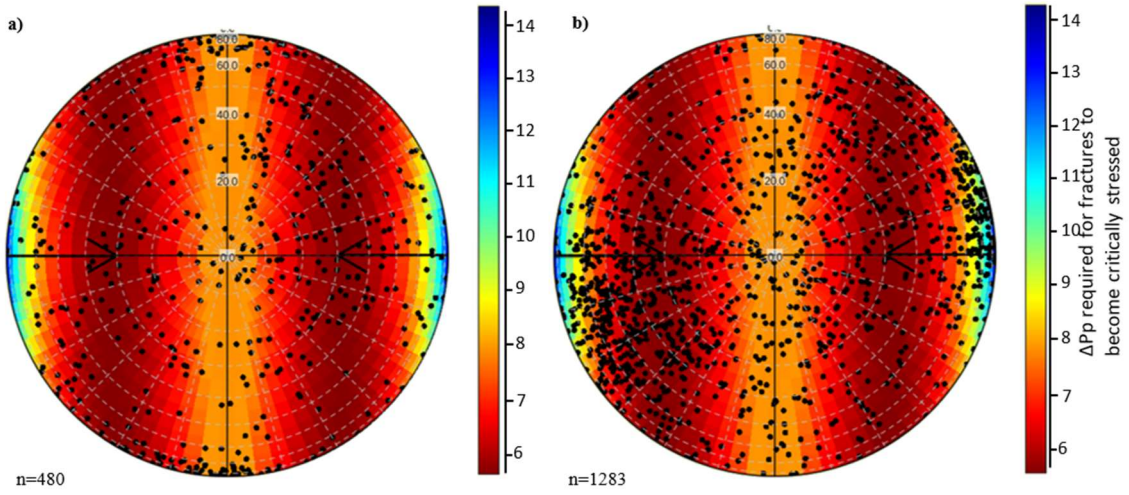

Figure 14: Fracture reactivation plots created for a transitional strike-slip to reverse fault stress regime as defined in the Perth Basin at 500 m depth, with coefficient of friction of 0.6 as per Byerlee (1978). a) illustrates the total number of conductive fractures interpreted, while b) highlights the total number of resistive fractures interpreted.

6.0 CONCLUSIONS

- Results gathered from calcite twin data could imply polyphase deformation as summarised below:
    - NPS1 tensor 2, is most consistent with a NNW-SSE compressional event and potentially attributed to Late-Early to Middle-Triassic N-S compression, through a reverse sense movement in basement structures (Hall, 1989).
    - NPS2 tensor 2 contains characteristics of an E-W extensional regime. This palaeo stress regime may represent Late Triassic extension, due to paralic sedimentary inputs along with the formation of the Cattamarra Coal Measures (Harris, 1994).
    - After rotations performed in NPS1 tensor 1, a NW-SE extensional regime is observed in-line with the breakup of Gondwana.
    - The reduced stress tensor established in NPS2 tensor 1, signifies N-S compression, autochthonous from complex interactions at plate boundaries.
- The stress regime in the Perth Basin is transpressional.
- The mean regional σ_{Hmax} orientation in the study area is 089.9°N, with a s.d. of 5.63. This orientation was determined from 186 borehole breakouts and 45 DITFs from six image logs.
- The σ_V ranges from 0.7 MPa to 22.69 MPa at 1km depth and from 0.8 MPa to 58.08 MPa in Bartsia 1 at 2.5km.
- The σ_{Hmin} ranges from 13.01 MPa at 800m in Eremia 2 to 26.60 MPa at 1525m in Dongara 28.

- The σ_{Hmax} varies from 23.97 MPa at 800m in Eremia 2 to 51.30 MPa at 1525m in Dongara 28.
- Natural fractures identified from wellbore image logs displayed a large disparity between percentage of electrically conductive (and potentially hydraulically active) and electrically resistive fractures (27% conductive compared to 73% resistive), defined by two clear sets, reflecting palaeo-basinal stresses and present-day *in-situ* stresses.
    - The primary set is composed of NW-SE dipping resistive fractures.
    - The secondary set of resistive fractures is significantly smaller, however, is dipping NE-SW.
    - The primary set of conductive fractures is observed dipping E-W in four of the eight wells, with the secondary set oberserved dipping NNE-SSW in seven of the eight wells although fewer in number.
- Resistive fractures observed are also optimally aligned to reactivation in both shallow reverse fault stress regimes (<500 m) and deep strike slip fault regimes (>550 m), however could be stress insensitive due to cementation properties (Bailey et al., 2012).
- From the tranpressional stress regime observed, <3% of total fractures require a Pp change of greater than 10 MPa to become critically stressed and thus likely to contribute to subsurface permeability.

Recommendations for future studies

From analysis and interpretation of these methodologies plus comparison of results to previous publications, the Perth Basin is believed to have undergone multiple stages of

extension and compression, leading to an extensive fracture network that provides secondary permeability in the subsurface. This interpretation should not be taken as representative of the entire basin due to small study area and errors inherent with certain CSIT methods. Therefore, further works centred around calcite stress inversion technique are encouraged to ascertain a wider degree of palaeo stresses. Improvements in U-stage measurements through implementation of new methods including electron backscatter diffraction (EBSD) (Parlangeau et al., 2015) will remove any human error associated with conventional U-stage measurements resulting in higher accuracy. Due to large volumes of work conducted in the area, a review paper regarding the collation of all previous works is encouraged particularly if tied in with new palaeo stress tensors to solidify both palaeo and well known *in-situ* stresses.

ACKNOWLEDGMENTS

A huge thank you to my supervisors, Dr. Rosalind King, Dr. Rowan Hansberry and Dr. Khalid Amrouch, for your constant support and time throughout the course of this year. Secondly thank you to Dr. Juraj Farkus for organising the honours program this year and Dr. Alan Collins and Dr. John Foden for support and guidance in New Zealand. Finally thank to you all my fellow honours students for making this year such an enjoyable year.

REFERENCES

AMROUCH, K., BEAUDOIN, N., LACOMBE, O., BELLAHSEN, N., & DANIEL, J. M. (2011). Paleostress magnitudes in folded sedimentary rocks. *Geophysical Research Letters*, *38*(17).

AMROUCH, K., LACOMBE, O., BELLAHSEN, N., DANIEL, J. M., & CALLOT, J. P. (2010a). Stress and strain patterns, kinematics and deformation mechanisms in a basement-cored anticline: Sheep Mountain Anticline, Wyoming. *Tectonics*, *29*(1).

AMROUCH, K., LACOMBE, O., BELLAHSEN, N., DANIEL, J. M., & CALLOT, J. P. (2010b). Stress and strain patterns, kinematics and deformation mechanisms in a basement-cored anticline: Sheep Mountain Anticline, Wyoming. *Tectonics*, *29*(1).

ANDERSON, E. M. (1951). *The Dynamics of Faulting and Dyke Formation with Applications to Brittan* (Vol. 2nd): Edinburgh: Oliver and Boyd

ANGELIER, J. (1984). Tectonic analysis of fault slip data sets. *Journal of Geophysical Research: Solid Earth*, *89*(B7), 5835-5848.

ANGELIER, J. (1990). Inversion of field data in fault tectonics to obtain the regional stress—III. A new rapid direct inversion method by analytical means. *Geophysical Journal International*, *103*(2), 363-376.

AUDLEY-CHARLES, M. G., BALLANTYNE, P. D., & HALL, R. (1988). Mesozoic-Cenozoic rift-drift sequence of Asian fragments from Gondwanaland. *Tectonophysics*, *155*(1-4), 317-330.

BAILEY, A., KING, R., & BACKÉ, G. (2012). Integration of structural, stress, and seismic data to define secondary permeability networks through deep-cemented sediments in the Northern Perth Basin. *The APPEA Journal*, *52*(1), 455-474.

BALME, B. E. (1980). Palynology and the Carboniferous-Permian boundary in Australia and other Gondwana continents. *Palynology*, *4*(1), 43-55.

BARTON, C. A., ZOBACK, M. D., & MOOS, D. (1995). Fluid flow along potentially active faults in crystalline rock. *Geology*, *23*(8), 683-686.

BEESON, J. (1992b). A field and experimental study of structures in the Albany Mobile Belt. Western Australia. *Ph. D Thesis, University of Western Australia, (Unpublished manuscript).* 154 pp.

BELL, J. (1996a). Petro Geoscience 1. In-situ stresses in sedimentary rocks (part 1): measurement techniques. *Geoscience Canada*, *23*(2).

BELL, J. (1996b). Petro geoscience 2. In-situ stresses in sedimentary rocks (part 2): applications of stress measurements. *Geoscience Canada,* 23(3).

BRUDY, M., & ZOBACK M.D. (1999). Drilling-induced tensile wall-fractures: implications for determination of in-situ stress orientation and magnitude. *International Journal of Rock Mechanics and Mining Sciences, 36*, 24.

BURKHARD, M. (1993). Calcite twins, their geometry, appearance and significance as stress-strain markers and indicators of tectonic regime: a review. *Journal of structural geology*, *15*(3-5), 351-368.

BYERLEE, J. (1978). Friction of rocks. *Pure and applied Geophysics*, *116*(4), 615-626.

CAWOOD, P. A., & NEMCHIN, A. A. (2000). Provenance record of a rift basin: U/Pb ages of detrital zircons from the Perth Basin, Western Australia. *Sedimentary Geology*, *134*(3), 209-234.

CLARK, D. (2005). A preliminary seismicity model for southwest Western Australia based on neotectonic data. *AEES Proceedings, paper*, (22).

CROSTELLA, A., & BACKHOUSE, J. (2000). *Geology and petroleum potential of the Abrolhos Sub-basin, Western Australia* (No. 75). Geological Survey of Western Australia.

DALY, M. C., CHOROWICZ, J., & FAIRHEAD, J. D. (1989). Rift basin evolution in Africa: the influence of reactivated steep basement shear zones. *Geological Society, London, Special Publications*, *44*(1), 309-334.

DALY, M. C., LAWRENCE, S. R., DIEMU-TSHIBAND, K., & MATOUANA, B. (1992). Tectonic evolution of the Cuvette Centrale, Zaire. *Journal of the Geological Society*, *149*(4), 539-546.

DALY, M. C., LAWRENCE, S. R., KIMUN'A, D., & BINGA, M. (1991). Late Palaeozoic deformation in central Africa: a result of distant collision? *Nature*, *350*(6319), 605-607.

DVORKIN, J., NUR, A., & YIN, H. (1994). Effective properties of cemented granular materials. *Mechanics of materials*, 18(4), 351-366.

ETCHECOPAR, A. (1984*), Etude des e tats de contraintes en tectonique cassante et simulation de de formation plastique (approche mathe matique), the se doctorates-sciences*, 270 pp., Univ. Sci. et Tech. du Langue-doc, Montpellier, France.

FALVEY, D. A., & MUTTER, J. C. (1981). Regional plate tectonics and the evolution of Australia's passive continental margins. *BMR J. Aust. Geol. Geophys*, *6*, 1-29.

FERRILL, D. A. (1998). Critical re-evaluation of differential stress estimates from calcite twins in coarse-grained limestone. *Tectonophysics*, *285*(1), 77-86.

FRUTH JR, L. S., ORME, G. R., & DONATH, F. A. (1966). Experimental compaction effects in carbonate sediments. *Journal of Sedimentary Research*, 36(3). 747‑754.

HALL, P. B. (1989) High Hopes for Australia's north Perth Basin.*The Oil and Gas Journal*. *87*(43).

HALL, P. B., & KNEALE, R. L. (1992). Perth Basin rejuvenated. *The APPEA Journal*, *32*(1), 33-43.

HARRIS, L. B. (1993). Correlations between the Central Indian Tectonic Zone and the Albany Mobile Belt of Western Australia: evidence for a continuous Proterozoic orogenic belt. *Gondwana*, *8*, 165-180.

HARRIS, L. B. (1994). Structural and tectonic synthesis for the Perth Basin, Western Australia. *Journal of Petroleum Geology*, *17*(2), 129-156.

HARRIS, L. B., & LI, Z. X. (1991). Tectonic controls on Cambrian dolerite dyke emplacement in the Albany Mobile Belt, Western Australia. In *Abstracts, (Unpublished manuscript) Gondwana* (Vol. 8, pp. 41-42).

HARRIS, L.B. (1987). *A tectonic framework for the Western Australian Shield and its significance to gold mineralisation: a personal view*. In: Ho, S. E. and Groves. D.I. (Eds.). Recent advances in understanding Precambrian gold deposits. *Geol. Dept. Univ. Extension, Univ. West. Australia Publ*., 11, 1-27.

HEALY, D., JONES, R. R., & HOLDSWORTH, R. E. (2006). Three-dimensional brittle shear fracturing by tensile crack interaction. *Nature*, *439*(7072), 64.

HEFFER, K., & LEAN, J. (1993). Earth stress orientation-a control on, and guide to, flooding directionality in a majority of reservoirs. *Reservoir characterization III: Tulsa, Oklahoma, PennWell Books*, 799-822.

HEFFER, K. J., FOX, R. J., MCGILL, C. A., & KOUTSABELOULIS, N. C. (1997). Novel techniques show links between reservoir flow directionality, earth stress, fault structure and geomechanical changes in mature waterfloods. *SPE Journal*, 2(02), 91-98.

HEIDBACH, O., TINGAY, M., BARTH, A., REINECKER, J., KURFEß, D., & MÜLLER, B. (2008). Global crustal stress pattern based on the World Stress Map database release 2008. *Tectonophysics*, *482*(1), 3-15.

HILLIS, R. R., & REYNOLDS, S. D. (2000). The Australian stress map. *Journal of the Geological Society*, *157*(5), 915-921.

IASKY, R. P., & MORY, A. J. (1993). Structural and tectonic framework of the onshore northern Perth Basin. *Exploration Geophysics*, *24*(4), 585-592.

KEMPTON, R., GONG, S., KENNARD, J., VOLK, H., MILLS, D., EADINGTON, P., & LIU, K. (2011). Detection of palaeo-oil columns in the offshore Northern Perth Basin: extension of the effective Permo-Triassic charge system. *The APPEA Journal*, *51*(1), 377-396.

KIRSCH, E. G. (1898). Die Theorie der Elastizit t und die Bed rfnisse der Festigkeitslehre. *Zeitshrift des Vereines deutscher Ingenieure, 42*, 797-807.

KING, R. C., HILLIS, R. R., & REYNOLDS, S. D. (2008). In-situ stresses and natural fractures in the Northern Perth Basin, Australia. *Australian Journal of Earth Sciences*, *55*(5), 685-701.

KING, R. C., TINGAY, M. R., HILLIS, R. R., MORLEY, C. K., & CLARK, J. (2010). Present-day stress orientations and tectonic provinces of the NW Borneo collisional margin. *Journal of Geophysical Research: Solid Earth*, *115*(B10).

KULIKOWSKI, D., & AMROUCH, K. (2017). Combining geophysical data and calcite twin stress inversion to refine the tectonic history of subsurface and offshore provinces: A case study on the Cooper-Eromanga Basin, Australia. *Tectonics*, *36*(3), 515-541.

LACOMBE, O. (2001). Paleostress magnitudes associated with development of mountain belts: Insights from tectonic analyses of calcite twins in the Taiwan Foothills. *Tectonics*, *20*(6), 834-849.

LACOMBE, O. (2010), Calcite twins, a tool for tectonic studies in thrust belts and stable orogenic forelands, *Oil Gas Sci. Technol.–Revue d'IFP Energies Nouvelles*, 65(6), 809–838.

LACOMBE, O. (2012). Do fault slip data inversions actually yield "paleostresses" that can be compared with contemporary stresses? A critical discussion. *Comptes Rendus Geoscience*, *344*(3), 159-173.

LACOMBE, O., & LAURENT, P. (1996). Determination of deviatoric stress tensors based on inversion of calcite twin data from experimentally deformed monophase samples: preliminary results. *Tectonophysics*, *255*(3-4), 189-202.

LACOMBE, O., AMROUCH, K., MOUTHEREAU, F., & DISSEZ, L. (2007). Calcite twinning constraints on late Neogene stress patterns and deformation mechanisms in the active Zagros collision belt. *Geology*, *35*(3), 263-266.

LACOMBE, O., ANGELIER, J., & LAURENT, P. (1992). Determining paleostress orientations from faults and calcite twins: a case study near the Sainte-Victoire Range (southern France). *Tectonophysics*, *201*(1-2), 141-156.

LACOMBE, O., ANGELIER, J., LAURENT, P., BERGERAT, F., & TOURNERET, C. (1990). Joint analyses of calcite twins and fault slips as a key for deciphering polyphase tectonics: Burgundy as a case study. *Tectonophysics*, *182*(3-4), 279-300.

LAUBACH, S. E. (2004). Practical approaches to identifying sealed and open fractures. *AAPG bulletin*, *87*(4), 561-579.

LAURENT, P. (1984), *Les macles de la calcite en tectonique: Nouvelles me thodes dynamiques et premieres applications, these doctorat-es-sciences*, 324 pp., Univ. Sci. et Tech. du Languedoc, Montpellier, France.

LAURENT, P., KERN, H., & LACOMBE, O. (2000). Determination of deviatoric stress tensors based on inversion of calcite twin data from experimentally deformed monophase samples. Part II. Axial and triaxial stress experiments. *Tectonophysics*, *327*(1), 131-148.

MARSHALL, J. F., LEE, C. S., RAMSAY, D. C., & MOORE, A. M. (1989). Tectonic controls on sedimentation and maturation in the offshore north Perth Basin. *The APPEA Journal*, *29*(1), 450-465.

MEANS, W. D. (1976). Stress and strain: basic concepts of continuum mechanics for geologists. New York: Springer-Verlag.

MORY, A. J., & IASKY, R. P. (1996). *Stratigraphy and structure of the onshore northern Perth Basin, Western Australia* (Vol. 46). Geological Survey of Western Australia.

MÜLLER, R. D., MIHUT, D., & BALDWIN, S. (1998). A new kinematic model for the formation and evolution of the west and northwest Australian margin. *The sedimentary basins of Western Australia*, 2, 55-72.

OLIEROOK, H. K., TIMMS, N. E., & HAMILTON, P. J. (2014). Mechanisms for permeability modification in the damage zone of a normal fault, northern Perth Basin, Western Australia. *Marine and Petroleum Geology*, *50*, 130-147.

PARLANGEAU, C., LACOMBE, O., BRISSET, F., KOHLER, E., DANIEL, J. M., & SCHUELLER, S. (2015, April). Inversion of calcite twin data for stress (2): EBSD as a tool for data measurements. In EGU General Assembly Conference Abstracts (Vol. 17).

PLAYFORD, P. E., LOW, G. H., & COCKBAIN, A. E. (1976). *Geology of the Perth Basin, Western Australia*. Geological Survey of Western Australia.

PLUMB, R. A., & HICKMAN, S. H. (1985). Stress-induced borehole elongation: A comparison between the four-arm dipmeter and the borehole televiewer in the Auburn Geothermal Well. *Journal of Geophysical Research: Solid Earth*, *90*(B7), 5513-5521.

RASMUSSEN, B., & GLOVER, J. E. (1996). Fluid evolution interpreted from diagenetic assemblages and salinity data in Permo-Triassic sandstone, northern Perth Basin, Western Australia. *Journal of Sedimentary Research*, *66*(3).

REYNOLDS, S. D., & HILLIS, R. R. (2000). The in-situ stress field of the Perth Basin, Australia. *Geophysical Research Letters*, *27*(20), 3421-3424.

REYNOLDS, S. D., MILDREN, S. D., HILLIS, R. R., & MEYER, J. J. (2006). Constraining stress magnitudes using petroleum exploration data in the Cooper–Eromanga Basins, Australia. *Tectonophysics, 415*(1), 123-140.

RICHARDSON, R. M. (1992). Ridge forces, absolute plate motions, and the intraplate stress field. Journal of Geophysical Research: Solid Earth, 97(B8), 11739-11748.

SANDIFORD, M., WALLACE, M., & COBLENTZ, D. (2004). Origin of the in-situ stress field in south-eastern Australia. *Basin Research*, *16*(3), 325-338.

SIBSON, R. H. (1996). Structural permeability of fluid-driven fault-fracture meshes. *Journal of Structural Geology*, *18*(8), 1031-1042.

SIBSON, R. H. (1983). Continental fault structure and the shallow earthquake source. *Journal of the Geological Society*, 140(5), 741-767.

SONG, T., & CAWOOD, P. A. (1999). Multistage deformation of linked fault systems in extensional regions: an example from the northern Perth Basin, Western Australia. *Australian Journal of Earth Sciences*, *46*(6), 897-903.

SONG, T., & CAWOOD, P. A. (2000). Structural styles in the Perth Basin associated with the Mesozoic break-up of Greater India and Australia. *Tectonophysics*, *317*(1), 55-72.

SONG, T., CAWOOD, P. A., & MIDDLETON, M. (2001). Transfer zones normal and oblique to rift trend: examples from the Perth Basin, Western Australia. *Geological Society, London, Special Publications*, *187*(1), 475-488.

TINGAY, M. R., HILLIS, R. R., MORLEY, C. K., SWARBRICK, R. E., & DRAKE, S. J. (2005). Present-day stress orientation in Brunei: a snapshot of 'prograding tectonics' in a Tertiary delta. *Journal of the Geological Society*, *162*(1), 39-49.

TURNER, F. J., D. T. GRIGGS, AND H. HEARD (1954), Experimental deformation of calcite crystals, *Geol. Soc. Am. Bull.*, 65(9), 883‐934.

VEEVERS, J. J. (1991). Mid-Cretaceous tectonic climax, Late Cretaceous recovery, and Cainozoic relaxation in the Australian region. *The Cainozoic in Australia: A Re-appraisal of the Evidence: Geological Society of Australia, Special Publication*, *18*, 1-15.

VEEVERS, J. J., & CONAGHAN, P. J. (1984). *Phanerozoic earth history of Australia*. Oxford University Press, USA.

VEEVERS, J. J., POWELL, C. M., & JOHNSON, B. D. (1975). Greater India's place in Gondwanaland and in Asia. *Earth and Planetary Science Letters*, *27*(3), 383-387.

WHITE, A. J., TRAUGOTT, M. O., & SWARBRICK, R. E. (2002). The use of leak-off tests as means of predicting minimum in-situ stress. *Petroleum Geoscience*, *8*(2), 189-193.

WILDE, S. A., & MURPHY, D. M. K. (1990). The nature and origin of Late Proterozoic high-grade gneisses of the Leeuwin Block, Western Australia. *Precambrian Research*, *47*(3-4), 251-270.

ZOBACK, M. L. (1992). First-and second-order patterns of stress in the lithosphere: The World Stress Map Project. *Journal of Geophysical Research: Solid Earth*, *97*(B8), 11703-11728.

APPENDIX A: NPS1 & NPS2 WHOLE ROCK SAMPLE

NPS1 WHOLE ROCK

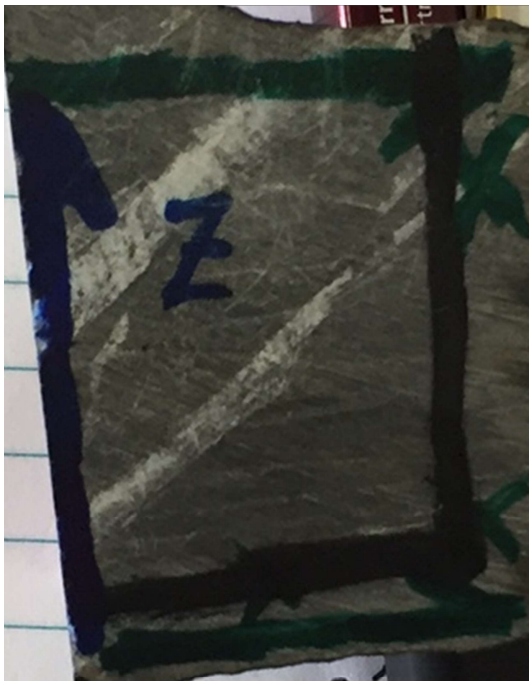

NPS1ZX

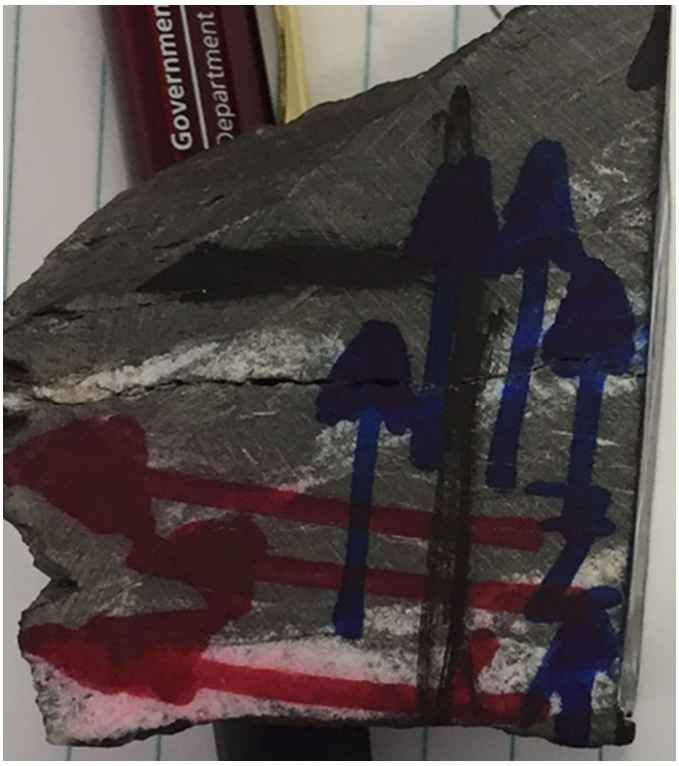

NPS1YZ

NPS1XY

NPS2 WHOLE ROCK

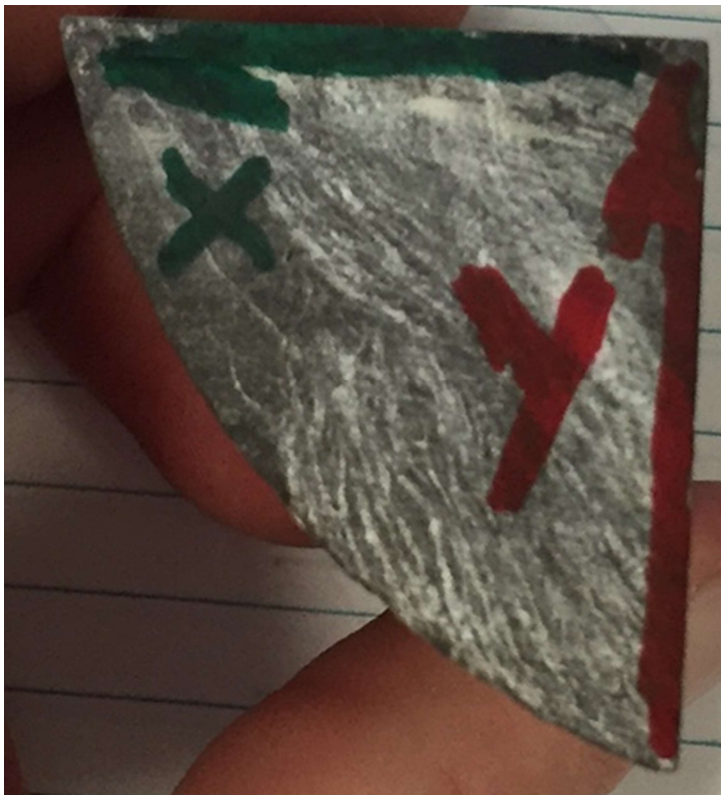

NPS2XY:

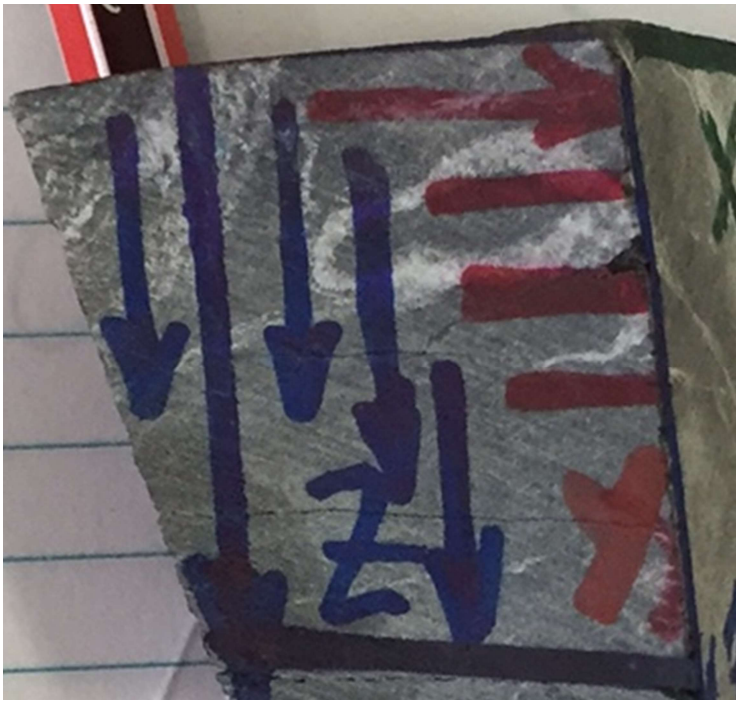

NPS2ZY:

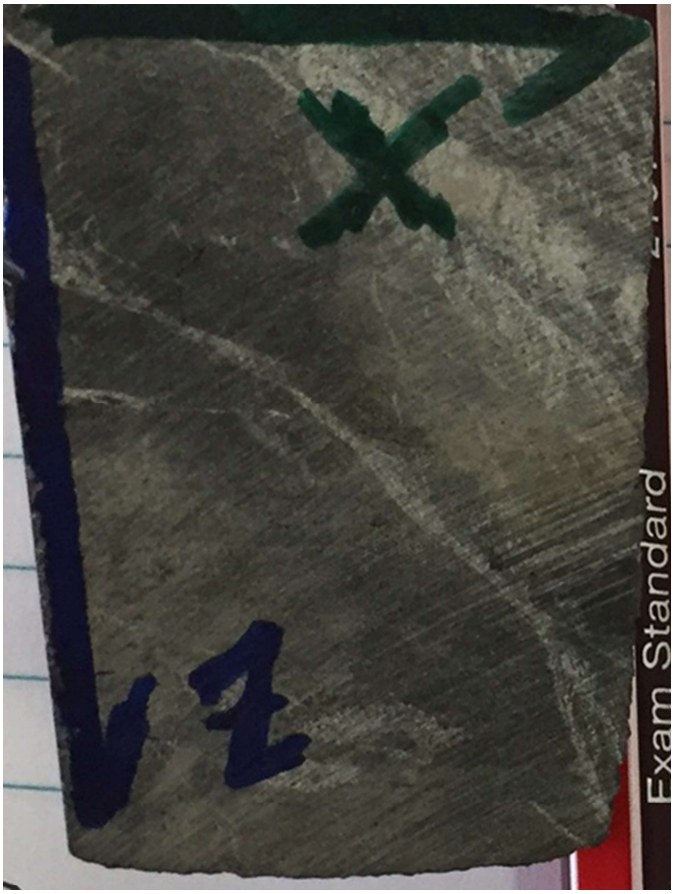

NPS2ZX:

APPENDIX B: THIN SECTIONS USED FOR CSIT ANALYSIS

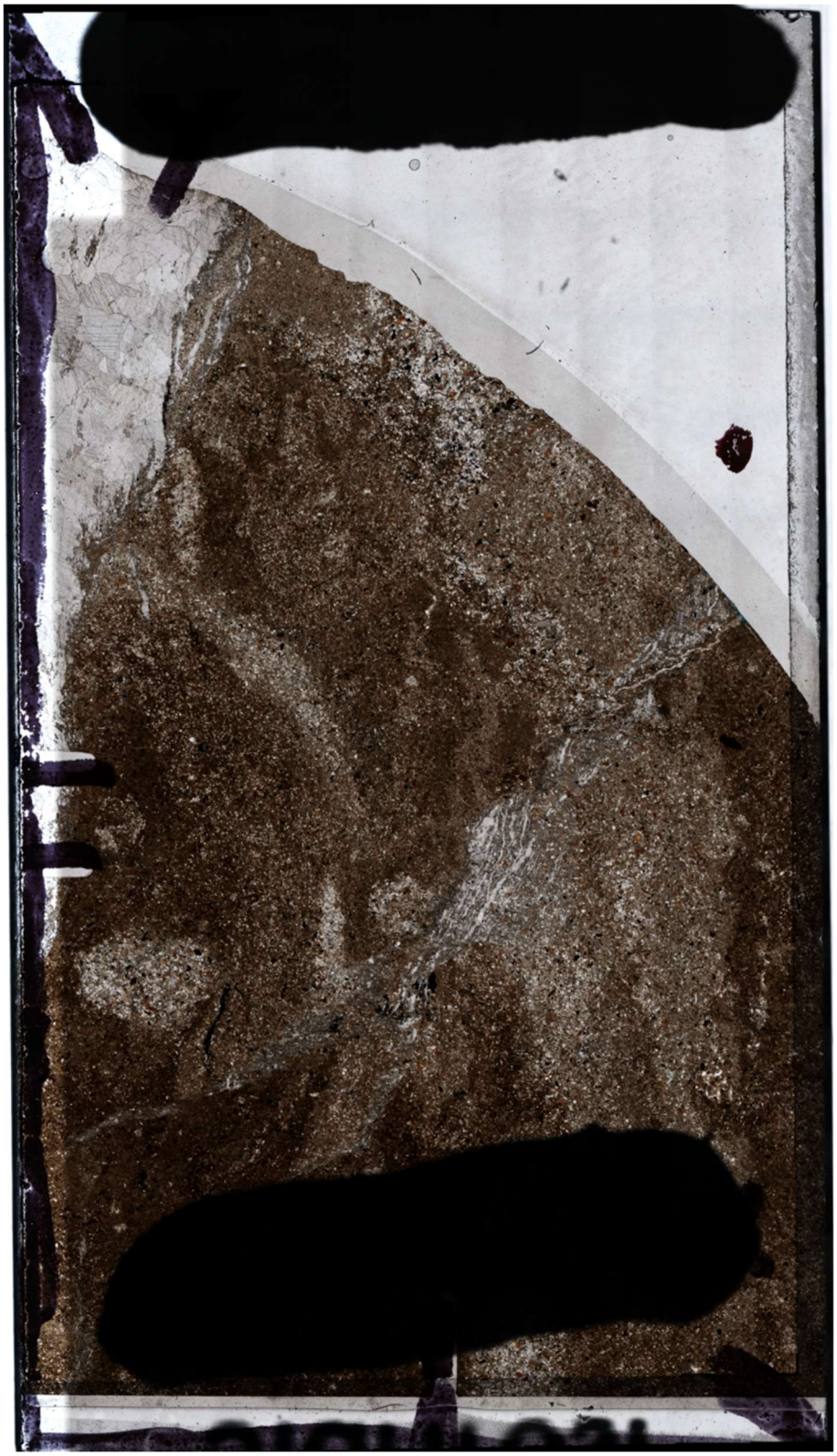

NPS1XY THIN SECTION

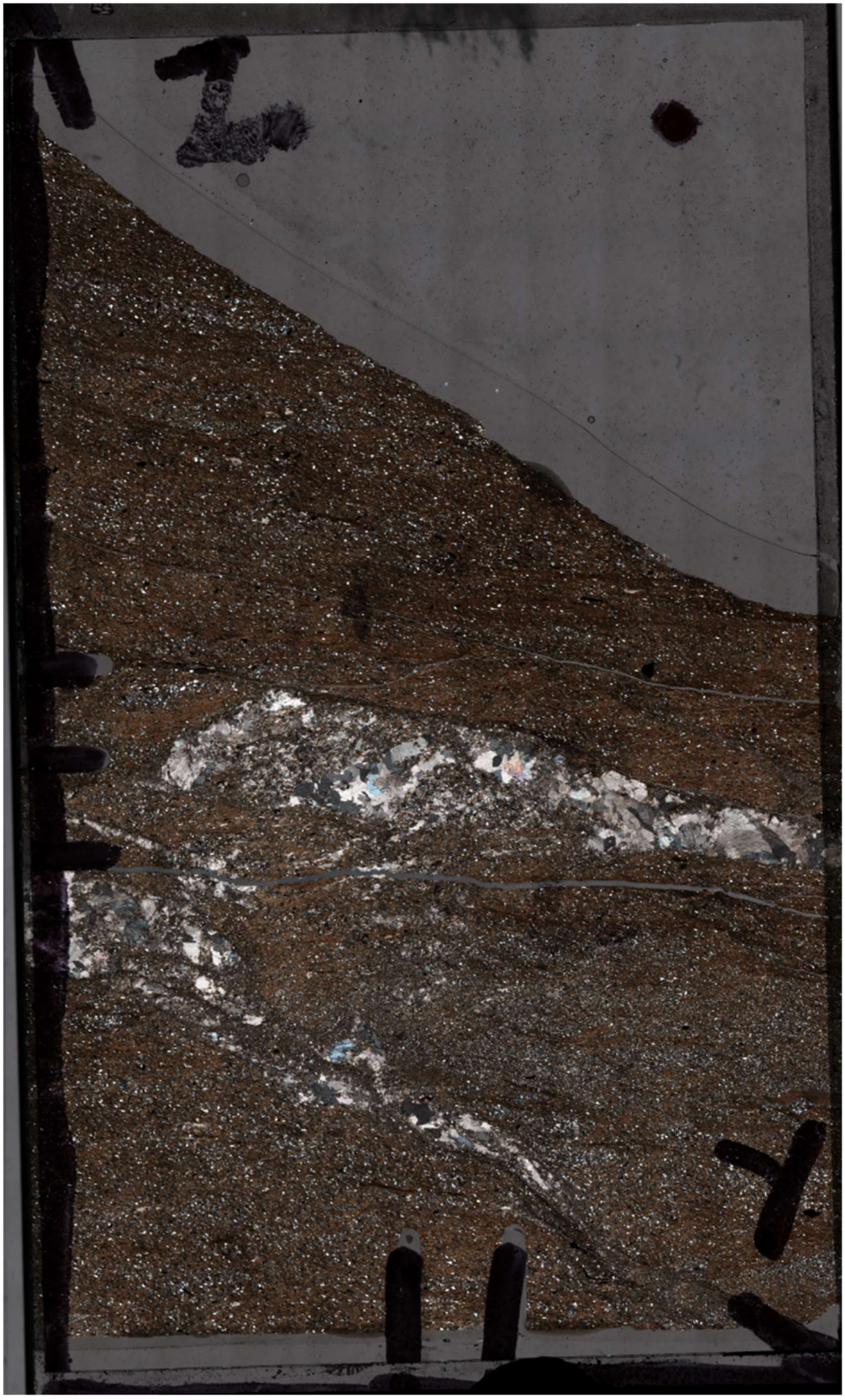

NPS1ZY THIN SECTION

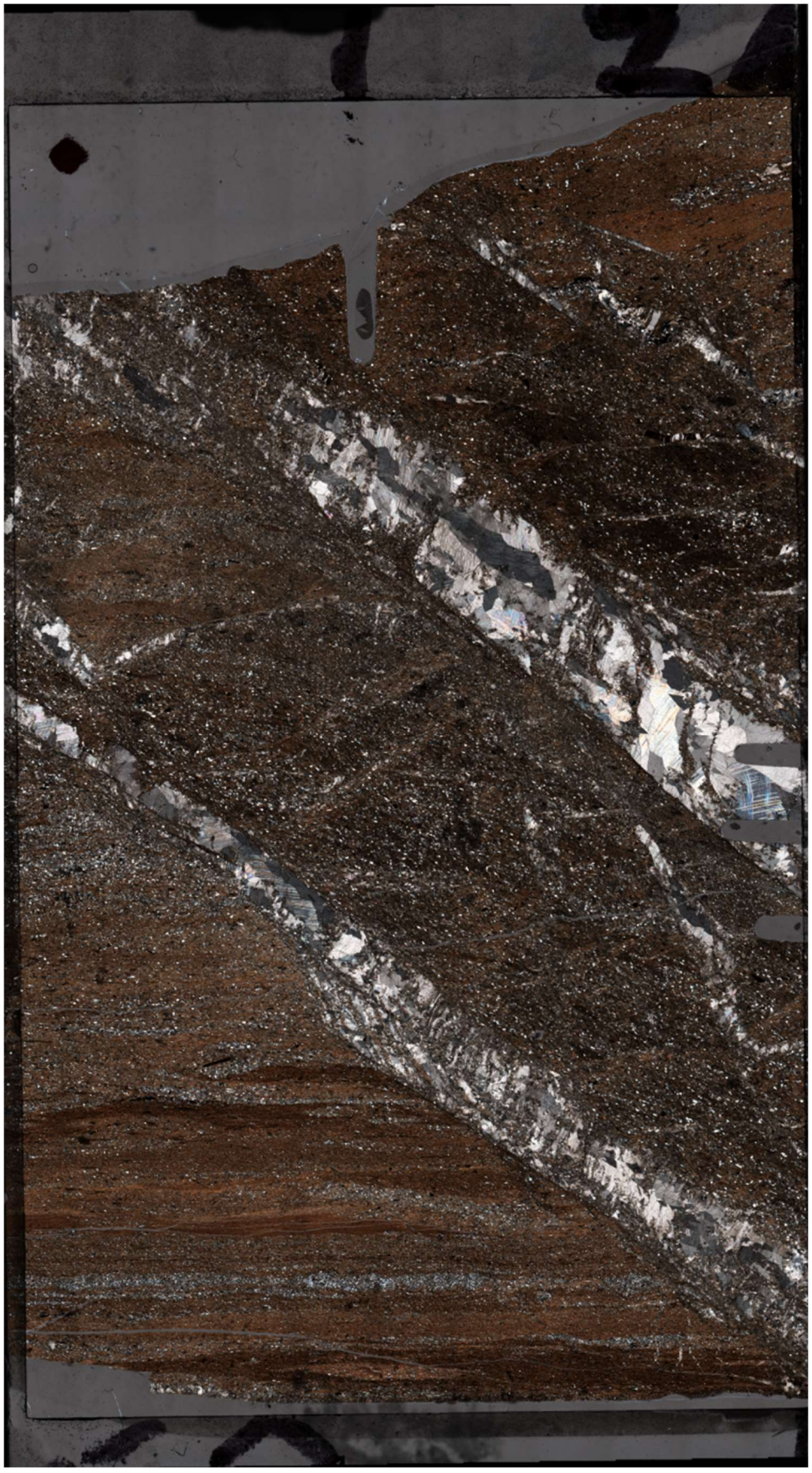

NPS1ZX THIN SECTION

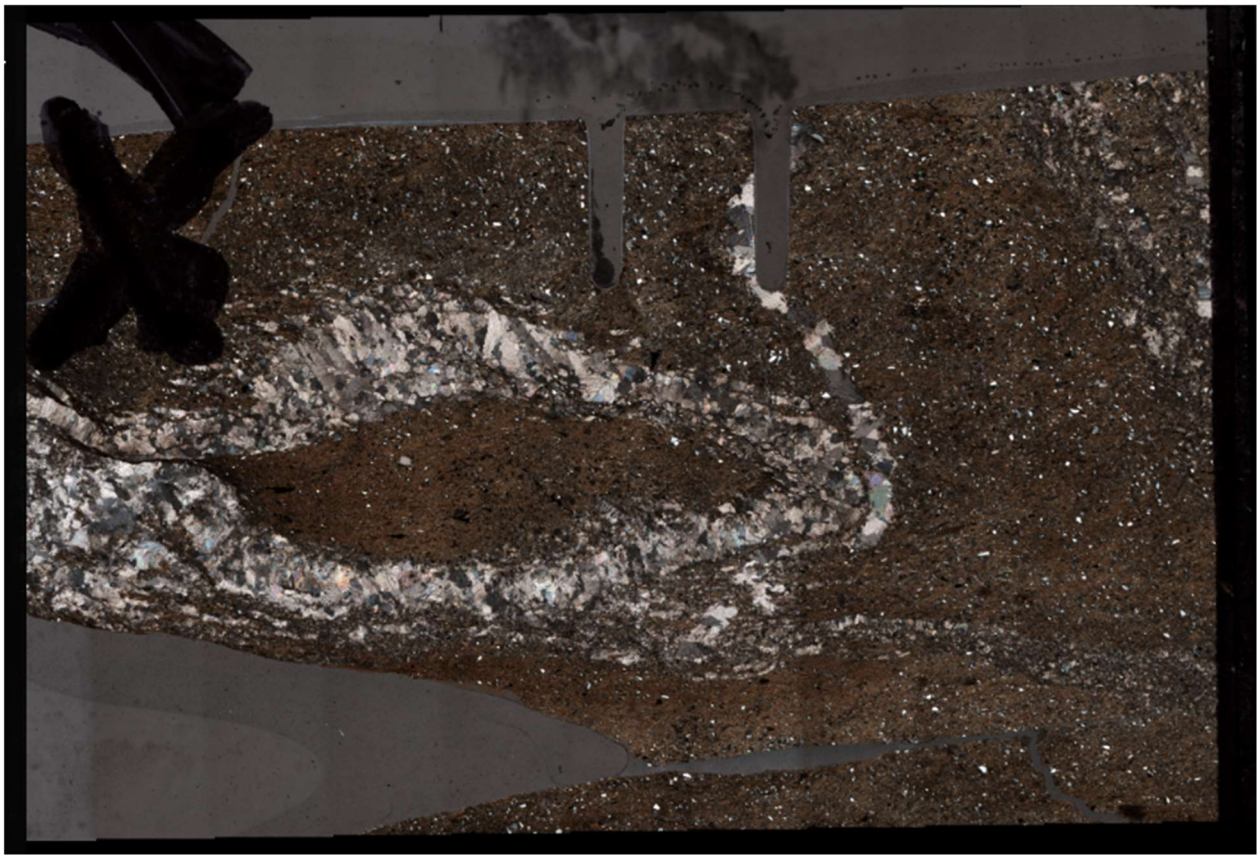

NPS2XZ THIN SECTION

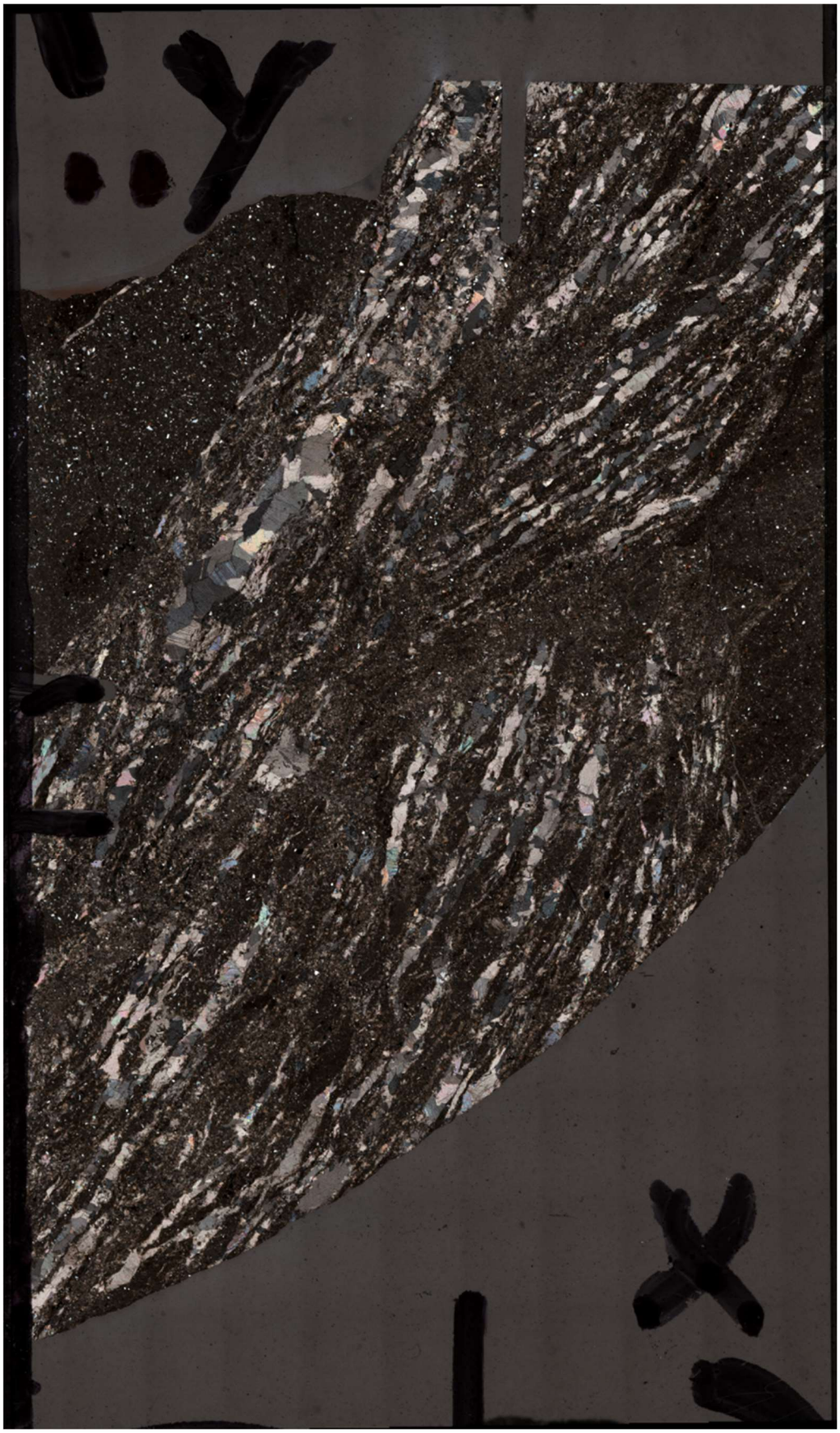

NPS2YX THIN SECTION

NPS2ZX THIN SECTION

APPENDIX C: WELL CARDS

Appendix C.1

Well Card 1: Bartsia 1

Latitude:	29.288°S
Longitude:	114.974°E
Total depth interval:	2510m
Image tool used:	FMI
Depth interval of image log (top/bottom):	1387/2487m
Max. deviation from vertical:	19.30°
Subcontracted drilling company:	Century Drilling Ltd
Parent company:	ARC Energy Limited Ltd

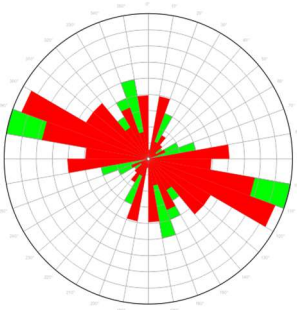

145 total fractures interpreted in Drakea 1. Conductive fractures in green with resistive fractures in red.

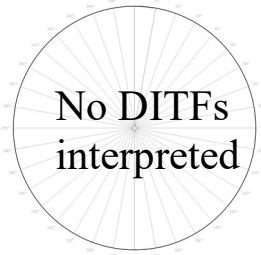

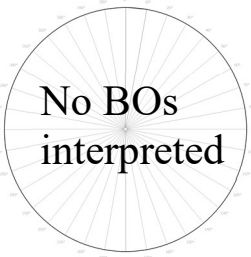

Example of the Bartsia 1 image log: showing the deviation of the well in pink, Gamma ray index in black, Pad 1 azimuth in green and interpretations in the far-right panel. Note the thin electrically resistive fractures 2351 m cross cutting the beds and tool malfunction on the first pad on the left.

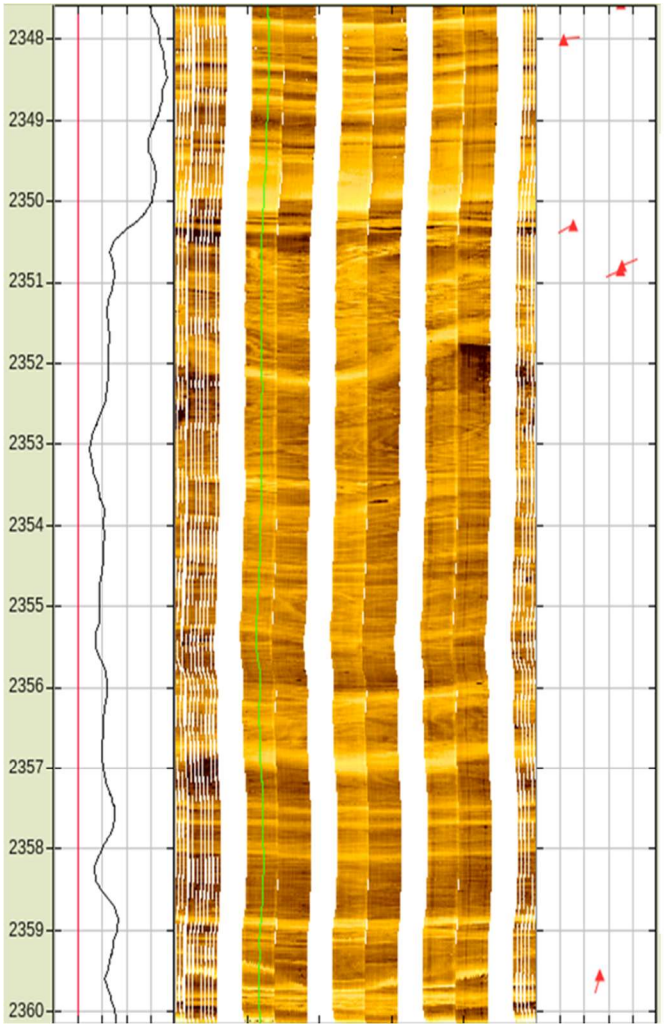

Fracture depth chart: with associated lithologies listed below.

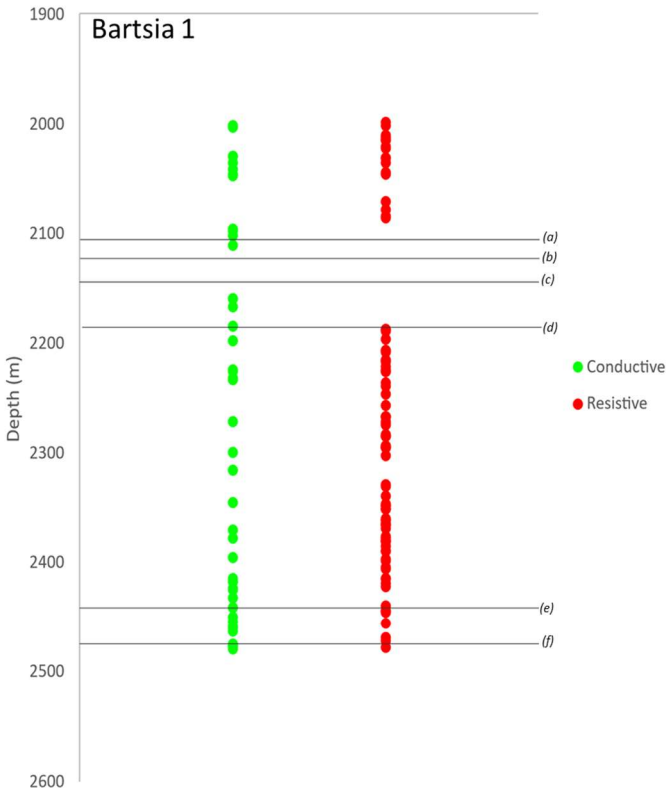

(a) Limestone Marker; 2107m, Bookara Sandstone; 2115m, (b) Dongara Sandstone; 2129m, Wagina Formation; 2136m, (c) Carynginia Formation; 2152m, (d) Irwin River Coal Measures; 2196m, (e) Kingia Formation; 2452m, (f) High cliff Sandstone; 2486m.

Appendix C.2

Well Card 2: Drakea 1

Latitude:	29.403°S
Longitude:	115.061°E
Total depth interval:	3080m
Image tool used:	FMI
Depth interval of image log (top/bottom):	773/3091m
Max. deviation from vertical:	45.93°
Subcontracted drilling company:	Century Drilling Ltd
Parent company:	ARC Energy Limited Ltd

Example of the Drakea 1 image log: showing the deviation of the well in pink, Gamma ray index in black. Note wavy bedding, easily confused as fractures as well as evidence of truncated bedding.

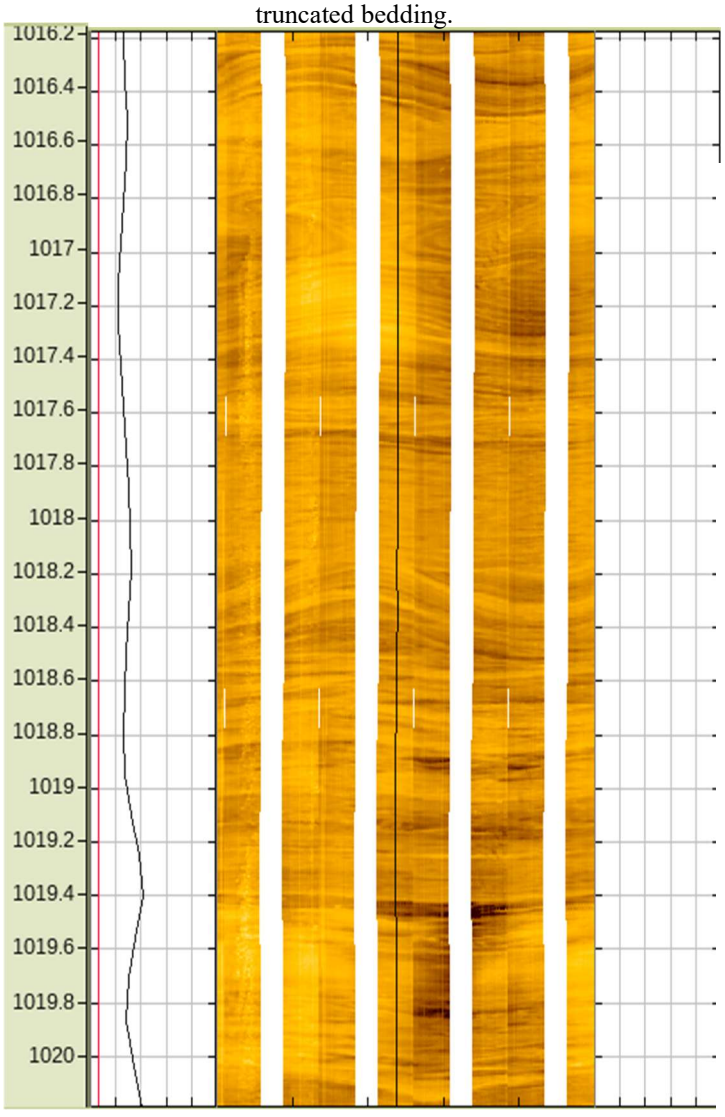

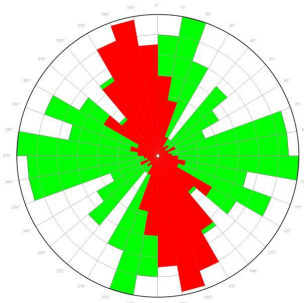

729 total fractures interpreted in Drakea 1. Conductive fractures in green with resistive fractures in red.

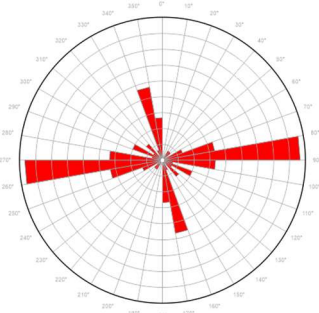

13 drilling-induced tensile fractures were interpreted in Drakea 1, amounting to accumulative length of 6.13 m, equating to a D ranking (questionable σ_{Hmax} orientation ± 25-40°) as per the World Stress Map Ranking Scheme (Heidback et al., 2008).

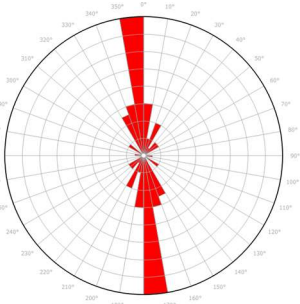

47 borehole breakouts were interpreted in Drakea 1, amounting to accumulative length of 80.35 m, equating to a B ranking (σ_{Hmax} believed to be within ±15-20°) as per the World Stress Map Ranking Scheme (Heidback et al., 2008).

Fracture depth chart: with associated lithologies listed below.

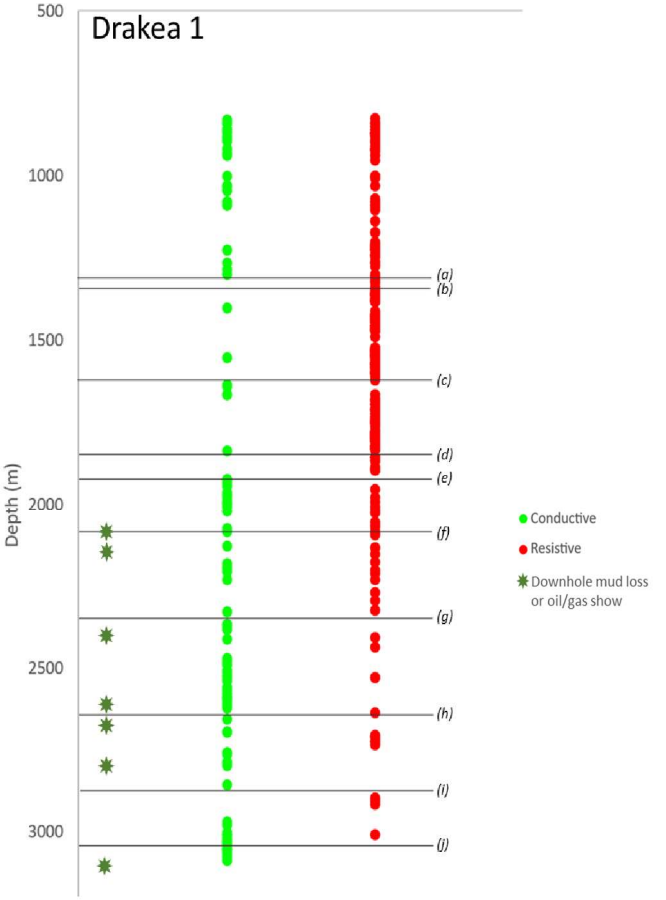

(a) Cadda Formation; 1269m (b) Cattamarra Coal Measures; 1298m, (c) Cattamarra Coal Marker; 1624m, (d) Eneabba Formation; 1835m, (e) Kockatea Shale; 1900m, (f) Basal Limestone; 2117m, Wagina Sandstone; 2168m, Carynginia Formation; 2191m, (g) Irwin River Coal Measures; 2320m, Nangetty Formation; 2375m (h) Kingia Formation; 2650m, High Cliff Sandstone; 2693m, (i) Holmwood Shale; 2753m, (j)

Appendix C.3

Well Card 3: Eremia 2

Latitude:	29.310°S
Longitude:	115.027°E
Total depth interval:	2124m
Image tool used:	FMI
Depth interval of image log (top/bottom):	503/2290m
Max. deviation from vertical:	28.42°
Subcontracted drilling company:	Century Drilling Ltd
Parent company:	ARC Energy Limited Ltd

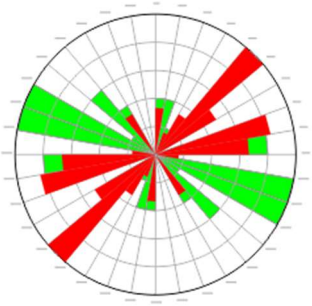

56 total fractures interpreted in Eremia 2. Conductive fractures in green with resistive fractures in red.

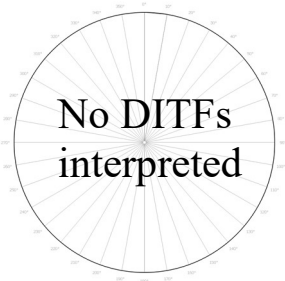

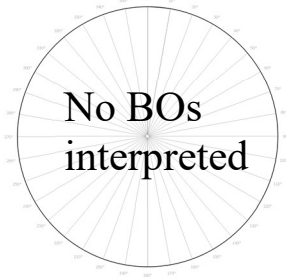

Example of the Eremia 2 image log: showing the Gamma ray index in black, Pad 1 azimuth in black and interpretations in the far-right panel. This example again highlights two examples of resistive fractures as observed at 2185.5 m and 2188.5 m.

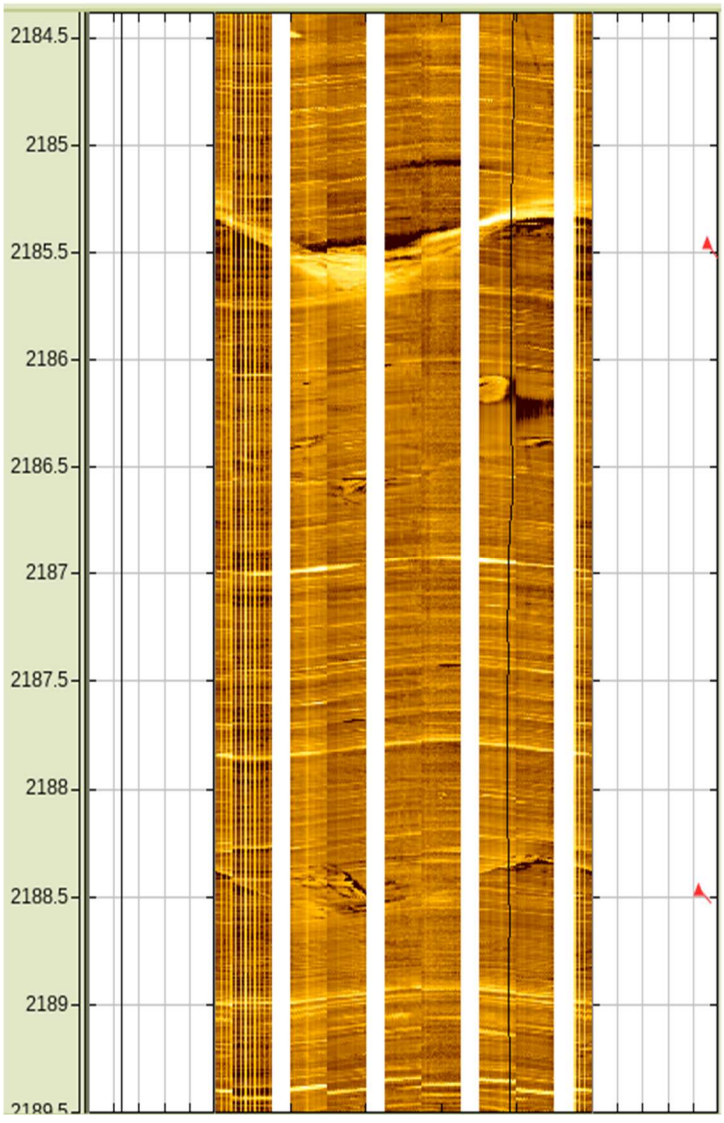

Fracture depth chart: with the only the Kockatea Shale recorded, in this section of the well.

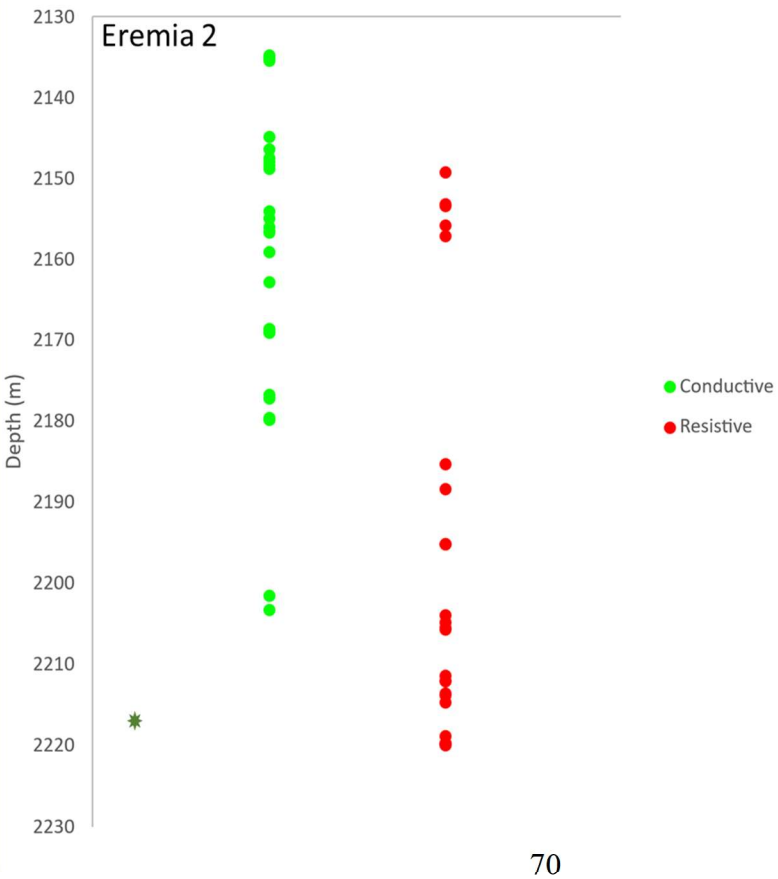

Appendix C.4

Well Card 4:Evandra 1

Latitude:	29.348°S
Longitude:	115.021°E
Total depth interval:	2352m
Image tool used:	FMI
Depth interval of image log (top/bottom):	1841/2325m
Max. deviation from vertical:	14.90°
Subcontracted drilling company:	Century Drilling Ltd
Parent company:	ARC Energy Limited Ltd

Example of the Evandra 1 image log: showing the deviation of the well in pink, Pad 1 azimuth in black and interpretations in the far-right panel. Examples of wing DITFs are observed in the middle two pads with a network of cross cutting electrically resistive fractures particularly at 2271 m.

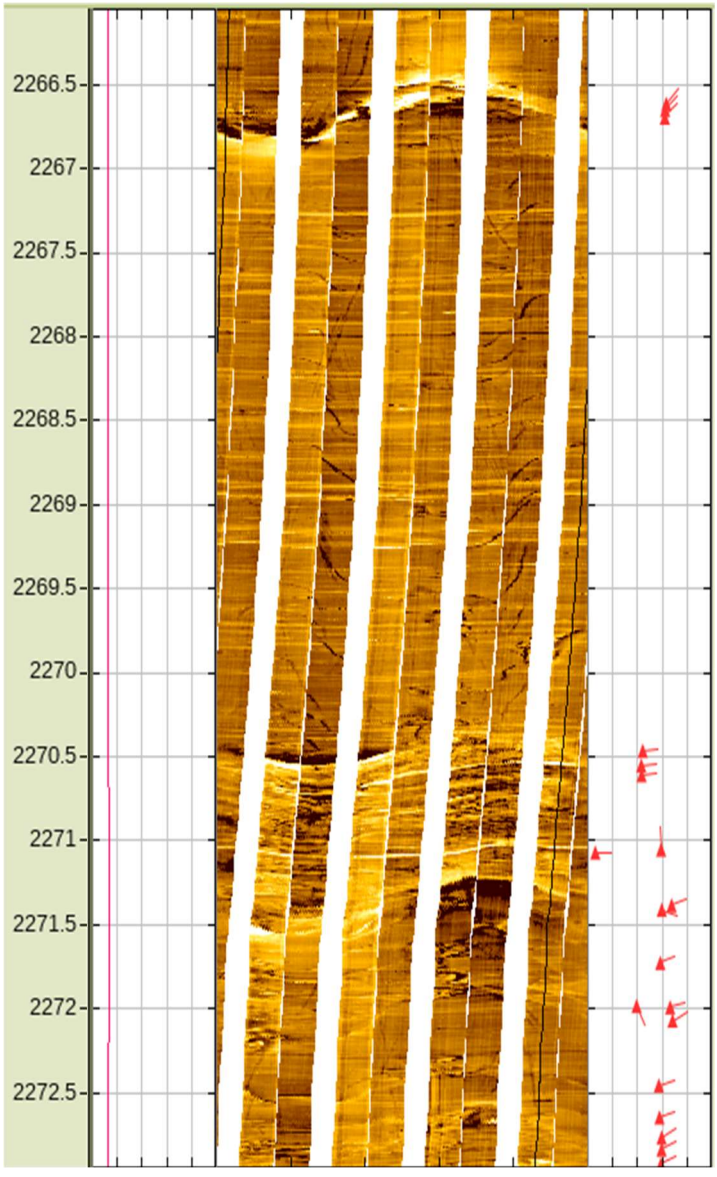

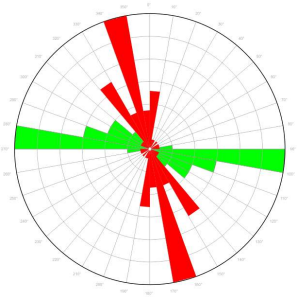

60 total fractures interpreted in Evandra 1. Conductive fractures in green with resistive fractures in red.

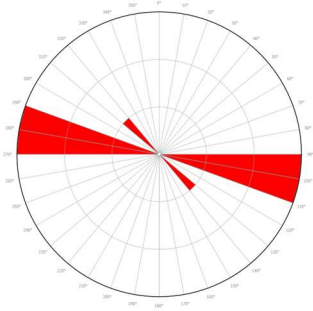

Seven drilling-induced tensile fractures were interpreted in Evandra 1, amounting to accumulative length of 6.09 m, equating to a D ranking (questionable σ_{Hmax} orientation ± 25-40°) as per the World Stress Map Ranking Scheme (Heidback et al., 2008).

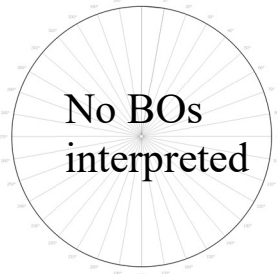

Fracture depth chart: with associated lithologies listed below.

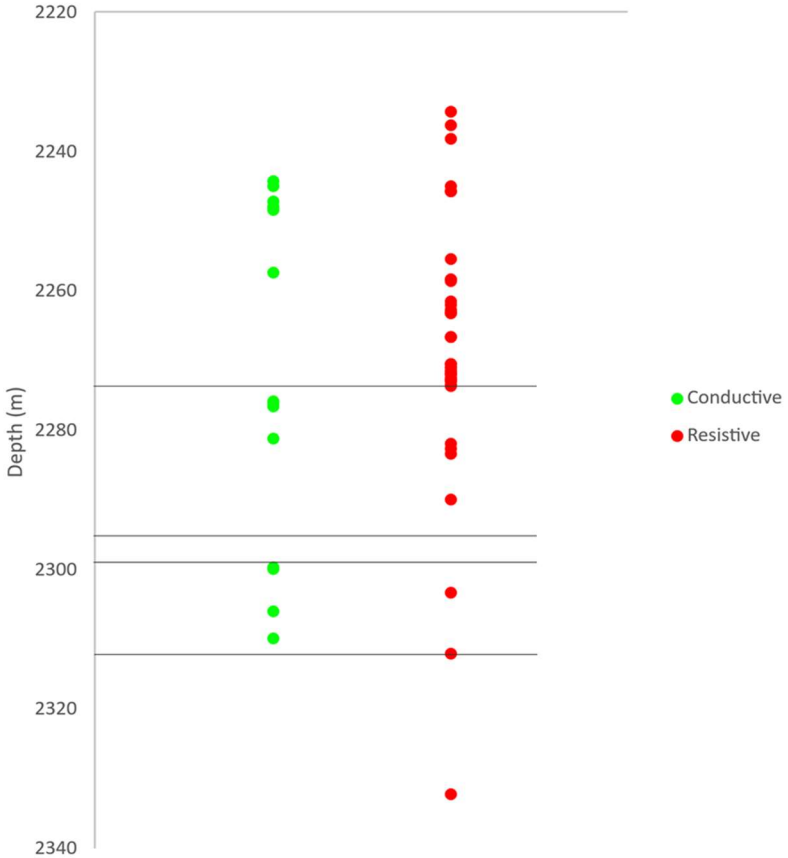

(a) Basal Limestone Marker; 2273m (b) Dongara Sandstone; 2293m, (c) Wagina Formation; 2298m, (d) Carynginia Formation; 2312m.

Appendix C.5

Well Card 5: Hovea 9

Latitude:	29.329°S
Longitude:	115.044°E
Total depth interval:	2114m
Image tool used:	FMI
Depth interval of image log (top/bottom):	498/2112.5m
Max. deviation from vertical:	15.92°
Subcontracted drilling company:	Century Drilling Ltd
Parent company:	ARC Energy Limited Ltd

Example of the Hovea 9 image log: exemplifying the deviation of the well in pink, Pad 1 azimuth in black and interpretations in the far-right panel. Again, see observed DITF running for the majority of the example shot (1928.4-1931 m). The DITF however appears to by intersected by the electrically conductive natural fracture at 1931 m.

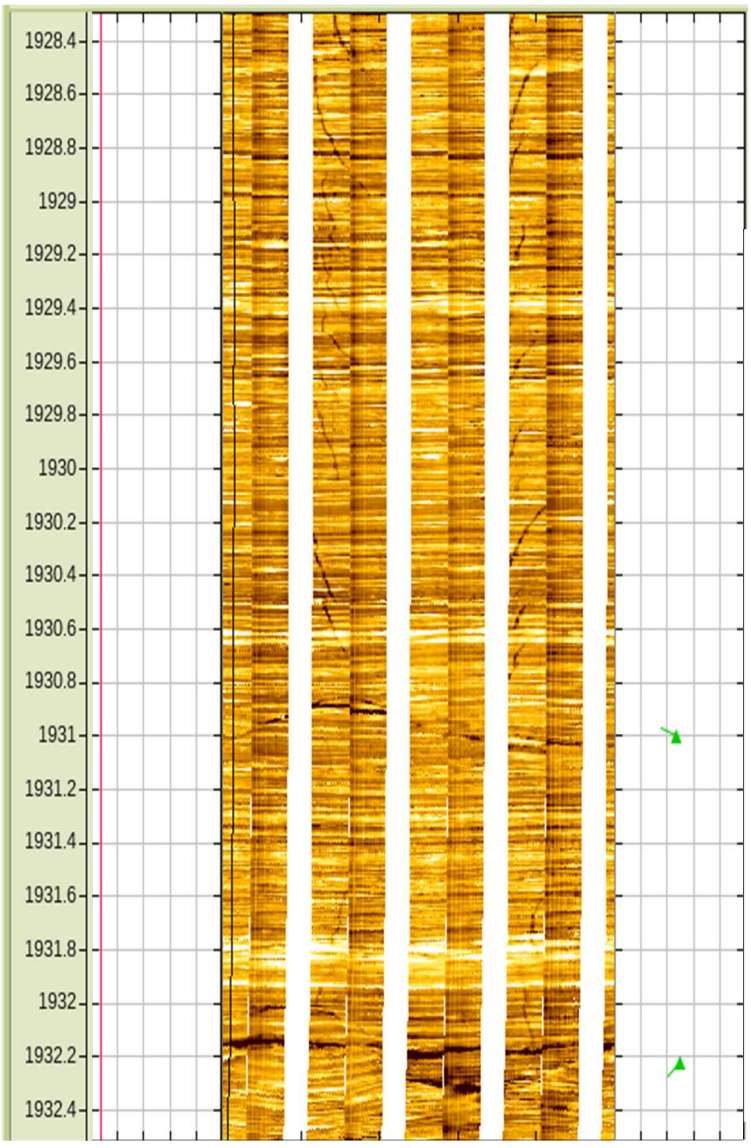

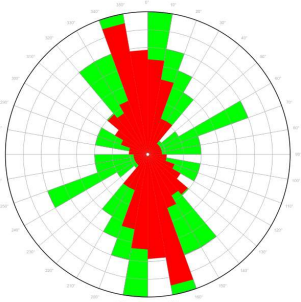

245 total fractures interpreted in Hovea 9. Conductive fractures in green with resistive fractures in red.

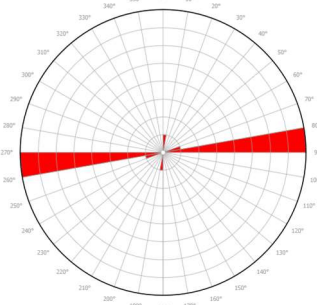

Ten drilling-induced tensile fractures were interpreted in Hovea 9, amounting to accumulative length of 8.92 m, equating to a D ranking (questionable σ_{Hmax} orientation ± 25-40°) as per the World Stress Map Ranking Scheme (Heidback et al., 2008).

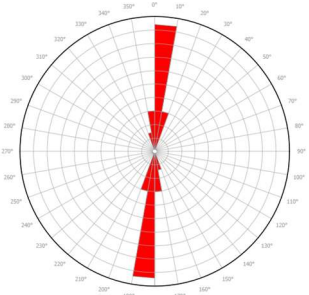

87 borehole breakouts were interpreted in Hovea 9, amounting to accumulative length of 195.86 m, equating to a A ranking (σ_{Hmax} believed to be within ±15°) as per the World Stress Map Ranking Scheme (Heidback et al., 2008).

Fracture depth chart: with associated lithologies listed below.

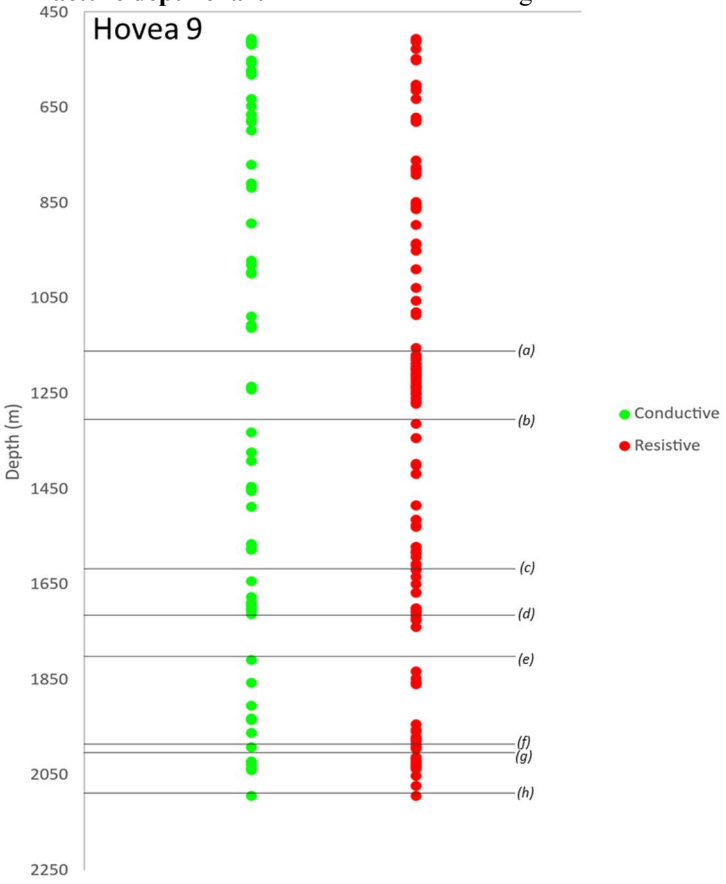

(a) Cadda Formation; 1175m (b) Mountain Bridge Fault; 1292m, Eneabba Member; 1292m, (c) Lesueur Sandstone; 1620m, (d) Woodada Formation; 1705m, (e) Kockatea Shale; 1819m, (f) Dongara Sandstone, Fault; 2004m, (g) Wagina Formation; 2031m, (h) Carynginia Formation; 2069m.

Appendix C.6

Well Card 6: Hovea 12

Latitude:	29.318°S
Longitude:	115.042°E
Total depth interval:	2482m
Image tool used:	FMI
Depth interval of image log (top/bottom):	1600/2475m
Max. deviation from vertical:	38.08°
Subcontracted drilling company:	Century Drilling Ltd
Parent company:	ARC Energy Limited Ltd

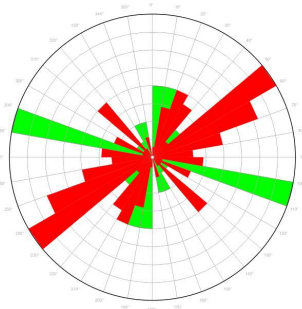

119 total fractures interpreted in Hovea 12. Conductive fractures in green with resistive fractures in red.

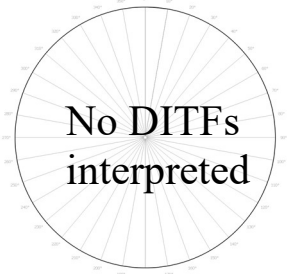

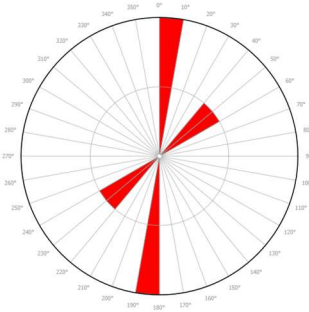

Four borehole breakouts were interpreted in Hovea 12, amounting to accumulative length of 12.01 m, equating to a D ranking (σ_{Hmax} believed to be within ±25-40°) as per the World Stress Map Ranking Scheme (Heidback et al., 2008).

Example of the Hovea 12 image log: showing the Gamma ray index in black, Pad 1 azimuth in black and interpretations in the far-right panel.

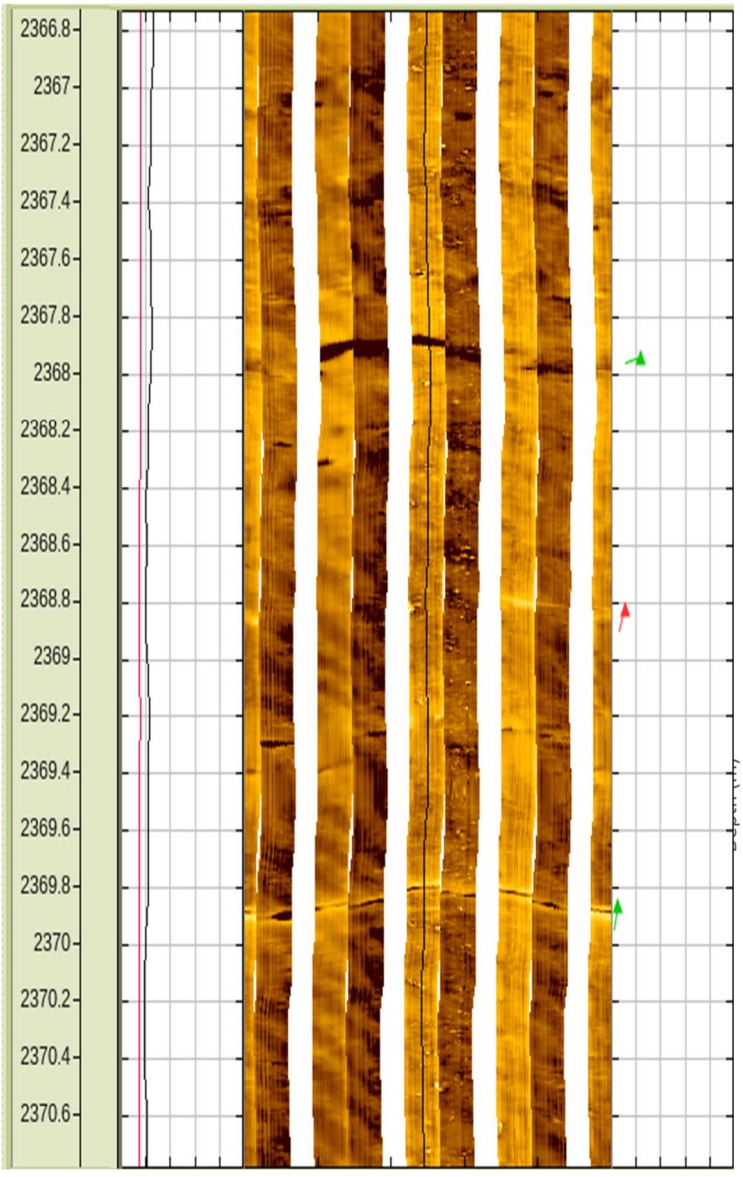

Fracture depth chart: with associated lithologies listed below.

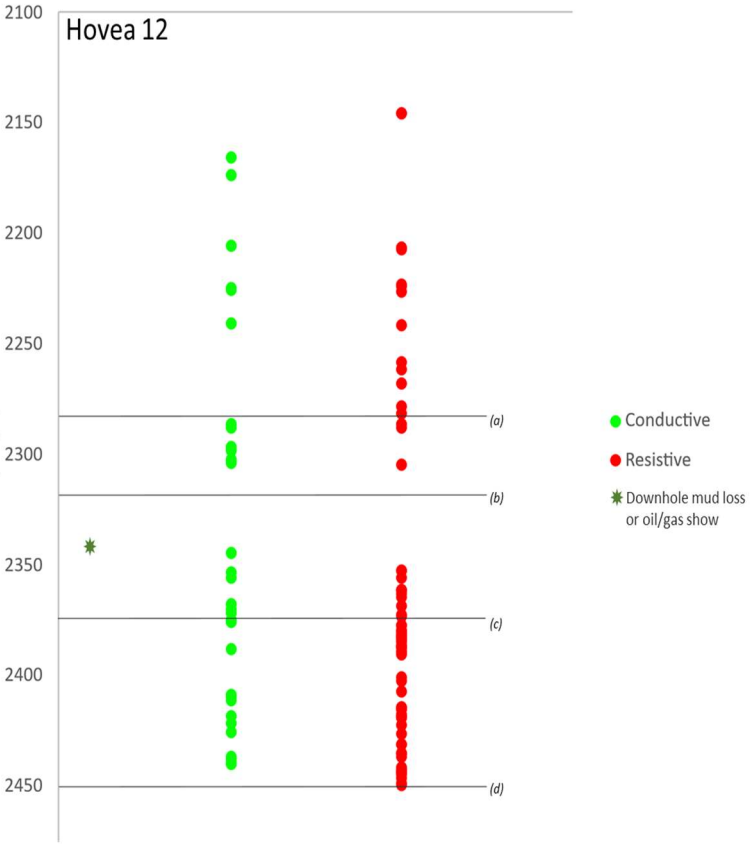

(a) Basal Limestone Marker; 2286m (b) Dongara Sandstone; 2324m, (c) Wagina Sandstone; 2375m, (d) Carynginia Formation; 2450m.

Appendix C.7

Well Card 7: Jingemia 2

Latitude:	29.339°S
Longitude:	114.990°E
Total depth interval:	2781m
Image tool used:	FMI
Depth interval of image log (top/bottom):	500/2778m
Max. deviation from vertical:	30.06°
Subcontracted drilling company:	Century Drilling Ltd
Parent company:	Origin Energy Developments Pty Ltd

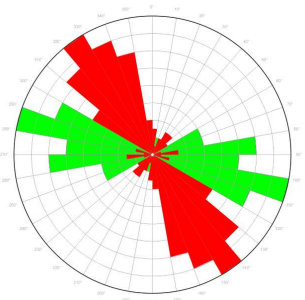

129 total fractures interpreted in Jingemia 2. Conductive fractures in green with resistive fractures in red.

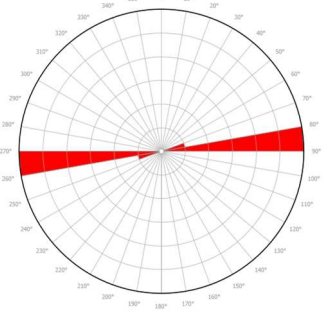

Seven drilling-induced tensile fractures were interpreted in Jingemia 2, amounting to accumulative length of 6.32 m, equating to a D ranking (questionable σ_{Hmax} orientation ± 25-40°) as per the World Stress Map Ranking Scheme (Heidback et al., 2008).

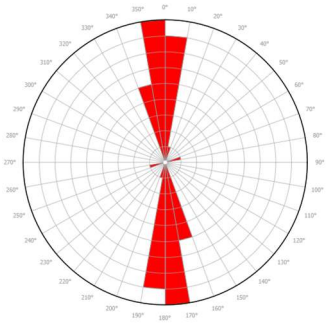

24 borehole breakouts were interpreted in Jingemia 2, amounting to accumulative length of 101.55 m, equating to a A ranking (σ_{Hmax} believed to be within ±15°) as per the World Stress Map Ranking Scheme (Heidback et al., 2008).

Example of the Jingemia 2 image log: showing the Gamma ray index in black, Pad 1 azimuth in black and interpretations in the far-right panel. An example of a complex electrically resistive natural fracture network (2176 m).

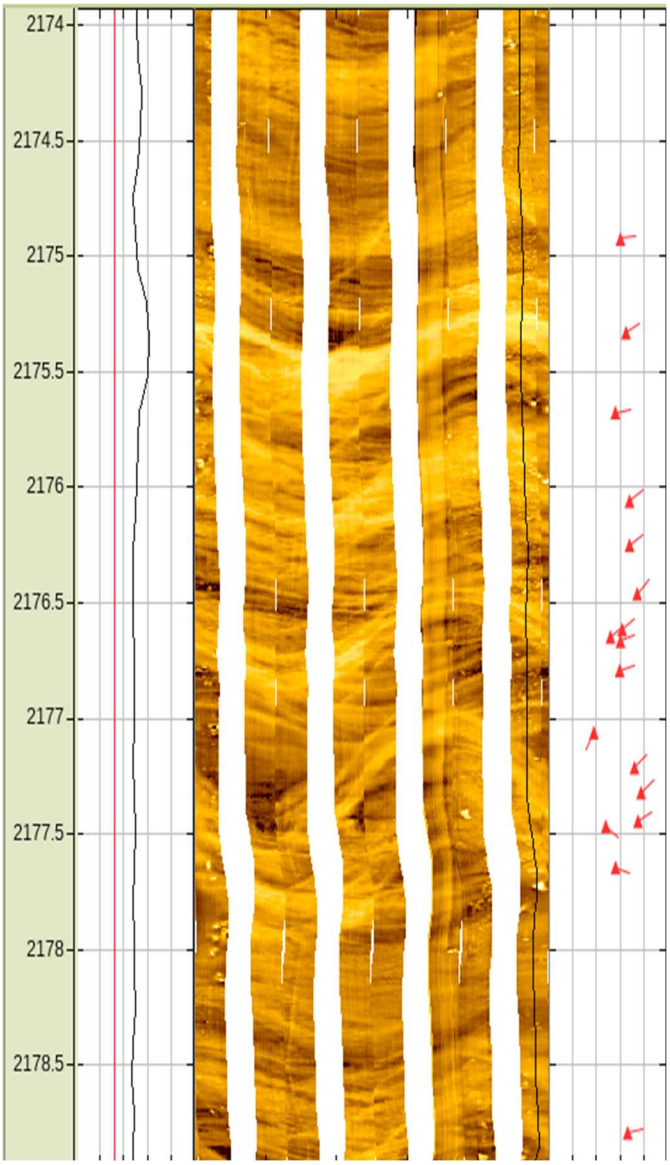

Fracture depth chart: with associated lithologies listed below.

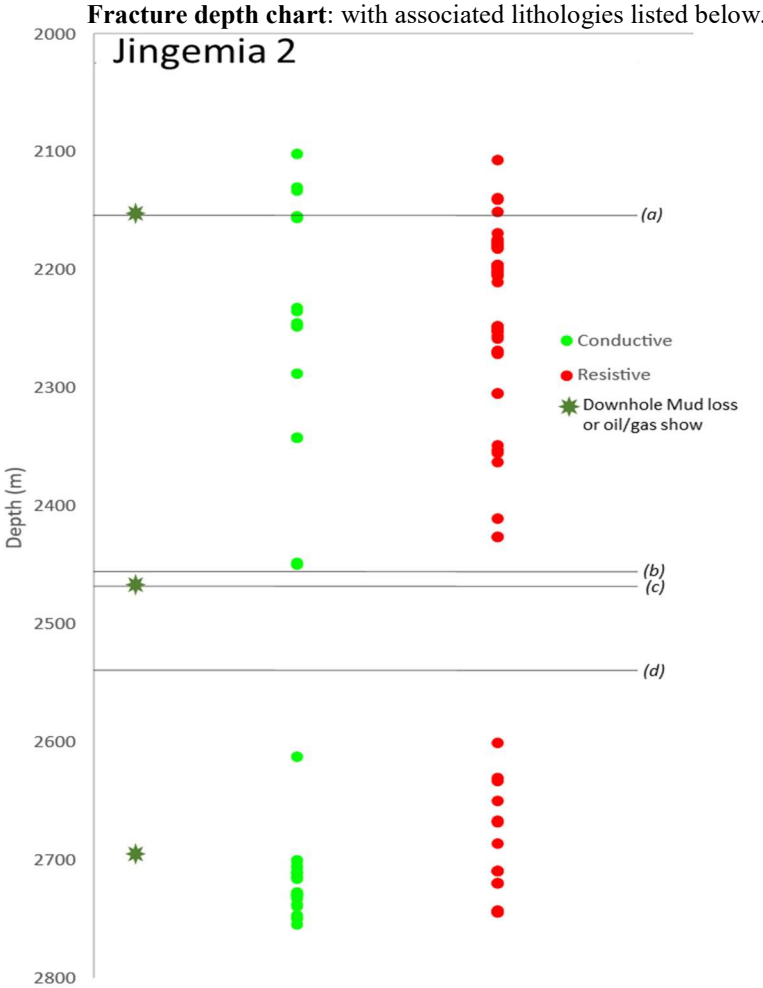

(a) Kockatea Shale; 2160m (b) Dongara Sandstone; 2455m, (c) Wagina Sandstone; 2465m, (d) Total Depth (Logged); 2468m.

Appendix C.8

Well Card 8: Jingemia 3

Latitude:	29.339°S
Longitude:	114.990°E
Total depth interval:	2625m
Image tool used:	FMI
Depth interval of image log (top/bottom):	500/2636.5m
Max. deviation from vertical:	21.36°
Subcontracted drilling company:	Century Drilling Ltd
Parent company:	Origin Energy-Developments Pty Ltd

Example of the Jingemia 3 image log: showing the Gamma ray index in black, Pad 1 azimuth in black and interpretations in the far-right panel. Note minor tool malfunction in pad 1, and series of cross cutting natural resistive fractures at 1945 m depth.

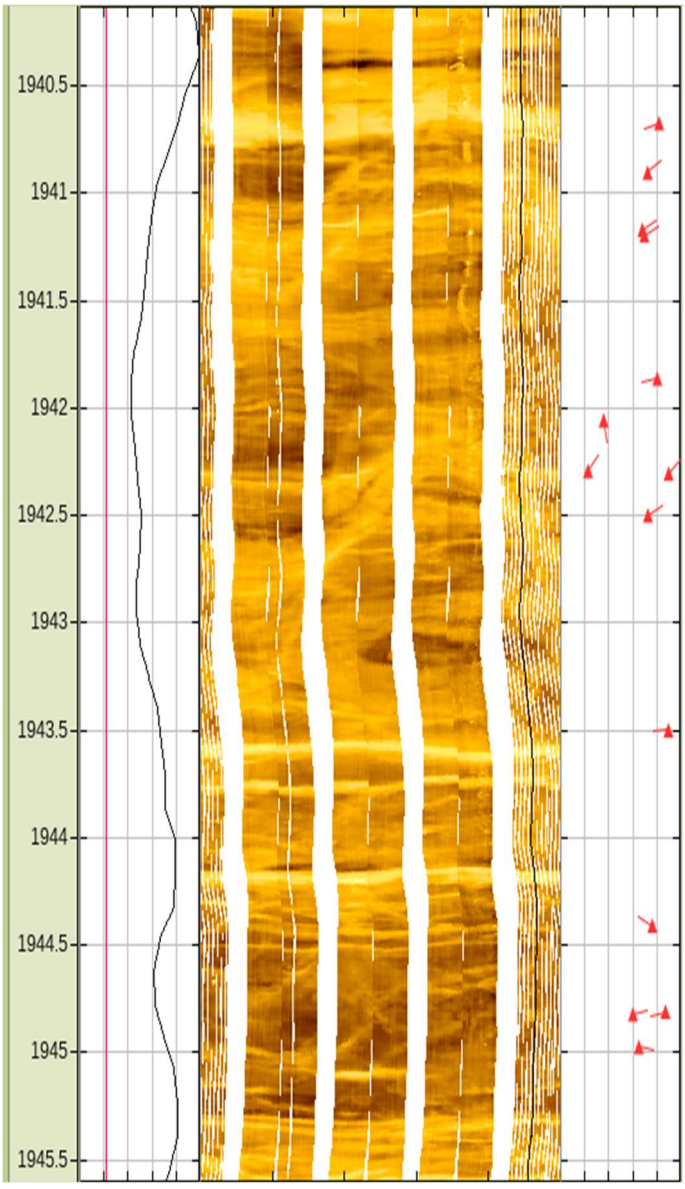

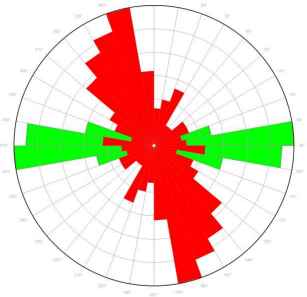

281 total fractures interpreted in Jingemia 3. Conductive fractures in green with resistive fractures in red.

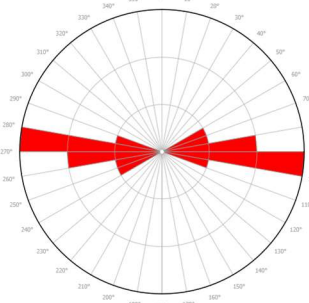

Eight drilling-induced tensile fractures were interpreted in Jingemia 2, amounting to accumulative length of 6.32 m, equating to a D ranking (questionable σ_{Hmax} orientation ± 25-40°) as per the World Stress Map Ranking Scheme (Heidback et al., 2008).

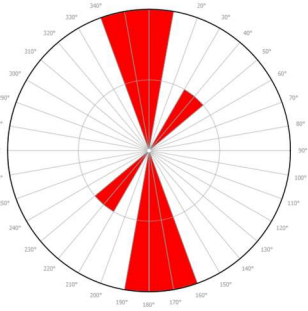

Eight borehole breakouts were interpreted in Hovea 12, amounting to accumulative length of 24.01 m, equating to a C ranking (σ_{Hmax} believed to be within ±20-25°) as per the World Stress Map Ranking Scheme (Heidback et al., 2008).

Fracture depth chart: with associated lithologies listed below.

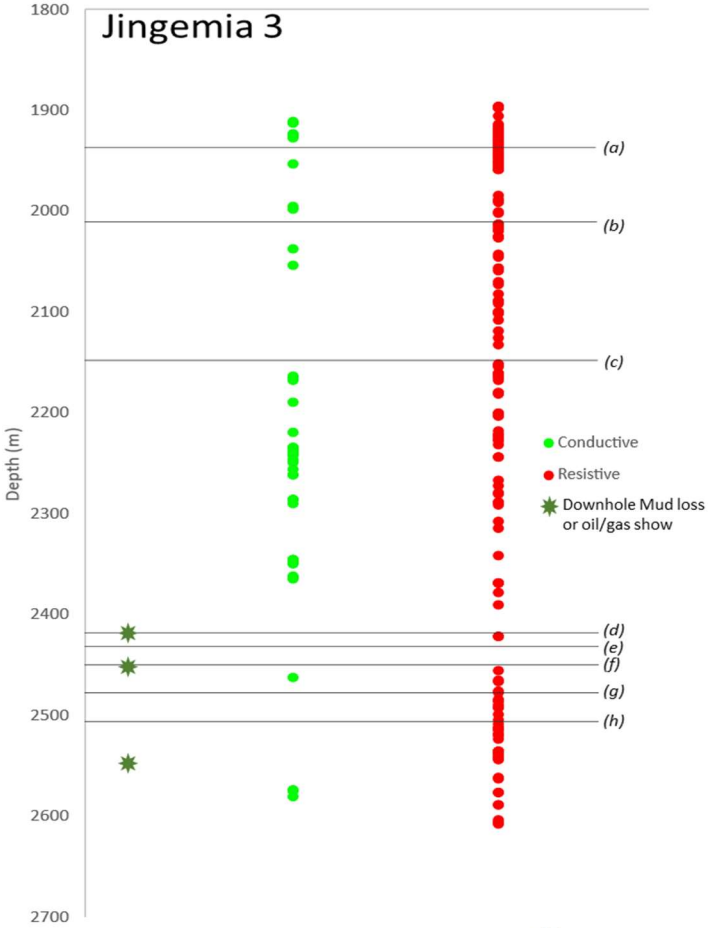

(a) Lesueur Sandstone; 1933m (b) Woodada Formation; 2038m, (c) Kockatea Shale; 2143m, (d)) Basal Kockatea Shale; 2410m, (e) Dongara Sandstone; 2425m, (f) Wagina Formation; 2446m, (g) Carynginia Formation; 2479m, (h) Total Depth (Logged); 2505m.

APPENDIX D: FULL STRESS INDICATOR SETS

Borehole Breakout

DRAKEA 1: TOTAL INTERPRETED BREAKOUT SET

Top Depth (m)	Bottom Depth (m)	Width (deg)	Azimuth (deg)	Apparent Mode	Image Log
1388.259944	1389.113103	70	127.5	North	FMI_SONIC_004PUP_FMI
1388.259944	1389.113103	70	307.5	North	FMI_SONIC_004PUP_FMI
1389.652802	1390.847037	83.75	128.125	North	FMI_SONIC_004PUP_FMI
1389.652802	1390.847037	83.75	308.125	North	FMI_SONIC_004PUP_FMI
1390.761868	1391.2934	70	96.25	North	FMI_SONIC_004PUP_FMI
1390.761868	1391.2934	70	276.25	North	FMI_SONIC_004PUP_FMI
1391.616399	1393.109193	92.5	153.75	North	FMI_SONIC_004PUP_FMI
1391.616399	1393.109193	92.5	333.75	North	FMI_SONIC_004PUP_FMI
1393.21978	1393.61589	40	152.5	North	FMI_SONIC_004PUP_FMI
1393.21978	1393.61589	40	332.5	North	FMI_SONIC_004PUP_FMI
1396.463141	1397.285831	52.5	165	North	FMI_SONIC_004PUP_FMI
1396.463141	1397.285831	52.5	345	North	FMI_SONIC_004PUP_FMI
1400.901602	1401.500845	68.75	158.125	North	FMI_SONIC_004PUP_FMI
1400.901602	1401.500845	68.75	338.125	North	FMI_SONIC_004PUP_FMI
1405.296051	1406.29479	41.25	56.875	North	FMI_SONIC_004PUP_FMI
1405.296051	1406.29479	41.25	236.875	North	FMI_SONIC_004PUP_FMI
1475.4515	1476.050744	61.25	153.125	North	FMI_SONIC_004PUP_FMI
1475.4515	1476.050744	61.25	333.125	North	FMI_SONIC_004PUP_FMI
1609.438184	1610.166078	82.5	173.75	North	FMI_SONIC_004PUP_FMI
1609.438184	1610.166078	82.5	353.75	North	FMI_SONIC_004PUP_FMI
1626.690967	1627.35115	72.5	206.25	North	FMI_SONIC_004PUP_FMI
1626.690967	1627.35115	72.5	26.25	North	FMI_SONIC_004PUP_FMI
1628.058731	1628.641046	68.75	191.875	North	FMI_SONIC_004PUP_FMI
1628.058731	1628.641046	68.75	11.875	North	FMI_SONIC_004PUP_FMI
1628.959057	1630.497783	77.5	205	North	FMI_SONIC_004PUP_FMI
1628.959057	1630.497783	77.5	25	North	FMI_SONIC_004PUP_FMI
1637.473956	1638.53702	110	182.5	North	FMI_SONIC_004PUP_FMI
1637.473956	1638.53702	110	2.5	North	FMI_SONIC_004PUP_FMI
1654.100412	1654.686113	87.5	171.25	North	FMI_SONIC_004PUP_FMI
1654.100412	1654.686113	87.5	351.25	North	FMI_SONIC_004PUP_FMI
1654.865547	1655.349681	72.5	176.25	North	FMI_SONIC_004PUP_FMI
1654.865547	1655.349681	72.5	356.25	North	FMI_SONIC_004PUP_FMI
1655.450397	1656.839844	88.75	181.875	North	FMI_SONIC_004PUP_FMI
1655.450397	1656.839844	88.75	1.875	North	FMI_SONIC_004PUP_FMI
1685.04099	1685.789197	86.25	221.875	North	FMI_SONIC_004PUP_FMI

1685.04099	1685.789197	86.25	41.875	North	FMI_SONIC_004PUP_FMI
1689.428667	1690.518816	130	195	North	FMI_SONIC_004PUP_FMI
1689.428667	1690.518816	130	15	North	FMI_SONIC_004PUP_FMI
1698.711856	1699.365268	108.75	186.875	North	FMI_SONIC_004PUP_FMI
1698.711856	1699.365268	108.75	6.875	North	FMI_SONIC_004PUP_FMI
1701.169769	1702.24976	72.5	166.25	North	FMI_SONIC_004PUP_FMI
1701.169769	1702.24976	72.5	346.25	North	FMI_SONIC_004PUP_FMI
1770.543155	1772.652355	60	186.25	North	FMI_SONIC_004PUP_FMI
1770.543155	1772.652355	60	6.25	North	FMI_SONIC_004PUP_FMI
1813.709457	1814.880726	98.75	186.875	North	FMI_SONIC_004PUP_FMI
1813.709457	1814.880726	98.75	6.875	North	FMI_SONIC_004PUP_FMI
1817.496662	1818.833057	87.5	151.25	North	FMI_SONIC_004PUP_FMI
1817.496662	1818.833057	87.5	331.25	North	FMI_SONIC_004PUP_FMI
1840.889779	1841.785455	73.75	203.125	North	FMI_SONIC_004PUP_FMI
1840.889779	1841.785455	73.75	23.125	North	FMI_SONIC_004PUP_FMI
1860.273127	1862.75346	62.5	213.75	North	FMI_SONIC_004PUP_FMI
1860.273127	1862.75346	62.5	33.75	North	FMI_SONIC_004PUP_FMI
1872.802839	1876.058159	67.5	221.25	North	FMI_SONIC_004PUP_FMI
1872.802839	1876.058159	67.5	41.25	North	FMI_SONIC_004PUP_FMI
1880.081346	1881.91863	72.5	205	North	FMI_SONIC_004PUP_FMI
1880.081346	1881.91863	72.5	25	North	FMI_SONIC_004PUP_FMI
2471.032297	2473.053309	62.5	166.25	North	FMI_SONIC_004PUP_FMI
2471.032297	2473.053309	62.5	346.25	North	FMI_SONIC_004PUP_FMI
2534.521946	2535.624316	78.75	160.625	North	FMI_SONIC_004PUP_FMI
2534.521946	2535.624316	78.75	340.625	North	FMI_SONIC_004PUP_FMI
2571.079523	2573.379644	50	178.75	North	FMI_SONIC_004PUP_FMI
2571.079523	2573.379644	50	358.75	North	FMI_SONIC_004PUP_FMI
2598.701698	2600.069338	35	236.25	North	FMI_SONIC_004PUP_FMI
2598.701698	2600.069338	35	56.25	North	FMI_SONIC_004PUP_FMI
2606.704245	2607.63437	61.25	166.875	North	FMI_SONIC_004PUP_FMI
2606.704245	2607.63437	61.25	346.875	North	FMI_SONIC_004PUP_FMI
2622.20633	2624.537384	47.5	178.75	North	FMI_SONIC_004PUP_FMI
2622.20633	2624.537384	47.5	358.75	North	FMI_SONIC_004PUP_FMI
2634.929522	2636.376383	53.75	170.625	North	FMI_SONIC_004PUP_FMI
2634.929522	2636.376383	53.75	350.625	North	FMI_SONIC_004PUP_FMI
2638.477777	2645.505389	55	175	North	FMI_SONIC_004PUP_FMI
2638.477777	2645.505389	55	355	North	FMI_SONIC_004PUP_FMI
2650.201946	2651.981815	45	178.75	North	FMI_SONIC_004PUP_FMI
2650.201946	2651.981815	45	358.75	North	FMI_SONIC_004PUP_FMI
2654.002828	2656.104221	57.5	175	North	FMI_SONIC_004PUP_FMI
2654.002828	2656.104221	57.5	355	North	FMI_SONIC_004PUP_FMI
2661.616074	2663.855264	61.25	170.625	North	FMI_SONIC_004PUP_FMI
2661.616074	2663.855264	61.25	350.625	North	FMI_SONIC_004PUP_FMI
2667.21979	2668.942244	62.5	176.25	North	FMI_SONIC_004PUP_FMI

2667.21979	2668.942244	62.5	356.25	North	FMI_SONIC_004PUP_FMI
2670.503936	2674.626342	68.75	170.625	North	FMI_SONIC_004PUP_FMI
2670.503936	2674.626342	68.75	350.625	North	FMI_SONIC_004PUP_FMI
2674.982316	2677.026294	77.5	168.75	North	FMI_SONIC_004PUP_FMI
2674.982316	2677.026294	77.5	348.75	North	FMI_SONIC_004PUP_FMI
2677.795657	2684.673989	62.5	180	North	FMI_SONIC_004PUP_FMI
2677.795657	2684.673989	62.5	0	North	FMI_SONIC_004PUP_FMI
2685.799326	2689.336098	50	172.5	North	FMI_SONIC_004PUP_FMI
2685.799326	2689.336098	50	352.5	North	FMI_SONIC_004PUP_FMI
2692.72359	2694.537908	51.25	170.625	North	FMI_SONIC_004PUP_FMI
2692.72359	2694.537908	51.25	350.625	North	FMI_SONIC_004PUP_FMI
2843.943556	2846.366474	71.25	171.875	North	FMI_SONIC_004PUP_FMI
2843.943556	2846.366474	71.25	351.875	North	FMI_SONIC_004PUP_FMI
2864.56707	2866.588082	76.25	175.625	North	FMI_SONIC_004PUP_FMI
2864.56707	2866.588082	76.25	355.625	North	FMI_SONIC_004PUP_FMI

HOVEA 9: TOTAL INTERPRETED BREAKOUT SET

Top Depth (m)	Bottom Depth (m)	Width (deg)	Azimuth (deg)	Apparent Mode	Image Log
2144.2	2146.437	57.91798	168.6435	North	FMI_TLD_MCFL_CNL_185PUC_FMI_final_SC
2144.2	2146.437	57.91798	348.6435	North	FMI_TLD_MCFL_CNL_185PUC_FMI_final_SC
2166.283	2167.162	72.68139	169.2114	North	FMI_TLD_MCFL_CNL_185PUC_FMI_final_SC
2166.283	2167.162	72.68139	349.2114	North	FMI_TLD_MCFL_CNL_185PUC_FMI_final_SC
2477.476	2478.78	64.73186	173.1861	North	FMI_TLD_MCFL_CNL_185PUC_FMI_final_SC
2477.476	2478.78	64.73186	353.1861	North	FMI_TLD_MCFL_CNL_185PUC_FMI_final_SC
2504.777	2505.187	51.1041	170.9148	North	FMI_TLD_MCFL_CNL_185PUC_FMI_final_SC
2504.777	2505.187	51.1041	350.9148	North	FMI_TLD_MCFL_CNL_185PUC_FMI_final_SC
2505.365	2508.906	43.15457	169.2114	North	FMI_TLD_MCFL_CNL_185PUC_FMI_final_SC
2505.365	2508.906	43.15457	349.2114	North	FMI_TLD_MCFL_CNL_185PUC_FMI_final_SC
2509.525	2510.929	31.79811	182.8391	North	FMI_TLD_MCFL_CNL_185PUC_FMI_final_SC
2509.525	2510.929	31.79811	2.839117	North	FMI_TLD_MCFL_CNL_185PUC_FMI_final_SC
2511.275	2512.911	55.64669	169.7792	North	FMI_TLD_MCFL_CNL_185PUC_FMI_final_SC
2511.275	2512.911	55.64669	349.7792	North	FMI_TLD_MCFL_CNL_185PUC_FMI_final_SC
2513.13	2514.625	63.59621	183.9748	North	FMI_TLD_MCFL_CNL_185PUC_FMI_final_SC
2513.13	2514.625	63.59621	3.974763	North	FMI_TLD_MCFL_CNL_185PUC_FMI_final_SC
2514.757	2515.809	73.81703	164.1009	North	FMI_TLD_MCFL_CNL_185PUC_FMI_final_SC
2514.757	2515.809	73.81703	344.1009	North	FMI_TLD_MCFL_CNL_185PUC_FMI_final_SC
2515.914	2521.104	52.23975	172.6183	North	FMI_TLD_MCFL_CNL_185PUC_FMI_final_SC
2515.914	2521.104	52.23975	352.6183	North	FMI_TLD_MCFL_CNL_185PUC_FMI_final_SC
2521.237	2522.121	57.91798	183.4069	North	FMI_TLD_MCFL_CNL_185PUC_FMI_final_SC
2521.237	2522.121	57.91798	3.40694	North	FMI_TLD_MCFL_CNL_185PUC_FMI_final_SC
2522.531	2524.317	52.23975	177.1609	North	FMI_TLD_MCFL_CNL_185PUC_FMI_final_SC
2522.531	2524.317	52.23975	357.1609	North	FMI_TLD_MCFL_CNL_185PUC_FMI_final_SC
2525.32	2526.669	52.23975	178.2965	North	FMI_TLD_MCFL_CNL_185PUC_FMI_final_SC
2525.32	2526.669	52.23975	358.2965	North	FMI_TLD_MCFL_CNL_185PUC_FMI_final_SC
2527.065	2527.835	60.18927	185.6782	North	FMI_TLD_MCFL_CNL_185PUC_FMI_final_SC
2527.065	2527.835	60.18927	5.678233	North	FMI_TLD_MCFL_CNL_185PUC_FMI_final_SC
2527.981	2552.958	59.05363	171.4826	North	FMI_TLD_MCFL_CNL_185PUC_FMI_final_SC
2527.981	2552.958	59.05363	351.4826	North	FMI_TLD_MCFL_CNL_185PUC_FMI_final_SC
2553.026	2553.258	38.61199	181.7035	North	FMI_TLD_MCFL_CNL_185PUC_FMI_final_SC
2553.026	2553.258	38.61199	1.70347	North	FMI_TLD_MCFL_CNL_185PUC_FMI_final_SC
2553.29	2553.723	48.83281	180	North	FMI_TLD_MCFL_CNL_185PUC_FMI_final_SC
2553.29	2553.723	48.83281	0	North	FMI_TLD_MCFL_CNL_185PUC_FMI_final_SC
2553.901	2568.601	51.1041	177.7287	North	FMI_TLD_MCFL_CNL_185PUC_FMI_final_SC
2553.901	2568.601	51.1041	357.7287	North	FMI_TLD_MCFL_CNL_185PUC_FMI_final_SC
2568.684	2579.433	70.41009	178.2965	North	FMI_TLD_MCFL_CNL_185PUC_FMI_final_SC
2568.684	2579.433	70.41009	358.2965	North	FMI_TLD_MCFL_CNL_185PUC_FMI_final_SC
2579.543	2585.585	57.91798	182.2713	North	FMI_TLD_MCFL_CNL_185PUC_FMI_final_SC
2579.543	2585.585	57.91798	2.271293	North	FMI_TLD_MCFL_CNL_185PUC_FMI_final_SC

2585.854	2586.56	52.23975	191.9243	North	FMI_TLD_MCFL_CNL_185PUC_FMI_final_SC
2585.854	2586.56	52.23975	11.92429	North	FMI_TLD_MCFL_CNL_185PUC_FMI_final_SC
2586.884	2589.892	65.86751	182.8391	North	FMI_TLD_MCFL_CNL_185PUC_FMI_final_SC
2586.884	2589.892	65.86751	2.839117	North	FMI_TLD_MCFL_CNL_185PUC_FMI_final_SC
2590.434	2605.207	52.23975	177.1609	North	FMI_TLD_MCFL_CNL_185PUC_FMI_final_SC
2590.434	2605.207	52.23975	357.1609	North	FMI_TLD_MCFL_CNL_185PUC_FMI_final_SC
2096.471	2101.964	61.25	199.375	North	FMI_TLD_MCFL_CNL_185PUC_FMI_final_SC
2096.471	2101.964	61.25	19.375	North	FMI_TLD_MCFL_CNL_185PUC_FMI_final_SC
2103.827	2108.765	82.5	203.75	North	FMI_TLD_MCFL_CNL_185PUC_FMI_final_SC
2103.827	2108.765	82.5	23.75	North	FMI_TLD_MCFL_CNL_185PUC_FMI_final_SC
2111.937	2115.27	53.75	199.375	North	FMI_TLD_MCFL_CNL_185PUC_FMI_final_SC
2111.937	2115.27	53.75	19.375	North	FMI_TLD_MCFL_CNL_185PUC_FMI_final_SC
2121.308	2123.447	60	42.5	North	FMI_TLD_MCFL_CNL_185PUC_FMI_final_SC
2121.308	2123.447	60	222.5	North	FMI_TLD_MCFL_CNL_185PUC_FMI_final_SC
2124.04	2125.893	52.5	61.25	North	FMI_TLD_MCFL_CNL_185PUC_FMI_final_SC
2124.04	2125.893	52.5	241.25	North	FMI_TLD_MCFL_CNL_185PUC_FMI_final_SC
2137.146	2138.378	66.25	189.375	North	FMI_TLD_MCFL_CNL_185PUC_FMI_final_SC
2137.146	2138.378	66.25	9.375	North	FMI_TLD_MCFL_CNL_185PUC_FMI_final_SC
2140.537	2141.396	28.75	189.375	North	FMI_TLD_MCFL_CNL_185PUC_FMI_final_SC
2140.537	2141.396	28.75	9.375	North	FMI_TLD_MCFL_CNL_185PUC_FMI_final_SC
2142.017	2142.524	45	183.75	North	FMI_TLD_MCFL_CNL_185PUC_FMI_final_SC
2142.017	2142.524	45	3.75	North	FMI_TLD_MCFL_CNL_185PUC_FMI_final_SC
2150.032	2151.236	63.75	188.125	North	FMI_TLD_MCFL_CNL_185PUC_FMI_final_SC
2150.032	2151.236	63.75	8.125	North	FMI_TLD_MCFL_CNL_185PUC_FMI_final_SC
2152.114	2153.117	52.5	182.5	North	FMI_TLD_MCFL_CNL_185PUC_FMI_final_SC
2152.114	2153.117	52.5	2.5	North	FMI_TLD_MCFL_CNL_185PUC_FMI_final_SC
2160.253	2161.848	80	166.25	North	FMI_TLD_MCFL_CNL_185PUC_FMI_final_SC
2160.253	2161.848	80	346.25	North	FMI_TLD_MCFL_CNL_185PUC_FMI_final_SC
2366.634	2367.207	43.75	176.875	North	FMI_TLD_MCFL_CNL_185PUC_FMI_final_SC
2366.634	2367.207	43.75	356.875	North	FMI_TLD_MCFL_CNL_185PUC_FMI_final_SC
2367.437	2367.637	40	176.25	North	FMI_TLD_MCFL_CNL_185PUC_FMI_final_SC
2367.437	2367.637	40	356.25	North	FMI_TLD_MCFL_CNL_185PUC_FMI_final_SC
2367.714	2367.952	41.25	169.375	North	FMI_TLD_MCFL_CNL_185PUC_FMI_final_SC
2367.714	2367.952	41.25	349.375	North	FMI_TLD_MCFL_CNL_185PUC_FMI_final_SC
2368.774	2369.529	32.5	178.75	North	FMI_TLD_MCFL_CNL_185PUC_FMI_final_SC
2368.774	2369.529	32.5	358.75	North	FMI_TLD_MCFL_CNL_185PUC_FMI_final_SC
2368.077	2368.506	36.25	175.625	North	FMI_TLD_MCFL_CNL_185PUC_FMI_final_SC
2368.077	2368.506	36.25	355.625	North	FMI_TLD_MCFL_CNL_185PUC_FMI_final_SC
2498.21	2499.022	37.5	172.5	North	FMI_TLD_MCFL_CNL_185PUC_FMI_final_SC
2498.21	2499.022	37.5	352.5	North	FMI_TLD_MCFL_CNL_185PUC_FMI_final_SC
2499.213	2499.748	38.75	175.625	North	FMI_TLD_MCFL_CNL_185PUC_FMI_final_SC
2499.213	2499.748	38.75	355.625	North	FMI_TLD_MCFL_CNL_185PUC_FMI_final_SC
2524.46	2525.167	47.5	180	North	FMI_TLD_MCFL_CNL_185PUC_FMI_final_SC
2524.46	2525.167	47.5	0	North	FMI_TLD_MCFL_CNL_185PUC_FMI_final_SC

2605.446	2606.124	50	180	North	FMI_TLD_MCFL_CNL_185PUC_FMI_final_SC
2605.446	2606.124	50	0	North	FMI_TLD_MCFL_CNL_185PUC_FMI_final_SC
2606.344	2606.65	40	186.25	North	FMI_TLD_MCFL_CNL_185PUC_FMI_final_SC
2606.344	2606.65	40	6.25	North	FMI_TLD_MCFL_CNL_185PUC_FMI_final_SC
2606.707	2607.223	41.25	189.375	North	FMI_TLD_MCFL_CNL_185PUC_FMI_final_SC
2606.707	2607.223	41.25	9.375	North	FMI_TLD_MCFL_CNL_185PUC_FMI_final_SC
2607.519	2608.226	41.25	184.375	North	FMI_TLD_MCFL_CNL_185PUC_FMI_final_SC
2607.519	2608.226	41.25	4.375	North	FMI_TLD_MCFL_CNL_185PUC_FMI_final_SC
2608.302	2609.745	43.75	184.375	North	FMI_TLD_MCFL_CNL_185PUC_FMI_final_SC
2608.302	2609.745	43.75	4.375	North	FMI_TLD_MCFL_CNL_185PUC_FMI_final_SC
2609.85	2613.852	41.25	186.875	North	FMI_TLD_MCFL_CNL_185PUC_FMI_final_SC
2609.85	2613.852	41.25	6.875	North	FMI_TLD_MCFL_CNL_185PUC_FMI_final_SC
2613.929	2614.483	41.25	185.625	North	FMI_TLD_MCFL_CNL_185PUC_FMI_final_SC
2613.929	2614.483	41.25	5.625	North	FMI_TLD_MCFL_CNL_185PUC_FMI_final_SC
2614.721	2615.839	43.75	188.125	North	FMI_TLD_MCFL_CNL_185PUC_FMI_final_SC
2614.721	2615.839	43.75	8.125	North	FMI_TLD_MCFL_CNL_185PUC_FMI_final_SC
2615.992	2619.087	41.25	185.625	North	FMI_TLD_MCFL_CNL_185PUC_FMI_final_SC
2615.992	2619.087	41.25	5.625	North	FMI_TLD_MCFL_CNL_185PUC_FMI_final_SC
2619.201	2620.386	37.5	183.75	North	FMI_TLD_MCFL_CNL_185PUC_FMI_final_SC
2619.201	2620.386	37.5	363.75	North	FMI_TLD_MCFL_CNL_185PUC_FMI_final_SC
2620.787	2624.379	45	180	North	FMI_TLD_MCFL_CNL_185PUC_FMI_final_SC
2620.787	2624.379	45	360	North	FMI_TLD_MCFL_CNL_185PUC_FMI_final_SC
2624.541	2626.165	36.25	181.875	North	FMI_TLD_MCFL_CNL_185PUC_FMI_final_SC
2624.541	2626.165	36.25	1.875	North	FMI_TLD_MCFL_CNL_185PUC_FMI_final_SC
2626.337	2627.063	37.5	183.75	North	FMI_TLD_MCFL_CNL_185PUC_FMI_final_SC
2626.337	2627.063	37.5	3.75	North	FMI_TLD_MCFL_CNL_185PUC_FMI_final_SC
2627.34	2631.066	42.5	183.75	North	FMI_TLD_MCFL_CNL_185PUC_FMI_final_SC
2627.34	2631.066	42.5	3.75	North	FMI_TLD_MCFL_CNL_185PUC_FMI_final_SC
2631.199	2631.667	33.75	183.125	North	FMI_TLD_MCFL_CNL_185PUC_FMI_final_SC
2631.199	2631.667	33.75	3.125	North	FMI_TLD_MCFL_CNL_185PUC_FMI_final_SC
2631.677	2632.919	40	188.75	North	FMI_TLD_MCFL_CNL_185PUC_FMI_final_SC
2631.677	2632.919	40	8.75	North	FMI_TLD_MCFL_CNL_185PUC_FMI_final_SC
2633.024	2636.205	28.75	190.625	North	FMI_TLD_MCFL_CNL_185PUC_FMI_final_SC
2633.024	2636.205	28.75	10.625	North	FMI_TLD_MCFL_CNL_185PUC_FMI_final_SC
2636.32	2637.351	35	191.25	North	FMI_TLD_MCFL_CNL_185PUC_FMI_final_SC
2636.32	2637.351	35	11.25	North	FMI_TLD_MCFL_CNL_185PUC_FMI_final_SC
2637.6	2638.44	48.75	184.375	North	FMI_TLD_MCFL_CNL_185PUC_FMI_final_SC
2637.6	2638.44	48.75	4.375	North	FMI_TLD_MCFL_CNL_185PUC_FMI_final_SC
2638.574	2640.418	41.25	183.125	North	FMI_TLD_MCFL_CNL_185PUC_FMI_final_SC
2638.574	2640.418	41.25	3.125	North	FMI_TLD_MCFL_CNL_185PUC_FMI_final_SC
2640.609	2643.981	41.25	185.625	North	FMI_TLD_MCFL_CNL_185PUC_FMI_final_SC
2640.609	2643.981	41.25	5.625	North	FMI_TLD_MCFL_CNL_185PUC_FMI_final_SC
2644.153	2645.127	35	187.5	North	FMI_TLD_MCFL_CNL_185PUC_FMI_final_SC
2644.153	2645.127	35	7.5	North	FMI_TLD_MCFL_CNL_185PUC_FMI_final_SC

2645.222	2646.178	47.5	187.5	North	FMI_TLD_MCFL_CNL_185PUC_FMI_final_SC
2645.222	2646.178	47.5	7.5	North	FMI_TLD_MCFL_CNL_185PUC_FMI_final_SC
2646.464	2647.849	50	182.5	North	FMI_TLD_MCFL_CNL_185PUC_FMI_final_SC
2646.464	2647.849	50	2.5	North	FMI_TLD_MCFL_CNL_185PUC_FMI_final_SC
2648.222	2648.442	22.5	185	North	FMI_TLD_MCFL_CNL_185PUC_FMI_final_SC
2648.222	2648.442	22.5	5	North	FMI_TLD_MCFL_CNL_185PUC_FMI_final_SC
2648.575	2648.852	35	188.75	North	FMI_TLD_MCFL_CNL_185PUC_FMI_final_SC
2648.575	2648.852	35	8.75	North	FMI_TLD_MCFL_CNL_185PUC_FMI_final_SC
2649.378	2649.951	40	185	North	FMI_TLD_MCFL_CNL_185PUC_FMI_final_SC
2649.378	2649.951	40	5	North	FMI_TLD_MCFL_CNL_185PUC_FMI_final_SC
2650.161	2650.715	37.5	181.25	North	FMI_TLD_MCFL_CNL_185PUC_FMI_final_SC
2650.161	2650.715	37.5	1.25	North	FMI_TLD_MCFL_CNL_185PUC_FMI_final_SC
2650.868	2651.441	36.25	185.625	North	FMI_TLD_MCFL_CNL_185PUC_FMI_final_SC
2650.868	2651.441	36.25	5.625	North	FMI_TLD_MCFL_CNL_185PUC_FMI_final_SC
2652.033	2654.565	35	188.75	North	FMI_TLD_MCFL_CNL_185PUC_FMI_final_SC
2652.033	2654.565	35	8.75	North	FMI_TLD_MCFL_CNL_185PUC_FMI_final_SC
2654.87	2656.494	47.5	182.5	North	FMI_TLD_MCFL_CNL_185PUC_FMI_final_SC
2654.87	2656.494	47.5	362.5	North	FMI_TLD_MCFL_CNL_185PUC_FMI_final_SC
2656.714	2660.764	55	183.75	North	FMI_TLD_MCFL_CNL_185PUC_FMI_final_SC
2656.714	2660.764	55	3.75	North	FMI_TLD_MCFL_CNL_185PUC_FMI_final_SC
2661.041	2661.548	40	187.5	North	FMI_TLD_MCFL_CNL_185PUC_FMI_final_SC
2661.041	2661.548	40	7.5	North	FMI_TLD_MCFL_CNL_185PUC_FMI_final_SC
2661.806	2663.955	46.25	185.625	North	FMI_TLD_MCFL_CNL_185PUC_FMI_final_SC
2661.806	2663.955	46.25	5.625	North	FMI_TLD_MCFL_CNL_185PUC_FMI_final_SC
2664.108	2664.7	47.5	183.75	North	FMI_TLD_MCFL_CNL_185PUC_FMI_final_SC
2664.108	2664.7	47.5	3.75	North	FMI_TLD_MCFL_CNL_185PUC_FMI_final_SC
2664.872	2666.295	48.75	190.625	North	FMI_TLD_MCFL_CNL_185PUC_FMI_final_SC
2664.872	2666.295	48.75	10.625	North	FMI_TLD_MCFL_CNL_185PUC_FMI_final_SC
2666.83	2669.419	53.75	194.375	North	FMI_TLD_MCFL_CNL_185PUC_FMI_final_SC
2666.83	2669.419	53.75	14.375	North	FMI_TLD_MCFL_CNL_185PUC_FMI_final_SC
2669.944	2670.842	55	191.25	North	FMI_TLD_MCFL_CNL_185PUC_FMI_final_SC
2669.944	2670.842	55	11.25	North	FMI_TLD_MCFL_CNL_185PUC_FMI_final_SC
2671.396	2674.004	61.25	195.625	North	FMI_TLD_MCFL_CNL_185PUC_FMI_final_SC
2671.396	2674.004	61.25	15.625	North	FMI_TLD_MCFL_CNL_185PUC_FMI_final_SC
2674.319	2675.017	61.25	195.625	North	FMI_TLD_MCFL_CNL_185PUC_FMI_final_SC
2674.319	2675.017	61.25	15.625	North	FMI_TLD_MCFL_CNL_185PUC_FMI_final_SC
2675.38	2677.137	62.5	196.25	North	FMI_TLD_MCFL_CNL_185PUC_FMI_final_SC
2675.38	2677.137	62.5	16.25	North	FMI_TLD_MCFL_CNL_185PUC_FMI_final_SC
2678.541	2681.474	56.25	198.125	North	FMI_TLD_MCFL_CNL_185PUC_FMI_final_SC
2678.541	2681.474	56.25	18.125	North	FMI_TLD_MCFL_CNL_185PUC_FMI_final_SC
2682.105	2682.754	58.75	193.125	North	FMI_TLD_MCFL_CNL_185PUC_FMI_final_SC
2682.105	2682.754	58.75	13.125	North	FMI_TLD_MCFL_CNL_185PUC_FMI_final_SC
2681.55	2682.047	63.75	195.625	North	FMI_TLD_MCFL_CNL_185PUC_FMI_final_SC
2681.55	2682.047	63.75	15.625	North	FMI_TLD_MCFL_CNL_185PUC_FMI_final_SC

2684.388	2686.021	53.75	194.375	North	FMI_TLD_MCFL_CNL_185PUC_FMI_final_SC
2684.388	2686.021	53.75	14.375	North	FMI_TLD_MCFL_CNL_185PUC_FMI_final_SC

HOVEA 12: TOTAL INTERPRETED BREAKOUT SET

Top Depth (m)	Bottom Depth (m)	Width (deg)	Azimuth (deg)	Apparent Mode	Image Log
2187.524	2190.453	66.25	43.125	North	FMI_005PUP_FMI
2187.524	2190.453	66.25	223.125	North	FMI_005PUP_FMI
2194.295	2199.132	96.25	50.625	North	FMI_005PUP_FMI
2194.295	2199.132	96.25	230.625	North	FMI_005PUP_FMI
2292.777	2295.549	78.75	185.625	North	FMI_005PUP_FMI
2292.777	2295.549	78.75	5.625	North	FMI_005PUP_FMI
2306.202	2307.68	68.75	185.625	North	FMI_005PUP_FMI
2306.202	2307.68	68.75	5.625	North	FMI_005PUP_FMI

JINGEMIA 2: TOTAL INTERPRETED BREAKOUT SET

Top Depth (m)	Bottom Depth (m)	Width (deg)	Azimuth (deg)	Apparent Mode	Image Log
2124.095	2126.068	65.86751	78.35962	North	FMI
2124.095	2126.068	65.86751	258.3596	North	FMI
2144.2	2146.437	57.91798	168.6435	North	FMI
2144.2	2146.437	57.91798	348.6435	North	FMI
2166.283	2167.162	72.68139	169.2114	North	FMI
2166.283	2167.162	72.68139	349.2114	North	FMI
2477.476	2478.78	64.73186	173.1861	North	FMI
2477.476	2478.78	64.73186	353.1861	North	FMI
2504.777	2505.187	51.1041	170.9148	North	FMI
2504.777	2505.187	51.1041	350.9148	North	FMI
2505.365	2508.906	43.15457	169.2114	North	FMI
2505.365	2508.906	43.15457	349.2114	North	FMI
2509.525	2510.929	31.79811	182.8391	North	FMI
2509.525	2510.929	31.79811	2.839117	North	FMI
2511.275	2512.911	55.64669	169.7792	North	FMI
2511.275	2512.911	55.64669	349.7792	North	FMI
2513.13	2514.625	63.59621	183.9748	North	FMI
2513.13	2514.625	63.59621	3.974763	North	FMI
2514.757	2515.809	73.81703	164.1009	North	FMI
2514.757	2515.809	73.81703	344.1009	North	FMI
2515.914	2521.104	52.23975	172.6183	North	FMI

2515.914	2521.104	52.23975	352.6183	North	FMI
2521.237	2522.121	57.91798	183.4069	North	FMI
2521.237	2522.121	57.91798	3.40694	North	FMI
2522.531	2524.317	52.23975	177.1609	North	FMI
2522.531	2524.317	52.23975	357.1609	North	FMI
2525.32	2526.669	52.23975	178.2965	North	FMI
2525.32	2526.669	52.23975	358.2965	North	FMI
2527.065	2527.835	60.18927	185.6782	North	FMI
2527.065	2527.835	60.18927	5.678233	North	FMI
2527.981	2552.958	59.05363	171.4826	North	FMI
2527.981	2552.958	59.05363	351.4826	North	FMI
2553.026	2553.258	38.61199	181.7035	North	FMI
2553.026	2553.258	38.61199	1.70347	North	FMI
2553.29	2553.723	48.83281	180	North	FMI
2553.29	2553.723	48.83281	0	North	FMI
2553.901	2568.601	51.1041	177.7287	North	FMI
2553.901	2568.601	51.1041	357.7287	North	FMI
2568.684	2579.433	70.41009	178.2965	North	FMI
2568.684	2579.433	70.41009	358.2965	North	FMI
2579.543	2585.585	57.91798	182.2713	North	FMI
2579.543	2585.585	57.91798	2.271293	North	FMI
2585.854	2586.56	52.23975	191.9243	North	FMI
2585.854	2586.56	52.23975	11.92429	North	FMI
2586.884	2589.892	65.86751	182.8391	North	FMI
2586.884	2589.892	65.86751	2.839117	North	FMI
2590.434	2605.207	52.23975	177.1609	North	FMI
2590.434	2605.207	52.23975	357.1609	North	FMI

JINGEMIA 3: TOTAL INTERPRETED BREAKOUT SET

Top Depth (m)	Bottom Depth (m)	Width (deg)	Azimuth (deg)	Apparent Mode	Image Log
1898.529	1901.308	87.5	187.5	North	FMI_007PUC_FMI
1898.529	1901.308	87.5	7.5	North	FMI_007PUC_FMI
1906.331	1910.572	90	173.75	North	FMI_007PUC_FMI
1906.331	1910.572	90	353.75	North	FMI_007PUC_FMI
1911.136	1919.114	93.75	170.625	North	FMI_007PUC_FMI
1911.136	1919.114	93.75	350.625	North	FMI_007PUC_FMI
1920.691	1922.16	83.75	210.625	North	FMI_007PUC_FMI
1920.691	1922.16	83.75	30.625	North	FMI_007PUC_FMI
1922.651	1923.646	110	223.75	North	FMI_007PUC_FMI
1922.651	1923.646	110	43.75	North	FMI_007PUC_FMI
1924.144	1925.442	61.25	165.625	North	FMI_007PUC_FMI
1924.144	1925.442	61.25	345.625	North	FMI_007PUC_FMI
1991.152	1994.258	80	180	North	FMI_007PUC_FMI

1991.152	1994.258	80	0	North	FMI_007PUC_FMI
1997.304	1999.452	78.75	165.625	North	FMI_007PUC_FMI
1997.304	1999.452	78.75	345.625	North	FMI_007PUC_FMI

Drilling Induced Tensile Fractures

DRAKEA 1: TOTAL INTERPRETED DITF SET

Top Depth (m)	Bottom Depth (m)	Width (deg)	Azimuth (deg)	Apparent Mode	Image Log
1643.463001	1644.377	83.75	136.875	North	FMI_SONIC_004PUP_FMI
1643.463001	1644.377	83.75	316.875	North	FMI_SONIC_004PUP_FMI
2838.856575	2840.636	92.5	80	North	FMI_SONIC_004PUP_FMI
2838.856575	2840.636	92.5	260	North	FMI_SONIC_004PUP_FMI
3010.77679	3013.385	57.5	75	North	FMI_SONIC_004PUP_FMI
3010.77679	3013.385	57.5	255	North	FMI_SONIC_004PUP_FMI
3014.387259	3015.565	72.5	81.25	North	FMI_SONIC_004PUP_FMI
3014.387259	3015.565	72.5	261.25	North	FMI_SONIC_004PUP_FMI
3016.674809	3017.801	65	70	North	FMI_SONIC_004PUP_FMI
3016.674809	3017.801	65	250	North	FMI_SONIC_004PUP_FMI
3024.553763	3025.698	87.5	71.25	North	FMI_SONIC_004PUP_FMI
3024.553763	3025.698	87.5	251.25	North	FMI_SONIC_004PUP_FMI
3039.708778	3044.363	73.75	68.125	North	FMI_SONIC_004PUP_FMI
3039.708778	3044.363	73.75	248.125	North	FMI_SONIC_004PUP_FMI
3048.307759	3049.448	76.25	71.875	North	FMI_SONIC_004PUP_FMI
3048.307759	3049.448	76.25	251.875	North	FMI_SONIC_004PUP_FMI
3058.326123	3059.725	76.25	70.625	North	FMI_SONIC_004PUP_FMI
3058.326123	3059.725	76.25	250.625	North	FMI_SONIC_004PUP_FMI
3062.725522	3064.128	81.25	81.875	North	FMI_SONIC_004PUP_FMI
3062.725522	3064.128	81.25	261.875	North	FMI_SONIC_004PUP_FMI
3065.443709	3066.016	73.75	78.125	North	FMI_SONIC_004PUP_FMI
3065.443709	3066.016	73.75	258.125	North	FMI_SONIC_004PUP_FMI
3066.236083	3067.204	66.25	78.125	North	FMI_SONIC_004PUP_FMI
3066.236083	3067.204	66.25	258.125	North	FMI_SONIC_004PUP_FMI
3067.362632	3068.589	66.25	85.625	North	FMI_SONIC_004PUP_FMI
3067.362632	3068.589	66.25	265.625	North	FMI_SONIC_004PUP_FMI

EVANDRA 1: TOTAL INTERPRETED DITF SET

Top Depth (m)	Bottom Depth (m)	Width (deg)	Azimuth (deg)	Apparent Mode	Image Log
2234.2	2243.617	61.25	101.875	North	FMI_079PUP_FMI
2234.2	2243.617	61.25	281.875	North	FMI_079PUP_FMI
2239.785	2243.32	55	95	North	FMI_079PUP_FMI
2239.785	2243.32	55	275	North	FMI_079PUP_FMI
2251.074	2253.465	48.75	91.875	North	FMI_079PUP_FMI
2251.074	2253.465	48.75	271.875	North	FMI_079PUP_FMI
2254.049	2255.301	56.25	93.125	North	FMI_079PUP_FMI
2254.049	2255.301	56.25	273.125	North	FMI_079PUP_FMI
2255.485	2256.358	78.75	108.125	North	FMI_079PUP_FMI
2255.485	2256.358	78.75	288.125	North	FMI_079PUP_FMI
2268.158	2269.496	68.75	108.125	North	FMI_079PUP_FMI
2268.158	2269.496	68.75	288.125	North	FMI_079PUP_FMI
2274.016	2275.209	60	133.75	North	FMI_079PUP_FMI
2274.016	2275.209	60	313.75	North	FMI_079PUP_FMI

HOVEA 9: TOTAL INTERPRETED DITF SET

Top Depth (m)	Bottom Depth (m)	Width (deg)	Azimuth (deg)	Apparent Mode	Image Log
2190.79	2192.686	54.51104	89.71609	North	FMI
2190.79	2192.686	54.51104	269.7161	North	FMI
2238.26	2242.065	78.35962	80.06309	North	FMI
2238.26	2242.065	78.35962	260.0631	North	FMI
2373.437	2377.442	45.42587	84.03785	North	FMI
2373.437	2377.442	45.42587	264.0379	North	FMI
2396.313	2399.762	49.96845	81.76656	North	FMI
2396.313	2399.762	49.96845	261.7666	North	FMI
2400.318	2401.808	53.37539	85.74132	North	FMI
2400.318	2401.808	53.37539	265.7413	North	FMI
2402.187	2403.376	62.46057	85.74132	North	FMI
2402.187	2403.376	62.46057	265.7413	North	FMI
2403.599	2408.489	52.23975	77.22397	North	FMI
2403.599	2408.489	52.23975	257.224	North	FMI
2293.491	2294.332	43.75	188.125	North	FMI
2293.491	2294.332	43.75	8.125	North	FMI
2417.625	2423.376	36.25	81.875	North	FMI
2417.625	2423.376	36.25	261.875	North	FMI
2423.596	2425.554	43.75	86.875	North	FMI
2423.596	2425.554	43.75	266.875	North	FMI

JINGEMIA 2: TOTAL INTERPRETED DITF SET

Top Depth (m)	Bottom Depth (m)	Width (deg)	Azimuth (deg)	Apparent Mode	Image Log
2190.79	2192.686	54.51104	89.71609	North	FMI
2190.79	2192.686	54.51104	269.7161	North	FMI
2238.26	2242.065	78.35962	80.06309	North	FMI
2238.26	2242.065	78.35962	260.0631	North	FMI
2373.437	2377.442	45.42587	84.03785	North	FMI
2373.437	2377.442	45.42587	264.0379	North	FMI
2396.313	2399.762	49.96845	81.76656	North	FMI
2396.313	2399.762	49.96845	261.7666	North	FMI
2400.318	2401.808	53.37539	85.74132	North	FMI
2400.318	2401.808	53.37539	265.7413	North	FMI
2402.187	2403.376	62.46057	85.74132	North	FMI
2402.187	2403.376	62.46057	265.7413	North	FMI
2403.599	2408.489	52.23975	77.22397	North	FMI
2403.599	2408.489	52.23975	257.224	North	FMI

JINGEMIA 3: TOTAL INTERPRETED DITF SET

Top Depth (m)	Bottom Depth (m)	Width (deg)	Azimuth (deg)	Apparent Mode	Image Log
2033.553	2036.18	68.75	69.375	North	FMI_007PUC_FMI
2033.553	2036.18	68.75	249.375	North	FMI_007PUC_FMI
2103.195	2107.12	72.5	91.25	North	FMI_007PUC_FMI
2103.195	2107.12	72.5	271.25	North	FMI_007PUC_FMI
2293.021	2299.44	46.25	79.375	North	FMI_007PUC_FMI
2293.021	2299.44	46.25	259.375	North	FMI_007PUC_FMI
2306.289	2309.044	38.75	88.125	North	FMI_007PUC_FMI
2306.289	2309.044	38.75	268.125	North	FMI_007PUC_FMI
2349.85	2352.731	63.75	98.125	North	FMI_007PUC_FMI
2349.85	2352.731	63.75	278.125	North	FMI_007PUC_FMI
2352.798	2355.419	73.75	104.375	North	FMI_007PUC_FMI
2352.798	2355.419	73.75	284.375	North	FMI_007PUC_FMI
2356.99	2360.066	76.25	94.375	North	FMI_007PUC_FMI
2356.99	2360.066	76.25	274.375	North	FMI_007PUC_FMI
2571.406	2573.857	91.25	85.625	North	FMI_007PUC_FMI
2571.406	2573.857	91.25	265.625	North	FMI_007PUC_FMI

APPENDIX E: FULL FRACTURE SETS

Drakea 1: Total interpreted fracture set

Top Depth (m)	Bottom Depth (m)	Depth (m)	True Dip (deg)	True Azimuth (deg)	Surface Type	Apparent Mode	Image Log
826.4158458	826.4996	826.4577	21.34389	233.9074	RFracC	North	FMI_SONIC_004PUP_FMI
830.5597638	830.6435	830.6017	26.35421	310.042	ConFracC	North	FMI_SONIC_004PUP_FMI
830.5868482	830.6706	830.6287	26.16192	304.7157	ConFracC	North	FMI_SONIC_004PUP_FMI
838.5699845	838.6944	838.6322	27.74845	191.0453	RFracC	North	FMI_SONIC_004PUP_FMI
839.2606375	839.3106	839.2856	11.87309	75.79223	RFracC	North	FMI_SONIC_004PUP_FMI
839.3148064	839.4189	839.3669	24.56265	212.8015	RFracC	North	FMI_SONIC_004PUP_FMI
839.5416385	839.7744	839.658	47.2706	225.0502	ConFracC	North	FMI_SONIC_004PUP_FMI
841.4341631	841.5789	841.5065	38.82065	299.413	RFracC	North	FMI_SONIC_004PUP_FMI
842.7139025	842.8586	842.7863	32.84278	210.2405	ConFracC	North	FMI_SONIC_004PUP_FMI
849.3089617	849.4537	849.3813	36.44809	41.06552	RFracC	North	FMI_SONIC_004PUP_FMI
849.3157328	849.4131	849.3644	26.78197	37.46389	RFracC	North	FMI_SONIC_004PUP_FMI
849.5831915	849.8159	849.6996	48.8855	247.1976	RFracC	North	FMI_SONIC_004PUP_FMI
858.9442482	859.177	859.0606	51.34779	289.5876	RFracC	North	FMI_SONIC_004PUP_FMI
859.2049359	859.3971	859.301	43.80966	48.66818	RFracC	North	FMI_SONIC_004PUP_FMI
859.4182258	859.5291	859.4737	26.63686	86.23691	RFracC	North	FMI_SONIC_004PUP_FMI
861.1617861	861.2726	861.2172	32.08144	340.1562	ConFracC	North	FMI_SONIC_004PUP_FMI
861.1279305	861.2388	861.1834	32.13037	327.8552	ConFracC	North	FMI_SONIC_004PUP_FMI
862.0284879	862.2071	862.1178	41.21243	245.4618	ConFracC	North	FMI_SONIC_004PUP_FMI
864.3069657	864.5194	864.4132	49.16327	314.6245	ConFracC	North	FMI_SONIC_004PUP_FMI
864.5304123	864.6345	864.5825	29.97402	310.9484	ConFracC	North	FMI_SONIC_004PUP_FMI
869.9134431	870.0852	869.9993	36.70214	149.9714	RFracC	North	FMI_SONIC_004PUP_FMI
869.9202142	870.092	870.0061	42.4543	291.1686	RFracC	North	FMI_SONIC_004PUP_FMI
869.943913	870.1157	870.0298	38.70224	81.3245	RFracC	North	FMI_SONIC_004PUP_FMI
869.9472986	870.1326	870.04	40.94021	220.9398	RFracC	North	FMI_SONIC_004PUP_FMI
869.7678642	869.8652	869.8165	28.59697	319.965	RFracC	North	FMI_SONIC_004PUP_FMI
869.6392132	869.7027	869.6709	13.95726	156.0657	RFracC	North	FMI_SONIC_004PUP_FMI
869.595201	869.6925	869.6439	27.97303	6.038721	RFracC	North	FMI_SONIC_004PUP_FMI
869.7069243	869.8042	869.7556	27.802	10.60104	RFracC	North	FMI_SONIC_004PUP_FMI
869.7373942	869.8347	869.7861	28.64627	334.5042	RFracC	North	FMI_SONIC_004PUP_FMI
869.8423464	870.0141	869.9282	37.78757	100.737	RFracC	North	FMI_SONIC_004PUP_FMI
872.3781263	872.4077	872.3929	6.907829	228.5169	RFracC	North	FMI_SONIC_004PUP_FMI
871.006977	871.1314	871.0692	30.24744	225.2491	ConFracC	North	FMI_SONIC_004PUP_FMI
876.7996598	876.809	876.8043	0.323615	331.0505	RFracC	North	FMI_SONIC_004PUP_FMI
876.8165876	876.8259	876.8212	0.350134	312.2286	RFracC	North	FMI_SONIC_004PUP_FMI
876.8301298	876.8597	876.8449	5.803037	194.6738	RFracC	North	FMI_SONIC_004PUP_FMI
877.3210351	877.3506	877.3358	6.859472	225.6004	RFracC	North	FMI_SONIC_004PUP_FMI
877.6697472	877.7197	877.6947	11.63891	104.8163	RFracC	North	FMI_SONIC_004PUP_FMI
883.4962855	883.5462	883.5212	13.75781	251.1704	ConFracC	North	FMI_SONIC_004PUP_FMI

882.9545969	883.0045	882.9796	15.56181	291.3289	ConFracC	North	FMI_SONIC_004PUP_FMI
888.0701689	888.33	888.2001	54.26901	316.8675	RFracC	North	FMI_SONIC_004PUP_FMI
892.4705267	892.5493	892.5099	22.2139	276.8827	RFracC	North	FMI_SONIC_004PUP_FMI
892.4535989	892.5459	892.4997	25.78329	285.5517	RFracC	North	FMI_SONIC_004PUP_FMI
894.8370289	894.9835	894.9102	36.80926	279.1027	ConFracC	North	FMI_SONIC_004PUP_FMI
895.0063066	895.1527	895.0795	34.51839	223.1518	ConFracC	North	FMI_SONIC_004PUP_FMI
897.9652808	898.0508	898.008	24.13529	286.8532	RFracC	North	FMI_SONIC_004PUP_FMI
898.0431485	898.1286	898.0859	23.88394	279.7814	RFracC	North	FMI_SONIC_004PUP_FMI
909.9467562	910.0593	910.003	27.89731	88.87048	RFracC	North	FMI_SONIC_004PUP_FMI
914.1922409	914.2371	914.2147	13.86206	298.635	RFracC	North	FMI_SONIC_004PUP_FMI
916.3352966	916.3599	916.3476	7.010765	261.5096	RFracC	North	FMI_SONIC_004PUP_FMI
919.6836094	919.7488	919.7162	17.0878	80.26318	RFracC	North	FMI_SONIC_004PUP_FMI
919.6091273	919.6743	919.6417	17.09231	233.4856	RFracC	North	FMI_SONIC_004PUP_FMI
919.4567773	919.522	919.4894	15.77162	139.3977	RFracC	North	FMI_SONIC_004PUP_FMI
919.4737051	919.5389	919.5063	18.77712	284.8225	RFracC	North	FMI_SONIC_004PUP_FMI
920.9938188	921.059	921.0264	18.68607	281.3467	ConFracC	North	FMI_SONIC_004PUP_FMI
921.4610253	921.5262	921.4936	16.16011	200.567	RFracC	North	FMI_SONIC_004PUP_FMI
921.6641585	921.7293	921.6968	16.31737	207.322	RFracC	North	FMI_SONIC_004PUP_FMI
921.9553161	922.0205	921.9879	19.61986	339.6921	RFracC	North	FMI_SONIC_004PUP_FMI
924.362445	924.475	924.4187	27.01126	183.022	RFracC	North	FMI_SONIC_004PUP_FMI
931.1233963	931.2902	931.2068	39.17933	238.8041	ConFracC	North	FMI_SONIC_004PUP_FMI
934.586818	934.7671	934.677	39.7964	187.9237	ConFracC	North	FMI_SONIC_004PUP_FMI
938.0807097	938.1459	938.1133	18.80017	266.8205	ConFracC	North	FMI_SONIC_004PUP_FMI
938.7171938	938.8162	938.7667	27.90011	306.1626	RFracC	North	FMI_SONIC_004PUP_FMI
1000.791326	1000.924	1000.858	34.63055	209.8481	ConFracC	North	FMI_SONIC_004PUP_FMI
1002.528115	1002.661	1002.595	37.23621	256.9412	RFracC	North	FMI_SONIC_004PUP_FMI
1003.20184	1003.301	1003.251	28.55504	224.4886	RFracC	North	FMI_SONIC_004PUP_FMI
1003.71983	1003.819	1003.769	23.06328	150.5142	RFracC	North	FMI_SONIC_004PUP_FMI
1005.974609	1006.04	1006.007	22.29475	272.4954	RFracC	North	FMI_SONIC_004PUP_FMI
1006.001693	1006.067	1006.034	16.41367	10.2877	RFracC	North	FMI_SONIC_004PUP_FMI
1028.637507	1029.028	1028.833	68.28997	268.6581	ConFracC	North	FMI_SONIC_004PUP_FMI
1028.786471	1029.177	1028.982	68.15633	254.3615	ConFracC	North	FMI_SONIC_004PUP_FMI
1028.674748	1029.065	1028.87	68.28438	269.8492	ConFracC	North	FMI_SONIC_004PUP_FMI
1032.673087	1032.941	1032.807	47.6996	124.3473	RFracC	North	FMI_SONIC_004PUP_FMI
1045.846278	1045.952	1045.899	33.84308	280.0552	ConFracC	North	FMI_SONIC_004PUP_FMI
1071.46815	1071.554	1071.511	26.95458	207.7135	RFracC	North	FMI_SONIC_004PUP_FMI
1081.056039	1081.196	1081.126	41.66361	272.6037	RFracC	North	FMI_SONIC_004PUP_FMI
1081.232088	1081.318	1081.275	29.9122	273.5952	RFracC	North	FMI_SONIC_004PUP_FMI
1081.861801	1081.941	1081.901	21.51541	176.728	ConFracC	North	FMI_SONIC_004PUP_FMI
1081.886362	1082.038	1081.962	29.03207	95.57671	ConFracC	North	FMI_SONIC_004PUP_FMI
1088.711639	1088.802	1088.757	26.74646	189.9319	ConFracC	North	FMI_SONIC_004PUP_FMI
1089.009568	1089.168	1089.089	31.40366	27.40315	ConFracC	North	FMI_SONIC_004PUP_FMI
1091.159394	1091.277	1091.218	34.66755	299.4632	RFracC	North	FMI_SONIC_004PUP_FMI
1091.210178	1091.328	1091.269	33.54325	193.1351	RFracC	North	FMI_SONIC_004PUP_FMI

1092.137819	1092.337	1092.237	44.77587	331.6755	RFracC	North	FMI_SONIC_004PUP_FMI
1103.438799	1103.441	1103.44	8.841424	249.9856	RFracC	North	FMI_SONIC_004PUP_FMI
1138.840674	1138.96	1138.9	36.88006	279.848	RFracC	North	FMI_SONIC_004PUP_FMI
1171.7855	1171.932	1171.859	45.72914	259.1531	RFracC	North	FMI_SONIC_004PUP_FMI
1174.866354	1174.965	1174.916	22.84401	143.6583	RFracC	North	FMI_SONIC_004PUP_FMI
1203.558923	1203.902	1203.73	46.5979	60.92736	RFracC	North	FMI_SONIC_004PUP_FMI
1210.0795	1210.348	1210.214	40.88753	79.44919	RFracC	North	FMI_SONIC_004PUP_FMI
1210.434984	1211.299	1210.867	89.06282	245.9534	RFracC	North	FMI_SONIC_004PUP_FMI
1212.46293	1212.955	1212.709	54.8169	59.183	RFracC	North	FMI_SONIC_004PUP_FMI
1213.400729	1213.892	1213.647	54.95632	64.8131	RFracC	North	FMI_SONIC_004PUP_FMI
1216.996187	1217.488	1217.242	56.41939	87.08183	RFracC	North	FMI_SONIC_004PUP_FMI
1217.598816	1217.948	1217.774	47.02738	59.26502	RFracC	North	FMI_SONIC_004PUP_FMI
1218.150661	1218.243	1218.197	36.7539	230.1469	RFracC	North	FMI_SONIC_004PUP_FMI
1218.292854	1218.385	1218.339	36.8501	235.2837	RFracC	North	FMI_SONIC_004PUP_FMI
1220.872646	1221.06	1220.966	30.09972	69.87037	RFracC	North	FMI_SONIC_004PUP_FMI
1221.255214	1221.442	1221.349	33.84502	109.3574	RFracC	North	FMI_SONIC_004PUP_FMI
1222.060976	1222.289	1222.175	38.51058	101.2608	RFracC	North	FMI_SONIC_004PUP_FMI
1222.010193	1222.238	1222.124	39.10709	105.6079	RFracC	North	FMI_SONIC_004PUP_FMI
1224.126164	1224.212	1224.169	26.67956	177.2963	RFracC	North	FMI_SONIC_004PUP_FMI
1224.782961	1225.133	1224.958	47.89276	76.77428	RFracC	North	FMI_SONIC_004PUP_FMI
1225.270481	1225.607	1225.438	46.79634	75.43743	RFracC	North	FMI_SONIC_004PUP_FMI
1225.581952	1225.918	1225.75	64.17759	296.4171	ConFracC	North	FMI_SONIC_004PUP_FMI
1225.971291	1226.152	1226.061	51.59935	267.047	RFracC	North	FMI_SONIC_004PUP_FMI
1227.978924	1228.403	1228.191	76.56012	243.1678	RFracC	North	FMI_SONIC_004PUP_FMI
1227.691152	1228.081	1227.886	65.93573	165.8038	RFracC	North	FMI_SONIC_004PUP_FMI
1238.670504	1239.061	1238.866	50.85092	82.13952	RFracC	North	FMI_SONIC_004PUP_FMI
1239.303602	1239.599	1239.451	42.94206	68.31875	RFracC	North	FMI_SONIC_004PUP_FMI
1239.865604	1240.053	1239.959	29.94906	64.66541	RFracC	North	FMI_SONIC_004PUP_FMI
1240.468233	1240.676	1240.572	33.88952	83.74221	RFracC	North	FMI_SONIC_004PUP_FMI
1241.020078	1241.099	1241.059	31.57773	210.1986	RFracC	North	FMI_SONIC_004PUP_FMI
1241.395875	1242.016	1241.706	59.234	50.70484	RFracC	North	FMI_SONIC_004PUP_FMI
1243.44752	1243.784	1243.616	46.11473	57.67996	RFracC	North	FMI_SONIC_004PUP_FMI
1246.690881	1246.939	1246.815	38.07894	48.34858	RFracC	North	FMI_SONIC_004PUP_FMI
1261.604246	1261.852	1261.728	37.39645	51.61948	RFracC	North	FMI_SONIC_004PUP_FMI
1263.012637	1263.261	1263.137	43.2173	117.8634	RFracC	North	FMI_SONIC_004PUP_FMI
1262.955082	1263.142	1263.049	32.04316	99.52437	RFracC	North	FMI_SONIC_004PUP_FMI
1264.092628	1264.381	1264.237	45.18384	104.0279	RFracC	North	FMI_SONIC_004PUP_FMI
1264.180653	1264.469	1264.325	43.01493	86.71134	RFracC	North	FMI_SONIC_004PUP_FMI
1264.431184	1264.672	1264.552	46.76871	139.0523	RFracC	North	FMI_SONIC_004PUP_FMI
1265.490862	1265.671	1265.581	32.03077	107.6961	RFracC	North	FMI_SONIC_004PUP_FMI
1266.536998	1266.67	1266.603	20.2103	74.36259	ConFracC	North	FMI_SONIC_004PUP_FMI
1273.7313	1273.864	1273.798	20.51374	83.77863	RFracC	North	FMI_SONIC_004PUP_FMI
1283.237936	1283.344	1283.291	29.69147	171.0665	ConFracC	North	FMI_SONIC_004PUP_FMI
1297.135635	1297.296	1297.216	38.00873	322.6291	ConFracC	North	FMI_SONIC_004PUP_FMI

1301.479301	1301.639	1301.559	24.56283	68.70654	RFracC	North	FMI_SONIC_004PUP_FMI
1303.910128	1304.158	1304.034	36.99861	58.08495	RFracC	North	FMI_SONIC_004PUP_FMI
1303.85596	1304.104	1303.98	37.01558	62.89094	RFracC	North	FMI_SONIC_004PUP_FMI
1303.784863	1304.033	1303.909	37.107	53.2954	RFracC	North	FMI_SONIC_004PUP_FMI
1306.669355	1307.188	1306.929	55.08169	61.24261	RFracC	North	FMI_SONIC_004PUP_FMI
1311.47007	1311.894	1311.682	50.93059	58.38206	RFracC	North	FMI_SONIC_004PUP_FMI
1322.185349	1323.192	1322.689	89.05195	79.57393	RFracC	North	FMI_SONIC_004PUP_FMI
1325.601373	1326.323	1325.962	86.85942	254.3973	RFracC	North	FMI_SONIC_004PUP_FMI
1339.901953	1340.265	1340.084	50.92737	103.724	RFracC	North	FMI_SONIC_004PUP_FMI
1344.160979	1344.409	1344.285	37.24024	49.82042	RFracC	North	FMI_SONIC_004PUP_FMI
1344.171136	1344.379	1344.275	32.98134	81.00884	RFracC	North	FMI_SONIC_004PUP_FMI
1349.323949	1349.531	1349.428	36.04717	3.610952	RFracC	North	FMI_SONIC_004PUP_FMI
1349.364576	1349.572	1349.468	35.5982	6.550567	RFracC	North	FMI_SONIC_004PUP_FMI
1355.140331	1355.47	1355.305	46.56256	89.22188	RFracC	North	FMI_SONIC_004PUP_FMI
1355.370549	1355.984	1355.677	58.06536	52.21054	RFracC	North	FMI_SONIC_004PUP_FMI
1355.634622	1356.235	1355.935	57.66033	53.60387	RFracC	North	FMI_SONIC_004PUP_FMI
1355.709104	1356.133	1355.921	50.72151	56.4593	RFracC	North	FMI_SONIC_004PUP_FMI
1357.252917	1357.359	1357.306	25.77069	152.178	RFracC	North	FMI_SONIC_004PUP_FMI
1356.728156	1358.1	1357.414	85.93993	76.06013	RFracC	North	FMI_SONIC_004PUP_FMI
1358.06545	1358.686	1358.376	58.36899	46.64117	RFracC	North	FMI_SONIC_004PUP_FMI
1358.139932	1358.76	1358.45	58.66111	39.69103	RFracC	North	FMI_SONIC_004PUP_FMI
1358.268583	1358.889	1358.579	59.35428	30.03036	RFracC	North	FMI_SONIC_004PUP_FMI
1358.657922	1359.096	1358.877	53.48421	89.31392	RFracC	North	FMI_SONIC_004PUP_FMI
1358.722247	1359.16	1358.941	78.26875	241.9238	RFracC	North	FMI_SONIC_004PUP_FMI
1359.531394	1360.118	1359.825	57.78448	71.81392	RFracC	North	FMI_SONIC_004PUP_FMI
1359.697287	1360.108	1359.903	76.21927	216.6155	RFracC	North	FMI_SONIC_004PUP_FMI
1358.129775	1358.594	1358.362	78.83123	215.2372	RFracC	North	FMI_SONIC_004PUP_FMI
1359.121742	1359.519	1359.32	49.31074	62.35697	RFracC	North	FMI_SONIC_004PUP_FMI
1358.434475	1358.987	1358.711	56.20171	50.78216	RFracC	North	FMI_SONIC_004PUP_FMI
1360.428566	1360.866	1360.647	51.45278	50.71806	RFracC	North	FMI_SONIC_004PUP_FMI
1360.333771	1361.151	1360.742	86.82401	270.0403	RFracC	North	FMI_SONIC_004PUP_FMI
1360.560603	1361.377	1360.969	64.93495	91.55237	RFracC	North	FMI_SONIC_004PUP_FMI
1360.401482	1361.218	1360.81	64.64626	19.8266	RFracC	North	FMI_SONIC_004PUP_FMI
1363.241962	1363.415	1363.329	27.68665	80.13721	RFracC	North	FMI_SONIC_004PUP_FMI
1363.654999	1363.835	1363.745	28.74844	79.80639	RFracC	North	FMI_SONIC_004PUP_FMI
1365.926706	1366.1	1366.013	50.42372	271.0165	RFracC	North	FMI_SONIC_004PUP_FMI
1363.241962	1363.829	1363.535	58.49616	27.22428	RFracC	North	FMI_SONIC_004PUP_FMI
1372.345716	1372.932	1372.639	83.3519	255.0627	RFracC	North	FMI_SONIC_004PUP_FMI
1372.873863	1372.966	1372.92	10.78154	40.24218	RFracC	North	FMI_SONIC_004PUP_FMI
1372.765525	1373.352	1373.059	67.43256	334.9261	RFracC	North	FMI_SONIC_004PUP_FMI
1376.425309	1376.585	1376.505	30.72248	346.5956	RFracC	North	FMI_SONIC_004PUP_FMI
1376.875587	1376.961	1376.918	20.76128	153.4405	RFracC	North	FMI_SONIC_004PUP_FMI
1376.641984	1376.727	1376.685	21.56371	310.8283	RFracC	North	FMI_SONIC_004PUP_FMI
1376.442236	1376.501	1376.471	29.48318	237.8509	RFracC	North	FMI_SONIC_004PUP_FMI

1376.550574	1376.609	1376.58	20.35687	285.5123	RFracC	North	FMI_SONIC_004PUP_FMI
1379.204849	1379.812	1379.508	59.52778	85.6822	RFracC	North	FMI_SONIC_004PUP_FMI
1380.179888	1380.787	1380.483	84.22384	252.7543	RFracC	North	FMI_SONIC_004PUP_FMI
1382.573475	1382.849	1382.711	44.16763	106.525	RFracC	North	FMI_SONIC_004PUP_FMI
1382.705511	1383.36	1383.033	77.17162	164.7551	RFracC	North	FMI_SONIC_004PUP_FMI
1383.934467	1384.284	1384.109	51.54234	111.3977	RFracC	North	FMI_SONIC_004PUP_FMI
1384.506626	1385.046	1384.776	59.73703	102.2826	RFracC	North	FMI_SONIC_004PUP_FMI
1399.609582	1399.837	1399.723	60.95053	248.3203	ConFracC	North	FMI_SONIC_004PUP_FMI
1413.537751	1413.962	1413.75	52.95576	92.4811	RFracC	North	FMI_SONIC_004PUP_FMI
1421.453176	1423.753	1422.603	70.85875	70.92926	RFracC	North	FMI_SONIC_004PUP_FMI
1422.655048	1423.086	1422.87	77.70544	258.9797	RFracC	North	FMI_SONIC_004PUP_FMI
1423.305074	1423.587	1423.446	40.82202	83.74001	RFracC	North	FMI_SONIC_004PUP_FMI
1421.784961	1422.994	1422.39	85.56202	69.81102	RFracC	North	FMI_SONIC_004PUP_FMI
1425.322865	1425.842	1425.582	82.95253	244.2673	RFracC	North	FMI_SONIC_004PUP_FMI
1426.42317	1426.983	1426.703	84.24038	246.7029	RFracC	North	FMI_SONIC_004PUP_FMI
1426.761725	1427.572	1427.167	85.72062	280.7047	RFracC	North	FMI_SONIC_004PUP_FMI
1427.601342	1428.154	1427.878	57.48235	90.44727	RFracC	North	FMI_SONIC_004PUP_FMI
1427.147678	1427.836	1427.492	87.90744	244.5295	RFracC	North	FMI_SONIC_004PUP_FMI
1427.408366	1428.002	1427.705	84.86048	252.6851	RFracC	North	FMI_SONIC_004PUP_FMI
1427.912813	1428.506	1428.209	83.18257	266.8412	RFracC	North	FMI_SONIC_004PUP_FMI
1428.346164	1428.858	1428.602	82.45279	247.7806	RFracC	North	FMI_SONIC_004PUP_FMI
1428.864154	1429.634	1429.249	89.7279	238.586	RFracC	North	FMI_SONIC_004PUP_FMI
1429.558193	1430.057	1429.807	53.74535	73.88496	RFracC	North	FMI_SONIC_004PUP_FMI
1429.48371	1429.982	1429.733	54.09013	78.15988	RFracC	North	FMI_SONIC_004PUP_FMI
1429.663145	1430.162	1429.912	53.09176	60.94186	RFracC	North	FMI_SONIC_004PUP_FMI
1433.864617	1434.086	1433.975	33.24815	73.83409	RFracC	North	FMI_SONIC_004PUP_FMI
1434.240414	1434.522	1434.381	39.46139	55.22941	RFracC	North	FMI_SONIC_004PUP_FMI
1434.724548	1435.006	1434.865	52.3859	143.3673	RFracC	North	FMI_SONIC_004PUP_FMI
1435.273008	1435.744	1435.509	78.45829	267.3919	RFracC	North	FMI_SONIC_004PUP_FMI
1438.424958	1438.592	1438.508	28.81322	106.3296	RFracC	North	FMI_SONIC_004PUP_FMI
1439.708083	1439.868	1439.788	24.18865	72.48179	RFracC	North	FMI_SONIC_004PUP_FMI
1441.549825	1441.981	1441.765	78.68758	232.6292	RFracC	North	FMI_SONIC_004PUP_FMI
1443.445735	1443.626	1443.536	54.48019	252.9004	RFracC	North	FMI_SONIC_004PUP_FMI
1445.314561	1445.488	1445.401	27.46453	24.96676	RFracC	North	FMI_SONIC_004PUP_FMI
1445.653116	1445.698	1445.676	24.57377	254.255	RFracC	North	FMI_SONIC_004PUP_FMI
1447.135989	1447.391	1447.263	61.55853	195.0102	RFracC	North	FMI_SONIC_004PUP_FMI
1447.978992	1448.078	1448.029	39.72005	234.7025	RFracC	North	FMI_SONIC_004PUP_FMI
1454.814425	1455.144	1454.979	70.52346	258.3982	RFracC	North	FMI_SONIC_004PUP_FMI
1455.505078	1455.834	1455.67	48.88306	106.3672	RFracC	North	FMI_SONIC_004PUP_FMI
1455.555861	1455.682	1455.619	35.93821	296.5256	RFracC	North	FMI_SONIC_004PUP_FMI
1455.586331	1455.712	1455.649	40.98451	193.8872	RFracC	North	FMI_SONIC_004PUP_FMI
1456.236358	1456.985	1456.611	61.70256	74.29486	RFracC	North	FMI_SONIC_004PUP_FMI
1457.218168	1457.771	1457.495	58.55981	92.71556	RFracC	North	FMI_SONIC_004PUP_FMI
1456.79836	1457.134	1456.966	46.18691	82.04979	RFracC	North	FMI_SONIC_004PUP_FMI

1458.379413	1458.952	1458.666	57.81308	80.27469	RFracC	North	FMI_SONIC_004PUP_FMI
1459.256272	1459.579	1459.418	44.45277	73.30073	RFracC	North	FMI_SONIC_004PUP_FMI
1460.647735	1461.045	1460.846	52.31393	98.24919	RFracC	North	FMI_SONIC_004PUP_FMI
1461.307918	1462.043	1461.676	61.93084	79.75832	RFracC	North	FMI_SONIC_004PUP_FMI
1465.834403	1466.313	1466.074	80.41096	239.6068	RFracC	North	FMI_SONIC_004PUP_FMI
1465.986753	1466.424	1466.206	52.4929	81.04089	RFracC	North	FMI_SONIC_004PUP_FMI
1466.54537	1466.997	1466.771	52.30763	69.55208	RFracC	North	FMI_SONIC_004PUP_FMI
1466.680792	1467.132	1466.906	76.34745	270.8211	RFracC	North	FMI_SONIC_004PUP_FMI
1467.31389	1468.334	1467.824	87.71929	58.6616	RFracC	North	FMI_SONIC_004PUP_FMI
1467.428999	1467.84	1467.634	49.83337	59.54892	RFracC	North	FMI_SONIC_004PUP_FMI
1468.620714	1469.167	1468.894	57.8772	88.71294	RFracC	North	FMI_SONIC_004PUP_FMI
1468.559774	1469.106	1468.833	82.28814	253.7854	RFracC	North	FMI_SONIC_004PUP_FMI
1468.50222	1469.048	1468.775	63.40614	347.0794	RFracC	North	FMI_SONIC_004PUP_FMI
1469.067607	1469.417	1469.242	46.60136	74.64034	RFracC	North	FMI_SONIC_004PUP_FMI
1468.840775	1469.326	1469.083	55.23424	86.36441	RFracC	North	FMI_SONIC_004PUP_FMI
1468.664726	1469.15	1468.907	76.21606	187.1746	RFracC	North	FMI_SONIC_004PUP_FMI
1469.677007	1470.06	1469.869	48.16603	61.14638	RFracC	North	FMI_SONIC_004PUP_FMI
1469.622838	1470.765	1470.194	86.34938	52.51728	RFracC	North	FMI_SONIC_004PUP_FMI
1469.08115	1470.196	1469.639	86.64351	53.7512	RFracC	North	FMI_SONIC_004PUP_FMI
1469.937695	1470.186	1470.062	36.76037	63.42154	RFracC	North	FMI_SONIC_004PUP_FMI
1470.381202	1470.501	1470.441	17.30886	82.01878	RFracC	North	FMI_SONIC_004PUP_FMI
1470.662203	1470.985	1470.823	44.33977	73.51241	RFracC	North	FMI_SONIC_004PUP_FMI
1470.455684	1470.697	1470.576	36.13048	68.3623	RFracC	North	FMI_SONIC_004PUP_FMI
1471.122639	1471.933	1471.528	88.38238	259.1457	RFracC	North	FMI_SONIC_004PUP_FMI
1471.816677	1472.112	1471.964	42.8327	84.51111	RFracC	North	FMI_SONIC_004PUP_FMI
1490.261175	1490.387	1490.324	33.13006	306.9816	RFracC	North	FMI_SONIC_004PUP_FMI
1524.018534	1525.431	1524.725	67.80781	57.62941	RFracC	North	FMI_SONIC_004PUP_FMI
1525.826419	1526.007	1525.917	28.09923	33.43881	RFracC	North	FMI_SONIC_004PUP_FMI
1526.93011	1527.137	1527.034	31.76379	39.54461	RFracC	North	FMI_SONIC_004PUP_FMI
1527.109544	1527.317	1527.213	31.37721	54.84334	RFracC	North	FMI_SONIC_004PUP_FMI
1527.373618	1527.581	1527.477	38.4913	347.5536	RFracC	North	FMI_SONIC_004PUP_FMI
1527.779884	1527.987	1527.884	31.85779	37.91182	RFracC	North	FMI_SONIC_004PUP_FMI
1527.66139	1527.869	1527.765	31.39608	53.16541	RFracC	North	FMI_SONIC_004PUP_FMI
1527.515811	1527.723	1527.62	31.62097	42.9569	RFracC	North	FMI_SONIC_004PUP_FMI
1527.068918	1527.33	1527.2	65.48674	247.9987	RFracC	North	FMI_SONIC_004PUP_FMI
1527.465028	1527.727	1527.596	40.90887	12.98171	RFracC	North	FMI_SONIC_004PUP_FMI
1528.304645	1528.553	1528.429	39.43923	12.52529	RFracC	North	FMI_SONIC_004PUP_FMI
1528.849719	1529.037	1528.943	52.01917	193.2198	RFracC	North	FMI_SONIC_004PUP_FMI
1529.174732	1529.362	1529.268	30.2191	20.46075	RFracC	North	FMI_SONIC_004PUP_FMI
1528.578875	1528.827	1528.703	41.47553	359.5283	RFracC	North	FMI_SONIC_004PUP_FMI
1529.784132	1529.924	1529.854	20.82021	34.88844	RFracC	North	FMI_SONIC_004PUP_FMI
1530.200555	1530.381	1530.291	27.34722	53.17867	RFracC	North	FMI_SONIC_004PUP_FMI
1530.613593	1531.43	1531.022	89.37337	250.7502	RFracC	North	FMI_SONIC_004PUP_FMI
1530.745629	1530.912	1530.829	26.4934	85.82744	RFracC	North	FMI_SONIC_004PUP_FMI

1531.321174	1531.562	1531.442	35.92618	41.95941	RFracC	North	FMI_SONIC_004PUP_FMI
1531.957658	1532.151	1532.055	29.58196	44.53044	RFracC	North	FMI_SONIC_004PUP_FMI
1532.912384	1533.106	1533.009	31.02207	87.46312	RFracC	North	FMI_SONIC_004PUP_FMI
1532.824359	1533.018	1532.921	29.64942	67.18653	RFracC	North	FMI_SONIC_004PUP_FMI
1533.098589	1533.272	1533.185	31.16142	112.4956	RFracC	North	FMI_SONIC_004PUP_FMI
1533.274638	1533.57	1533.422	45.61039	105.942	RFracC	North	FMI_SONIC_004PUP_FMI
1533.362663	1533.597	1533.48	37.8263	97.97891	RFracC	North	FMI_SONIC_004PUP_FMI
1533.372819	1533.601	1533.487	34.11153	61.61325	RFracC	North	FMI_SONIC_004PUP_FMI
1533.369434	1533.577	1533.473	34.43288	10.64216	RFracC	North	FMI_SONIC_004PUP_FMI
1533.752001	1534.867	1534.309	65.7167	61.73335	RFracC	North	FMI_SONIC_004PUP_FMI
1533.999147	1534.227	1534.113	37.47616	8.704761	RFracC	North	FMI_SONIC_004PUP_FMI
1534.144726	1535.124	1534.634	64.76615	38.72008	RFracC	North	FMI_SONIC_004PUP_FMI
1534.970801	1535.07	1535.02	12.42809	31.50812	RFracC	North	FMI_SONIC_004PUP_FMI
1535.048668	1535.209	1535.129	31.54337	343.2103	RFracC	North	FMI_SONIC_004PUP_FMI
1536.538312	1536.8	1536.669	39.81093	21.95704	RFracC	North	FMI_SONIC_004PUP_FMI
1536.931036	1537.057	1536.994	17.67419	52.58152	RFracC	North	FMI_SONIC_004PUP_FMI
1538.505319	1538.841	1538.673	45.83773	29.34059	RFracC	North	FMI_SONIC_004PUP_FMI
1540.997087	1541.11	1541.053	15.08248	40.6922	RFracC	North	FMI_SONIC_004PUP_FMI
1540.909062	1541.116	1541.013	32.84726	24.73146	RFracC	North	FMI_SONIC_004PUP_FMI
1540.726242	1540.934	1540.83	31.8227	71.83248	RFracC	North	FMI_SONIC_004PUP_FMI
1540.810881	1541.018	1540.915	32.05826	34.56508	RFracC	North	FMI_SONIC_004PUP_FMI
1543.014877	1543.29	1543.152	39.85402	39.16959	RFracC	North	FMI_SONIC_004PUP_FMI
1543.170612	1543.297	1543.234	19.55409	93.7314	RFracC	North	FMI_SONIC_004PUP_FMI
1543.912049	1544.038	1543.975	23.23681	350.6201	RFracC	North	FMI_SONIC_004PUP_FMI
1543.658132	1544.035	1543.846	50.18838	94.33835	RFracC	North	FMI_SONIC_004PUP_FMI
1543.861265	1544.177	1544.019	49.53413	117.568	RFracC	North	FMI_SONIC_004PUP_FMI
1544.958185	1545.186	1545.072	36.97342	98.14828	RFracC	North	FMI_SONIC_004PUP_FMI
1544.99204	1545.45	1545.221	53.1083	80.80642	RFracC	North	FMI_SONIC_004PUP_FMI
1544.826148	1545.027	1544.926	51.87737	183.1103	RFracC	North	FMI_SONIC_004PUP_FMI
1545.110535	1545.44	1545.275	49.99849	356.7126	RFracC	North	FMI_SONIC_004PUP_FMI
1546.975975	1547.305	1547.141	70.93668	257.3787	RFracC	North	FMI_SONIC_004PUP_FMI
1546.921806	1547.251	1547.086	44.67648	73.07711	RFracC	North	FMI_SONIC_004PUP_FMI
1547.118168	1547.563	1547.34	51.70228	40.3968	RFracC	North	FMI_SONIC_004PUP_FMI
1547.629387	1547.999	1547.814	47.19363	63.83636	RFracC	North	FMI_SONIC_004PUP_FMI
1548.140606	1548.45	1548.295	69.04685	259.4102	RFracC	North	FMI_SONIC_004PUP_FMI
1548.8685	1549.117	1548.993	62.95196	259.7061	RFracC	North	FMI_SONIC_004PUP_FMI
1549.305236	1549.553	1549.429	64.13471	244.7191	RFracC	North	FMI_SONIC_004PUP_FMI
1549.515141	1549.763	1549.639	36.52355	56.42022	RFracC	North	FMI_SONIC_004PUP_FMI
1549.477899	1549.726	1549.602	63.48236	254.3531	RFracC	North	FMI_SONIC_004PUP_FMI
1548.577342	1549.137	1548.857	59.0231	96.70786	RFracC	North	FMI_SONIC_004PUP_FMI
1548.042425	1548.866	1548.454	65.07786	95.57498	RFracC	North	FMI_SONIC_004PUP_FMI
1550.188866	1550.478	1550.333	66.8215	262.4996	RFracC	North	FMI_SONIC_004PUP_FMI
1551.40428	1552.214	1551.809	63.1301	80.87357	ConFracC	North	FMI_SONIC_004PUP_FMI
1554.698424	1555.129	1554.914	50.66939	60.65265	RFracC	North	FMI_SONIC_004PUP_FMI

1554.180434	1554.483	1554.332	69.6553	242.8421	RFracC	North	FMI_SONIC_004PUP_FMI
1555.83597	1556.165	1556.001	44.29929	65.39105	RFracC	North	FMI_SONIC_004PUP_FMI
1554.579929	1555.139	1554.86	82.46795	211.4746	RFracC	North	FMI_SONIC_004PUP_FMI
1557.325613	1557.709	1557.517	52.7352	109.3871	RFracC	North	FMI_SONIC_004PUP_FMI
1560.518191	1560.963	1560.74	52.31976	31.58232	RFracC	North	FMI_SONIC_004PUP_FMI
1566.77808	1566.965	1566.872	28.8279	71.64734	RFracC	North	FMI_SONIC_004PUP_FMI
1567.38748	1567.575	1567.481	29.38403	33.184	RFracC	North	FMI_SONIC_004PUP_FMI
1567.84453	1568.167	1568.006	43.78594	49.90439	RFracC	North	FMI_SONIC_004PUP_FMI
1567.638011	1568.123	1567.881	58.70905	113.1987	RFracC	North	FMI_SONIC_004PUP_FMI
1568.335435	1568.651	1568.493	43.45039	43.76572	RFracC	North	FMI_SONIC_004PUP_FMI
1569.317246	1569.633	1569.475	43.90426	36.18505	RFracC	North	FMI_SONIC_004PUP_FMI
1571.077734	1571.305	1571.192	34.4435	44.26187	RFracC	North	FMI_SONIC_004PUP_FMI
1570.407394	1570.635	1570.521	34.21833	50.86774	RFracC	North	FMI_SONIC_004PUP_FMI
1569.946959	1570.175	1570.061	34.29453	47.58354	RFracC	North	FMI_SONIC_004PUP_FMI
1569.848778	1570.076	1569.963	34.13895	57.49748	RFracC	North	FMI_SONIC_004PUP_FMI
1570.051911	1570.28	1570.166	38.42646	5.448212	RFracC	North	FMI_SONIC_004PUP_FMI
1570.16702	1570.334	1570.25	28.72291	8.617202	RFracC	North	FMI_SONIC_004PUP_FMI
1571.355349	1571.522	1571.439	26.80968	25.03795	RFracC	North	FMI_SONIC_004PUP_FMI
1568.799256	1569	1568.9	31.13874	37.0451	RFracC	North	FMI_SONIC_004PUP_FMI
1568.013807	1568.194	1568.104	27.53636	50.41479	RFracC	North	FMI_SONIC_004PUP_FMI
1570.989709	1571.163	1571.076	26.42074	61.07443	RFracC	North	FMI_SONIC_004PUP_FMI
1571.639736	1571.82	1571.73	28.41293	32.73847	RFracC	North	FMI_SONIC_004PUP_FMI
1572.134027	1572.314	1572.224	27.53126	53.81546	RFracC	North	FMI_SONIC_004PUP_FMI
1572.614775	1572.863	1572.739	37.14381	39.7375	RFracC	North	FMI_SONIC_004PUP_FMI
1572.889005	1573.137	1573.013	36.9846	42.9153	RFracC	North	FMI_SONIC_004PUP_FMI
1572.922861	1573.171	1573.047	37.46779	34.98959	RFracC	North	FMI_SONIC_004PUP_FMI
1572.946559	1573.195	1573.071	38.80109	21.10017	RFracC	North	FMI_SONIC_004PUP_FMI
1571.226698	1571.475	1571.351	37.89522	86.14787	RFracC	North	FMI_SONIC_004PUP_FMI
1573.068439	1573.432	1573.25	46.7583	57.42547	RFracC	North	FMI_SONIC_004PUP_FMI
1576.047727	1576.594	1576.321	55.97356	70.15199	RFracC	North	FMI_SONIC_004PUP_FMI
1577.127719	1577.619	1577.374	53.85166	67.41238	RFracC	North	FMI_SONIC_004PUP_FMI
1574.41589	1574.853	1574.635	51.55894	73.36934	RFracC	North	FMI_SONIC_004PUP_FMI
1576.765464	1577.013	1576.889	37.37569	38.12457	RFracC	North	FMI_SONIC_004PUP_FMI
1580.662237	1580.822	1580.742	24.4632	51.26314	RFracC	North	FMI_SONIC_004PUP_FMI
1580.939852	1581.303	1581.121	47.3674	43.8684	RFracC	North	FMI_SONIC_004PUP_FMI
1581.850566	1582.044	1581.947	30.71523	34.748	RFracC	North	FMI_SONIC_004PUP_FMI
1583.963152	1584.617	1584.29	86.03038	247.142	RFracC	North	FMI_SONIC_004PUP_FMI
1583.58397	1584.238	1583.911	85.12276	261.4649	RFracC	North	FMI_SONIC_004PUP_FMI
1583.743091	1583.937	1583.84	30.09202	72.3109	RFracC	North	FMI_SONIC_004PUP_FMI
1583.776947	1583.971	1583.874	56.92606	242.9437	RFracC	North	FMI_SONIC_004PUP_FMI
1585.171795	1585.406	1585.289	35.45315	69.95046	RFracC	North	FMI_SONIC_004PUP_FMI
1587.991961	1588.491	1588.241	54.24699	67.18082	RFracC	North	FMI_SONIC_004PUP_FMI
1587.961491	1588.284	1588.123	69.67454	264.5096	RFracC	North	FMI_SONIC_004PUP_FMI
1592.816376	1593.098	1592.957	65.53026	268.482	RFracC	North	FMI_SONIC_004PUP_FMI

1593.679692	1593.874	1593.777	51.78887	286.6014	RFracC	North	FMI_SONIC_004PUP_FMI
1596.212086	1596.663	1596.438	74.99343	284.0053	RFracC	North	FMI_SONIC_004PUP_FMI
1595.495211	1595.694	1595.595	57.51158	245.1426	RFracC	North	FMI_SONIC_004PUP_FMI
1595.867622	1596.026	1595.947	42.59325	301.2374	RFracC	North	FMI_SONIC_004PUP_FMI
1596.091069	1596.317	1596.204	56.11201	287.8587	RFracC	North	FMI_SONIC_004PUP_FMI
1596.886674	1597.153	1597.02	65.86822	232.3887	RFracC	North	FMI_SONIC_004PUP_FMI
1597.340338	1597.607	1597.474	60.70238	289.0738	RFracC	North	FMI_SONIC_004PUP_FMI
1597.428363	1597.668	1597.548	61.06661	268.8201	RFracC	North	FMI_SONIC_004PUP_FMI
1597.766918	1598.169	1597.968	73.83136	275.4883	RFracC	North	FMI_SONIC_004PUP_FMI
1598.119016	1598.758	1598.439	58.66747	64.17602	RFracC	North	FMI_SONIC_004PUP_FMI
1598.975561	1599.615	1599.295	60.61828	93.10681	RFracC	North	FMI_SONIC_004PUP_FMI
1599.852419	1600.383	1600.118	81.79256	257.6382	RFracC	North	FMI_SONIC_004PUP_FMI
1600.502446	1600.837	1600.67	69.40289	274.7603	RFracC	North	FMI_SONIC_004PUP_FMI
1600.448277	1600.783	1600.615	69.05911	277.0098	RFracC	North	FMI_SONIC_004PUP_FMI
1600.641253	1600.888	1600.764	60.93016	275.4485	RFracC	North	FMI_SONIC_004PUP_FMI
1600.878242	1601.07	1600.974	54.58905	269.7576	RFracC	North	FMI_SONIC_004PUP_FMI
1600.969652	1601.27	1601.12	67.96173	264.3077	RFracC	North	FMI_SONIC_004PUP_FMI
1601.728016	1602.028	1601.878	68.44095	259.8923	RFracC	North	FMI_SONIC_004PUP_FMI
1606.73525	1607.151	1606.943	77.20426	245.8281	RFracC	North	FMI_SONIC_004PUP_FMI
1613.685793	1613.973	1613.829	41.69588	39.30559	RFracC	North	FMI_SONIC_004PUP_FMI
1619.167005	1619.461	1619.314	41.11382	76.48517	RFracC	North	FMI_SONIC_004PUP_FMI
1633.728272	1634.022	1633.875	68.55959	259.1924	ConFracC	North	FMI_SONIC_004PUP_FMI
1642.747388	1643.095	1642.921	73.32877	240.6483	ConFracC	North	FMI_SONIC_004PUP_FMI
1663.199519	1663.439	1663.319	58.60057	292.2198	RFracC	North	FMI_SONIC_004PUP_FMI
1666.703568	1666.943	1666.823	63.21802	249.5113	ConFracC	North	FMI_SONIC_004PUP_FMI
1667.458546	1667.698	1667.578	35.58381	64.45702	ConFracC	North	FMI_SONIC_004PUP_FMI
1678.26862	1678.569	1678.419	42.5081	87.68538	RFracC	North	FMI_SONIC_004PUP_FMI
1678.613947	1678.786	1678.7	26.64738	46.13173	RFracC	North	FMI_SONIC_004PUP_FMI
1678.549621	1678.972	1678.761	77.23987	227.8988	RFracC	North	FMI_SONIC_004PUP_FMI
1679.934313	1680.357	1680.145	72.80769	196.8288	RFracC	North	FMI_SONIC_004PUP_FMI
1683.211529	1683.586	1683.399	48.96987	94.35599	RFracC	North	FMI_SONIC_004PUP_FMI
1684.095158	1684.389	1684.242	41.2968	61.87084	RFracC	North	FMI_SONIC_004PUP_FMI
1684.396473	1684.69	1684.543	41.35468	69.66711	RFracC	North	FMI_SONIC_004PUP_FMI
1692.487947	1692.87	1692.679	75.45396	241.4398	RFracC	North	FMI_SONIC_004PUP_FMI
1695.352125	1695.971	1695.661	59.94943	95.75106	RFracC	North	FMI_SONIC_004PUP_FMI
1696.022465	1696.316	1696.169	42.51532	88.63659	RFracC	North	FMI_SONIC_004PUP_FMI
1695.755006	1696.049	1695.902	42.6308	90.12407	RFracC	North	FMI_SONIC_004PUP_FMI
1695.826103	1696.12	1695.973	54.72865	329.0457	RFracC	North	FMI_SONIC_004PUP_FMI
1696.39149	1696.685	1696.538	68.38535	255.6619	RFracC	North	FMI_SONIC_004PUP_FMI
1706.896864	1707.191	1707.044	67.6902	260.882	RFaultC	North	FMI_SONIC_004PUP_FMI
1707.519806	1707.712	1707.616	29.57817	67.07611	RFracC	North	FMI_SONIC_004PUP_FMI
1707.516421	1708.101	1707.809	57.10216	65.67145	RFracC	North	FMI_SONIC_004PUP_FMI
1708.176604	1708.409	1708.293	36.2332	31.10562	RFracC	North	FMI_SONIC_004PUP_FMI
1708.315411	1708.609	1708.462	41.86172	75.54802	RFracC	North	FMI_SONIC_004PUP_FMI

1708.809702	1709.056	1708.933	63.65001	230.2697	RFracC	North	FMI_SONIC_004PUP_FMI
1709.432644	1709.767	1709.6	72.09758	241.0228	RFracC	North	FMI_SONIC_004PUP_FMI
1708.298484	1708.565	1708.432	65.79547	250.7743	RFracC	North	FMI_SONIC_004PUP_FMI
1715.127146	1715.373	1715.25	62.96295	258.8789	RFracC	North	FMI_SONIC_004PUP_FMI
1715.293038	1715.614	1715.453	69.99424	260.8485	RFracC	North	FMI_SONIC_004PUP_FMI
1715.55034	1716.067	1715.809	80.47523	265.5905	RFracC	North	FMI_SONIC_004PUP_FMI
1715.841498	1716.223	1716.032	73.47015	268.1486	RFracC	North	FMI_SONIC_004PUP_FMI
1724.610083	1725.371	1724.991	88.80047	250.6475	RFracC	North	FMI_SONIC_004PUP_FMI
1725.639291	1725.974	1725.806	44.07459	56.73783	RFracC	North	FMI_SONIC_004PUP_FMI
1731.608023	1732.525	1732.066	85.7293	286.984	RFracC	North	FMI_SONIC_004PUP_FMI
1735.443855	1735.717	1735.581	39.91081	81.0231	RFracC	North	FMI_SONIC_004PUP_FMI
1736.429052	1736.675	1736.552	36.00973	68.97361	RFracC	North	FMI_SONIC_004PUP_FMI
1736.429052	1736.675	1736.552	36.00973	68.97361	RFracC	North	FMI_SONIC_004PUP_FMI
1741.64619	1741.892	1741.769	38.29641	94.35215	RFracC	North	FMI_SONIC_004PUP_FMI
1742.116782	1742.363	1742.24	35.34426	57.5421	RFracC	North	FMI_SONIC_004PUP_FMI
1742.817592	1743.064	1742.941	35.72737	36.01308	RFracC	North	FMI_SONIC_004PUP_FMI
1745.228106	1745.474	1745.351	35.94147	72.37703	RFracC	North	FMI_SONIC_004PUP_FMI
1746.189604	1746.524	1746.357	43.90979	37.12611	RFracC	North	FMI_SONIC_004PUP_FMI
1747.02245	1747.289	1747.156	37.48979	46.06234	RFracC	North	FMI_SONIC_004PUP_FMI
1747.434625	1747.534	1747.484	39.45648	252.414	RFracC	North	FMI_SONIC_004PUP_FMI
1747.732554	1748.075	1747.904	44.30018	63.34883	RFracC	North	FMI_SONIC_004PUP_FMI
1750.738926	1751.082	1750.91	44.91344	74.0304	RFracC	North	FMI_SONIC_004PUP_FMI
1750.986071	1751.227	1751.107	34.59085	47.58858	RFracC	North	FMI_SONIC_004PUP_FMI
1751.37541	1751.698	1751.537	43.23863	72.7566	RFracC	North	FMI_SONIC_004PUP_FMI
1752.052521	1752.341	1752.197	39.65172	60.58187	RFracC	North	FMI_SONIC_004PUP_FMI
1752.394462	1752.832	1752.613	50.90158	76.07739	RFracC	North	FMI_SONIC_004PUP_FMI
1754.303914	1754.66	1754.482	46.02898	75.33292	RFracC	North	FMI_SONIC_004PUP_FMI
1758.606953	1758.889	1758.748	43.02149	100.4396	RFracC	North	FMI_SONIC_004PUP_FMI
1760.783864	1760.937	1760.86	22.9367	81.91404	RFracC	North	FMI_SONIC_004PUP_FMI
1777.498344	1777.936	1777.717	77.03375	269.369	RFracC	North	FMI_SONIC_004PUP_FMI
1777.677779	1778.258	1777.968	56.07287	72.21367	RFracC	North	FMI_SONIC_004PUP_FMI
1777.911382	1778.491	1778.201	85.57623	237.3255	RFracC	North	FMI_SONIC_004PUP_FMI
1777.972322	1778.552	1778.262	82.57336	270.313	RFracC	North	FMI_SONIC_004PUP_FMI
1777.86737	1778.447	1778.157	78.1116	176.1832	RFracC	North	FMI_SONIC_004PUP_FMI
1778.646047	1778.833	1778.74	55.31904	261.9292	RFracC	North	FMI_SONIC_004PUP_FMI
1778.747614	1778.982	1778.865	61.51745	264.2899	RFracC	North	FMI_SONIC_004PUP_FMI
1778.798397	1779.033	1778.916	61.35582	265.3475	RFracC	North	FMI_SONIC_004PUP_FMI
1779.008301	1779.243	1779.126	58.54617	280.2081	RFracC	North	FMI_SONIC_004PUP_FMI
1779.052313	1779.287	1779.17	60.06868	272.7563	RFracC	North	FMI_SONIC_004PUP_FMI
1780.765404	1781.332	1781.049	85.25459	231.4601	RFracC	North	FMI_SONIC_004PUP_FMI
1781.066718	1781.85	1781.458	89.99475	220.5067	RFracC	North	FMI_SONIC_004PUP_FMI
1781.575414	1781.977	1781.776	74.78991	272.5441	RFracC	North	FMI_SONIC_004PUP_FMI
1781.73792	1782.086	1781.912	70.10922	278.6151	RFracC	North	FMI_SONIC_004PUP_FMI
1781.82933	1782.13	1781.98	68.01772	268.98	RFracC	North	FMI_SONIC_004PUP_FMI

1782.262681	1782.563	1782.413	44.22078	100.8398	RFracC	North	FMI_SONIC_004PUP_FMI
1782.005379	1782.306	1782.156	67.27322	273.3849	RFracC	North	FMI_SONIC_004PUP_FMI
1782.083247	1782.384	1782.233	66.21408	278.8844	RFracC	North	FMI_SONIC_004PUP_FMI
1782.709574	1783.457	1783.083	60.04914	70.18755	RFracC	North	FMI_SONIC_004PUP_FMI
1783.274962	1783.609	1783.442	45.74652	91.15266	RFracC	North	FMI_SONIC_004PUP_FMI
1783.820036	1784.195	1784.008	75.52098	253.2022	RFracC	North	FMI_SONIC_004PUP_FMI
1783.90806	1784.283	1784.096	46.52564	62.26311	RFracC	North	FMI_SONIC_004PUP_FMI
1784.338026	1784.713	1784.525	49.38594	96.16907	RFracC	North	FMI_SONIC_004PUP_FMI
1785.610994	1786.027	1785.819	76.6779	264.8018	RFracC	North	FMI_SONIC_004PUP_FMI
1785.946164	1786.504	1786.225	54.88066	56.27292	RFracC	North	FMI_SONIC_004PUP_FMI
1786.203466	1786.49	1786.347	68.87328	250.3572	RFracC	North	FMI_SONIC_004PUP_FMI
1786.030803	1786.473	1786.252	51.14628	78.2762	RFracC	North	FMI_SONIC_004PUP_FMI
1786.569106	1786.951	1786.76	47.70987	33.78608	RFracC	North	FMI_SONIC_004PUP_FMI
1786.968601	1787.35	1787.159	76.02289	253.1915	RFracC	North	FMI_SONIC_004PUP_FMI
1787.452735	1787.733	1787.593	67.88745	254.6134	RFracC	North	FMI_SONIC_004PUP_FMI
1788.018123	1788.325	1788.172	69.01063	265.8728	RFracC	North	FMI_SONIC_004PUP_FMI
1788.163702	1788.41	1788.287	63.73779	259.5059	RFracC	North	FMI_SONIC_004PUP_FMI
1788.448088	1788.755	1788.602	42.76832	84.31031	RFracC	North	FMI_SONIC_004PUP_FMI
1788.404076	1788.732	1788.568	72.59559	247.2929	RFracC	North	FMI_SONIC_004PUP_FMI
1789.006705	1789.192	1789.099	56.92967	243.1596	RFracC	North	FMI_SONIC_004PUP_FMI
1789.145512	1789.331	1789.238	56.77859	246.1559	RFracC	North	FMI_SONIC_004PUP_FMI
1789.209838	1789.395	1789.303	56.50015	250.1544	RFracC	North	FMI_SONIC_004PUP_FMI
1789.291091	1789.497	1789.394	53.9571	284.6034	RFracC	North	FMI_SONIC_004PUP_FMI
1789.396043	1790.157	1789.776	60.07652	63.26898	RFracC	North	FMI_SONIC_004PUP_FMI
1789.748141	1790.069	1789.909	70.851	260.513	RFracC	North	FMI_SONIC_004PUP_FMI
1789.900491	1790.099	1790	56.8459	264.6428	RFracC	North	FMI_SONIC_004PUP_FMI
1790.117166	1790.289	1790.203	52.60608	264.6953	RFracC	North	FMI_SONIC_004PUP_FMI
1790.269516	1790.435	1790.352	49.31114	276.2732	RFracC	North	FMI_SONIC_004PUP_FMI
1790.401553	1790.688	1790.545	66.698	268.8159	RFracC	North	FMI_SONIC_004PUP_FMI
1790.442179	1790.688	1790.565	61.21095	275.4665	RFracC	North	FMI_SONIC_004PUP_FMI
1790.577602	1790.837	1790.708	64.02073	268.291	RFracC	North	FMI_SONIC_004PUP_FMI
1790.980482	1791.714	1791.347	59.53281	64.67504	RFracC	North	FMI_SONIC_004PUP_FMI
1791.301248	1791.705	1791.503	76.92395	257.8543	RFracC	North	FMI_SONIC_004PUP_FMI
1790.830656	1791.038	1790.934	56.84733	272.1335	RFracC	North	FMI_SONIC_004PUP_FMI
1790.928837	1791.136	1791.033	57.57449	267.9932	RFracC	North	FMI_SONIC_004PUP_FMI
1791.1015	1791.309	1791.205	59.48797	253.5927	RFracC	North	FMI_SONIC_004PUP_FMI
1793.403677	1793.821	1793.612	75.276	275.0913	RFracC	North	FMI_SONIC_004PUP_FMI
1793.901353	1794.413	1794.157	55.80793	93.30309	RFracC	North	FMI_SONIC_004PUP_FMI
1793.803172	1794.315	1794.059	54.45528	82.10777	RFracC	North	FMI_SONIC_004PUP_FMI
1795.181093	1795.598	1795.39	49.16638	69.57732	RFracC	North	FMI_SONIC_004PUP_FMI
1794.981345	1795.399	1795.19	77.19668	262.5544	RFracC	North	FMI_SONIC_004PUP_FMI
1794.869622	1795.287	1795.078	77.59654	259.13	RFracC	North	FMI_SONIC_004PUP_FMI
1795.157394	1795.575	1795.366	49.16638	69.57732	RFracC	North	FMI_SONIC_004PUP_FMI
1795.150623	1795.568	1795.359	72.78605	287.6736	RFracC	North	FMI_SONIC_004PUP_FMI

1795.495949	1795.791	1795.644	40.45736	67.27575	RFracC	North	FMI_SONIC_004PUP_FMI
1795.543347	1795.839	1795.691	40.59901	70.42516	RFracC	North	FMI_SONIC_004PUP_FMI
1796.085035	1796.685	1796.385	58.01402	87.20944	RFracC	North	FMI_SONIC_004PUP_FMI
1795.851432	1796.716	1796.284	84.21256	295.3065	RFracC	North	FMI_SONIC_004PUP_FMI
1796.741833	1796.983	1796.862	63.73446	218.3649	RFracC	North	FMI_SONIC_004PUP_FMI
1795.980083	1796.628	1796.304	86.47059	256.5212	RFracC	North	FMI_SONIC_004PUP_FMI
1796.992364	1797.437	1797.215	50.93546	75.29359	RFracC	North	FMI_SONIC_004PUP_FMI
1798.232339	1798.485	1798.359	65.77518	227.7886	RFracC	North	FMI_SONIC_004PUP_FMI
1799.30556	1799.545	1799.425	59.94904	278.5713	RFracC	North	FMI_SONIC_004PUP_FMI
1799.667814	1800.016	1799.842	47.05485	93.80826	RFracC	North	FMI_SONIC_004PUP_FMI
1801.126988	1801.766	1801.446	57.23961	56.21349	RFracC	North	FMI_SONIC_004PUP_FMI
1802.044473	1802.277	1802.161	40.88722	350.646	RFracC	North	FMI_SONIC_004PUP_FMI
1801.81087	1802.044	1801.927	40.60305	352.04	RFracC	North	FMI_SONIC_004PUP_FMI
1801.055891	1801.343	1801.199	39.83627	70.52721	RFracC	North	FMI_SONIC_004PUP_FMI
1801.455386	1802.027	1801.741	61.47756	359.5187	RFracC	North	FMI_SONIC_004PUP_FMI
1803.574743	1803.889	1803.732	69.05276	270.4292	RFracC	North	FMI_SONIC_004PUP_FMI
1803.757563	1804.072	1803.915	41.99782	67.15992	RFracC	North	FMI_SONIC_004PUP_FMI
1803.916684	1804.149	1804.033	58.292	282.5849	RFracC	North	FMI_SONIC_004PUP_FMI
1804.383891	1805.023	1804.703	57.25233	47.71652	RFracC	North	FMI_SONIC_004PUP_FMI
1804.928965	1805.568	1805.248	87.08688	246.9834	RFracC	North	FMI_SONIC_004PUP_FMI
1804.942507	1806.083	1805.513	64.68091	58.94828	RFracC	North	FMI_SONIC_004PUP_FMI
1805.345388	1805.741	1805.543	76.9276	254.4379	RFracC	North	FMI_SONIC_004PUP_FMI
1806.09021	1806.255	1806.173	49.15952	278.2599	RFracC	North	FMI_SONIC_004PUP_FMI
1806.584501	1806.75	1806.667	38.68035	155.3982	RFracC	North	FMI_SONIC_004PUP_FMI
1811.551108	1811.852	1811.701	40.60201	46.75784	RFracC	North	FMI_SONIC_004PUP_FMI
1815.133024	1815.23	1815.182	22.20166	319.6906	RFracC	North	FMI_SONIC_004PUP_FMI
1821.186395	1821.446	1821.316	65.54477	262.7493	RFracC	North	FMI_SONIC_004PUP_FMI
1821.873662	1822.31	1822.092	77.23184	272.8166	RFracC	North	FMI_SONIC_004PUP_FMI
1822.588014	1823.538	1823.063	63.13191	79.70503	RFracC	North	FMI_SONIC_004PUP_FMI
1822.689581	1822.936	1822.813	62.9495	269.848	RFracC	North	FMI_SONIC_004PUP_FMI
1823.373463	1823.62	1823.497	65.77252	247.7256	RFracC	North	FMI_SONIC_004PUP_FMI
1823.684934	1823.931	1823.808	34.26747	56.43584	RFracC	North	FMI_SONIC_004PUP_FMI
1823.837284	1824.084	1823.96	65.86139	246.6701	RFracC	North	FMI_SONIC_004PUP_FMI
1824.683672	1825.004	1824.844	73.06304	247.1655	RFracC	North	FMI_SONIC_004PUP_FMI
1825.861845	1826.413	1826.137	53.82316	67.99014	RFracC	North	FMI_SONIC_004PUP_FMI
1826.549112	1827.1	1826.825	84.99811	218.6029	RFracC	North	FMI_SONIC_004PUP_FMI
1827.78484	1828.464	1828.125	57.26918	67.75927	RFracC	North	FMI_SONIC_004PUP_FMI
1827.788225	1828.468	1828.128	86.01934	198.11	RFracC	North	FMI_SONIC_004PUP_FMI
1829.111114	1829.312	1829.211	60.45617	226.0457	RFracC	North	FMI_SONIC_004PUP_FMI
1829.124657	1829.413	1829.269	40.17535	87.16125	RFracC	North	FMI_SONIC_004PUP_FMI
1830.27913	1831.197	1830.738	88.06163	83.01864	RFracC	North	FMI_SONIC_004PUP_FMI
1833.106068	1833.266	1833.186	53.29169	254.777	RFracC	North	FMI_SONIC_004PUP_FMI
1833.11961	1833.618	1833.369	81.47546	267.416	RFracC	North	FMI_SONIC_004PUP_FMI
1833.373527	1834.285	1833.829	86.99509	74.51329	RFracC	North	FMI_SONIC_004PUP_FMI

1853.940767	1854.412	1854.176	48.78516	65.72143	RFracC	North	FMI_SONIC_004PUP_FMI
1854.096503	1855.096	1854.596	60.47159	59.24489	RFracC	North	FMI_SONIC_004PUP_FMI
1853.998322	1854.923	1854.461	84.52628	52.54506	RFracC	North	FMI_SONIC_004PUP_FMI
1855.623387	1856.156	1855.89	50.9244	59.574	RFracC	North	FMI_SONIC_004PUP_FMI
1857.634406	1858.675	1858.155	83.9686	73.48327	RFracC	North	FMI_SONIC_004PUP_FMI
1864.916733	1865.28	1865.098	43.83481	79.03206	RFracC	North	FMI_SONIC_004PUP_FMI
1865.377168	1865.74	1865.559	43.2746	72.76648	RFracC	North	FMI_SONIC_004PUP_FMI
1865.746194	1866.265	1866.006	85.25373	254.717	RFracC	North	FMI_SONIC_004PUP_FMI
1865.475349	1865.764	1865.62	71.96192	219.9555	RFracC	North	FMI_SONIC_004PUP_FMI
1890.365942	1890.594	1890.48	65.41031	245.0534	RFracC	North	FMI_SONIC_004PUP_FMI
1892.028249	1892.256	1892.142	65.00925	218.6162	RFracC	North	FMI_SONIC_004PUP_FMI
1892.119659	1892.347	1892.234	65.78796	230.8357	RFracC	North	FMI_SONIC_004PUP_FMI
1892.471757	1892.699	1892.586	44.17049	140.6848	RFracC	North	FMI_SONIC_004PUP_FMI
1892.91865	1893.072	1892.995	19.63324	32.83828	RFracC	North	FMI_SONIC_004PUP_FMI
1892.867867	1893.278	1893.073	80.50298	217.9815	RFracC	North	FMI_SONIC_004PUP_FMI
1923.056851	1923.244	1923.15	29.33163	100.6693	ConFracC	North	FMI_SONIC_004PUP_FMI
1923.175346	1923.362	1923.269	31.55857	111.4625	ConFracC	North	FMI_SONIC_004PUP_FMI
1924.224867	1924.412	1924.318	25.69376	24.94156	ConFracC	North	FMI_SONIC_004PUP_FMI
1923.56807	1924.168	1923.868	54.20371	31.14405	ConFracC	North	FMI_SONIC_004PUP_FMI
1925.822849	1926.044	1925.933	60.3274	266.2737	ConFracC	North	FMI_SONIC_004PUP_FMI
1929.198246	1929.534	1929.366	57.09444	138.7005	ConFracC	North	FMI_SONIC_004PUP_FMI
1935.085724	1935.28	1935.183	29.6907	94.41523	ConFracC	North	FMI_SONIC_004PUP_FMI
1942.621968	1942.816	1942.719	50.98858	281.1484	ConFracC	North	FMI_SONIC_004PUP_FMI
1954.772721	1954.967	1954.87	27.32997	70.14958	RFracC	North	FMI_SONIC_004PUP_FMI
1965.376276	1965.794	1965.585	67.95846	147.6702	ConFracC	North	FMI_SONIC_004PUP_FMI
1966.909932	1967.144	1967.027	31.63033	52.29102	ConFracC	North	FMI_SONIC_004PUP_FMI
1969.411856	1969.646	1969.529	52.81963	151.4301	ConFracC	North	FMI_SONIC_004PUP_FMI
1970.342883	1970.692	1970.518	58.75837	134.1858	ConFracC	North	FMI_SONIC_004PUP_FMI
1972.563807	1972.71	1972.637	25.69211	111.2851	ConFracC	North	FMI_SONIC_004PUP_FMI
1974.070378	1974.217	1974.144	23.6412	102.1775	ConFracC	North	FMI_SONIC_004PUP_FMI
1976.044156	1976.191	1976.117	18.12552	52.42738	ConFracC	North	FMI_SONIC_004PUP_FMI
1976.162651	1976.512	1976.337	42.71551	60.28171	RFracC	North	FMI_SONIC_004PUP_FMI
1991.698958	1992.049	1991.874	43.42302	58.56193	RFracC	North	FMI_SONIC_004PUP_FMI
1992.640142	1992.841	1992.74	55.34205	265.4545	ConFracC	North	FMI_SONIC_004PUP_FMI
1993.496687	1993.758	1993.627	38.84855	85.37463	ConFracC	North	FMI_SONIC_004PUP_FMI
1992.959246	1993.057	1993.008	38.01578	254.2256	ConFracC	North	FMI_SONIC_004PUP_FMI
1997.688865	1997.935	1997.812	37.55907	87.45703	ConFracC	North	FMI_SONIC_004PUP_FMI
1997.363852	1997.678	1997.521	42.26239	72.93056	ConFracC	North	FMI_SONIC_004PUP_FMI
1998.968605	1999.14	1999.055	50.22321	266.9941	ConFracC	North	FMI_SONIC_004PUP_FMI
2001.1726	2001.378	2001.275	33.54118	94.18934	ConFracC	North	FMI_SONIC_004PUP_FMI
2006.599643	2006.805	2006.702	34.65017	99.85892	ConFracC	North	FMI_SONIC_004PUP_FMI
2015.104155	2015.432	2015.268	49.35898	102.9909	RFracC	North	FMI_SONIC_004PUP_FMI
2019.583243	2019.816	2019.7	34.80275	19.17853	ConFracC	North	FMI_SONIC_004PUP_FMI
2028.196092	2028.679	2028.438	54.91685	73.89158	RFracC	North	FMI_SONIC_004PUP_FMI

2054.163291	2054.274	2054.219	40.10098	203.367	RFracC	North	FMI_SONIC_004PUP_FMI
2064.597568	2064.708	2064.653	28.85325	150.9634	RFracC	North	FMI_SONIC_004PUP_FMI
2070.948867	2071.127	2071.038	32.53666	102.4633	RFracC	North	FMI_SONIC_004PUP_FMI
2074.75423	2074.885	2074.82	21.1969	78.93964	ConFracC	North	FMI_SONIC_004PUP_FMI
2081.505025	2081.636	2081.571	20.68788	70.58718	ConFracC	North	FMI_SONIC_004PUP_FMI
2084.77547	2084.873	2084.824	32.72519	186.9047	ConFracC	North	FMI_SONIC_004PUP_FMI
2086.468247	2086.606	2086.537	21.91398	67.62065	RFracC	North	FMI_SONIC_004PUP_FMI
2092.284628	2092.389	2092.337	37.57495	208.3913	RFracC	North	FMI_SONIC_004PUP_FMI
2096.208485	2096.346	2096.277	41.79995	277.9446	RFracC	North	FMI_SONIC_004PUP_FMI
2128.93325	2129.254	2129.094	45.63561	30.99356	ConFracC	North	FMI_SONIC_004PUP_FMI
2133.036541	2133.357	2133.197	45.70036	86.04799	RFracC	North	FMI_SONIC_004PUP_FMI
2133.510519	2133.77	2133.64	64.07597	255.7944	RFracC	North	FMI_SONIC_004PUP_FMI
2153.43789	2153.589	2153.514	30.29309	343.2454	RFracC	North	FMI_SONIC_004PUP_FMI
2179.330606	2179.482	2179.406	23.236	104.9872	RFracC	North	FMI_SONIC_004PUP_FMI
2183.44744	2183.599	2183.523	23.09043	107.2725	ConFracC	North	FMI_SONIC_004PUP_FMI
2190.38444	2190.536	2190.46	23.85893	4.72847	ConFracC	North	FMI_SONIC_004PUP_FMI
2199.518664	2199.569	2199.544	4.387864	246.5639	ConFracC	North	FMI_SONIC_004PUP_FMI
2204.431103	2204.481	2204.456	5.783117	272.3881	RFracC	North	FMI_SONIC_004PUP_FMI
2206.536918	2206.621	2206.579	9.362578	141.6262	ConFracC	North	FMI_SONIC_004PUP_FMI
2212.431167	2212.718	2212.575	42.48221	120.5656	RFracC	North	FMI_SONIC_004PUP_FMI
2232.307755	2232.547	2232.428	51.80558	170.7219	ConFracC	North	FMI_SONIC_004PUP_FMI
2270.056681	2270.168	2270.112	6.348988	8.902127	RFracC	North	FMI_SONIC_004PUP_FMI
2296.474159	2296.585	2296.53	39.94344	198.4787	RFracC	North	FMI_SONIC_004PUP_FMI
2323.264047	2323.768	2323.516	89.33334	208.5242	RFracC	North	FMI_SONIC_004PUP_FMI
2368.708338	2369.002	2368.855	26.31916	52.749	ConFracC	North	FMI_SONIC_004PUP_FMI
2368.644013	2368.938	2368.791	27.71275	39.5589	ConFracC	North	FMI_SONIC_004PUP_FMI
2368.633856	2368.928	2368.781	29.04227	31.39191	ConFracC	North	FMI_SONIC_004PUP_FMI
2368.616928	2368.911	2368.764	29.41856	29.43932	ConFracC	North	FMI_SONIC_004PUP_FMI
2368.606771	2368.9	2368.754	29.04227	31.39191	ConFracC	North	FMI_SONIC_004PUP_FMI
2372.337652	2372.577	2372.457	78.52669	240.9648	ConFracC	North	FMI_SONIC_004PUP_FMI
2384.386838	2384.992	2384.689	66.18218	155.713	ConFracC	North	FMI_SONIC_004PUP_FMI
2409.619372	2409.778	2409.699	7.29447	38.48653	RFracC	North	FMI_SONIC_004PUP_FMI
2410.418363	2410.705	2410.562	53.98774	329.1512	ConFracC	North	FMI_SONIC_004PUP_FMI
2434.638616	2435.135	2434.887	45.87355	11.68771	RFracC	North	FMI_SONIC_004PUP_FMI
2472.306289	2472.627	2472.467	22.23385	65.86746	ConFracC	North	FMI_SONIC_004PUP_FMI
2477.723176	2478.267	2477.995	80.98002	181.7699	ConFracC	North	FMI_SONIC_004PUP_FMI
2478.17684	2478.721	2478.449	80.98976	181.781	ConFracC	North	FMI_SONIC_004PUP_FMI
2489.078324	2489.623	2489.35	66.21394	161.6031	ConFracC	North	FMI_SONIC_004PUP_FMI
2489.352553	2489.897	2489.625	76.4239	175.1316	ConFracC	North	FMI_SONIC_004PUP_FMI
2508.717922	2509.181	2508.949	65.2903	166.185	ConFracC	North	FMI_SONIC_004PUP_FMI
2509.550768	2509.878	2509.715	58.51683	171.523	ConFracC	North	FMI_SONIC_004PUP_FMI
2509.767444	2510.095	2509.931	58.51518	171.5264	ConFracC	North	FMI_SONIC_004PUP_FMI
2515.499187	2515.888	2515.693	60.07534	166.4677	ConFracC	North	FMI_SONIC_004PUP_FMI
2522.808598	2523.197	2523.003	69.65074	178.3627	ConFracC	North	FMI_SONIC_004PUP_FMI

2528.330436	2528.543	2528.437	8.256757	68.12391	RFracC	North	FMI_SONIC_004PUP_FMI
2528.692691	2528.804	2528.748	11.92882	216.2433	RFracC	North	FMI_SONIC_004PUP_FMI
2536.316958	2536.861	2536.589	70.83924	168.3816	ConFracC	North	FMI_SONIC_004PUP_FMI
2541.395289	2541.736	2541.566	82.35384	57.99672	ConFracC	North	FMI_SONIC_004PUP_FMI
2557.998046	2558.339	2558.169	69.09403	182.5715	ConFracC	North	FMI_SONIC_004PUP_FMI
2568.774264	2569.379	2569.077	71.86142	166.8702	ConFracC	North	FMI_SONIC_004PUP_FMI
2576.814955	2577.156	2576.985	69.55578	183.105	ConFracC	North	FMI_SONIC_004PUP_FMI
2586.83958	2587.181	2587.01	79.57967	193.8182	ConFracC	North	FMI_SONIC_004PUP_FMI
2587.049484	2587.391	2587.22	58.83671	172.2647	ConFracC	North	FMI_SONIC_004PUP_FMI
2589.026648	2589.368	2589.197	70.17599	183.328	ConFracC	North	FMI_SONIC_004PUP_FMI
2588.813358	2589.236	2589.025	47.01845	151.438	ConFracC	North	FMI_SONIC_004PUP_FMI
2590.858232	2591.416	2591.137	71.35773	168.3947	ConFracC	North	FMI_SONIC_004PUP_FMI
2592.161671	2592.719	2592.441	75.57027	172.6853	ConFracC	North	FMI_SONIC_004PUP_FMI
2591.938224	2592.455	2592.197	67.02348	166.0253	ConFracC	North	FMI_SONIC_004PUP_FMI
2591.748633	2591.975	2591.862	62.09923	191.6325	ConFracC	North	FMI_SONIC_004PUP_FMI
2593.539591	2593.935	2593.737	68.08582	175.658	ConFracC	North	FMI_SONIC_004PUP_FMI
2595.865467	2596.112	2595.989	70.81816	196.7283	ConFracC	North	FMI_SONIC_004PUP_FMI
2608.094088	2608.239	2608.166	8.972047	254.6918	ConFracC	North	FMI_SONIC_004PUP_FMI
2619.191933	2619.486	2619.339	89.17296	210.3161	ConFracC	North	FMI_SONIC_004PUP_FMI
2621.588906	2621.74	2621.665	11.29788	211.0594	ConFracC	North	FMI_SONIC_004PUP_FMI
2637.487467	2638.126	2637.807	66.0854	335.3617	RFracC	North	FMI_SONIC_004PUP_FMI
2656.981487	2657.62	2657.301	89.09232	181.0858	ConFracC	North	FMI_SONIC_004PUP_FMI
2692.834503	2693.494	2693.164	82.12069	172.6105	ConFracC	North	FMI_SONIC_004PUP_FMI
2693.105348	2693.683	2693.394	77.00765	23.07384	ConFracC	North	FMI_SONIC_004PUP_FMI
2693.535313	2694.113	2693.824	51.39683	143.6253	ConFracC	North	FMI_SONIC_004PUP_FMI
2707.162168	2707.28	2707.221	18.63491	214.0278	RFracC	North	FMI_SONIC_004PUP_FMI
2707.57182	2707.798	2707.685	13.04411	146.8899	RFracC	North	FMI_SONIC_004PUP_FMI
2710.48001	2710.706	2710.593	5.570274	120.6913	RFracC	North	FMI_SONIC_004PUP_FMI
2711.390724	2711.617	2711.504	3.471871	79.24198	RFracC	North	FMI_SONIC_004PUP_FMI
2712.348836	2712.575	2712.462	4.180928	104.2198	RFracC	North	FMI_SONIC_004PUP_FMI
2725.75563	2725.982	2725.869	5.409658	119.2176	RFracC	North	FMI_SONIC_004PUP_FMI
2726.321017	2726.547	2726.434	89.20397	265.5167	RFracC	North	FMI_SONIC_004PUP_FMI
2726.510608	2726.886	2726.698	16.94658	68.97436	RFracC	North	FMI_SONIC_004PUP_FMI
2762.086009	2762.644	2762.365	65.2925	161.5614	ConFracC	North	FMI_SONIC_004PUP_FMI
2787.29823	2787.639	2787.469	84.69899	199.8385	ConFracC	North	FMI_SONIC_004PUP_FMI
2788.483174	2788.912	2788.698	69.93018	175.398	ConFracC	North	FMI_SONIC_004PUP_FMI
2798.826041	2799.255	2799.041	63.63103	169.8864	ConFracC	North	FMI_SONIC_004PUP_FMI
2854.670754	2854.829	2854.75	54.9533	202.7684	ConFracC	North	FMI_SONIC_004PUP_FMI
2893.814529	2894.101	2893.958	12.79105	93.94689	RFracC	North	FMI_SONIC_004PUP_FMI
2900.20984	2900.415	2900.313	6.456263	1.494085	RFracC	North	FMI_SONIC_004PUP_FMI
2903.013079	2904.16	2903.586	84.63685	138.2683	RFracC	North	FMI_SONIC_004PUP_FMI
2917.19855	2917.411	2917.305	4.280864	86.41726	RFracC	North	FMI_SONIC_004PUP_FMI
2970.64629	2970.981	2970.813	83.86764	50.80973	ConFracC	North	FMI_SONIC_004PUP_FMI
2977.102541	2977.437	2977.27	84.49336	91.20766	ConFracC	North	FMI_SONIC_004PUP_FMI

3001.02148	3001.193	3001.107	55.38908	198.8551	ConFracC	North	FMI_SONIC_004PUP_FMI
3005.046904	3005.171	3005.109	51.00102	208.4874	ConFracC	North	FMI_SONIC_004PUP_FMI
3005.737557	3005.862	3005.8	55.9154	213.6771	ConFracC	North	FMI_SONIC_004PUP_FMI
3006.174293	3006.299	3006.236	49.35135	206.986	ConFracC	North	FMI_SONIC_004PUP_FMI
3006.834476	3007.121	3006.978	75.0395	198.9714	ConFracC	North	FMI_SONIC_004PUP_FMI
3006.996983	3007.284	3007.14	69.25867	191.5105	ConFracC	North	FMI_SONIC_004PUP_FMI
3008.767628	3009.176	3008.972	78.36289	311.9686	ConFracC	North	FMI_SONIC_004PUP_FMI
3009.353329	3009.999	3009.676	86.25004	316.603	RFracC	North	FMI_SONIC_004PUP_FMI
3027.049619	3027.282	3027.166	25.00586	153.6765	ConFracC	North	FMI_SONIC_004PUP_FMI
3034.32856	3034.785	3034.557	87.60363	117.6453	ConFracC	North	FMI_SONIC_004PUP_FMI
3035.178334	3035.635	3035.406	85.83218	27.80209	ConFracC	North	FMI_SONIC_004PUP_FMI
3035.902843	3035.987	3035.945	32.41527	287.1743	ConFracC	North	FMI_SONIC_004PUP_FMI
3037.754741	3037.899	3037.827	7.755981	299.2461	ConFracC	North	FMI_SONIC_004PUP_FMI
3044.238077	3045.013	3044.625	71.25917	162.5942	ConFracC	North	FMI_SONIC_004PUP_FMI
3051.479776	3051.814	3051.647	88.02077	103.6817	ConFracC	North	FMI_SONIC_004PUP_FMI
3053.077758	3053.243	3053.16	67.29628	287.8391	ConFracC	North	FMI_SONIC_004PUP_FMI
3054.012171	3054.177	3054.095	76.16006	270.4768	ConFracC	North	FMI_SONIC_004PUP_FMI
3078.388159	3078.634	3078.511	67.29771	308.4087	ConFracC	North	FMI_SONIC_004PUP_FMI
1318.275896	1318.448	1318.362	31.2712	3.292922	RFracC	North	FMI_SONIC_004PUP_FMI
1318.154016	1318.272	1318.213	43.04667	245.4623	RFracC	North	FMI_SONIC_004PUP_FMI
1380.434667	1383.071	1381.753	72.74209	74.67343	RFracC	North	FMI_SONIC_004PUP_FMI
1441.205361	1441.343	1441.274	22.31054	10.65414	RFracC	North	FMI_SONIC_004PUP_FMI
2229.695002	2230.471	2230.083	89.48691	105.8023	RFracC	North	FMI_SONIC_004PUP_FMI
2328.108472	2328.884	2328.496	77.61953	58.82095	ConFracC	North	FMI_SONIC_004PUP_FMI
951.4631704	952.2388	951.851	73.33331	171.7126	RFracC	North	FMI_SONIC_004PUP_FMI
1099.6631	1100.002	1099.833	55.31794	1.444432	RFracC	North	FMI_SONIC_004PUP_FMI
1206.53562	1206.875	1206.705	70.71145	215.8368	RFracC	North	FMI_SONIC_004PUP_FMI
1206.638967	1206.978	1206.809	63.41808	300.9592	RFracC	North	FMI_SONIC_004PUP_FMI
1523.157087	1524.828	1523.993	69.81698	74.83865	RFracC	North	FMI_SONIC_004PUP_FMI
1525.361828	1525.954	1525.658	57.15118	66.18118	RFracC	North	FMI_SONIC_004PUP_FMI
1524.385771	1525.873	1525.13	68.52206	68.27829	RFracC	North	FMI_SONIC_004PUP_FMI
1544.641828	1545.762	1545.202	68.25939	18.91391	RFracC	North	FMI_SONIC_004PUP_FMI
1552.438803	1553.972	1553.206	69.87062	82.76751	RFracC	North	FMI_SONIC_004PUP_FMI
1733.112729	1734.462	1733.788	84.36079	63.67607	RFracC	North	FMI_SONIC_004PUP_FMI
1836.19585	1836.811	1836.503	57.99627	93.48717	ConFracC	North	FMI_SONIC_004PUP_FMI
1856.302628	1857.767	1857.035	63.92116	52.28992	RFracC	North	FMI_SONIC_004PUP_FMI
1885.251336	1886.05	1885.651	88.01159	75.53903	RFracC	North	FMI_SONIC_004PUP_FMI
2005.524547	2005.956	2005.74	52.62508	87.88111	RFracC	North	FMI_SONIC_004PUP_FMI
2027.296364	2027.727	2027.512	52.74943	77.16424	RFracC	North	FMI_SONIC_004PUP_FMI
2484.137057	2484.729	2484.433	62.29919	153.3171	ConFracC	North	FMI_SONIC_004PUP_FMI
2524.442477	2525.034	2524.738	33.83766	81.47542	ConFracC	North	FMI_SONIC_004PUP_FMI
2733.422062	2734.152	2733.787	29.8616	70.68756	RFracC	North	FMI_SONIC_004PUP_FMI
2756.881883	2757.612	2757.247	51.51605	138.3012	ConFracC	North	FMI_SONIC_004PUP_FMI
2757.306755	2758.036	2757.672	78.05773	167.6568	ConFracC	North	FMI_SONIC_004PUP_FMI

3024.195238	3024.925	3024.56	68.54942	49.24742	ConFracC	North	FMI_SONIC_004PUP_FMI
3024.12634	3024.856	3024.491	69.50264	45.51811	ConFracC	North	FMI_SONIC_004PUP_FMI
3025.251677	3025.981	3025.617	66.32584	79.15056	ConFracC	North	FMI_SONIC_004PUP_FMI
3028.329127	3028.668	3028.499	86.23703	98.6494	ConFracC	North	FMI_SONIC_004PUP_FMI
3029.029592	3029.369	3029.199	84.64204	296.7998	ConFracC	North	FMI_SONIC_004PUP_FMI
3029.385566	3029.725	3029.555	84.85053	205.5759	ConFracC	North	FMI_SONIC_004PUP_FMI
3038.962409	3039.715	3039.339	67.33148	51.60372	ConFracC	North	FMI_SONIC_004PUP_FMI
3057.541945	3057.812	3057.677	89.2234	275.9273	ConFracC	North	FMI_SONIC_004PUP_FMI
3056.531438	3056.917	3056.724	73.40129	318.2804	ConFracC	North	FMI_SONIC_004PUP_FMI
3050.204291	3050.727	3050.466	71.82973	329.9282	ConFracC	North	FMI_SONIC_004PUP_FMI
3049.848318	3050.371	3050.11	81.37946	113.059	ConFracC	North	FMI_SONIC_004PUP_FMI
3030.671665	3031.355	3031.014	69.7111	94.25935	ConFracC	North	FMI_SONIC_004PUP_FMI
3015.378653	3015.601	3015.49	15.37112	136.3561	ConFracC	North	FMI_SONIC_004PUP_FMI
3018.696288	3019.663	3019.179	88.12074	177.3367	ConFracC	North	FMI_SONIC_004PUP_FMI
3019.981312	3021.044	3020.513	87.9755	0.537268	ConFracC	North	FMI_SONIC_004PUP_FMI
3022.568586	3023.466	3023.017	80.37542	14.72245	ConFracC	North	FMI_SONIC_004PUP_FMI
3030.041018	3030.332	3030.187	88.43907	281.0516	ConFracC	North	FMI_SONIC_004PUP_FMI
3035.73233	3035.886	3035.809	60.13106	292.4153	ConFracC	North	FMI_SONIC_004PUP_FMI
3038.798473	3038.952	3038.875	64.65166	286.804	ConFracC	North	FMI_SONIC_004PUP_FMI
3050.918351	3051.306	3051.112	73.90377	186.3093	ConFracC	North	FMI_SONIC_004PUP_FMI
3050.790882	3051.041	3050.916	57.72186	186.4562	ConFracC	North	FMI_SONIC_004PUP_FMI
3050.904571	3051.154	3051.029	60.60889	189.4451	ConFracC	North	FMI_SONIC_004PUP_FMI
3051.05271	3051.544	3051.298	65.30106	168.4514	ConFracC	North	FMI_SONIC_004PUP_FMI
3054.84577	3055.219	3055.033	86.18599	106.8375	ConFracC	North	FMI_SONIC_004PUP_FMI
3057.853347	3058.034	3057.944	74.4161	281.4597	ConFracC	North	FMI_SONIC_004PUP_FMI
3062.307867	3062.716	3062.512	88.031	115.7539	ConFracC	North	FMI_SONIC_004PUP_FMI
3062.008143	3062.134	3062.071	14.76729	208.3205	ConFracC	North	FMI_SONIC_004PUP_FMI
3067.971619	3068.573	3068.272	69.94401	54.85884	ConFracC	North	FMI_SONIC_004PUP_FMI
3075.003077	3075.604	3075.304	82.77933	23.41388	ConFracC	North	FMI_SONIC_004PUP_FMI
3084.521901	3084.634	3084.578	56.98897	285.8514	ConFracC	North	FMI_SONIC_004PUP_FMI
3084.435774	3084.548	3084.492	65.02013	274.0646	ConFracC	North	FMI_SONIC_004PUP_FMI

Bartsia 1: Total interpreted fracture set

Top Depth (m)	Bottom Depth (m)	Depth (m)	True Dip (deg)	True Azimuth (deg)	Surface Type	Apparent Mode	Image Log
2000.666	2000.741	2000.704	11.55423	104.4627	RFracC	North	FMI_SONIC_051PUP_FMI
2001.628	2001.694	2001.661	19.60562	71.92249	ConFracC	North	FMI_SONIC_051PUP_FMI
1997.28	1997.632	1997.456	55.32107	280.025	RFracC	North	FMI_SONIC_051PUP_FMI
2040.907	2041.215	2041.061	50.09786	71.74133	ConFracC	North	FMI_SONIC_051PUP_FMI
2044.77	2045.144	2044.957	47.75408	100.7833	ConFracC	North	FMI_SONIC_051PUP_FMI
2044.574	2045.305	2044.939	60.63299	107.048	RFracC	North	FMI_SONIC_051PUP_FMI
2010.397	2010.724	2010.561	62.22032	73.99226	RFracC	North	FMI_SONIC_051PUP_FMI
2029.347	2029.473	2029.41	30.64867	60.94151	ConFracC	North	FMI_SONIC_051PUP_FMI
2046.788	2046.914	2046.851	42.0629	290.1274	ConFracC	North	FMI_SONIC_051PUP_FMI
2085.385	2085.51	2085.448	20.70454	205.9113	RFracC	North	FMI_SONIC_051PUP_FMI
2096.78	2096.987	2096.884	41.31486	229.964	ConFracC	North	FMI_SONIC_051PUP_FMI
2165.996	2166.21	2166.103	30.52148	199.6299	ConFracC	North	FMI_SONIC_051PUP_FMI
2186.681	2186.867	2186.774	46.43	305.1155	RFracC	North	FMI_SONIC_051PUP_FMI
2186.652	2186.837	2186.744	47.70995	310.3681	RFracC	North	FMI_SONIC_051PUP_FMI
2189.042	2189.336	2189.189	67.64086	1.654489	RFracC	North	FMI_SONIC_051PUP_FMI
2196.846	2197.126	2196.986	38.85276	197.6513	ConFracC	North	FMI_SONIC_051PUP_FMI
2207.407	2207.687	2207.547	39.17879	208.1198	RFracC	North	FMI_SONIC_051PUP_FMI
2216.262	2216.543	2216.403	40.36433	150.5115	RFracC	North	FMI_SONIC_051PUP_FMI
2223.568	2223.697	2223.632	33.1292	302.986	ConFracC	North	FMI_SONIC_051PUP_FMI
2224.907	2225.078	2224.993	24.79471	228.6499	ConFracC	North	FMI_SONIC_051PUP_FMI
2225.289	2225.46	2225.375	23.03568	204.0939	RFracC	North	FMI_SONIC_051PUP_FMI
2225.276	2225.446	2225.361	23.16528	178.4019	RFracC	North	FMI_SONIC_051PUP_FMI
2231.922	2232.093	2232.008	31.51065	119.5813	ConFracC	North	FMI_SONIC_051PUP_FMI
2232.03	2232.201	2232.115	28.71303	132.2664	ConFracC	North	FMI_SONIC_051PUP_FMI
2232.466	2232.637	2232.552	32.17057	117.0327	ConFracC	North	FMI_SONIC_051PUP_FMI
2234.993	2235.141	2235.067	36.7801	84.9215	RFracC	North	FMI_SONIC_051PUP_FMI
2238.969	2239.103	2239.036	16.37338	194.2917	RFracC	North	FMI_SONIC_051PUP_FMI
2255.791	2255.925	2255.858	16.00002	197.8107	RFracC	North	FMI_SONIC_051PUP_FMI
2267.017	2267.22	2267.119	27.04172	175.451	RFracC	North	FMI_SONIC_051PUP_FMI
2267.294	2267.497	2267.395	39.47013	105.1721	RFracC	North	FMI_SONIC_051PUP_FMI
2267.31	2267.513	2267.411	29.9263	237.6859	RFracC	North	FMI_SONIC_051PUP_FMI
2270.819	2271.022	2270.921	26.32633	202.8526	ConFracC	North	FMI_SONIC_051PUP_FMI
2271.03	2271.233	2271.131	30.41354	241.8654	RFracC	North	FMI_SONIC_051PUP_FMI
2272.015	2272.218	2272.117	59.53276	357.4448	RFracC	North	FMI_SONIC_051PUP_FMI
2273.431	2273.588	2273.509	18.5159	198.635	RFracC	North	FMI_SONIC_051PUP_FMI
2283.507	2283.664	2283.586	23.09509	237.951	RFracC	North	FMI_SONIC_051PUP_FMI
2283.759	2283.952	2283.855	31.25365	247.1838	RFracC	North	FMI_SONIC_051PUP_FMI
2284.337	2284.531	2284.434	29.7903	239.5877	RFracC	North	FMI_SONIC_051PUP_FMI
2292.712	2292.952	2292.832	32.20104	207.7918	RFracC	North	FMI_SONIC_051PUP_FMI
2295.067	2295.307	2295.187	39.26862	112.0045	RFracC	North	FMI_SONIC_051PUP_FMI
2295.127	2295.366	2295.247	36.40149	124.7855	RFracC	North	FMI_SONIC_051PUP_FMI

2295.184	2295.423	2295.304	33.30808	143.4793	RFracC	North	FMI_SONIC_051PUP_FMI
2298.41	2298.65	2298.53	45.03549	267.3078	ConFracC	North	FMI_SONIC_051PUP_FMI
2301.367	2301.606	2301.486	33.9812	219.1865	RFracC	North	FMI_SONIC_051PUP_FMI
2315.17	2315.354	2315.262	23.69041	204.5806	ConFracC	North	FMI_SONIC_051PUP_FMI
2328.898	2329.027	2328.963	26.65515	262.4371	RFracC	North	FMI_SONIC_051PUP_FMI
2338.652	2339.138	2338.895	49.69414	195.5822	RFracC	North	FMI_SONIC_051PUP_FMI
2344.91	2345.204	2345.057	71.01374	358.5531	ConFracC	North	FMI_SONIC_051PUP_FMI
2346.211	2346.405	2346.308	35.23114	244.339	RFracC	North	FMI_SONIC_051PUP_FMI
2347.949	2348.074	2348.011	20.8709	84.07387	RFracC	North	FMI_SONIC_051PUP_FMI
2350.224	2350.376	2350.3	28.05297	245.6206	RFracC	North	FMI_SONIC_051PUP_FMI
2359.342	2359.773	2359.558	47.82932	199.3449	RFracC	North	FMI_SONIC_051PUP_FMI
2361.459	2361.607	2361.533	21.77387	101.5383	RFracC	North	FMI_SONIC_051PUP_FMI
2363.494	2363.688	2363.591	37.42344	250.5026	RFracC	North	FMI_SONIC_051PUP_FMI
2363.579	2363.772	2363.676	46.16365	276.0476	RFracC	North	FMI_SONIC_051PUP_FMI
2368.547	2368.695	2368.621	16.04706	170.3816	RFracC	North	FMI_SONIC_051PUP_FMI
2369.544	2369.77	2369.657	32.25787	211.3132	ConFracC	North	FMI_SONIC_051PUP_FMI
2376.934	2377.036	2376.985	19.37962	256.4178	ConFracC	North	FMI_SONIC_051PUP_FMI
2379.36	2379.407	2379.384	6.784134	4.566379	RFracC	North	FMI_SONIC_051PUP_FMI
2379.952	2380.082	2380.017	15.14397	206.3268	RFracC	North	FMI_SONIC_051PUP_FMI
2380.691	2380.953	2380.822	32.48184	175.6388	RFracC	North	FMI_SONIC_051PUP_FMI
2380.782	2381.003	2380.893	28.01349	182.3723	RFracC	North	FMI_SONIC_051PUP_FMI
2384.246	2384.339	2384.293	5.300956	183.4109	RFracC	North	FMI_SONIC_051PUP_FMI
2395.992	2396.135	2396.063	47.88848	11.85299	RFracC	North	FMI_SONIC_051PUP_FMI
2398.031	2398.174	2398.103	24.30105	84.27429	RFracC	North	FMI_SONIC_051PUP_FMI
2403.112	2403.429	2403.27	70.94999	10.04483	RFracC	North	FMI_SONIC_051PUP_FMI
2413.933	2414.049	2413.991	45.99396	332.5779	ConFracC	North	FMI_SONIC_051PUP_FMI
2417.162	2417.474	2417.318	43.32766	215.922	ConFracC	North	FMI_SONIC_051PUP_FMI
2417.377	2417.603	2417.49	39.16424	237.3927	ConFracC	North	FMI_SONIC_051PUP_FMI
2418.394	2419.256	2418.825	88.51662	190.1927	RFracC	North	FMI_SONIC_051PUP_FMI
2423.587	2423.717	2423.652	12.91156	143.3198	ConFracC	North	FMI_SONIC_051PUP_FMI
2439.567	2439.642	2439.604	18.43046	42.09987	RFracC	North	FMI_SONIC_051PUP_FMI
2444.073	2444.226	2444.15	51.00583	2.880252	RFracC	North	FMI_SONIC_051PUP_FMI
2444.316	2444.583	2444.449	60.95519	29.62989	RFracC	North	FMI_SONIC_051PUP_FMI
2445.217	2445.378	2445.298	48.57515	296.4946	RFracC	North	FMI_SONIC_051PUP_FMI
2449.954	2450.23	2450.092	36.60239	198.2685	ConFracC	North	FMI_SONIC_051PUP_FMI
2456.011	2456.287	2456.149	61.22982	284.1297	RFracC	North	FMI_SONIC_051PUP_FMI
2459.064	2459.189	2459.126	22.55481	242.2904	ConFracC	North	FMI_SONIC_051PUP_FMI
2459.267	2459.461	2459.364	36.74878	242.9981	ConFracC	North	FMI_SONIC_051PUP_FMI
2394.565	2394.731	2394.648	29.63247	239.2081	ConFracC	North	FMI_SONIC_051PUP_FMI
2463.664	2463.775	2463.72	42.60766	2.101379	ConFracC	North	FMI_SONIC_051PUP_FMI
2468.173	2468.426	2468.299	38.0595	216.4722	RFracC	North	FMI_SONIC_051PUP_FMI
2475.185	2475.388	2475.287	28.54132	202.109	ConFracC	North	FMI_SONIC_051PUP_FMI
2475.656	2475.859	2475.758	25.70834	178.4972	ConFracC	North	FMI_SONIC_051PUP_FMI
2475.56	2475.763	2475.662	27.50608	195.1834	ConFracC	North	FMI_SONIC_051PUP_FMI

2476.045	2476.316	2476.181	33.21229	160.0278	ConFracC	North	FMI_SONIC_051PUP_FMI
2476.221	2476.438	2476.329	28.88837	190.5327	ConFracC	North	FMI_SONIC_051PUP_FMI
2476.386	2476.639	2476.512	34.122	195.1453	ConFracC	North	FMI_SONIC_051PUP_FMI
2477.785	2477.988	2477.886	28.05139	198.6841	RFracC	North	FMI_SONIC_051PUP_FMI
2293.846	2294.049	2293.948	28.4687	216.7946	RFracC	North	FMI_SONIC_051PUP_FMI
2293.995	2294.253	2294.124	36.70566	224.962	RFracC	North	FMI_SONIC_051PUP_FMI
2002.655	2002.922	2002.789	62.88125	51.04047	ConFracC	North	FMI_SONIC_051PUP_FMI
2011.19	2011.372	2011.281	52.05121	43.3412	RFracC	North	FMI_SONIC_051PUP_FMI
2013.351	2013.821	2013.586	75.47223	54.56208	RFracC	North	FMI_SONIC_051PUP_FMI
2013.458	2013.928	2013.693	77.05149	46.55153	RFracC	North	FMI_SONIC_051PUP_FMI
2013.533	2014.003	2013.768	79.13395	32.79612	RFracC	North	FMI_SONIC_051PUP_FMI
2020.667	2021.137	2020.902	54.55119	229.3069	RFracC	North	FMI_SONIC_051PUP_FMI
2021.014	2021.41	2021.212	50.49112	229.1736	RFracC	North	FMI_SONIC_051PUP_FMI
2028.336	2028.731	2028.534	46.7693	196.3537	ConFracC	North	FMI_SONIC_051PUP_FMI
2029.913	2030.309	2030.111	48.34799	206.9687	RFracC	North	FMI_SONIC_051PUP_FMI
2029.988	2030.384	2030.186	48.12412	205.5316	RFracC	North	FMI_SONIC_051PUP_FMI
2035.449	2035.577	2035.513	27.85853	63.44561	RFracC	North	FMI_SONIC_051PUP_FMI
2035.224	2035.587	2035.406	56.6686	72.39566	ConFracC	North	FMI_SONIC_051PUP_FMI
2044.102	2044.476	2044.289	45.01095	121.2296	RFracC	North	FMI_SONIC_051PUP_FMI
2070.884	2071.387	2071.135	53.01149	170.6345	RFracC	North	FMI_SONIC_051PUP_FMI
2077.542	2077.735	2077.639	32.86646	204.4873	RFracC	North	FMI_SONIC_051PUP_FMI
2082.42	2083.617	2083.019	67.92667	180.3062	RFracC	North	FMI_SONIC_051PUP_FMI
2096.153	2096.356	2096.255	33.14486	197.009	ConFracC	North	FMI_SONIC_051PUP_FMI
2101.758	2101.94	2101.849	44.39125	256.7771	ConFracC	North	FMI_SONIC_051PUP_FMI
2109.523	2109.651	2109.587	29.23097	242.0124	ConFracC	North	FMI_SONIC_051PUP_FMI
2159.163	2159.73	2159.446	83.22721	10.02393	ConFracC	North	FMI_SONIC_051PUP_FMI
2159.264	2159.831	2159.548	83.7303	2.99609	ConFracC	North	FMI_SONIC_051PUP_FMI
2184.09	2184.592	2184.341	52.95335	202.7193	ConFracC	North	FMI_SONIC_051PUP_FMI
2196.107	2196.609	2196.358	53.41172	200.7852	RFracC	North	FMI_SONIC_051PUP_FMI
2206	2206.503	2206.252	53.34118	201.9697	RFracC	North	FMI_SONIC_051PUP_FMI
2206.198	2206.701	2206.449	53.42377	203.3887	RFracC	North	FMI_SONIC_051PUP_FMI
2214.407	2214.578	2214.493	51.78478	26.52417	RFracC	North	FMI_SONIC_051PUP_FMI
2214.578	2214.749	2214.664	25.70379	227.0379	RFracC	North	FMI_SONIC_051PUP_FMI
2220.696	2221.103	2220.9	46.9792	198.6385	RFracC	North	FMI_SONIC_051PUP_FMI
2224.076	2224.483	2224.28	48.53124	223.8794	RFracC	North	FMI_SONIC_051PUP_FMI
2245.634	2246.04	2245.837	46.80176	209.6726	RFracC	North	FMI_SONIC_051PUP_FMI
2267.079	2267.486	2267.282	59.17932	106.9865	RFracC	North	FMI_SONIC_051PUP_FMI
2283.85	2284.257	2284.054	47.18679	218.668	RFracC	North	FMI_SONIC_051PUP_FMI
2329.699	2330.169	2329.934	48.40963	198.6277	RFracC	North	FMI_SONIC_051PUP_FMI
2347.411	2347.71	2347.561	63.67577	36.81116	RFracC	North	FMI_SONIC_051PUP_FMI
2347.267	2347.566	2347.416	63.6755	36.81354	RFracC	North	FMI_SONIC_051PUP_FMI
2350.561	2351.042	2350.801	64.40577	72.73197	RFracC	North	FMI_SONIC_051PUP_FMI
2350.614	2351.096	2350.855	63.25262	249.9449	RFracC	North	FMI_SONIC_051PUP_FMI
2360.759	2361.016	2360.888	32.74027	137.191	RFracC	North	FMI_SONIC_051PUP_FMI

2366.113	2366.369	2366.241	49.751	260.5293	RFracC	North	FMI_SONIC_051PUP_FMI
2365.979	2366.171	2366.075	58.7465	357.8655	RFracC	North	FMI_SONIC_051PUP_FMI
2375.231	2375.338	2375.284	25.02435	267.5665	RFracC	North	FMI_SONIC_051PUP_FMI
2377.579	2377.686	2377.632	24.29625	265.8297	RFracC	North	FMI_SONIC_051PUP_FMI
2389.376	2389.825	2389.601	46.18535	170.6407	RFracC	North	FMI_SONIC_051PUP_FMI
2389.334	2389.868	2389.601	49.82263	153.6869	RFracC	North	FMI_SONIC_051PUP_FMI
2405.265	2405.532	2405.399	37.25887	209.208	RFracC	North	FMI_SONIC_051PUP_FMI
2414.111	2414.378	2414.244	68.58026	351.3713	RFracC	North	FMI_SONIC_051PUP_FMI
2414.196	2415.127	2414.661	62.30974	199.145	RFracC	North	FMI_SONIC_051PUP_FMI
2421.673	2422.132	2421.903	52.48935	212.1392	RFracC	North	FMI_SONIC_051PUP_FMI
2425.053	2425.224	2425.138	39.9656	266.391	ConFracC	North	FMI_SONIC_051PUP_FMI
2431.711	2432.074	2431.893	40.95671	160.1844	ConFracC	North	FMI_SONIC_051PUP_FMI
2441.38	2441.743	2441.562	40.88185	158.755	ConFracC	North	FMI_SONIC_051PUP_FMI
2453.541	2454.814	2454.178	81.76493	167.4608	ConFracC	North	FMI_SONIC_051PUP_FMI
2471.692	2472.066	2471.879	43.48456	186.656	RFracC	North	FMI_SONIC_051PUP_FMI
2479.147	2480.623	2479.885	81.51341	177.5056	ConFracC	North	FMI_SONIC_051PUP_FMI

Eremia 2: Total interpreted fracture set

Top Depth (m)	Bottom Depth (m)	Depth (m)	True Dip (deg)	True Azimuth (deg)	Surface Type	Apparent Mode	Image Log
2144.679	2144.845	2144.762	61.99602	100.9159	ConFracC	North	FMI_024PUP_FMI
2147.408	2147.694	2147.551	81.27874	140.5511	ConFracC	North	FMI_024PUP_FMI
2147.739	2148.025	2147.882	78.67587	103.8744	ConFracC	North	FMI_024PUP_FMI
2149.116	2149.201	2149.158	42.82822	99.57948	RFracC	North	FMI_024PUP_FMI
2153.034	2153.182	2153.108	39.83739	58.87637	RFracC	North	FMI_024PUP_FMI
2158.851	2159.179	2159.015	48.18457	16.87935	ConFracC	North	FMI_024PUP_FMI
2185.292	2185.621	2185.457	82.35013	137.4206	RFracC	North	FMI_024PUP_FMI
2188.341	2188.596	2188.468	76.17153	130.2079	RFracC	North	FMI_024PUP_FMI
2195.054	2195.308	2195.181	74.74229	138.2489	RFracC	North	FMI_024PUP_FMI
2195.101	2195.356	2195.229	74.90369	137.2245	RFracC	North	FMI_024PUP_FMI
2194.985	2195.239	2195.112	74.57265	139.2727	RFracC	North	FMI_024PUP_FMI
2201.385	2201.575	2201.48	66.78235	134.6617	ConFracC	North	FMI_024PUP_FMI
2203.277	2203.521	2203.399	74.53711	127.627	ConFracC	North	FMI_024PUP_FMI
2204.789	2205.032	2204.91	72.05265	143.8117	RFracC	North	FMI_024PUP_FMI
2218.479	2219.094	2218.786	57.30525	351.9731	RFracC	North	FMI_024PUP_FMI
2219.327	2219.942	2219.635	55.43831	346.7262	RFracC	North	FMI_024PUP_FMI
2219.375	2219.99	2219.682	55.43831	346.7262	RFracC	North	FMI_024PUP_FMI
2219.486	2220.101	2219.794	53.7867	341.2344	RFracC	North	FMI_024PUP_FMI
2219.555	2220.17	2219.863	50.98402	329.6936	RFracC	North	FMI_024PUP_FMI
2219.783	2220.26	2220.022	45.12373	323.4817	RFracC	North	FMI_024PUP_FMI
2134.646	2134.848	2134.747	55.03376	194.6169	ConFracC	North	FMI_024PUP_FMI
2134.837	2135.038	2134.938	46.9229	210.1711	ConFracC	North	FMI_024PUP_FMI
2134.996	2135.198	2135.097	47.97865	208.1605	ConFracC	North	FMI_024PUP_FMI
2135.134	2135.304	2135.219	34.43758	222.326	ConFracC	North	FMI_024PUP_FMI
2135.245	2135.415	2135.33	33.34986	224.5872	ConFracC	North	FMI_024PUP_FMI
2146.258	2146.428	2146.343	62.01922	98.75942	ConFracC	North	FMI_024PUP_FMI
2148.204	2148.437	2148.32	66.07504	177.3066	ConFracC	North	FMI_024PUP_FMI
2148.495	2149.004	2148.75	76.20768	201.1213	ConFracC	North	FMI_024PUP_FMI
2153.331	2153.384	2153.357	38.74808	116.0832	RFracC	North	FMI_024PUP_FMI
2153.962	2154.248	2154.105	36.18818	351.4227	ConFracC	North	FMI_024PUP_FMI
2154.736	2155.224	2154.98	48.33498	347.3561	ConFracC	North	FMI_024PUP_FMI
2155.94	2156.268	2156.104	42.0319	358.8462	ConFracC	North	FMI_024PUP_FMI
2155.706	2156.035	2155.871	42.39414	0.342931	RFracC	North	FMI_024PUP_FMI
2156.369	2156.581	2156.475	72.10355	118.9051	ConFracC	North	FMI_024PUP_FMI
2156.534	2156.979	2156.756	89.67243	323.6249	ConFracC	North	FMI_024PUP_FMI
2162.795	2162.933	2162.864	50.18227	170.0526	ConFracC	North	FMI_024PUP_FMI
2169.1	2169.375	2169.237	54.25704	208.0067	ConFracC	North	FMI_024PUP_FMI
2168.983	2169.195	2169.089	45.50762	208.6601	ConFracC	North	FMI_024PUP_FMI
2168.829	2169.031	2168.93	48.24576	199.0869	ConFracC	North	FMI_024PUP_FMI
2168.686	2168.887	2168.787	50.18916	195.035	ConFracC	North	FMI_024PUP_FMI
2168.67	2168.872	2168.771	47.29042	201.1858	ConFracC	North	FMI_024PUP_FMI

2176.74	2176.941	2176.841	33.21556	233.2376	ConFracC	North	FMI_024PUP_FMI
2177.053	2177.254	2177.154	34.60947	229.1078	ConFracC	North	FMI_024PUP_FMI
2179.545	2179.746	2179.646	24.46343	274.079	ConFracC	North	FMI_024PUP_FMI
2179.715	2179.916	2179.815	49.21036	194.5901	ConFracC	North	FMI_024PUP_FMI
2179.784	2179.985	2179.884	52.45373	54.97692	ConFracC	North	FMI_024PUP_FMI
2203.792	2203.993	2203.892	52.80402	51.59031	RFracC	North	FMI_024PUP_FMI
2211.305	2211.506	2211.406	70.25084	123.6925	RFracC	North	FMI_024PUP_FMI
2211.835	2212.153	2211.994	81.92838	132.2603	RFracC	North	FMI_024PUP_FMI
2212.005	2212.323	2212.164	44.76937	356.7318	RFracC	North	FMI_024PUP_FMI
2214.513	2214.725	2214.619	72.45432	120.8027	RFracC	North	FMI_024PUP_FMI
2213.606	2213.913	2213.76	69.76979	171.8356	RFracC	North	FMI_024PUP_FMI
2213.516	2213.823	2213.67	71.43618	167.6999	RFracC	North	FMI_024PUP_FMI
2205.594	2205.902	2205.748	72.72631	164.153	RFracC	North	FMI_024PUP_FMI
2205.366	2205.674	2205.52	78.62595	90.60916	RFracC	North	FMI_024PUP_FMI
2156.804	2157.387	2157.096	88.09202	175.4775	RFracC	North	FMI_024PUP_FMI

Evandra 1: Total interpreted fracture set

Top Depth (m)	Bottom Depth (m)	Depth (m)	True Dip (deg)	True Azimuth (deg)	Surface Type	Apparent Mode	Image Log
2243.629	2244.726	2244.178	89.33658	190.7993	ConFracC	North	FMI_079PUP_FMI
2244.376	2245.473	2244.925	88.92807	185.9117	ConFracC	North	FMI_079PUP_FMI
2246.68	2247.777	2247.229	88.47636	176.1276	ConFracC	North	FMI_079PUP_FMI
2247.411	2248.509	2247.96	89.07469	188.396	ConFracC	North	FMI_079PUP_FMI
2247.52	2248.618	2248.069	88.98943	187.1723	ConFracC	North	FMI_079PUP_FMI
2247.738	2249.178	2248.458	86.84308	192.2838	ConFracC	North	FMI_079PUP_FMI
2257.062	2257.723	2257.393	82.18769	27.19591	ConFracC	North	FMI_079PUP_FMI
2299.135	2300.014	2299.575	88.4033	7.929441	ConFracC	North	FMI_079PUP_FMI
2299.571	2300.45	2300.011	87.70256	13.95914	ConFracC	North	FMI_079PUP_FMI
2309.424	2310.303	2309.863	89.52698	1.695968	ConFracC	North	FMI_079PUP_FMI
2305.626	2306.505	2306.065	88.70426	7.804448	ConFracC	North	FMI_079PUP_FMI
2331.962	2332.375	2332.169	66.22049	257.4024	RFracC	North	FMI_079PUP_FMI
2234.133	2234.545	2234.339	66.58004	51.62653	RFracC	North	FMI_079PUP_FMI
2236.156	2236.425	2236.29	49.19942	78.41236	RFracC	North	FMI_079PUP_FMI
2237.743	2238.502	2238.123	65.71334	210.8008	RFracC	North	FMI_079PUP_FMI
2244.892	2245.225	2245.058	61.28448	57.86903	RFracC	North	FMI_079PUP_FMI
2245.465	2245.726	2245.595	51.02325	73.56373	RFracC	North	FMI_079PUP_FMI
2245.577	2245.989	2245.783	62.22683	78.47712	RFracC	North	FMI_079PUP_FMI
2245.541	2245.888	2245.715	58.7328	74.85583	RFracC	North	FMI_079PUP_FMI
2255.311	2255.478	2255.395	34.00538	95.75389	RFracC	North	FMI_079PUP_FMI
2258.207	2258.374	2258.291	35.04852	92.0659	RFracC	North	FMI_079PUP_FMI
2258.366	2258.533	2258.449	34.30048	95.95211	RFracC	North	FMI_079PUP_FMI
2258.586	2258.753	2258.669	30.54926	118.1047	RFracC	North	FMI_079PUP_FMI
2261.424	2261.837	2261.63	63.32717	79.00882	RFracC	North	FMI_079PUP_FMI
2261.879	2262.118	2261.998	48.45133	79.55128	RFracC	North	FMI_079PUP_FMI
2262.564	2262.803	2262.684	45.63591	254.3499	RFracC	North	FMI_079PUP_FMI
2262.802	2263.041	2262.922	53.2985	56.21079	RFracC	North	FMI_079PUP_FMI
2263.036	2263.276	2263.156	47.67186	264.2803	RFracC	North	FMI_079PUP_FMI
2263.206	2263.445	2263.326	52.60142	59.63372	RFracC	North	FMI_079PUP_FMI
2266.571	2266.832	2266.701	56.22655	53.51319	RFracC	North	FMI_079PUP_FMI
2266.524	2266.785	2266.654	56.44422	52.37409	RFracC	North	FMI_079PUP_FMI
2266.488	2266.749	2266.618	57.28828	47.83844	RFracC	North	FMI_079PUP_FMI
2270.376	2270.565	2270.47	40.14963	84.11151	RFracC	North	FMI_079PUP_FMI
2270.462	2270.651	2270.557	39.12958	89.08333	RFracC	North	FMI_079PUP_FMI
2270.52	2270.709	2270.614	39.38192	87.82648	RFracC	North	FMI_079PUP_FMI
2270.964	2271.152	2271.058	53.5557	356.6054	RFracC	North	FMI_079PUP_FMI
2271.05	2271.102	2271.076	5.790759	90.61522	RFracC	North	FMI_079PUP_FMI
2271.209	2271.571	2271.39	61.19519	72.13779	RFracC	North	FMI_079PUP_FMI
2271.234	2271.596	2271.415	54.01854	108.3227	RFracC	North	FMI_079PUP_FMI
2271.894	2272.256	2272.075	61.91508	68.5459	RFracC	North	FMI_079PUP_FMI
2271.815	2272.177	2271.996	60.16785	76.95333	RFracC	North	FMI_079PUP_FMI

2271.876	2272.101	2271.989	35.80019	150.5762	RFracC	North	FMI_079PUP_FMI
2271.598	2271.867	2271.733	52.96917	72.22491	RFracC	North	FMI_079PUP_FMI
2272.327	2272.595	2272.461	51.93773	77.01904	RFracC	North	FMI_079PUP_FMI
2272.518	2272.786	2272.652	52.4356	74.62097	RFracC	North	FMI_079PUP_FMI
2272.637	2272.905	2272.771	53.92294	67.49843	RFracC	North	FMI_079PUP_FMI
2272.709	2272.977	2272.843	53.91981	67.498	RFracC	North	FMI_079PUP_FMI
2272.796	2273.064	2272.93	53.42659	69.86042	RFracC	North	FMI_079PUP_FMI
2273.438	2273.706	2273.572	40.28155	163.5069	RFracC	North	FMI_079PUP_FMI
2273.312	2273.616	2273.464	54.98816	79.33757	RFracC	North	FMI_079PUP_FMI
2275.515	2276.137	2275.826	79.5426	35.33234	ConFracC	North	FMI_079PUP_FMI
2275.692	2276.314	2276.003	80.52372	28.18734	ConFracC	North	FMI_079PUP_FMI
2276.251	2276.952	2276.601	79.94428	45.1945	ConFracC	North	FMI_079PUP_FMI
2281.769	2282.066	2281.918	49.66883	238.5387	RFracC	North	FMI_079PUP_FMI
2282.512	2282.809	2282.661	50.31733	95.10496	RFracC	North	FMI_079PUP_FMI
2281.131	2281.428	2281.279	63.38425	30.00944	ConFracC	North	FMI_079PUP_FMI
2283.223	2283.577	2283.4	53.08508	230.7548	RFracF	North	FMI_079PUP_FMI
2289.898	2290.188	2290.043	63.84827	21.49613	RFracF	North	FMI_079PUP_FMI
2303.25	2303.475	2303.362	39.14427	96.32539	RFracF	North	FMI_079PUP_FMI
2312.061	2312.214	2312.137	49.1948	311.0215	RFracF	North	FMI_079PUP_FMI

Hovea 9: Total interpreted fracture set

Top Depth (m)	Bottom Depth (m)	Depth (m)	True Dip (deg)	True Azimuth (deg)	Surface Type	Apparent Mode	Image Log
506.5366	506.6444	506.5905	29.85287	272.3002	ConFracC	North	FMI_035PUC_FMI
512.7461	512.8539	512.8	28.94155	305.8029	ConFracC	North	FMI_035PUC_FMI
507.5987	507.7065	507.6526	25.13483	54.66988	RFracC	North	FMI_035PUC_FMI
510.0092	510.117	510.0631	26.73105	355.1427	RFracC	North	FMI_035PUC_FMI
509.7591	509.8524	509.8058	24.18991	339.3001	ConFracC	North	FMI_035PUC_FMI
509.799	509.8923	509.8456	23.91092	345.5508	ConFracC	North	FMI_035PUC_FMI
510.2159	510.3092	510.2625	26.48601	278.6293	ConFracC	North	FMI_035PUC_FMI
510.5349	510.6426	510.5888	29.02587	302.3591	RFracC	North	FMI_035PUC_FMI
513.9314	513.8435	513.8874	21.20259	122.3882	RFracC	North	FMI_035PUC_FMI
515.385	515.5508	515.4679	40.79586	283.319	ConFracC	North	FMI_035PUC_FMI
515.2799	515.4457	515.3628	40.70221	286.9019	ConFracC	North	FMI_035PUC_FMI
516.0882	516.254	516.1711	41.16347	257.162	ConFracC	North	FMI_035PUC_FMI
516.9057	517.0474	516.9765	33.73785	352.6051	ConFracC	North	FMI_035PUC_FMI
517.049	517.1449	517.097	25.00508	333.3172	ConFracC	North	FMI_035PUC_FMI
526.6672	526.7631	526.7151	24.03094	355.6304	RFracC	North	FMI_035PUC_FMI
547.8133	548.0469	547.9301	50.11423	200.7751	RFracC	North	FMI_035PUC_FMI
549.7347	549.8076	549.7711	18.12827	7.680532	RFracC	North	FMI_035PUC_FMI
552.2697	552.4114	552.3406	36.75286	279.7176	ConFracC	North	FMI_035PUC_FMI
551.9428	552.0386	551.9907	26.88625	292.8323	RFracC	North	FMI_035PUC_FMI
556.1754	556.2254	556.2004	14.90456	309.1911	ConFracC	North	FMI_035PUC_FMI
571.6321	571.7739	571.703	34.27497	343.6757	ConFracC	North	FMI_035PUC_FMI
574.4654	574.6071	574.5363	36.17511	297.4815	ConFracC	North	FMI_035PUC_FMI
581.646	581.7878	581.7169	36.1236	300.9566	ConFracC	North	FMI_035PUC_FMI
602.253	602.3948	602.3239	31.67566	98.03584	RFracC	North	FMI_035PUC_FMI
611.831	612.0187	611.9249	44.1436	210.8975	RFracC	North	FMI_035PUC_FMI
603.9564	604.0294	603.9929	16.78918	43.26074	RFracC	North	FMI_035PUC_FMI
615.3124	615.3853	615.3488	21.65785	289.1129	RFracC	North	FMI_035PUC_FMI
631.8989	632.0292	631.9641	35.04532	241.0586	RFracC	North	FMI_035PUC_FMI
631.9334	632.0636	631.9985	35.10275	246.8404	ConFracC	North	FMI_035PUC_FMI
646.5756	646.7059	646.6408	34.50516	288.5443	ConFracC	North	FMI_035PUC_FMI
665.9668	666.1085	666.0377	32.29452	20.10097	ConFracC	North	FMI_035PUC_FMI
666.1331	666.2749	666.204	32.63933	12.23616	ConFracC	North	FMI_035PUC_FMI
666.2306	666.3724	666.3015	32.24812	21.39182	ConFracC	North	FMI_035PUC_FMI
670.2052	670.2781	670.2417	19.3295	166.5844	RFracC	North	FMI_035PUC_FMI
676.2043	676.3117	676.258	30.30369	271.8143	RFracC	North	FMI_035PUC_FMI
676.256	676.3633	676.3096	30.16906	277.5127	ConFracC	North	FMI_035PUC_FMI
677.3629	677.4358	677.3993	22.25558	273.1456	RFracC	North	FMI_035PUC_FMI
680.5919	680.6304	680.6111	13.67509	253.6345	RFracC	North	FMI_035PUC_FMI
681.8995	682.0527	681.9761	36.44797	164.286	ConFracC	North	FMI_035PUC_FMI
698.9105	699.0981	699.0043	45.19951	270.1753	ConFracC	North	FMI_035PUC_FMI
760.0089	760.1277	760.0683	30.59633	324.1855	RFracC	North	FMI_035PUC_FMI

770.9806	771.2026	771.0916	50.3957	256.1673	ConFracC	North	FMI_035PUC_FMI
776.6299	776.7487	776.6893	31.69499	307.6526	RFracC	North	FMI_035PUC_FMI
777.2608	777.3796	777.3202	33.23417	257.0361	RFracC	North	FMI_035PUC_FMI
780.4095	780.4939	780.4517	24.95164	286.755	RFracC	North	FMI_035PUC_FMI
784.5274	784.6692	784.5983	36.95598	213.2147	RFracC	North	FMI_035PUC_FMI
791.6794	791.7867	791.7331	30.67624	271.4682	RFracC	North	FMI_035PUC_FMI
808.0824	808.1898	808.1361	28.49149	317.5214	ConFracC	North	FMI_035PUC_FMI
819.6965	819.8038	819.7501	29.42566	303.4071	ConFracC	North	FMI_035PUC_FMI
847.811	847.9184	847.8647	27.60333	169.5616	RFracC	North	FMI_035PUC_FMI
851.1949	851.2449	851.2199	17.02309	235.5861	RFracC	North	FMI_035PUC_FMI
854.55	854.6574	854.6037	30.95793	244.6382	RFracC	North	FMI_035PUC_FMI
859.0981	859.3087	859.2034	47.07885	191.9366	RFracC	North	FMI_035PUC_FMI
859.9527	860.3583	860.1555	66.05968	222.2103	RFracC	North	FMI_035PUC_FMI
861.094	861.1899	861.142	21.2345	93.98991	RFracC	North	FMI_035PUC_FMI
862.2526	862.3484	862.3005	27.46915	295.9678	RFracC	North	FMI_035PUC_FMI
892.5466	892.6424	892.5945	28.5296	230.2396	ConFracC	North	FMI_035PUC_FMI
894.3475	894.5007	894.4241	40.276	232.2548	ConFracC	North	FMI_035PUC_FMI
898.0123	898.1656	898.0889	38.08067	190.0417	RFracC	North	FMI_035PUC_FMI
936.1178	936.2252	936.1715	31.21624	286.0382	RFracC	North	FMI_035PUC_FMI
938.412	938.5193	938.4656	29.77405	204.4268	RFracC	North	FMI_035PUC_FMI
949.441	949.491	949.466	9.434226	105.7975	RFracC	North	FMI_035PUC_FMI
971.3041	971.572	971.438	52.17744	350.3745	ConFracC	North	FMI_035PUC_FMI
979.6662	979.8423	979.7542	44.53478	274.03	ConFracC	North	FMI_035PUC_FMI
988.9574	989.1336	989.0455	42.07597	330.4008	RFracF	North	FMI_035PUC_FMI
989.0377	989.2139	989.1258	41.54507	337.6374	RFracF	North	FMI_035PUC_FMI
996.3445	996.4518	996.3982	30.99965	233.5197	ConFracC	North	FMI_035PUC_FMI
997.5489	997.6563	997.6026	28.64005	198.1839	ConFracC	North	FMI_035PUC_FMI
1028.828	1029.042	1028.935	45.05012	9.448108	RFracC	North	FMI_035PUC_FMI
1055.101	1055.212	1055.157	31.83573	301.6128	RFracC	North	FMI_035PUC_FMI
1079.849	1080.075	1079.962	49.22749	217.1347	RFracC	North	FMI_035PUC_FMI
1085.762	1085.884	1085.823	26.17967	87.187	RFracC	North	FMI_035PUC_FMI
1087.569	1088.058	1087.814	71.31844	289.6829	ConFracC	North	FMI_035PUC_FMI
1107.931	1108.004	1107.967	19.82169	201.9083	ConFracC	North	FMI_035PUC_FMI
1110.386	1110.447	1110.416	12.28149	91.69687	ConFracC	North	FMI_035PUC_FMI
1112.496	1112.581	1112.539	17.97468	113.7699	ConFracC	North	FMI_035PUC_FMI
1154.834	1154.919	1154.877	17.97176	90.37298	RFracC	North	FMI_035PUC_FMI
1170.979	1171.374	1171.176	57.95386	90.85809	RFracC	North	FMI_035PUC_FMI
1172.494	1172.83	1172.662	54.09373	92.06683	RFracC	North	FMI_035PUC_FMI
1172.757	1173.094	1172.926	54.05813	97.32121	RFracC	North	FMI_035PUC_FMI
1176.931	1177.11	1177.021	43.8423	238.321	RFracC	North	FMI_035PUC_FMI
1177.614	1177.931	1177.772	52.90006	77.53042	RFracC	North	FMI_035PUC_FMI
1178.015	1178.458	1178.237	60.76862	88.22946	RFracC	North	FMI_035PUC_FMI
1187.559	1188.231	1187.895	68.753	93.51799	RFracC	North	FMI_035PUC_FMI
1188.58	1188.954	1188.767	56.87963	97.2688	RFracC	North	FMI_035PUC_FMI

1194.745	1195.223	1194.984	63.38404	62.49213	RFracC	North	FMI_035PUC_FMI
1194.917	1195.762	1195.339	72.64178	73.16339	RFracC	North	FMI_035PUC_FMI
1196.787	1197.241	1197.014	61.79869	76.5484	RFracC	North	FMI_035PUC_FMI
1197.624	1198.079	1197.851	61.61123	82.99365	RFracC	North	FMI_035PUC_FMI
1197.894	1199.22	1198.557	77.88887	65.76609	RFracC	North	FMI_035PUC_FMI
1198.708	1199.197	1198.953	64.185	57.37281	RFracC	North	FMI_035PUC_FMI
1199.064	1200.092	1199.578	75.38382	65.6418	RFracC	North	FMI_035PUC_FMI
1199.935	1200.826	1200.381	74.34995	52.90939	RFracC	North	FMI_035PUC_FMI
1201.994	1203.08	1202.537	75.87275	69.45578	RFracC	North	FMI_035PUC_FMI
1205.057	1206.028	1205.543	74.61966	70.66374	RFracC	North	FMI_035PUC_FMI
1208.275	1208.443	1208.359	35.32144	81.54321	RFracC	North	FMI_035PUC_FMI
1209.267	1210.272	1209.769	75.92323	54.27112	RFracC	North	FMI_035PUC_FMI
1209.967	1210.157	1210.062	39.39916	69.76398	RFracC	North	FMI_035PUC_FMI
1210.19	1210.381	1210.286	38.99562	81.79049	RFracC	North	FMI_035PUC_FMI
1210.878	1211.069	1210.974	40.85381	42.23488	RFracC	North	FMI_035PUC_FMI
1211.607	1211.798	1211.702	40.86856	42.23349	RFracC	North	FMI_035PUC_FMI
1215.547	1216.208	1215.878	69.15667	78.05205	RFracC	North	FMI_035PUC_FMI
1219.94	1220.601	1220.271	69.91152	62.78242	RFracC	North	FMI_035PUC_FMI
1219.2	1219.357	1219.279	33.42305	85.30599	RFracC	North	FMI_035PUC_FMI
1225.463	1226.262	1225.863	71.59455	103.6398	RFracC	North	FMI_035PUC_FMI
1226.501	1227.048	1226.775	65.97715	75.37218	RFracC	North	FMI_035PUC_FMI
1231.795	1232.72	1232.258	73.88759	84.57022	RFracC	North	FMI_035PUC_FMI
1234.411	1235.026	1234.718	68.05936	80.53211	RFracC	North	FMI_035PUC_FMI
1235.649	1235.84	1235.745	41.07687	43.60125	RFracC	North	FMI_035PUC_FMI
1235.896	1236.087	1235.991	40.92542	46.17277	RFracC	North	FMI_035PUC_FMI
1236.068	1236.224	1236.146	33.51286	87.90551	RFracC	North	FMI_035PUC_FMI
1236.343	1236.431	1236.387	25.89525	256.4066	ConFracC	North	FMI_035PUC_FMI
1239.314	1239.459	1239.387	32.96737	51.51833	RFracC	North	FMI_035PUC_FMI
1240.272	1240.417	1240.345	37.33154	243.949	ConFracC	North	FMI_035PUC_FMI
1240.886	1241.031	1240.958	38.68154	292.4835	ConFracC	North	FMI_035PUC_FMI
1241.408	1241.553	1241.48	31.45694	90.45828	RFracC	North	FMI_035PUC_FMI
1248.095	1248.24	1248.167	37.97516	254.4585	RFracC	North	FMI_035PUC_FMI
1250.332	1250.603	1250.467	49.47694	74.38011	RFracC	North	FMI_035PUC_FMI
1250.687	1250.936	1250.811	53.40207	261.5927	RFracC	North	FMI_035PUC_FMI
1251.771	1251.974	1251.873	41.06587	77.65949	RFracC	North	FMI_035PUC_FMI
1259.302	1259.481	1259.392	39.26778	181.6986	RFracC	North	FMI_035PUC_FMI
1265.142	1265.743	1265.442	74.86692	307.152	RFracC	North	FMI_035PUC_FMI
1268.822	1269.036	1268.929	49.56194	315.8751	RFracC	North	FMI_035PUC_FMI
1269.362	1269.575	1269.468	43.7026	50.22938	RFracC	North	FMI_035PUC_FMI
1272.103	1272.397	1272.25	57.96367	328.2411	RFracC	North	FMI_035PUC_FMI
1314.889	1315.091	1314.99	43.94996	22.7917	RFracC	North	FMI_035PUC_FMI
1332.485	1332.848	1332.666	61.26296	6.479758	ConFracC	North	FMI_035PUC_FMI
1343.378	1343.473	1343.426	28.46168	258.7337	RFracC	North	FMI_035PUC_FMI
1345.133	1345.274	1345.203	37.68875	251.6484	RFracC	North	FMI_035PUC_FMI

1373.138	1373.509	1373.324	57.9452	62.89878	ConFracC	North	FMI_035PUC_FMI
1391.784	1392.04	1391.912	47.06386	141.3517	ConFracC	North	FMI_035PUC_FMI
1398.058	1398.28	1398.169	43.43631	84.95759	RFracC	North	FMI_035PUC_FMI
1401.012	1401.154	1401.083	35.755	234.5591	RFracC	North	FMI_035PUC_FMI
1419.508	1419.558	1419.533	16.47113	256.6814	RFracC	North	FMI_035PUC_FMI
1419.921	1419.971	1419.946	14.05449	225.855	RFracC	North	FMI_035PUC_FMI
1444.663	1444.989	1444.826	53.19325	92.35244	ConFracC	North	FMI_035PUC_FMI
1449.95	1450.015	1449.982	19.79187	245.918	ConFracC	North	FMI_035PUC_FMI
1452.188	1452.445	1452.316	54.82196	259.0073	ConFracC	North	FMI_035PUC_FMI
1455.589	1455.777	1455.683	45.99836	261.1781	ConFracC	North	FMI_035PUC_FMI
1483.377	1484.058	1483.717	67.4106	83.53012	RFracC	North	FMI_035PUC_FMI
1484.467	1484.941	1484.704	71.75529	260.4995	RFracC	North	FMI_035PUC_FMI
1488.17	1488.292	1488.231	32.73106	232.9662	ConFracC	North	FMI_035PUC_FMI
1515.179	1515.505	1515.342	63.05876	254.6156	RFracC	North	FMI_035PUC_FMI
1516.057	1516.508	1516.283	69.914	245.2546	RFracC	North	FMI_035PUC_FMI
1527.281	1527.503	1527.392	44.38504	45.22737	RFracC	North	FMI_035PUC_FMI
1531.181	1531.3	1531.24	36.94745	278.373	RFracC	North	FMI_035PUC_FMI
1564.744	1564.863	1564.803	36.79731	265.5815	ConFracC	North	FMI_035PUC_FMI
1572.537	1572.888	1572.712	65.78706	254.8484	RFracC	North	FMI_035PUC_FMI
1572.973	1573.324	1573.148	66.88842	272.4274	RFracC	North	FMI_035PUC_FMI
1576.379	1576.49	1576.435	27.18802	17.82581	ConFracC	North	FMI_035PUC_FMI
1576.809	1576.886	1576.848	26.65198	260.8581	ConFracC	North	FMI_035PUC_FMI
1576.551	1576.673	1576.612	35.1404	336.7372	ConFracC	North	FMI_035PUC_FMI
1579.535	1579.952	1579.744	66.10077	219.5992	RFracC	North	FMI_035PUC_FMI
1582.558	1583.044	1582.801	72.95184	252.8275	RFracC	North	FMI_035PUC_FMI
1583.367	1583.738	1583.552	66.53689	248.5948	RFracC	North	FMI_035PUC_FMI
1592.891	1593.048	1592.97	43.82855	268.7639	RFracC	North	FMI_035PUC_FMI
1606.891	1607.185	1607.038	51.02906	160.8629	RFracC	North	FMI_035PUC_FMI
1610.013	1610.109	1610.061	31.79487	265.7893	RFracC	North	FMI_035PUC_FMI
1619.379	1619.475	1619.427	31.27372	259.3644	RFracC	North	FMI_035PUC_FMI
1619.069	1619.165	1619.117	23.80948	186.4101	RFracC	North	FMI_035PUC_FMI
1635.202	1635.642	1635.422	59.67856	41.69596	RFracC	North	FMI_035PUC_FMI
1645.113	1645.392	1645.253	60.44618	243.6991	ConFracC	North	FMI_035PUC_FMI
1651.019	1651.152	1651.086	40.35402	253.3649	RFracC	North	FMI_035PUC_FMI
1666.693	1666.827	1666.76	40.5851	255.7292	RFracC	North	FMI_035PUC_FMI
1666.969	1667.102	1667.036	40.65644	258.8347	RFracC	North	FMI_035PUC_FMI
1677.774	1677.862	1677.818	30.59623	257.0829	ConFracC	North	FMI_035PUC_FMI
1688.334	1688.717	1688.526	68.93413	250.6161	ConFracC	North	FMI_035PUC_FMI
1691	1691.179	1691.09	47.65888	281.9118	ConFracC	North	FMI_035PUC_FMI
1697.177	1697.356	1697.266	48.15587	260.7733	ConFracC	North	FMI_035PUC_FMI
1700.721	1700.901	1700.811	34.22281	48.1277	RFracC	North	FMI_035PUC_FMI
1700.899	1701.124	1701.012	41.02444	43.47708	RFracC	North	FMI_035PUC_FMI
1701.191	1701.681	1701.436	59.56245	80.18505	RFracC	North	FMI_035PUC_FMI
1702.126	1702.971	1702.549	68.6907	81.42566	RFracC	North	FMI_035PUC_FMI

1702.631	1703.384	1703.008	67.09527	84.06575	RFracC	North	FMI_035PUC_FMI
1703.411	1703.682	1703.547	45.05633	69.15294	ConFracC	North	FMI_035PUC_FMI
1704.565	1704.627	1704.596	24.11874	258.0305	ConFracC	North	FMI_035PUC_FMI
1707.54	1707.903	1707.722	67.84563	259.6837	RFracC	North	FMI_035PUC_FMI
1708.464	1708.953	1708.708	59.37443	76.37591	RFracC	North	FMI_035PUC_FMI
1709.238	1709.693	1709.465	57.82678	69.69165	RFracC	North	FMI_035PUC_FMI
1712.519	1712.675	1712.597	29.46779	84.74317	ConFracC	North	FMI_035PUC_FMI
1717.445	1717.533	1717.489	15.79036	96.89489	RFracC	North	FMI_035PUC_FMI
1721.787	1722.139	1721.963	52.61912	38.8649	RFracC	North	FMI_035PUC_FMI
1723.169	1723.521	1723.345	67.05306	253.2591	RFracC	North	FMI_035PUC_FMI
1724.041	1724.392	1724.217	66.85921	259.0438	RFracC	North	FMI_035PUC_FMI
1724.689	1725.041	1724.865	67.05963	250.8108	RFracC	North	FMI_035PUC_FMI
1740.725	1741.077	1740.901	65.39161	264.3864	RFracC	North	FMI_035PUC_FMI
1810.547	1810.784	1810.665	48.70865	234.3077	ConFracC	North	FMI_035PUC_FMI
1831.687	1831.924	1831.806	50.35397	51.27229	RFracC	North	FMI_035PUC_FMI
1849.249	1849.543	1849.396	57.05904	38.74886	RFracC	North	FMI_035PUC_FMI
1856.303	1856.402	1856.353	23.02155	209.0079	RFracC	North	FMI_035PUC_FMI
1857.089	1857.372	1857.23	54.1892	171.654	ConFracC	North	FMI_035PUC_FMI
1858.357	1858.548	1858.452	39.62445	215.849	RFracC	North	FMI_035PUC_FMI
1858.729	1858.978	1858.854	48.60396	194.9156	RFracC	North	FMI_035PUC_FMI
1858.466	1858.702	1858.584	46.62389	203.6987	RFracC	North	FMI_035PUC_FMI
1906.023	1906.26	1906.141	44.86362	332.7683	ConFracC	North	FMI_035PUC_FMI
1930.886	1931.122	1931.004	42.57775	290.517	ConFracC	North	FMI_035PUC_FMI
1932.107	1932.344	1932.226	45.07861	229.0344	ConFracC	North	FMI_035PUC_FMI
1935.382	1935.55	1935.466	34.61304	334.9741	ConFracC	North	FMI_035PUC_FMI
1944.117	1944.285	1944.201	32.54393	308.5739	RFracC	North	FMI_035PUC_FMI
1956.299	1956.467	1956.383	30.80262	294.2703	RFracC	North	FMI_035PUC_FMI
1959.579	1959.656	1959.617	12.11876	312.5859	RFracC	North	FMI_035PUC_FMI
1960.785	1960.985	1960.885	38.25562	229.606	ConFracC	North	FMI_035PUC_FMI
1971.895	1972.128	1972.012	47.46057	194.2634	RFracC	North	FMI_035PUC_FMI
1974.912	1975.145	1975.028	59.34033	103.7963	RFracC	North	FMI_035PUC_FMI
1974.544	1974.778	1974.661	59.26731	104.8771	RFracC	North	FMI_035PUC_FMI
1975.944	1976.063	1976.003	26.00544	203.8417	RFracC	North	FMI_035PUC_FMI
1981.57	1981.689	1981.63	23.13615	351.5211	RFracC	North	FMI_035PUC_FMI
1987.105	1987.224	1987.164	19.42225	330.7115	RFracC	North	FMI_035PUC_FMI
1989.978	1990.097	1990.038	22.14105	218.4319	RFracC	North	FMI_035PUC_FMI
1992.014	1992.167	1992.091	22.834	288.3872	ConFracC	North	FMI_035PUC_FMI
1993.448	1993.601	1993.525	50.28079	109.0666	RFracC	North	FMI_035PUC_FMI
1994.601	1994.697	1994.649	10.78207	289.4832	RFracC	North	FMI_035PUC_FMI
2013.671	2013.916	2013.793	63.51739	78.96157	RFracC	North	FMI_035PUC_FMI
2014.204	2014.633	2014.419	50.42374	318.8924	RFracC	North	FMI_035PUC_FMI
2014.692	2015.12	2014.906	48.33789	289.2718	RFracC	North	FMI_035PUC_FMI
2015.569	2015.883	2015.726	72.35758	101.8906	RFracC	North	FMI_035PUC_FMI
2017.657	2017.89	2017.774	63.77097	92.80321	RFracC	North	FMI_035PUC_FMI

2020.57	2020.804	2020.687	64.19661	104.1614	RFracC	North	FMI_035PUC_FMI
2021.161	2021.395	2021.278	62.15325	79.22414	RFracC	North	FMI_035PUC_FMI
2021.069	2021.303	2021.186	62.31076	80.26301	RFracC	North	FMI_035PUC_FMI
2021.58	2021.813	2021.697	34.93147	323.3203	ConFracC	North	FMI_035PUC_FMI
2021.895	2022.129	2022.012	58.99816	150.0283	ConFracC	North	FMI_035PUC_FMI
2024.344	2024.555	2024.45	61.09642	106.2503	RFracC	North	FMI_035PUC_FMI
2024.729	2024.939	2024.834	61.09141	105.2292	RFracC	North	FMI_035PUC_FMI
2027.682	2028.042	2027.862	75.54431	111.8211	RFracC	North	FMI_035PUC_FMI
2028.015	2028.283	2028.149	66.49683	83.809	RFracC	North	FMI_035PUC_FMI
2028.348	2028.581	2028.464	63.3886	91.65326	RFracC	North	FMI_035PUC_FMI
2029.414	2029.487	2029.451	5.016627	239.5691	ConFracC	North	FMI_035PUC_FMI
2029.311	2029.418	2029.365	42.8041	100.2759	RFracC	North	FMI_035PUC_FMI
2030.928	2031.724	2031.326	89.16918	291.0794	RFracC	North	FMI_035PUC_FMI
2031.726	2033.221	2032.473	82.59198	277.5098	RFracC	North	FMI_035PUC_FMI
2033.726	2033.859	2033.792	18.2145	260.0884	RFracC	North	FMI_035PUC_FMI
2034.271	2034.404	2034.337	19.9314	242.1549	RFracC	North	FMI_035PUC_FMI
2035.475	2035.551	2035.513	35.38181	111.2227	RFracC	North	FMI_035PUC_FMI
2035.234	2035.368	2035.301	17.68055	300.1415	RFracC	North	FMI_035PUC_FMI
2037.809	2037.897	2037.853	38.18006	106.0379	RFracC	North	FMI_035PUC_FMI
2038.331	2038.419	2038.375	37.87197	114.7044	RFracC	North	FMI_035PUC_FMI
2037.339	2037.427	2037.383	8.682046	321.3141	RFracC	North	FMI_035PUC_FMI
2038.532	2038.757	2038.645	38.78088	222.5509	ConFracC	North	FMI_035PUC_FMI
2017.202	2017.783	2017.493	85.91975	94.47054	RFracC	North	FMI_035PUC_FMI
2039.595	2039.805	2039.7	31.50399	256.939	ConFracC	North	FMI_035PUC_FMI
2052.608	2053.277	2052.943	87.21205	119.3351	RFracC	North	FMI_035PUC_FMI
2073.363	2073.703	2073.533	44.62756	271.3777	RFracC	North	FMI_035PUC_FMI
2093.436	2093.776	2093.606	46.16706	307.3485	RFracC	North	FMI_035PUC_FMI
2094.264	2094.463	2094.363	30.70198	291.7405	ConFracC	North	FMI_035PUC_FMI

Hovea 12: Total interpreted fracture set

Top Depth (m)	Bottom Depth (m)	Depth (m)	True Dip (deg)	True Azimuth (deg)	Surface Type	Apparent Mode	Image Log
2145.527	2146.495	2146.011	43.27805	45.98324	RFracC	North	FMI_005PUP_FMI
2145.96	2146.928	2146.444	43.27805	45.98324	RFracC	North	FMI_005PUP_FMI
2165.629	2166.118	2165.874	35.46605	41.6127	ConFracD	North	FMI_005PUP_FMI
2173.994	2174.483	2174.239	38.30856	52.98563	ConFracD	North	FMI_005PUP_FMI
2205.318	2205.807	2205.562	33.91582	27.18282	ConFracD	North	FMI_005PUP_FMI
2206.884	2207.373	2207.128	33.97816	29.22122	RFracF	North	FMI_005PUP_FMI
2206.515	2207.004	2206.76	75.92009	116.571	RFracF	North	FMI_005PUP_FMI
2226.452	2226.775	2226.613	28.3705	49.49374	RFracF	North	FMI_005PUP_FMI
2224.066	2224.389	2224.227	23.48991	1.94397	RFracF	North	FMI_005PUP_FMI
2223.006	2223.33	2223.168	25.488	34.78312	RFracF	North	FMI_005PUP_FMI
2225.088	2225.412	2225.25	23.78487	354.0857	ConFracC	North	FMI_005PUP_FMI
2225.54	2225.863	2225.701	80.82016	143.4969	ConFracC	North	FMI_005PUP_FMI
2240.934	2241.258	2241.096	43.50733	286.7087	ConFracC	North	FMI_005PUP_FMI
2241.238	2241.562	2241.4	80.87419	145.3814	RFracC	North	FMI_005PUP_FMI
2258.586	2258.909	2258.748	38.05265	72.98999	RFracC	North	FMI_005PUP_FMI
2261.313	2261.765	2261.539	40.63597	324.3758	RFracC	North	FMI_005PUP_FMI
2281.213	2281.665	2281.439	39.97091	45.92468	RFracC	North	FMI_005PUP_FMI
2286.059	2286.511	2286.285	47.17467	70.13541	RFracC	North	FMI_005PUP_FMI
2288.085	2288.538	2288.312	40.21931	45.33429	RFracC	North	FMI_005PUP_FMI
2302.983	2303.435	2303.209	87.06804	15.24316	ConFracC	North	FMI_005PUP_FMI
2302.66	2303.112	2302.886	87.06154	19.78259	ConFracC	North	FMI_005PUP_FMI
2303.756	2304.209	2303.983	87.34823	10.72005	ConFracC	North	FMI_005PUP_FMI
2304.705	2305.158	2304.931	61.76893	288.669	RFracC	North	FMI_005PUP_FMI
2267.766	2268.054	2267.91	27.15546	332.854	RFracC	North	FMI_005PUP_FMI
2277.824	2278.388	2278.106	42.3267	348.3679	RFracC	North	FMI_005PUP_FMI
2286.422	2286.799	2286.611	89.27839	198.9363	ConFracC	North	FMI_005PUP_FMI
2287.746	2287.944	2287.845	71.88552	190.5194	ConFracC	North	FMI_005PUP_FMI
2296.682	2296.879	2296.78	70.92635	185.0938	ConFracC	North	FMI_005PUP_FMI
2296.786	2296.984	2296.885	69.24431	175.1745	ConFracC	North	FMI_005PUP_FMI
2297.187	2297.384	2297.286	71.4803	196.0299	ConFracC	North	FMI_005PUP_FMI
2298.118	2298.316	2298.217	70.69472	184.3122	ConFracC	North	FMI_005PUP_FMI
2301.942	2302.327	2302.135	73.74535	137.9623	ConFracC	North	FMI_005PUP_FMI
2344.41	2344.526	2344.468	5.892785	310.069	ConFracC	North	FMI_005PUP_FMI
2352.219	2352.335	2352.277	8.683804	298.3365	RFracC	North	FMI_005PUP_FMI
2352.803	2352.918	2352.86	4.341708	93.06561	RFracC	North	FMI_005PUP_FMI
2353.678	2353.794	2353.736	16.2468	123.3816	ConFracC	North	FMI_005PUP_FMI
2355.414	2355.53	2355.472	7.227208	106.22	ConFracC	North	FMI_005PUP_FMI
2355.826	2355.941	2355.884	1.886106	5.190824	RFracC	North	FMI_005PUP_FMI
2361.169	2361.285	2361.227	6.573945	103.1138	RFracC	North	FMI_005PUP_FMI
2361.487	2361.558	2361.522	17.27728	159.0941	RFracC	North	FMI_005PUP_FMI
2361.667	2361.872	2361.769	18.11945	1.875584	RFracC	North	FMI_005PUP_FMI

2362.8	2362.878	2362.839	20.12444	152.9469	RFracC	North	FMI_005PUP_FMI
2364.338	2364.611	2364.475	26.11889	40.49017	RFracC	North	FMI_005PUP_FMI
2367.9	2367.986	2367.943	21.66948	256.6331	ConFracC	North	FMI_005PUP_FMI
2369.82	2369.905	2369.863	4.802165	193.7748	ConFracC	North	FMI_005PUP_FMI
2374.508	2374.639	2374.573	8.517345	321.4602	ConFracC	North	FMI_005PUP_FMI
2374.748	2374.878	2374.813	6.679971	336.4594	ConFracC	North	FMI_005PUP_FMI
2375.017	2375.147	2375.082	7.92041	77.33345	ConFracC	North	FMI_005PUP_FMI
2376.027	2376.18	2376.104	10.07886	47.31119	ConFracC	North	FMI_005PUP_FMI
2375.803	2375.971	2375.887	16.01237	329.8783	ConFracC	North	FMI_005PUP_FMI
2373.46	2373.628	2373.544	14.77837	337.0443	RFracC	North	FMI_005PUP_FMI
2368.795	2368.858	2368.826	10.26616	201.2326	RFracC	North	FMI_005PUP_FMI
2371.754	2371.817	2371.786	12.1401	226.915	ConFracC	North	FMI_005PUP_FMI
2372.491	2372.554	2372.523	11.8706	225.4575	RFracC	North	FMI_005PUP_FMI
2377.453	2377.651	2377.552	22.68537	325.424	RFracC	North	FMI_005PUP_FMI
2377.505	2377.703	2377.604	24.64046	318.3347	RFracC	North	FMI_005PUP_FMI
2379.657	2379.854	2379.755	19.33453	342.6352	RFracC	North	FMI_005PUP_FMI
2379.892	2380.09	2379.991	16.69309	18.43396	RFracC	North	FMI_005PUP_FMI
2380.199	2380.397	2380.298	18.07791	352.6772	RFracC	North	FMI_005PUP_FMI
2381.299	2381.497	2381.398	19.36399	342.5917	RFracC	North	FMI_005PUP_FMI
2381.943	2382.111	2382.027	16.55739	328.1038	RFracC	North	FMI_005PUP_FMI
2381.793	2381.961	2381.877	21.58399	309.3453	RFracC	North	FMI_005PUP_FMI
2382.526	2382.694	2382.61	17.97526	321.7192	RFracC	North	FMI_005PUP_FMI
2382.44	2382.608	2382.524	14.8748	337.9175	RFracC	North	FMI_005PUP_FMI
2383.282	2383.45	2383.366	16.11802	330.4513	RFracC	North	FMI_005PUP_FMI
2383.361	2383.529	2383.445	14.14123	343.5166	RFracC	North	FMI_005PUP_FMI
2384.51	2384.677	2384.593	12.11056	25.1313	RFracC	North	FMI_005PUP_FMI
2385.232	2385.34	2385.286	5.141438	293.0578	RFracC	North	FMI_005PUP_FMI
2386.683	2386.829	2386.756	18.31155	302.3933	RFracC	North	FMI_005PUP_FMI
2386.459	2386.604	2386.532	12.51781	322.9463	RFracC	North	FMI_005PUP_FMI
2387.23	2387.375	2387.302	8.490666	1.454668	RFracC	North	FMI_005PUP_FMI
2387.342	2387.487	2387.415	11.5788	328.1197	RFracC	North	FMI_005PUP_FMI
2387.739	2387.884	2387.811	8.931221	352.3612	RFracC	North	FMI_005PUP_FMI
2388.61	2388.756	2388.683	8.037244	15.84554	ConFracC	North	FMI_005PUP_FMI
2389.523	2389.669	2389.596	21.17669	295.4061	RFracC	North	FMI_005PUP_FMI
2389.621	2389.856	2389.738	27.86389	327.6743	RFracC	North	FMI_005PUP_FMI
2390.496	2390.731	2390.614	26.55432	332.9975	RFracC	North	FMI_005PUP_FMI
2401.007	2401.115	2401.061	5.472768	290.596	RFracC	North	FMI_005PUP_FMI
2403.087	2403.195	2403.141	12.11962	281.0272	RFracC	North	FMI_005PUP_FMI
2407.689	2407.932	2407.81	28.34707	331.2275	RFracC	North	FMI_005PUP_FMI
2409.242	2409.342	2409.292	14.22073	274.2402	ConFracC	North	FMI_005PUP_FMI
2409.384	2409.485	2409.434	13.16419	275.1896	ConFracC	North	FMI_005PUP_FMI
2409.87	2409.971	2409.921	11.05307	277.1553	ConFracC	North	FMI_005PUP_FMI
2411.337	2411.438	2411.387	3.593976	279.5339	ConFracC	North	FMI_005PUP_FMI
2414.364	2414.831	2414.598	43.26173	346.555	RFracC	North	FMI_005PUP_FMI

2414.791	2415.258	2415.024	41.09092	359.8197	RFracC	North	FMI_005PUP_FMI
2415.547	2415.67	2415.608	22.20937	122.262	RFracC	North	FMI_005PUP_FMI
2415.681	2415.849	2415.765	18.52515	323.1034	RFracC	North	FMI_005PUP_FMI
2418.035	2418.248	2418.141	22.26512	343.1534	RFracC	North	FMI_005PUP_FMI
2419.303	2419.516	2419.41	25.97854	325.2746	RFracC	North	FMI_005PUP_FMI
2418.764	2418.91	2418.837	26.45129	286.9937	RFracC	North	FMI_005PUP_FMI
2418.63	2418.775	2418.702	20.8978	298.3926	RFracC	North	FMI_005PUP_FMI
2418.199	2418.629	2418.414	83.3158	243.3058	ConFracF	North	FMI_005PUP_FMI
2421.694	2421.87	2421.782	13.68993	30.78073	ConFracF	North	FMI_005PUP_FMI
2422.521	2422.637	2422.579	2.950609	58.50525	RFracC	North	FMI_005PUP_FMI
2426.513	2426.764	2426.638	24.35496	5.275948	RFracC	North	FMI_005PUP_FMI
2425.99	2426.24	2426.115	26.91211	346.1233	ConFracC	North	FMI_005PUP_FMI
2431.239	2431.355	2431.297	9.498339	300.4861	RFracC	North	FMI_005PUP_FMI
2431.827	2431.942	2431.884	16.73419	287.1776	RFracC	North	FMI_005PUP_FMI
2435.68	2435.923	2435.802	22.48147	26.4843	RFracC	North	FMI_005PUP_FMI
2435.119	2435.242	2435.181	5.952683	329.8598	RFracC	North	FMI_005PUP_FMI
2435.347	2435.47	2435.409	11.27315	304.8989	RFracC	North	FMI_005PUP_FMI
2436.81	2436.933	2436.872	14.70618	296.8858	RFracC	North	FMI_005PUP_FMI
2437.237	2437.36	2437.298	5.990698	329.3222	ConFracC	North	FMI_005PUP_FMI
2437.952	2438.075	2438.013	19.87892	287.819	ConFracC	North	FMI_005PUP_FMI
2438.154	2438.277	2438.215	19.90676	287.8511	ConFracC	North	FMI_005PUP_FMI
2439.007	2439.13	2439.068	13.17094	300.324	ConFracC	North	FMI_005PUP_FMI
2440.387	2440.51	2440.449	4.192495	60.68611	ConFracC	North	FMI_005PUP_FMI
2439.905	2440.028	2439.966	13.22122	300.133	ConFracC	North	FMI_005PUP_FMI
2441.839	2442.164	2442.002	36.25549	338.2371	RFracC	North	FMI_005PUP_FMI
2444.271	2444.454	2444.363	16.89401	346.3709	RFracC	North	FMI_005PUP_FMI
2444.125	2444.308	2444.217	20.33942	328.5438	RFracC	North	FMI_005PUP_FMI
2442.288	2442.411	2442.35	12.65489	301.15	RFracC	North	FMI_005PUP_FMI
2442.995	2443.343	2443.169	82.67526	178.5764	RFracC	North	FMI_005PUP_FMI
2442.928	2443.41	2443.169	48.75536	330.4875	RFracC	North	FMI_005PUP_FMI
2449.693	2449.906	2449.799	27.00606	324.3815	RFracC	North	FMI_005PUP_FMI
2449.027	2449.285	2449.156	30.72339	333.4664	RFracC	North	FMI_005PUP_FMI
2446.314	2446.445	2446.379	10.69034	316.3533	RFracC	North	FMI_005PUP_FMI
2445.308	2445.438	2445.373	9.06132	323.3953	RFracC	North	FMI_005PUP_FMI

Jingemia 2: Total interpreted fracture set

Top Depth (m)	Bottom Depth (m)	Depth (m)	True Dip (deg)	True Azimuth (deg)	Surface Type	Apparent Mode	Image Log
2101.9186	2102.488	2102.203	85.82158	28.0598	ConFracC	North	FMI_TLD_MCFL_CNL_185PUC_FMI_final_SC
2106.4254	2107.368	2106.897	80.96586	54.01607	RFracC	North	FMI_TLD_MCFL_CNL_185PUC_FMI_final_SC
2129.7843	2130.727	2130.256	80.63509	194.9791	ConFracC	North	FMI_TLD_MCFL_CNL_185PUC_FMI_final_SC
2132.2861	2132.718	2132.502	60.64776	248.4859	ConFracC	North	FMI_TLD_MCFL_CNL_185PUC_FMI_final_SC
2139.2217	2139.8	2139.511	59.18296	232.4288	RFracC	North	FMI_TLD_MCFL_CNL_185PUC_FMI_final_SC
2140.8395	2141.418	2141.129	81.50944	36.99369	RFracC	North	FMI_TLD_MCFL_CNL_185PUC_FMI_final_SC
2150.3498	2150.928	2150.639	89.20386	195.5593	RFracC	North	FMI_TLD_MCFL_CNL_185PUC_FMI_final_SC
2154.4738	2155.052	2154.763	84.28769	31.26283	ConFracC	North	FMI_TLD_MCFL_CNL_185PUC_FMI_final_SC
2154.3007	2154.879	2154.59	82.11822	159.0573	ConFracC	North	FMI_TLD_MCFL_CNL_185PUC_FMI_final_SC
2155.5493	2156.127	2155.838	85.09446	29.31671	ConFracC	North	FMI_TLD_MCFL_CNL_185PUC_FMI_final_SC
2169.3294	2169.662	2169.496	81.24937	2.983805	RFracC	North	FMI_TLD_MCFL_CNL_185PUC_FMI_final_SC
2174.6656	2175.189	2174.927	54.71718	82.55047	RFracC	North	FMI_TLD_MCFL_CNL_185PUC_FMI_final_SC
2175.1076	2175.558	2175.333	58.92081	66.80999	RFracC	North	FMI_TLD_MCFL_CNL_185PUC_FMI_final_SC
2175.454	2175.905	2175.679	50.84617	82.80117	RFracC	North	FMI_TLD_MCFL_CNL_185PUC_FMI_final_SC
2175.8368	2176.287	2176.062	61.63218	61.85487	RFracC	North	FMI_TLD_MCFL_CNL_185PUC_FMI_final_SC
2176.0281	2176.479	2176.253	61.61923	61.86874	RFracC	North	FMI_TLD_MCFL_CNL_185PUC_FMI_final_SC
2176.2378	2176.688	2176.463	67.53852	51.31589	RFracC	North	FMI_TLD_MCFL_CNL_185PUC_FMI_final_SC
2176.4428	2176.793	2176.618	55.95946	58.93661	RFracC	North	FMI_TLD_MCFL_CNL_185PUC_FMI_final_SC
2176.5112	2176.789	2176.65	47.06663	60.933	RFracC	North	FMI_TLD_MCFL_CNL_185PUC_FMI_final_SC
2176.4474	2176.889	2176.668	54.70062	73.75878	RFracC	North	FMI_TLD_MCFL_CNL_185PUC_FMI_final_SC
2176.575	2177.017	2176.796	54.16253	74.81893	RFracC	North	FMI_TLD_MCFL_CNL_185PUC_FMI_final_SC
2176.9122	2177.217	2177.065	34.43269	214.0912	RFracC	North	FMI_TLD_MCFL_CNL_185PUC_FMI_final_SC
2176.976	2177.454	2177.215	65.43043	57.79722	RFracC	North	FMI_TLD_MCFL_CNL_185PUC_FMI_final_SC
2177.3178	2177.978	2177.648	50.96073	104.1919	RFracC	North	FMI_TLD_MCFL_CNL_185PUC_FMI_final_SC
2177.1173	2177.778	2177.447	68.09753	66.24414	RFracC	North	FMI_TLD_MCFL_CNL_185PUC_FMI_final_SC
2177.0352	2177.613	2177.324	70.37776	57.05736	RFracC	North	FMI_TLD_MCFL_CNL_185PUC_FMI_final_SC
2177.1811	2177.759	2177.47	43.63864	122.3328	RFracC	North	FMI_TLD_MCFL_CNL_185PUC_FMI_final_SC
2178.4843	2179.108	2178.796	60.2306	79.14375	RFracC	North	FMI_TLD_MCFL_CNL_185PUC_FMI_final_SC
2178.9172	2179.359	2179.138	52.55193	78.09035	RFracC	North	FMI_TLD_MCFL_CNL_185PUC_FMI_final_SC
2180.5988	2181.542	2181.07	80.77464	255.2908	RFracC	North	FMI_TLD_MCFL_CNL_185PUC_FMI_final_SC
2180.9952	2181.264	2181.129	45.74022	61.15427	RFracC	North	FMI_TLD_MCFL_CNL_185PUC_FMI_final_SC
2182.3441	2182.74	2182.542	64.36992	50.50652	RFracC	North	FMI_TLD_MCFL_CNL_185PUC_FMI_final_SC
2195.8919	2196.188	2196.04	52.49311	54.66452	RFracC	North	FMI_TLD_MCFL_CNL_185PUC_FMI_final_SC
2196.1334	2196.274	2196.204	30.33117	43.57781	RFracC	North	FMI_TLD_MCFL_CNL_185PUC_FMI_final_SC
2196.0559	2196.197	2196.126	30.84242	42.91932	RFracC	North	FMI_TLD_MCFL_CNL_185PUC_FMI_final_SC
2196.024	2196.283	2196.154	44.71244	60.1446	RFracC	North	FMI_TLD_MCFL_CNL_185PUC_FMI_final_SC
2196.6756	2196.999	2196.837	56.58244	52.63331	RFracC	North	FMI_TLD_MCFL_CNL_185PUC_FMI_final_SC
2197.2407	2197.609	2197.425	59.96154	53.93211	RFracC	North	FMI_TLD_MCFL_CNL_185PUC_FMI_final_SC
2197.587	2197.956	2197.771	58.38247	251.5439	RFracC	North	FMI_TLD_MCFL_CNL_185PUC_FMI_final_SC
2197.2999	2197.669	2197.484	55.61863	61.59419	RFracC	North	FMI_TLD_MCFL_CNL_185PUC_FMI_final_SC
2197.5734	2197.76	2197.667	11.91045	136.2107	RFracC	North	FMI_TLD_MCFL_CNL_185PUC_FMI_final_SC

2197.464	2197.65	2197.557	25.8232	71.21247	RFracC	North	FMI_TLD_MCFL_CNL_185PUC_FMI_final_SC
2200.6812	2200.868	2200.774	17.55217	94.21917	RFracC	North	FMI_TLD_MCFL_CNL_185PUC_FMI_final_SC
2201.0731	2201.259	2201.166	50.69679	278.0421	RFracC	North	FMI_TLD_MCFL_CNL_185PUC_FMI_final_SC
2201.8113	2202.772	2202.292	67.16474	79.38981	RFracC	North	FMI_TLD_MCFL_CNL_185PUC_FMI_final_SC
2201.9207	2202.681	2202.301	59.17236	88.60695	RFracC	North	FMI_TLD_MCFL_CNL_185PUC_FMI_final_SC
2202.4493	2203.046	2202.748	71.59941	55.30182	RFracC	North	FMI_TLD_MCFL_CNL_185PUC_FMI_final_SC
2202.7273	2203.141	2202.934	62.83677	54.76599	RFracC	North	FMI_TLD_MCFL_CNL_185PUC_FMI_final_SC
2202.4949	2202.909	2202.702	62.30912	55.72273	RFracC	North	FMI_TLD_MCFL_CNL_185PUC_FMI_final_SC
2202.39	2202.822	2202.606	57.71686	66.14717	RFracC	North	FMI_TLD_MCFL_CNL_185PUC_FMI_final_SC
2202.3673	2202.763	2202.565	55.96226	64.78728	RFracC	North	FMI_TLD_MCFL_CNL_185PUC_FMI_final_SC
2202.2852	2202.681	2202.483	52.69516	70.9242	RFracC	North	FMI_TLD_MCFL_CNL_185PUC_FMI_final_SC
2203.4336	2203.629	2203.531	32.84519	246.3855	RFracC	North	FMI_TLD_MCFL_CNL_185PUC_FMI_final_SC
2205.7166	2205.912	2205.814	12.96313	161.3808	RFracC	North	FMI_TLD_MCFL_CNL_185PUC_FMI_final_SC
2210.0867	2210.282	2210.184	45.37868	41.21964	RFracC	North	FMI_TLD_MCFL_CNL_185PUC_FMI_final_SC
2232.835	2233.194	2233.015	85.62324	353.8134	ConFracC	North	FMI_TLD_MCFL_CNL_185PUC_FMI_final_SC
2234.635	2234.994	2234.815	83.2479	3.244151	ConFracC	North	FMI_TLD_MCFL_CNL_185PUC_FMI_final_SC
2244.7833	2245.671	2245.227	83.98765	199.7866	ConFracC	North	FMI_TLD_MCFL_CNL_185PUC_FMI_final_SC
2245.8086	2246.487	2246.148	84.87479	190.1532	ConFracC	North	FMI_TLD_MCFL_CNL_185PUC_FMI_final_SC
2247.2303	2247.909	2247.57	82.30955	180.7294	ConFracC	North	FMI_TLD_MCFL_CNL_185PUC_FMI_final_SC
2248.3286	2248.752	2248.54	68.23312	45.4245	RFracC	North	FMI_TLD_MCFL_CNL_185PUC_FMI_final_SC
2248.0597	2248.483	2248.271	59.04448	61.59295	RFracC	North	FMI_TLD_MCFL_CNL_185PUC_FMI_final_SC
2249.7367	2250.005	2249.871	61.64572	32.24406	RFracC	North	FMI_TLD_MCFL_CNL_185PUC_FMI_final_SC
2251.4364	2251.705	2251.571	35.68748	227.3333	RFracC	North	FMI_TLD_MCFL_CNL_185PUC_FMI_final_SC
2251.8101	2252.078	2251.944	52.52652	47.65428	RFracC	North	FMI_TLD_MCFL_CNL_185PUC_FMI_final_SC
2252.2339	2252.666	2252.45	71.72059	40.12574	RFracC	North	FMI_TLD_MCFL_CNL_185PUC_FMI_final_SC
2254.9316	2255.364	2255.148	51.76011	76.39071	RFracC	North	FMI_TLD_MCFL_CNL_185PUC_FMI_final_SC
2258.1078	2258.276	2258.192	40.45488	38.67757	RFracC	North	FMI_TLD_MCFL_CNL_185PUC_FMI_final_SC
2267.773	2268.652	2268.213	65.76714	227.474	RFracC	North	FMI_TLD_MCFL_CNL_185PUC_FMI_final_SC
2270.9447	2271.167	2271.056	38.53557	58.90204	RFracC	North	FMI_TLD_MCFL_CNL_185PUC_FMI_final_SC
2270.293	2270.516	2270.404	23.00166	210.3874	RFracC	North	FMI_TLD_MCFL_CNL_185PUC_FMI_final_SC
2270.2474	2270.47	2270.359	51.32092	38.23748	RFracC	North	FMI_TLD_MCFL_CNL_185PUC_FMI_final_SC
2288.0924	2288.798	2288.445	76.3769	51.74303	ConFracC	North	FMI_TLD_MCFL_CNL_185PUC_FMI_final_SC
2304.7025	2305.253	2304.978	89.91369	114.1003	RFracC	North	FMI_TLD_MCFL_CNL_185PUC_FMI_final_SC
2304.584	2305.135	2304.859	84.09465	138.7408	RFracC	North	FMI_TLD_MCFL_CNL_185PUC_FMI_final_SC
2342.0147	2342.566	2342.29	84.94506	164.0239	ConFracC	North	FMI_TLD_MCFL_CNL_185PUC_FMI_final_SC
2342.557	2343.108	2342.832	84.42031	157.6877	ConFracC	North	FMI_TLD_MCFL_CNL_185PUC_FMI_final_SC
2348.5175	2348.941	2348.729	74.91083	30.56511	RFracC	North	FMI_TLD_MCFL_CNL_185PUC_FMI_final_SC
2352.081	2352.24	2352.16	13.9541	84.95712	RFracC	North	FMI_TLD_MCFL_CNL_185PUC_FMI_final_SC
2355.7311	2356.145	2355.938	34.00415	146.9164	RFracC	North	FMI_TLD_MCFL_CNL_185PUC_FMI_final_SC
2363.4187	2363.942	2363.68	39.88386	170.3045	RFracC	North	FMI_TLD_MCFL_CNL_185PUC_FMI_final_SC
2411.3622	2411.758	2411.56	83.69896	355.5913	RFracC	North	FMI_TLD_MCFL_CNL_185PUC_FMI_final_SC
2426.3865	2426.782	2426.584	77.73722	12.69577	RFracC	North	FMI_TLD_MCFL_CNL_185PUC_FMI_final_SC
2426.7282	2427.124	2426.926	83.29612	354.4177	RFracC	North	FMI_TLD_MCFL_CNL_185PUC_FMI_final_SC
2448.442	2448.993	2448.717	82.94944	139.2396	ConFracC	North	FMI_TLD_MCFL_CNL_185PUC_FMI_final_SC

2449.0618	2449.959	2449.51	86.91748	199.0211	ConFracC	North	FMI_TLD_MCFL_CNL_185PUC_FMI_final_SC
2449.9777	2450.246	2450.112	73.82318	358.1058	ConFracC	North	FMI_TLD_MCFL_CNL_185PUC_FMI_final_SC
2600.735	2601.559	2601.147	50.14312	133.0721	RFracC	North	FMI_TLD_MCFL_CNL_185PUC_FMI_final_SC
2613.0387	2613.353	2613.196	72.00119	283.8552	ConFracC	North	FMI_TLD_MCFL_CNL_185PUC_FMI_final_SC
2630.7105	2631.024	2630.868	55.50455	46.09082	RFracC	North	FMI_TLD_MCFL_CNL_185PUC_FMI_final_SC
2632.8933	2633.025	2632.959	11.67128	210.8929	RFracC	North	FMI_TLD_MCFL_CNL_185PUC_FMI_final_SC
2649.9727	2650.332	2650.152	35.67257	123.1205	RFracC	North	FMI_TLD_MCFL_CNL_185PUC_FMI_final_SC
2666.6967	2666.856	2666.776	25.04621	227.3918	RFracC	North	FMI_TLD_MCFL_CNL_185PUC_FMI_final_SC
2668.5514	2668.601	2668.576	35.8343	328.4439	RFracC	North	FMI_TLD_MCFL_CNL_185PUC_FMI_final_SC
2686.3964	2686.692	2686.544	43.23124	220.1059	RFracC	North	FMI_TLD_MCFL_CNL_185PUC_FMI_final_SC
2700.6368	2700.996	2700.817	72.99083	12.64338	ConFracC	North	FMI_TLD_MCFL_CNL_185PUC_FMI_final_SC
2700.6915	2701.051	2700.871	68.5481	24.0168	ConFracC	North	FMI_TLD_MCFL_CNL_185PUC_FMI_final_SC
2705.6403	2706.118	2705.879	88.2972	338.8787	ConFracC	North	FMI_TLD_MCFL_CNL_185PUC_FMI_final_SC
2705.7087	2705.913	2705.811	30.74833	219.0093	ConFracC	North	FMI_TLD_MCFL_CNL_185PUC_FMI_final_SC
2709.1218	2709.326	2709.224	20.09753	123.3368	RFracC	North	FMI_TLD_MCFL_CNL_185PUC_FMI_final_SC
2709.0854	2709.29	2709.188	61.65931	291.6233	RFracC	North	FMI_TLD_MCFL_CNL_185PUC_FMI_final_SC
2709.1081	2709.313	2709.21	41.66193	43.65868	RFracC	North	FMI_TLD_MCFL_CNL_185PUC_FMI_final_SC
2710.3066	2710.457	2710.382	16.02358	203.524	ConFracC	North	FMI_TLD_MCFL_CNL_185PUC_FMI_final_SC
2710.334	2710.42	2710.377	4.383402	21.3681	ConFracC	North	FMI_TLD_MCFL_CNL_185PUC_FMI_final_SC
2710.375	2710.461	2710.418	6.794964	259.2117	ConFracC	North	FMI_TLD_MCFL_CNL_185PUC_FMI_final_SC
2714.2438	2714.366	2714.305	20.62464	238.6292	ConFracC	North	FMI_TLD_MCFL_CNL_185PUC_FMI_final_SC
2715.4058	2715.528	2715.467	6.958095	175.5782	ConFracC	North	FMI_TLD_MCFL_CNL_185PUC_FMI_final_SC
2716.3901	2716.485	2716.438	13.62424	247.2672	ConFracC	North	FMI_TLD_MCFL_CNL_185PUC_FMI_final_SC
2720.382	2720.477	2720.43	13.68586	245.5177	RFracC	North	FMI_TLD_MCFL_CNL_185PUC_FMI_final_SC
2720.4413	2720.536	2720.489	20.30405	255.3281	RFracC	North	FMI_TLD_MCFL_CNL_185PUC_FMI_final_SC
2720.4321	2720.527	2720.48	4.832897	57.04758	RFracC	North	FMI_TLD_MCFL_CNL_185PUC_FMI_final_SC
2727.7825	2728.042	2727.912	61.41513	13.10841	ConFracC	North	FMI_TLD_MCFL_CNL_185PUC_FMI_final_SC
2728.3703	2728.73	2728.55	73.07866	6.054505	ConFracC	North	FMI_TLD_MCFL_CNL_185PUC_FMI_final_SC
2728.7212	2729.081	2728.901	71.2065	11.85024	ConFracC	North	FMI_TLD_MCFL_CNL_185PUC_FMI_final_SC
2730.5805	2731.086	2730.833	80.42912	8.472619	ConFracC	North	FMI_TLD_MCFL_CNL_185PUC_FMI_final_SC
2729.9881	2730.493	2730.241	83.22785	358.3335	ConFracC	North	FMI_TLD_MCFL_CNL_185PUC_FMI_final_SC
2731.1273	2731.788	2731.457	89.8972	351.1109	ConFracC	North	FMI_TLD_MCFL_CNL_185PUC_FMI_final_SC
2732.5536	2732.977	2732.765	70.03768	26.11521	ConFracC	North	FMI_TLD_MCFL_CNL_185PUC_FMI_final_SC
2737.6756	2738.5	2738.088	89.04363	179.2108	ConFracC	North	FMI_TLD_MCFL_CNL_185PUC_FMI_final_SC
2738.6736	2739.097	2738.885	80.21262	349.2818	ConFracC	North	FMI_TLD_MCFL_CNL_185PUC_FMI_final_SC
2743.586	2743.736	2743.661	16.57506	96.60056	RFracC	North	FMI_TLD_MCFL_CNL_185PUC_FMI_final_SC
2743.7136	2743.863	2743.788	36.71474	249.9202	RFracC	North	FMI_TLD_MCFL_CNL_185PUC_FMI_final_SC
2744.6113	2744.761	2744.686	27.09086	52.14859	RFracC	North	FMI_TLD_MCFL_CNL_185PUC_FMI_final_SC
2744.6614	2744.811	2744.736	37.46253	251.5574	RFracC	North	FMI_TLD_MCFL_CNL_185PUC_FMI_final_SC
2744.4928	2744.779	2744.636	49.84415	229.5369	RFracC	North	FMI_TLD_MCFL_CNL_185PUC_FMI_final_SC
2748.8264	2749.468	2749.147	80.4455	17.92114	ConFracC	North	FMI_TLD_MCFL_CNL_185PUC_FMI_final_SC
2749.2776	2749.92	2749.599	83.56773	7.547694	ConFracC	North	FMI_TLD_MCFL_CNL_185PUC_FMI_final_SC
2746.147	2747.108	2746.627	85.42726	167.6335	ConFracC	North	FMI_TLD_MCFL_CNL_185PUC_FMI_final_SC
2754.4953	2754.846	2754.67	55.46893	48.17961	ConFracC	North	FMI_TLD_MCFL_CNL_185PUC_FMI_final_SC

Jingemia 3: Total interpreted fracture set

Top Depth (m)	Bottom Depth (m)	Depth (m)	True Dip (deg)	True Azimuth (deg)	Surface Type	Apparent Mode	Image Log
1895.885	1896.247	1896.066	62.86434	34.36508	RFracC	North	FMI_007PUC_FMI
1895.934	1896.296	1896.115	62.01508	232.1046	RFracC	North	FMI_007PUC_FMI
1896.765	1897.127	1896.946	58.19225	47.15166	RFracC	North	FMI_007PUC_FMI
1896.995	1897.357	1897.176	59.04626	223.9811	RFracC	North	FMI_007PUC_FMI
1897.62	1898.091	1897.856	64.51472	47.31055	RFracC	North	FMI_007PUC_FMI
1905.325	1905.566	1905.445	70.08776	308.7543	RFracC	North	FMI_007PUC_FMI
1911.356	1911.669	1911.512	48.2163	65.38096	ConFracC	North	FMI_007PUC_FMI
1911.72	1912.47	1912.095	58.67644	97.68353	ConFracC	North	FMI_007PUC_FMI
1911.677	1912.427	1912.052	86.79652	261.3315	ConFracC	North	FMI_007PUC_FMI
1912.787	1913.477	1913.132	87.88991	110.9946	RFracC	North	FMI_007PUC_FMI
1914.729	1915.418	1915.074	61.74745	78.51372	RFracC	North	FMI_007PUC_FMI
1916.33	1916.535	1916.433	26.31142	119.1678	RFracC	North	FMI_007PUC_FMI
1918.891	1919.422	1919.157	73.57553	239.0451	RFracC	North	FMI_007PUC_FMI
1919.37	1919.902	1919.636	76.38831	247.0137	RFracC	North	FMI_007PUC_FMI
1919.801	1919.981	1919.891	27.60071	79.88142	RFracC	North	FMI_007PUC_FMI
1920.444	1920.624	1920.534	24.0941	101.5026	RFracC	North	FMI_007PUC_FMI
1921.96	1923.56	1922.76	81.74486	46.0538	RFracC	North	FMI_007PUC_FMI
1922.792	1923.603	1923.197	72.06513	53.17533	RFracC	North	FMI_007PUC_FMI
1922.998	1923.53	1923.264	64.12812	55.42252	RFracC	North	FMI_007PUC_FMI
1923.089	1923.621	1923.355	64.54715	54.20963	RFracC	North	FMI_007PUC_FMI
1919.594	1919.92	1919.757	64.20151	245.49	RFracC	North	FMI_007PUC_FMI
1919.461	1919.908	1919.684	71.93008	244.8512	RFracC	North	FMI_007PUC_FMI
1922.003	1922.972	1922.487	85.02483	23.48726	RFracC	North	FMI_007PUC_FMI
1923.938	1924.349	1924.144	45.29984	112.9275	RFracC	North	FMI_007PUC_FMI
1923.568	1924.331	1923.949	65.61781	70.02284	ConFracC	North	FMI_007PUC_FMI
1925.036	1925.823	1925.43	87.50017	101.1328	RFracC	North	FMI_007PUC_FMI
1924.43	1924.84	1924.635	52.56819	193.8915	ConFracC	North	FMI_007PUC_FMI
1924.824	1925.235	1925.029	83.9415	306.9906	ConFracC	North	FMI_007PUC_FMI
1926.99	1927.4	1927.195	78.57306	355.3063	ConFracC	North	FMI_007PUC_FMI
1925.625	1926.266	1925.945	56.72848	94.32954	ConFracC	North	FMI_007PUC_FMI
1927.378	1927.813	1927.596	67.40006	33.76548	RFracC	North	FMI_007PUC_FMI
1927.111	1927.546	1927.329	55.36919	68.83527	RFracC	North	FMI_007PUC_FMI
1927.324	1927.758	1927.541	52.40979	187.9757	RFracC	North	FMI_007PUC_FMI
1927.773	1928.207	1927.99	61.47294	50.12814	RFracC	North	FMI_007PUC_FMI
1927.712	1928.147	1927.929	60.21038	53.76463	RFracC	North	FMI_007PUC_FMI
1927.597	1928.031	1927.814	60.21038	53.76463	RFracC	North	FMI_007PUC_FMI
1927.415	1927.849	1927.632	62.31734	47.74465	RFracC	North	FMI_007PUC_FMI
1927.542	1927.977	1927.759	73.02861	249.5625	RFracC	North	FMI_007PUC_FMI
1927.736	1928.171	1927.954	71.86563	246.2073	RFracC	North	FMI_007PUC_FMI
1927.797	1928.232	1928.014	70.67127	242.8346	RFracC	North	FMI_007PUC_FMI
1927.851	1928.286	1928.069	69.45235	239.4468	RFracC	North	FMI_007PUC_FMI

1929.429	1929.985	1929.707	79.1952	252.4156	RFracC	North	FMI_007PUC_FMI
1929.216	1929.773	1929.495	57.08365	81.29004	RFracC	North	FMI_007PUC_FMI
1928.743	1929.299	1929.021	86.18961	277.5475	RFracC	North	FMI_007PUC_FMI
1930.824	1931.38	1931.102	58.82159	74.64486	RFracC	North	FMI_007PUC_FMI
1930.224	1930.78	1930.502	72.75382	33.34661	RFracC	North	FMI_007PUC_FMI
1931.655	1932.345	1932	67.67788	58.32184	RFracC	North	FMI_007PUC_FMI
1931.637	1932.048	1931.842	76.48335	264.4235	RFracC	North	FMI_007PUC_FMI
1931.115	1931.526	1931.321	77.70535	268.8487	RFracC	North	FMI_007PUC_FMI
1931.018	1931.477	1931.248	54.89535	74.56168	RFracC	North	FMI_007PUC_FMI
1933.56	1933.837	1933.699	63.0205	254.7785	RFracC	North	FMI_007PUC_FMI
1933.9	1934.359	1934.13	77.79406	260.3503	RFracC	North	FMI_007PUC_FMI
1933.7	1934.159	1933.929	71.79404	242.3806	RFracC	North	FMI_007PUC_FMI
1934.513	1934.923	1934.718	78.00082	269.9587	RFracC	North	FMI_007PUC_FMI
1934.064	1934.474	1934.269	52.60588	73.6087	RFracC	North	FMI_007PUC_FMI
1934.009	1934.881	1934.445	65.32948	76.99982	RFracC	North	FMI_007PUC_FMI
1935.211	1935.742	1935.476	57.65781	75.71572	RFracC	North	FMI_007PUC_FMI
1934.871	1935.403	1935.137	88.71606	299.6988	RFracC	North	FMI_007PUC_FMI
1934.628	1934.929	1934.779	45.4905	70.16528	RFracC	North	FMI_007PUC_FMI
1933.815	1934.116	1933.966	50.3174	54.5479	RFracC	North	FMI_007PUC_FMI
1936.084	1936.385	1936.235	59.70637	238.5997	RFracC	North	FMI_007PUC_FMI
1936.206	1936.507	1936.356	55.77027	39.01885	RFracC	North	FMI_007PUC_FMI
1939.136	1939.437	1939.286	69.50332	267.7616	RFracC	North	FMI_007PUC_FMI
1939.166	1939.467	1939.317	69.19715	266.6959	RFracC	North	FMI_007PUC_FMI
1940.471	1940.881	1940.676	74.08649	256.6421	RFracC	North	FMI_007PUC_FMI
1940.883	1941.512	1941.197	63.08825	67.76254	RFracC	North	FMI_007PUC_FMI
1940.592	1941.221	1940.906	65.46624	60.27572	RFracC	North	FMI_007PUC_FMI
1940.895	1941.451	1941.173	61.4671	65.71995	RFracC	North	FMI_007PUC_FMI
1941.678	1942.052	1941.865	72.777	259.5553	RFracC	North	FMI_007PUC_FMI
1942.145	1942.859	1942.502	65.71898	65.94426	RFracC	North	FMI_007PUC_FMI
1941.939	1942.179	1942.059	32.54474	165.1725	RFracC	North	FMI_007PUC_FMI
1942.242	1942.349	1942.296	20.80195	42.91801	RFracC	North	FMI_007PUC_FMI
1941.296	1943.32	1942.308	81.24546	51.25223	RFracC	North	FMI_007PUC_FMI
1943.261	1943.745	1943.503	81.09424	267.8979	RFracC	North	FMI_007PUC_FMI
1944.584	1945.067	1944.825	54.45186	80.42749	RFracC	North	FMI_007PUC_FMI
1944.572	1945.055	1944.813	78.84905	259.9835	RFracC	North	FMI_007PUC_FMI
1944.293	1944.533	1944.413	69.07169	295.259	RFracC	North	FMI_007PUC_FMI
1944.59	1945.364	1944.977	58.92056	97.91509	RFracC	North	FMI_007PUC_FMI
1946.41	1946.954	1946.682	60.2357	68.07294	RFracC	North	FMI_007PUC_FMI
1946.143	1946.687	1946.415	84.51437	271.8495	RFracC	North	FMI_007PUC_FMI
1945.912	1946.299	1946.106	50.1305	77.17371	RFracC	North	FMI_007PUC_FMI
1946.859	1947.342	1947.101	61.28517	57.16051	RFracC	North	FMI_007PUC_FMI
1949.765	1950.248	1950.007	48.39636	118.4456	RFracC	North	FMI_007PUC_FMI
1950.366	1950.91	1950.638	76.20614	21.7203	RFracC	North	FMI_007PUC_FMI
1951.439	1952.529	1951.984	72.4831	61.61131	RFracC	North	FMI_007PUC_FMI

1951.646	1952.736	1952.191	85.10432	93.11317	RFracC	North	FMI_007PUC_FMI
1953.539	1953.985	1953.762	57.9982	61.50554	ConFracC	North	FMI_007PUC_FMI
1954.776	1955.223	1955	53.47529	77.16429	RFracC	North	FMI_007PUC_FMI
1954.576	1955.023	1954.799	55.66018	69.19814	RFracC	North	FMI_007PUC_FMI
1955.183	1955.957	1955.57	87.28762	259.9433	RFracC	North	FMI_007PUC_FMI
1955.444	1956.218	1955.831	87.29626	259.9498	RFracC	North	FMI_007PUC_FMI
1955.255	1956.03	1955.643	69.20142	207.2742	RFracC	North	FMI_007PUC_FMI
1956.165	1956.564	1956.365	71.44489	250.1335	RFracC	North	FMI_007PUC_FMI
1955.953	1956.376	1956.164	73.44504	251.8931	RFracC	North	FMI_007PUC_FMI
1955.51	1956.443	1955.976	77.68279	224.334	RFracC	North	FMI_007PUC_FMI
1955.504	1956.546	1956.025	84.29313	239.0643	RFracC	North	FMI_007PUC_FMI
1957.063	1958.299	1957.681	72.4007	65.67247	RFracC	North	FMI_007PUC_FMI
1957.063	1958.299	1957.681	68.00887	80.71274	RFracC	North	FMI_007PUC_FMI
1957.591	1958.827	1958.209	79.81011	44.10092	RFracC	North	FMI_007PUC_FMI
1957.804	1958.712	1958.258	74.26437	50.0723	RFracC	North	FMI_007PUC_FMI
1956.511	1957.419	1956.965	61.61119	94.35205	RFracC	North	FMI_007PUC_FMI
1958.143	1958.59	1958.367	66.14111	227.6214	RFracC	North	FMI_007PUC_FMI
1959.047	1959.349	1959.198	66.17487	9.20688	RFracC	North	FMI_007PUC_FMI
1984.668	1984.969	1984.818	63.91414	15.60847	RFracC	North	FMI_007PUC_FMI
1988.83	1989.131	1988.98	73.38578	342.4663	RFracC	North	FMI_007PUC_FMI
1989.139	1989.44	1989.29	39.21095	166.4501	RFracC	North	FMI_007PUC_FMI
1990.765	1991.515	1991.14	85.59306	145.8166	RFracC	North	FMI_007PUC_FMI
1994.684	1994.876	1994.78	24.35066	143.0488	ConFracC	North	FMI_007PUC_FMI
1997.893	1998.668	1998.281	60.0688	91.13442	ConFracC	North	FMI_007PUC_FMI
1999.853	2000.421	2000.137	89.56829	126.6083	RFracC	North	FMI_007PUC_FMI
2001.303	2001.531	2001.417	35.16073	187.4305	RFracC	North	FMI_007PUC_FMI
2012.333	2012.488	2012.41	25.22703	69.5143	RFracC	North	FMI_007PUC_FMI
2012.879	2013.034	2012.956	19.07884	109.9997	RFracC	North	FMI_007PUC_FMI
2018.818	2018.974	2018.896	49.2486	1.207687	RFracC	North	FMI_007PUC_FMI
2019.188	2019.344	2019.266	23.852	191.6845	RFracC	North	FMI_007PUC_FMI
2015.148	2015.303	2015.225	19.88335	100.9606	RFracC	North	FMI_007PUC_FMI
2024.466	2024.622	2024.544	21.45655	178.79	RFracC	North	FMI_007PUC_FMI
2025.637	2025.938	2025.788	56.19031	229.5825	RFracC	North	FMI_007PUC_FMI
2026.747	2026.976	2026.862	53.00693	243.415	RFracC	North	FMI_007PUC_FMI
2036.806	2037.775	2037.291	85.68287	170.497	ConFracC	North	FMI_007PUC_FMI
2043.268	2043.472	2043.37	27.04346	159.2051	RFracC	North	FMI_007PUC_FMI
2044.954	2045.158	2045.056	25.93917	133.0768	RFracC	North	FMI_007PUC_FMI
2053.563	2053.828	2053.695	67.51185	354.5963	ConFracC	North	FMI_007PUC_FMI
2056.463	2056.606	2056.535	39.02383	22.72049	RFracC	North	FMI_007PUC_FMI
2059.163	2059.306	2059.234	53.0238	339.7465	RFracC	North	FMI_007PUC_FMI
2069.58	2069.723	2069.651	16.37059	119.2734	RFracC	North	FMI_007PUC_FMI
2072.413	2072.629	2072.521	35.5801	71.54775	RFracC	North	FMI_007PUC_FMI
2081.537	2081.754	2081.645	42.42851	49.22043	RFracC	North	FMI_007PUC_FMI
2088.229	2088.445	2088.337	55.02859	254.9	RFracC	North	FMI_007PUC_FMI

2088.441	2088.658	2088.55	45.39511	229.027	RFracC	North	FMI_007PUC_FMI
2092.136	2092.522	2092.329	43.08569	141.2964	RFracC	North	FMI_007PUC_FMI
2099.374	2099.517	2099.446	45.86131	265.0676	RFracC	North	FMI_007PUC_FMI
2099.513	2099.657	2099.585	23.04792	200.2753	RFracC	North	FMI_007PUC_FMI
2101.085	2101.968	2101.527	68.64396	68.25299	RFracC	North	FMI_007PUC_FMI
2101.455	2102.339	2101.897	83.47191	148.5014	RFracC	North	FMI_007PUC_FMI
2108.001	2108.327	2108.164	74.10299	352.0496	RFracC	North	FMI_007PUC_FMI
2118.563	2118.889	2118.726	56.36414	46.04737	RFracC	North	FMI_007PUC_FMI
2125.352	2125.484	2125.418	52.41226	329.9468	RFracC	North	FMI_007PUC_FMI
2132.402	2132.667	2132.534	39.2238	188.739	RFracC	North	FMI_007PUC_FMI
2151.197	2151.377	2151.287	24.74115	98.91385	RFracC	North	FMI_007PUC_FMI
2153.296	2153.476	2153.386	45.15733	244.5178	RFracC	North	FMI_007PUC_FMI
2153.278	2153.458	2153.368	24.98645	97.09704	RFracC	North	FMI_007PUC_FMI
2154.03	2154.162	2154.096	16.34478	92.13582	RFracC	North	FMI_007PUC_FMI
2160.892	2161.023	2160.958	15.1882	101.7932	RFracC	North	FMI_007PUC_FMI
2161.207	2161.484	2161.346	34.57589	136.7184	RFracC	North	FMI_007PUC_FMI
2161.11	2161.387	2161.249	70.38601	282.3624	RFracC	North	FMI_007PUC_FMI
2164.453	2164.876	2164.665	65.01759	230.6313	ConFracC	North	FMI_007PUC_FMI
2164.071	2164.275	2164.173	32.7025	76.241	ConFracC	North	FMI_007PUC_FMI
2163.689	2163.893	2163.791	31.46627	188.9407	RFracC	North	FMI_007PUC_FMI
2161.984	2162.188	2162.086	54.65907	11.34079	RFracC	North	FMI_007PUC_FMI
2165.339	2165.543	2165.441	54.71013	11.29179	RFracC	North	FMI_007PUC_FMI
2167.462	2167.557	2167.51	31.22154	258.7281	RFracC	North	FMI_007PUC_FMI
2167.735	2168.025	2167.88	38.19754	169.298	ConFracC	North	FMI_007PUC_FMI
2179.505	2179.819	2179.662	58.83149	233.6024	RFracC	North	FMI_007PUC_FMI
2180.64	2180.953	2180.796	40.26162	100.2311	RFracC	North	FMI_007PUC_FMI
2179.681	2179.994	2179.838	41.24321	173.4854	RFracC	North	FMI_007PUC_FMI
2189.977	2190.375	2190.176	57.62494	54.19464	ConFracC	North	FMI_007PUC_FMI
2199.732	2200.13	2199.931	77.68858	269.9044	RFracC	North	FMI_007PUC_FMI
2199.932	2200.331	2200.131	72.49511	252.2225	RFracC	North	FMI_007PUC_FMI
2202.869	2203.267	2203.068	81.23345	337.1359	RFracC	North	FMI_007PUC_FMI
2203.184	2203.582	2203.383	65.80656	233.1765	RFracC	North	FMI_007PUC_FMI
2217.884	2218.076	2217.98	36.86788	210.7923	RFracC	North	FMI_007PUC_FMI
2218.861	2219.053	2218.957	30.5918	188.3553	ConFracC	North	FMI_007PUC_FMI
2222.562	2222.754	2222.658	49.7452	245.499	RFracC	North	FMI_007PUC_FMI
2222.222	2222.414	2222.318	37.39314	212.0839	RFracC	North	FMI_007PUC_FMI
2221.943	2222.208	2222.075	57.18859	238.6573	RFracC	North	FMI_007PUC_FMI
2225.589	2225.854	2225.721	40.99961	68.76067	RFracC	North	FMI_007PUC_FMI
2225.65	2225.915	2225.782	63.43968	255.6457	RFracC	North	FMI_007PUC_FMI
2225.953	2226.218	2226.085	37.86928	82.10322	RFracC	North	FMI_007PUC_FMI
2226.93	2227.377	2227.153	58.97217	203.5951	RFracC	North	FMI_007PUC_FMI
2231.644	2232.43	2232.037	81.14588	235.231	RFracC	North	FMI_007PUC_FMI
2234.441	2234.96	2234.7	81.50917	357.0717	ConFracC	North	FMI_007PUC_FMI
2234.653	2235.173	2234.913	83.66128	349.1139	ConFracC	North	FMI_007PUC_FMI

2235.272	2235.791	2235.532	86.349	336.5035	ConFracC	North	FMI_007PUC_FMI
2235.605	2236.125	2235.865	84.14114	346.8041	ConFracC	North	FMI_007PUC_FMI
2235.909	2236.259	2236.084	68.90517	7.540696	ConFracC	North	FMI_007PUC_FMI
2236.133	2236.483	2236.308	77.89371	333.764	ConFracC	North	FMI_007PUC_FMI
2236.594	2236.847	2236.721	52.45457	26.70956	ConFracC	North	FMI_007PUC_FMI
2236.934	2237.187	2237.06	63.16421	356.7988	ConFracC	North	FMI_007PUC_FMI
2239.798	2240.05	2239.924	60.91308	1.740666	ConFracC	North	FMI_007PUC_FMI
2239.585	2239.777	2239.681	57.21562	347.4548	ConFracC	North	FMI_007PUC_FMI
2240.168	2240.36	2240.264	55.00644	354.2577	ConFracC	North	FMI_007PUC_FMI
2241.599	2242.156	2241.878	80.32205	1.687467	ConFracC	North	FMI_007PUC_FMI
2240.35	2240.906	2240.628	74.64473	18.79012	ConFracC	North	FMI_007PUC_FMI
2243.529	2243.915	2243.722	76.34078	258.0836	RFracC	North	FMI_007PUC_FMI
2244.372	2244.637	2244.504	33.53089	107.9226	RFracC	North	FMI_007PUC_FMI
2246.01	2246.967	2246.488	64.63912	72.50931	ConFracC	North	FMI_007PUC_FMI
2249.456	2249.903	2249.68	51.8892	72.61038	ConFracC	North	FMI_007PUC_FMI
2255.923	2256.746	2256.335	59.94117	86.75395	ConFracC	North	FMI_007PUC_FMI
2260.674	2261.703	2261.188	76.16676	40.67182	ConFracC	North	FMI_007PUC_FMI
2261.705	2262.601	2262.153	87.31733	3.946223	ConFracC	North	FMI_007PUC_FMI
2266.692	2267.03	2266.861	47.47855	68.27202	RFracC	North	FMI_007PUC_FMI
2272.638	2272.975	2272.806	47.28204	71.00778	RFracC	North	FMI_007PUC_FMI
2279.056	2279.394	2279.225	59.04899	34.81286	RFracC	North	FMI_007PUC_FMI
2279.918	2280.353	2280.135	66.59845	31.51378	RFracC	North	FMI_007PUC_FMI
2285.954	2286.183	2286.069	37.13876	70.54544	ConFracC	North	FMI_007PUC_FMI
2286.422	2286.808	2286.615	56.65218	53.38718	ConFracC	North	FMI_007PUC_FMI
2288.211	2288.415	2288.313	38.08361	205.3638	RFracC	North	FMI_007PUC_FMI
2288.169	2288.373	2288.271	32.24629	77.66222	RFracC	North	FMI_007PUC_FMI
2291.239	2291.443	2291.341	44.59806	226.0771	RFracC	North	FMI_007PUC_FMI
2290.244	2290.654	2290.449	78.79326	346.1467	ConFracC	North	FMI_007PUC_FMI
2307.164	2307.478	2307.321	46.1736	77.70879	RFracC	North	FMI_007PUC_FMI
2313.947	2314.26	2314.104	44.21236	87.5934	RFracC	North	FMI_007PUC_FMI
2341.066	2341.488	2341.277	68.83055	242.6553	RFracC	North	FMI_007PUC_FMI
2345.118	2345.541	2345.33	75.1368	8.239783	ConFracC	North	FMI_007PUC_FMI
2345.24	2345.662	2345.451	77.19165	0.36237	ConFracC	North	FMI_007PUC_FMI
2345.671	2346.093	2345.882	77.72036	358.1046	ConFracC	North	FMI_007PUC_FMI
2345.968	2346.39	2346.179	71.77855	19.50478	ConFracC	North	FMI_007PUC_FMI
2346.126	2346.609	2346.367	77.5012	10.15836	ConFracC	North	FMI_007PUC_FMI
2346.295	2346.779	2346.537	81.46791	354.2045	ConFracC	North	FMI_007PUC_FMI
2347.054	2347.537	2347.295	78.39275	6.73283	ConFracC	North	FMI_007PUC_FMI
2346.854	2347.337	2347.095	79.00913	4.4587	ConFracC	North	FMI_007PUC_FMI
2346.556	2346.955	2346.755	75.56085	1.126965	ConFracC	North	FMI_007PUC_FMI
2349.147	2349.545	2349.346	77.0295	354.3708	ConFracC	North	FMI_007PUC_FMI
2348.164	2348.526	2348.345	71.8497	6.042749	ConFracC	North	FMI_007PUC_FMI
2347.454	2347.816	2347.635	73.89005	358.3117	ConFracC	North	FMI_007PUC_FMI
2347.988	2348.35	2348.169	74.36888	356.0859	ConFracC	North	FMI_007PUC_FMI

2348.158	2348.799	2348.478	85.59289	358.7733	ConFracC	North	FMI_007PUC_FMI
2363.908	2364.354	2364.131	73.56724	15.31607	ConFracC	North	FMI_007PUC_FMI
2361.165	2361.612	2361.389	72.96783	17.58299	ConFracC	North	FMI_007PUC_FMI
2362.585	2363.032	2362.808	82.15509	336.6639	ConFracC	North	FMI_007PUC_FMI
2363.167	2363.663	2363.415	69.49791	35.61015	ConFracC	North	FMI_007PUC_FMI
2368.652	2368.868	2368.76	48.14485	233.5239	RFracC	North	FMI_007PUC_FMI
2368.7	2369.172	2368.936	61.34417	208.0381	RFracC	North	FMI_007PUC_FMI
2368.767	2369.238	2369.003	58.53389	197.8968	RFracC	North	FMI_007PUC_FMI
2378.79	2379.054	2378.922	57.84405	244.0793	RFracC	North	FMI_007PUC_FMI
2390.159	2390.594	2390.376	53.60276	80.94969	RFracC	North	FMI_007PUC_FMI
2421.992	2422.244	2422.118	44.25085	211.1831	RFracC	North	FMI_007PUC_FMI
2422.18	2422.433	2422.306	34.08783	107.83	RFracC	North	FMI_007PUC_FMI
2455.693	2456.067	2455.88	41.85936	157.6621	RFracC	North	FMI_007PUC_FMI
2462.488	2462.692	2462.59	50.46942	248.8866	ConFracC	North	FMI_007PUC_FMI
2465.534	2465.883	2465.709	43.64435	180.4361	RFracF	North	FMI_007PUC_FMI
2465.879	2466.229	2466.054	40.23838	158.19	RFracF	North	FMI_007PUC_FMI
2476.43	2476.78	2476.605	41.66665	168.2183	RFracF	North	FMI_007PUC_FMI
2477.51	2477.957	2477.733	44.87393	133.1836	RFracF	North	FMI_007PUC_FMI
2484.778	2485.043	2484.91	35.10314	172.9991	RFracF	North	FMI_007PUC_FMI
2485.591	2485.759	2485.675	20.44406	163.7021	RFracF	North	FMI_007PUC_FMI
2485.585	2485.752	2485.669	60.17925	330.5843	RFracF	North	FMI_007PUC_FMI
2489.128	2489.854	2489.491	82.06548	22.13023	RFracF	North	FMI_007PUC_FMI
2492.094	2492.323	2492.209	41.31346	213.7908	RFracF	North	FMI_007PUC_FMI
2492.191	2492.42	2492.306	28.50233	153.3466	RFracF	North	FMI_007PUC_FMI
2499.538	2499.913	2499.725	61.70426	229.0228	RFracF	North	FMI_007PUC_FMI
2505.168	2505.324	2505.246	21.57636	187.514	RFracF	North	FMI_007PUC_FMI
2508.19	2508.406	2508.298	44.76172	226.9529	RFracF	North	FMI_007PUC_FMI
2512.242	2512.386	2512.314	53.93642	286.6327	RFracF	North	FMI_007PUC_FMI
2512.242	2512.386	2512.314	14.58692	140.1997	RFracF	North	FMI_007PUC_FMI
2512.461	2512.568	2512.514	14.47385	57.11097	RFracF	North	FMI_007PUC_FMI
2513.359	2513.709	2513.534	41.81277	167.4186	RFracF	North	FMI_007PUC_FMI
2519.759	2519.951	2519.855	39.37187	222.5132	RFracF	North	FMI_007PUC_FMI
2523.181	2523.422	2523.301	34.004	180.3484	RFracF	North	FMI_007PUC_FMI
2519.225	2519.466	2519.346	32.02395	170.1605	RFracF	North	FMI_007PUC_FMI
2518.607	2518.847	2518.727	64.69961	356.0392	RFracF	North	FMI_007PUC_FMI
2514.147	2514.388	2514.268	44.81661	217.8556	RFracF	North	FMI_007PUC_FMI
2535.382	2535.622	2535.502	37.44213	68.22876	RFracF	North	FMI_007PUC_FMI
2535.473	2535.713	2535.593	52.07806	233.5575	RFracF	North	FMI_007PUC_FMI
2535.096	2535.337	2535.217	29.16994	125.7098	RFracF	North	FMI_007PUC_FMI
2535.29	2535.531	2535.411	63.87707	264.6405	RFracF	North	FMI_007PUC_FMI
2535.758	2535.998	2535.878	30.33982	154.9524	RFracF	North	FMI_007PUC_FMI
2536.261	2536.842	2536.551	88.61617	147.7359	RFracF	North	FMI_007PUC_FMI
2536.103	2536.296	2536.199	63.98884	328.2641	RFracF	North	FMI_007PUC_FMI
2537.317	2537.655	2537.486	38.66823	115.9659	RFracF	North	FMI_007PUC_FMI

2537.353	2537.521	2537.437	61.42443	307.3666	RFracF	North	FMI_007PUC_FMI
2536.298	2537.812	2537.055	61.93533	114.4484	RFracF	North	FMI_007PUC_FMI
2540.083	2540.288	2540.185	30.92265	187.607	RFracF	North	FMI_007PUC_FMI
2543.912	2544.116	2544.014	25.34181	108.4666	RFracF	North	FMI_007PUC_FMI
2542.085	2542.399	2542.242	36.39266	136.9604	RFracF	North	FMI_007PUC_FMI
2542.231	2542.338	2542.285	36.25288	257.292	RFracF	North	FMI_007PUC_FMI
2541.636	2541.744	2541.69	7.09035	119.1446	RFracF	North	FMI_007PUC_FMI
2562.385	2562.492	2562.439	22.01892	227.8705	RFracF	North	FMI_007PUC_FMI
2562.288	2562.395	2562.342	47.60856	290.8819	RFracF	North	FMI_007PUC_FMI
2574.276	2574.383	2574.33	13.52983	203.2954	ConFracC	North	FMI_007PUC_FMI
2574.889	2575.251	2575.07	40.0343	138.2658	ConFracC	North	FMI_007PUC_FMI
2576.491	2576.658	2576.575	21.56362	171.1905	RFracC	North	FMI_007PUC_FMI
2576.454	2576.622	2576.538	19.00101	141.5924	RFracC	North	FMI_007PUC_FMI
2580.828	2580.996	2580.912	27.89331	200.5569	ConFracC	North	FMI_007PUC_FMI
2587.993	2588.537	2588.265	89.13461	120.6865	RFracC	North	FMI_007PUC_FMI
2588.539	2589.083	2588.811	89.81547	113.6758	RFracC	North	FMI_007PUC_FMI
2603.895	2603.953	2603.924	14.33492	259.2431	RFracC	North	FMI_007PUC_FMI
2606.182	2607.078	2606.63	56.3961	137.2309	RFracC	North	FMI_007PUC_FMI
2607.662	2607.854	2607.758	42.4412	227.8939	RFracC	North	FMI_007PUC_FMI
2606.964	2607.157	2607.061	29.35944	188.9118	RFracC	North	FMI_007PUC_FMI

APPENDIX F: CALCITE STRESS INVERSION TECHNIQUE TENSORS

NPS1 TENSOR 1

```
 ****************************************
 ****************************************
 ***** ECHANTILLON NPS1 ******************
 ****************************************
 ****************************************
 ****************************************
 ****************************************
 ****************************************
 ****************************************
 ****************************************
  1 400  54 113 200 1

      ****************************************

TENSEUR N°1
      ****************************************

POURCENTAGE: 54
NOMBRE DE MACLES        211.
NOMBRE DE NON MACLES     89.
MACLES INCORPOREES      113
POURCENTAGE DU NOMBRE DE NON MACLES SUR MACLES=   42. %

      ****************************************
   SIGMA 1   DIRECTION  207.   PENDAGE   71.     -1.599
   SIGMA 2   DIRECTION  112.   PENDAGE    2.     -1.903
   SIGMA 3   DIRECTION   22.   PENDAGE   19.     -2.761
      f=  .63  RAPPORT R= 0.1       .138

347 305 101 327 102  29  48 346 320 326  36  16  19 454
312 150 452 315  59 440  22 323  34 360   3  30 433 353
129  21  32 126  51 136 432 314  44 331   1 617  38 151
105 441  11 428 127 356 146 125 442 324 112 131 310 103
414 135  28 352 116 434 409 435 118 345   4 124  31  58
 45 317  25 145 123 406-704 334-609 431 604 147-611 134
 49  41  24 737 325 447-625-613  55 405  42 645  39 128
348 313-751 321 641-755 344 426 301-729 601-624   5-749
351  53 446 120 119-615-621 706 402 303 359 614 110

      ****************************************

 347  305  101  327  102   29   48  346  320  326   36   16   19  454
.486 .485 .475 .467 .463 .459 .455 .452 .445 .441 .429 .429 .429 .426
```

312 150 452 315 59 440 22 323 34 360 3 30 433 353
.426 .425 .425 .424 .422 .422 .422 .420 .419 .418 .418 .413 .407 .405

129 21 32 126 51 136 432 314 44 331 1 617 38 151
.402 .402 .402 .400 .398 .395 .395 .394 .393 .391 .390 .390 .389 .381

105 441 11 428 127 356 146 125 442 324 112 131 310 103
.371 .368 .356 .352 .351 .349 .348 .340 .338 .330 .329 .329 .323 .322

414 135 28 352 116 434 409 435 118 345 4 124 31 58
.301 .295 .295 .292 .290 .287 .282 .275 .265 .245 .241 .240 .230 .223

45 317 25 145 123 406 -704 334 -609 431 604 147 -611 134
.213 .208 .206 .199 .198 .196 .185 .178 .177 .174 .172 .168 .166 .158

49 41 24 737 325 447 -625 -613 55 405 42 645 39 128
.150 .148 .143 .139 .138 .135 .135 .134 .128 .126 .122 .116 .116 .111

348 313 -751 321 641 -755 344 426 301 -729 601 -624 5 -749
.104 .102 .102 .094 .092 .091 .085 .082 .081 .078 .078 .077 .077 .077

351 53 446 120 119 -615 -621 706 402 303 359 614 110 -728
.073 .071 .070 .069 .067 .065 .065 .062 .062 .062 .062 .060 .060 .059

46 -648 -712 427 -747 -627 455 -644 -651 304 -653 605 -646 154
.058 .056 .056 .051 .047 .045 .039 .037 .036 .035 .035 .035 .033 .031

734 108 13 106 -629 26 429 311 -750 144 -659 726 -744 -631
.030 .029 .029 .029 .026 .023 .023 .022 .021 .018 .018 .012 .008 .007

-450 -636 52 425 -445 -652 -603 401 141 -746 403 407 17 138
.003 .002 .001 .001 .001 .001-.002-.003-.004-.011-.015-.016-.017-.019

336 -703 -723 -451 731 -423 47 437 -745 -412 9 -725 738 -702
-.019-.020-.027-.027-.029-.029-.032-.035-.037-.038-.041-.042-.042-.046

114 -634 -626 -741 -735 152 443 404 -705 -743 132 104 -616 27
-.047-.052-.052-.058-.058-.062-.062-.065-.066-.071-.076-.077-.077-.081

727 -660 -752 -701 -647 408 137 329 -620 -612 14 -630 730 341
-.081-.082-.082-.084-.084-.086-.088-.090-.091-.091-.094-.094-.094-.095

15 155 35 -714 60 -619 33 -628 -643 411 -622 632 623 133
-.099-.100-.102-.104-.107-.108-.109-.111-.115-.115-.118-.125-.127-.130

-754 -649 316 -736 -733 436 140 444 -748 309 -638 732 716 20
-.132-.139-.148-.151-.156-.162-.162-.164-.166-.167-.170-.173-.173-.178

142 -742 12 319 330 -656 -740 -655 322 10 338 -642 -416 332
-.178-.186-.187-.187-.189-.191-.196-.197-.197-.199-.206-.208-.208-.209

56 23 328 -710 -610 109 449 349 418 438 -724 358 -339 -658
-.212-.213-.217-.220-.220-.236-.239-.254-.264-.269-.272-.275-.288-.299

130 -709 753 8 608 -718 107 -424 335 148 149 -633 355 -453
-.302-.305-.308-.310-.311-.316-.321-.328-.331-.345-.345-.347-.348-.349

420 111 720 -719 342 419 -639 43 -635 430 -343 143 708 -308
-.354-.368-.370-.382-.384-.392-.403-.413-.416-.420-.420-.422-.423-.428

153 410 333 -711 -707 -448
-.432-.434-.437-.455-.459-.484

SEUIL INTERNE = 0.0605
TAILLE DES CRISTAUX = 100 MICRONS
SEUIL CALCULE = 11.5 MPa
SIGMA1-SIGMA3 = 190.2
SIGMA2-SIGMA3 = 26.3
SIGMA1d = 118.0

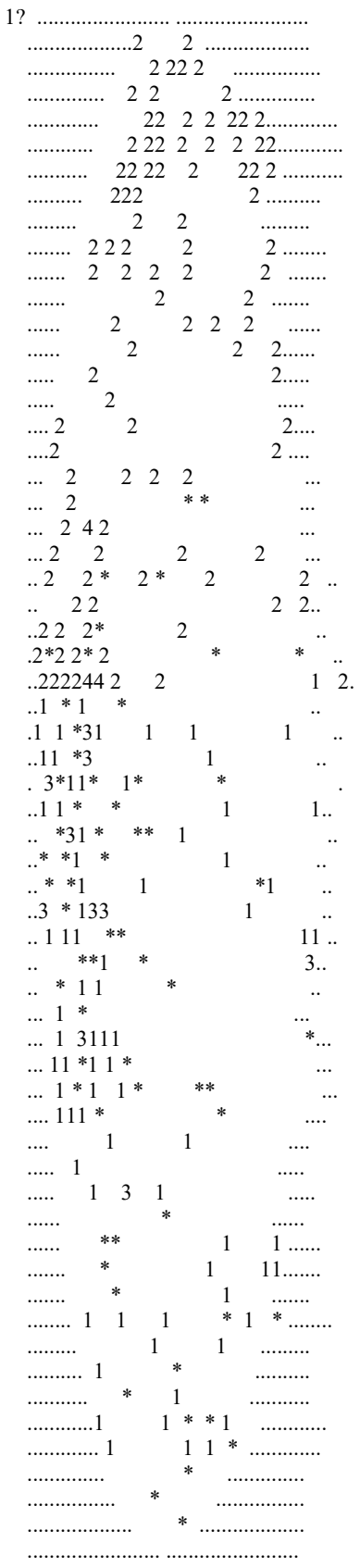

1 .2

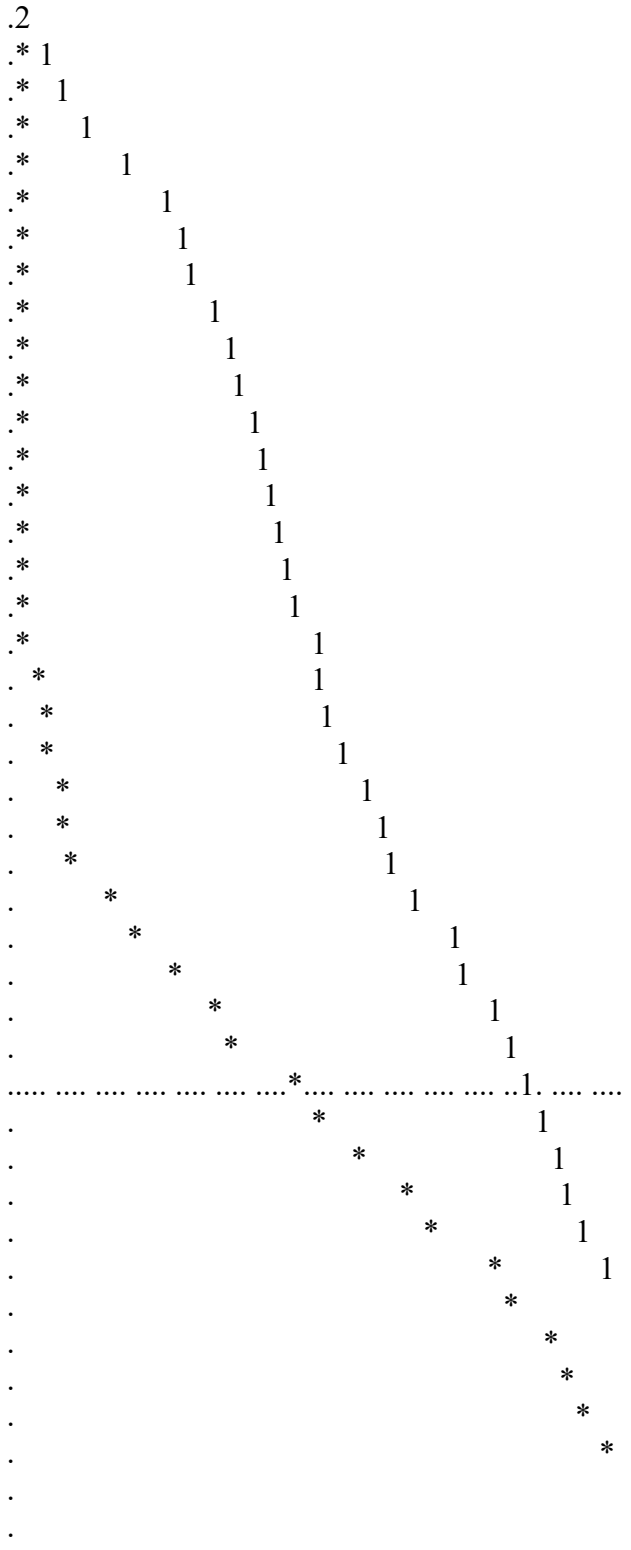

NPS 1 TENSOR 2

```
 ****************************************
 ****************************************
 ***** ECHANTILLON NPS1 ******************
 ****************************************
 ****************************************
 ****************************************
 ****************************************
 ****************************************
 ****************************************
 ****************************************
  1 400  50 113 200 1

      ****************************************
```

TENSEUR N°2

```
      LES DONNEES SUIVANTES SONT RETIREES
347 305 101 327 102  29  48 346 320 326  36  16  19 454
312 150 452 315  59 440  22 323  34 360   3  30 433 353
129  21  32 126  51 136 432 314  44 331   1 617  38 151
105 441  11 428 127 356 146 125 442 324 112 131 310 103
414 135  28 352 116 434 409 435 118 345   4 124  31  58
 45 317  25 145 123 406 334 431 604 147 134  49  41  24
737 325 447  55 405  42 645  39 128 348 313 321 641 344
426 301 601   5 351  53 446 120 119 706 402 303 359 614
110

      ****************************************
```

POURCENTAGE: 50
NOMBRE DE MACLES 98.
NOMBRE DE NON MACLES 89.
MACLES INCORPOREES 49
POURCENTAGE DU NOMBRE DE NON MACLES SUR MACLES= 91. %

```
      ****************************************

   SIGMA 1   DIRECTION  179.   PENDAGE   19.     -1.049
   SIGMA 2   DIRECTION  272.   PENDAGE   11.     -2.757
   SIGMA 3   DIRECTION   30.   PENDAGE   68.     -2.611
      f=  .61  RAPPORT R= 0.4       .419

 359  49 120 608  55-755 348  46  42   9-647  39 730-725
 106 641 403 134 325 140 408 332 335 319 341  45 322 338
 143-453-656-712 142 124  27 442  20 330 443  43 110 328
-749 708 352 402 344-724-729-728 329 304 356 738 425   5
```

52 351 420 28 23

****

359 49 120 608 55 -755 348 46 42 9 -647 39 730 -725
.447 .442 .439 .437 .424 .422 .419 .417 .414 .406 .404 .397 .387 .380

106 641 403 134 325 140 408 332 335 319 341 45 322 338
.376 .353 .353 .352 .351 .345 .345 .343 .343 .341 .338 .334 .334 .334

143 -453 -656 -712 142 124 27 442 20 330 443 43 110 328
.332 .331 .326 .321 .315 .310 .306 .306 .304 .303 .301 .301 .298 .296

-749 708 352 402 344 -724 -729 -728 329 304 356 738 425 5
.294 .294 .291 .290 .290 .289 .284 .281 .281 .281 .280 .280 .279 .275

52 351 420 28 23 431 -630 438 410 632 -745 426 -339 418
.275 .274 .274 .273 .273 .261 .260 .250 .248 .245 .244 .243 .239 .236

355 -628 623 -622 -634 349 -619 -450 109 -743 -742 342 -655 -642
.235 .234 .227 .225 .223 .223 .222 .221 .220 .219 .218 .215 .215 .213

56 407 -620 -710 -638 13 -747 104 309 -660 436 15 336 107
.210 .210 .208 .208 .206 .202 .201 .199 .198 .195 .194 .194 .191 .191

-744 -451 108 -612 -616 316 -711 -704 429 47 -448 12 17 -701
.187 .185 .182 .179 .177 .173 .170 .169 .168 .167 .163 .162 .162 .154

-627 -631 14 -629 -740 -646 -659 -754 -707 155 -639 -719 401 10
.152 .150 .148 .146 .142 .141 .141 .141 .140 .139 .138 .134 .134 .134

60 -649 -611 -621 -636 -644 -615 -651 -424 -652 -633 154 -648 152
.129 .126 .120 .120 .118 .117 .117 .115 .114 .112 .108 .107 .098 .094

430 720 -746 605 419 -752 -626 -705 -416 -653 132 -625 133 -709
.087 .084 .066 .058 .054 .048 .042 .036 .035 .035 .034 .026 .026 .025

149 -702 -703 -423 -635 153 311 8 -718 -412 732 411 333 -736
.015 .008 .005 .004 .003-.011-.017-.045-.045-.050-.054-.057-.063-.065

130 -610 -308 111 449 -735 455 -609 726 -603 -624 -733 -750 404
-.068-.070-.080-.082-.093-.095-.099-.100-.105-.106-.106-.111-.113-.114

-445 148 444 358 -714 -613 -343 753 -658 734 138 731 -643 -748
-.114-.120-.123-.129-.139-.159-.160-.161-.167-.168-.169-.170-.181-.184

137 427 -751 716 727 35 -723 -741 141 114 26 437 144 33
-.185-.187-.188-.218-.227-.243-.296-.303-.310-.328-.347-.381-.394-.399

SEUIL INTERNE = 0.2727
SEUIL CALCULE = 11.5 MPa
SIGMA1-SIGMA3 = 42.2
SIGMA2-SIGMA3 = 17.7
SIGMA1d = 22.2

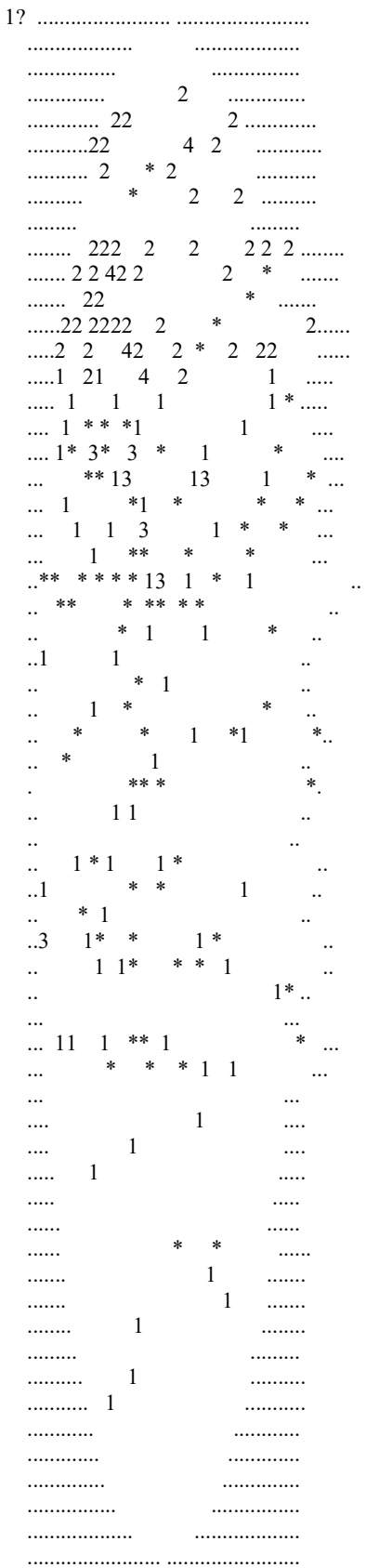

```
1   .2
    .2
    .2
    .2
    .*   1
    . *    1
    .  *     1
    .   *      1
    .   *      1
    .   *             1
    .     *                1
    .       *                 1
    .       *                        1
    .            *                           1
    .             *                              1
    .              *                                 1
    .                 *                                1
    .                         *                            1
    .                               *                            1
    .                                   *                          1
    .                                       *                          1
    .                                           *                       1
    .                                                     *                1
    .                                                               *       1
    .                                                                 *       1
    .                                                                 *         1
    .                                                                   *       1
    .                                                                     *      1
    .                                                                         *
    .                                                                          *
    ..... .... .... .... .... .... .... .... .... .... .... .... .... .... ....
    .
```

NPS 2 TENSOR 1

```
    ****************************************
 ****************************************
 ***** ECHANTILLON NPS2 ******************
 ****************************************
 ****************************************
 ****************************************
 ****************************************
 ****************************************
 ****************************************
 ****************************************
  1 400  30 113 200 1

      ****************************************

 TENSEUR N°1
      ****************************************

 POURCENTAGE: 30
 NOMBRE DE MACLES        195.
 NOMBRE DE NON MACLES     90.
 MACLES INCORPOREES       58
 POURCENTAGE DU NOMBRE DE NON MACLES SUR MACLES=   46. %
    SIGMA 1   DIRECTION  171.   PENDAGE   32.      -.668
    SIGMA 2   DIRECTION  296.   PENDAGE   42.     -2.106
    SIGMA 3   DIRECTION   59.   PENDAGE   31.     -2.106
       f= 1.01  RAPPORT R= 0.1        .093

-615 422 320 136 333 310-639  22 726 231-707 319 502 305
 331   2 207-608 318-723 220  40 311 328 316  44 427 321
 503  24 129 128 307 518 228 501  43 530 337-638 412 215
-617  23 232 504 327 114 223   6 301 431 415 341 408  29
 26 133 117 112 214-623-609 424 108 338 435

      ****************************************

 -615  422  320  136  333  310 -639   22  726  231 -707  319  502  305
 .483 .481 .478 .471 .464 .463 .450 .439 .432 .427 .421 .421 .417 .413

  331    2  207 -608  318 -723  220   40  311  328  316   44  427  321
 .412 .408 .404 .402 .395 .393 .387 .384 .384 .382 .381 .381 .379 .377

  503   24  129  128  307  518  228  501   43  530  337 -638  412  215
 .374 .371 .371 .367 .362 .355 .352 .352 .349 .345 .341 .336 .334 .328

 -617   23  232  504  327  114  223    6  301  431  415  341  408   29
 .314 .309 .307 .304 .296 .295 .294 .290 .287 .283 .281 .278 .275 .275
```

26 133 117 112 214 -623 -609 424 108 338 435 -636 -614 -642
.275 .271 .269 .268 .262 .261 .260 .257 .256 .256 .256 .249 .247 .243

37 -703 -626 31 211 103 430 306 632 428 213 -716 -727 -643
.238 .238 .232 .218 .218 .218 .217 .216 .215 .215 .192 .187 .184 .179

130 -815 -604 -618 32 340 -624 -822 41 -830 -832 644 201 116
.177 .167 .164 .163 .159 .159 .159 .152 .144 .143 .141 .138 .135 .127

-730 344 403 -732 -827 -804 -820 308 -801 343 204 -622 322 432
.127 .120 .120 .117 .110 .108 .107 .101 .099 .097 .094 .094 .093 .092

708 525 332 230 202 -606 323 5 107 416 39 -610 42 38
.087 .084 .083 .081 .081 .078 .078 .077 .076 .070 .069 .067 .064 .061

-712 315 -641 10 -605 126 520 3 127 342 11 -728 -714 -620
.061 .060 .060 .057 .056 .056 .055 .045 .045 .042 .039 .038 .037 .031

15 -631 532 17 317 414 -802 324 8 325 425 -637 -640 36
.031 .028 .024 .019 .018 .018 .013 .006 .006 .005 .001-.003-.005-.006

426 434 515 27 -627 339 -616 -821 326 218 20 407 -611 423
-.007-.009-.010-.012-.012-.013-.016-.017-.021-.022-.025-.028-.029-.030

123 -722 16 122 18 621 224 -731 -807 436 429 507 7 633
-.031-.031-.038-.041-.041-.041-.063-.068-.072-.074-.075-.084-.093-.095

-717 132 514 -607 -729 824 -531 118 736 -309 33 -619 -831 -508
-.095-.096-.100-.100-.101-.102-.104-.111-.112-.113-.116-.117-.120-.122

21 -818 131 527 -510 336 -828 612 -735 9 -528 13 19 30
-.124-.128-.131-.138-.138-.140-.141-.148-.149-.162-.163-.166-.166-.176

121 14 104 -511 -733 -814 -715 523 603 28 302 -823 -834 203
-.177-.178-.184-.186-.186-.187-.188-.191-.191-.191-.198-.202-.205-.208

1 -417 -602 -628 -803 124 -811 227 334 304 222 135 314 313
-.214-.219-.219-.220-.235-.236-.238-.242-.255-.258-.263-.268-.271-.276

329 115 433 -601 -734 724 -629 -813 -513 4 35 303 335 106
-.277-.279-.288-.292-.304-.306-.309-.315-.321-.328-.331-.333-.336-.340

-825 418 -808 330 -634 -625 406 312 534 521 -725 522 404 225
-.347-.364-.364-.364-.367-.367-.369-.371-.374-.379-.386-.391-.392-.393

125 -810 221 25 524 210 421 -706 208 -721 718 -704 12 234
-.396-.403-.411-.412-.413-.417-.418-.422-.423-.423-.426-.430-.435-.435

```
  134   34 -630 -635  613
-.453-.465-.465-.466-.489
        SEUIL INTERNE = 0.2564
        TAILLE DES CRISTAUX = 100 MICRONS
        SEUIL CALCULE =   11.5 MPa
        SIGMA1-SIGMA3 =    44.9
        SIGMA2-SIGMA3 =     4.2
        SIGMA1d =          28.5
```

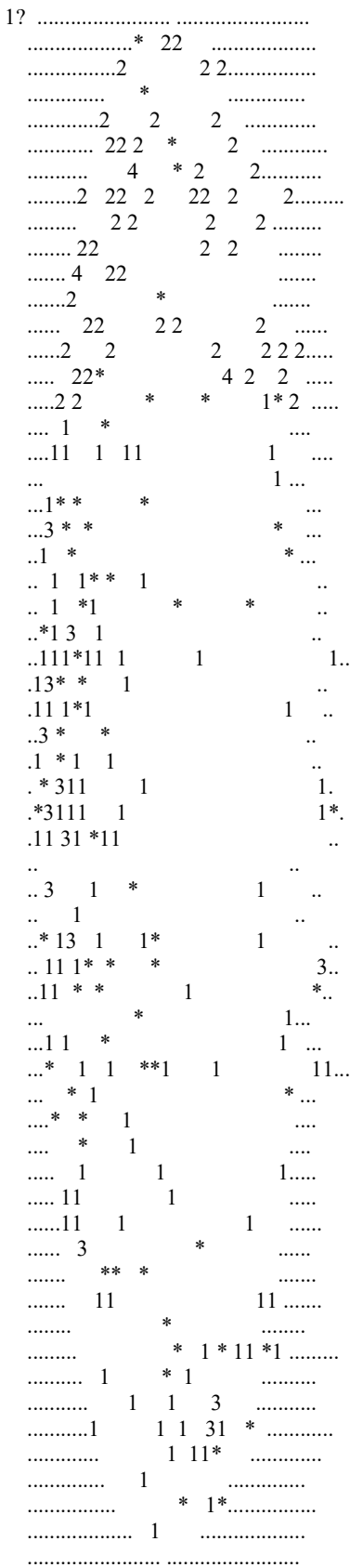

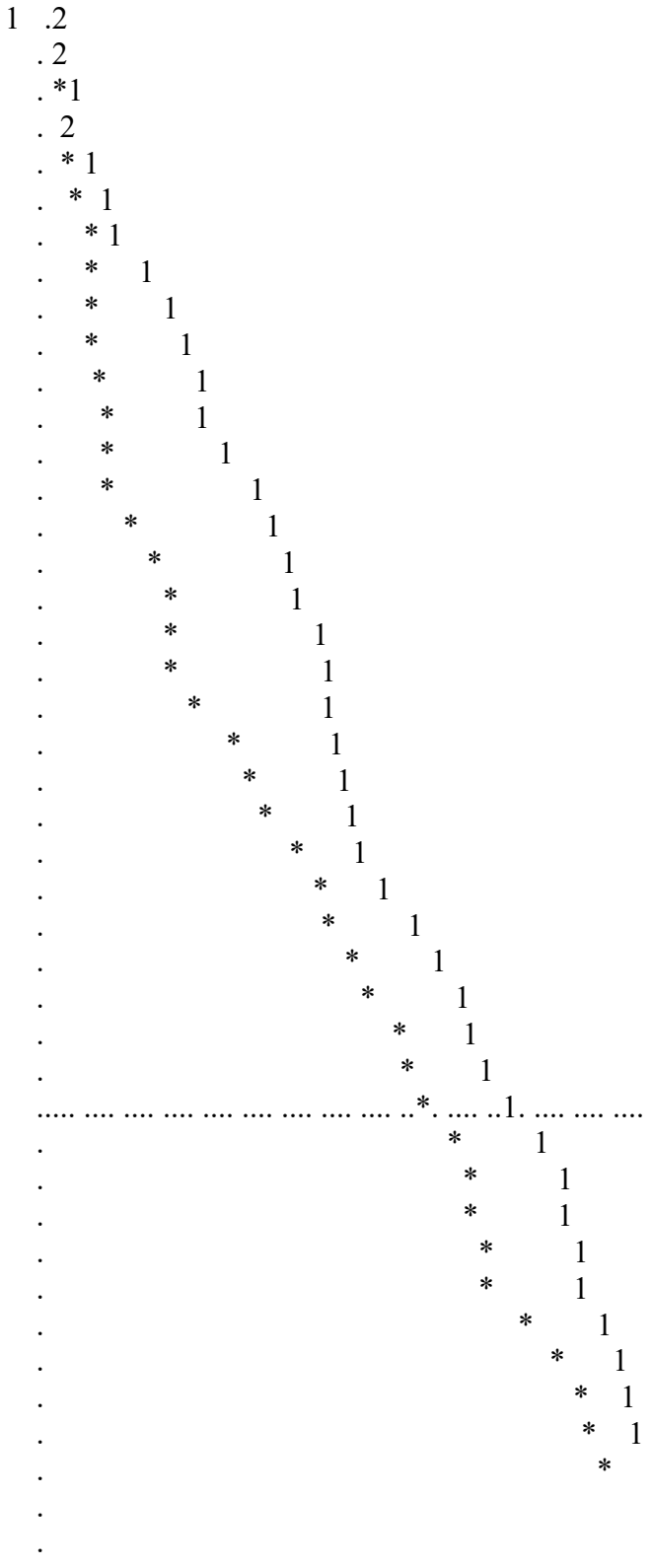

NPS 2 TENSOR 2

```
 ****************************************
 ****************************************
 ***** ECHANTILLON NPS2 ******************
 ****************************************
 ****************************************
 ****************************************
 ****************************************
 ****************************************
 ****************************************
 ****************************************
  1 400  39 113 200 1

      ****************************************

 TENSEUR N°2

      LES DONNEES SUIVANTES SONT RETIREES
422 320 136 333 310  22 726 231 319 502 305 331   2   0
207 318 220  40 311 328 316  44 427 321 503  24 129   0
128 307 518 228 501  43 530 337 412 215  23 232 504   0
327 114 223   6 301 431 415 341 408  29  26 133 117   0
112 214 424 108 338 435   0   0   0

      ****************************************

 POURCENTAGE: 39
 NOMBRE DE MACLES        138.
 NOMBRE DE NON MACLES     89.
 MACLES INCORPOREES       53
 POURCENTAGE DU NOMBRE DE NON MACLES SUR MACLES=   64. %

      ****************************************

    SIGMA 1   DIRECTION  262.   PENDAGE   47.      -.974
    SIGMA 2   DIRECTION   28.   PENDAGE   30.     -2.072
    SIGMA 3   DIRECTION  136.   PENDAGE   29.      -.763
       f= 1.14  RAPPORT R= 0.6       .639

 303-823 334 824 404 521 227 621 210 313 234 208-625-513
  30 335 434 406 121  11 222 302-619   4 811 225   9 131
 312 317-602 423 514-417-822-630  10-721 342 203 522 524
  17 134-828-627 718  37-731 403  25 414-309-607  15-717
  16 708  41 325   3  12 523  19 436 525 127-734 304  27

      ****************************************
```

303 -823 334 824 404 521 227 621 210 313 234 208 -625 -513
.490 .481 .471 .466 .460 .441 .441 .440 .434 .432 .411 .406 .395 .394

30 335 434 406 121 11 222 302 -619 4 811 225 9 131
.392 .392 .387 .386 .382 .375 .369 .368 .368 .359 .355 .348 .341 .329

312 317 -602 423 514 -417 -822 -630 10 -721 342 203 522 524
.324 .318 .316 .313 .311 .309 .300 .300 .300 .299 .293 .290 .285 .285

17 134 -828 -627 718 37 -731 403 25 414 -309 -607 15 -717
.284 .283 .281 .278 .276 .264 .260 .254 .253 .252 .252 .251 .251 .249

16 708 41 325 3 12 523 19 436 525 127 -734 304 27
.248 .247 .247 .246 .246 .244 .243 .243 .243 .241 .241 .240 .240 .240

-641 -616 -611 421 8 -634 -629 -725 -635 -605 -706 -508 130 7
.236 .232 .232 .232 .226 .223 .222 .217 .216 .215 .208 .203 .201 .198

-622 329 -623 -511 213 736 -803 104 432 -728 123 -821 1 -834
.192 .192 .192 .179 .178 .174 .172 .167 .165 .162 .162 .160 .160 .159

116 -827 -528 613 315 -638 42 -714 430 603 21 224 308 633
.158 .156 .154 .152 .150 .147 .139 .138 .138 .137 .133 .130 .130 .128

-610 -813 103 34 344 -631 38 426 324 322 -618 -825 221 632
.126 .125 .114 .113 .111 .111 .110 .107 .104 .102 .097 .095 .094 .093

-814 -510 407 612 -733 -715 -712 -727 339 429 106 -642 418 28
.089 .089 .087 .086 .083 .077 .074 .071 .069 .065 .065 .052 .051 .045

-606 -636 135 -722 5 -637 323 343 433 -735 -620 -704 -730 -815
.043 .039 .039 .037 .035 .033 .033 .028 .026 .022 .019 .013 .013 .011

107 -808 507 125 132 330 -640 -628 13 -802 202 20 -639 -801
.010 .008 .005 .004 .004 .003 .002-.002-.004-.004-.009-.017-.022-.029

527 -601 124 -830 14 18 515 -810 -609 -604 314 -624 36 534
-.029-.030-.035-.040-.042-.046-.050-.061-.061-.062-.066-.070-.071-.071

-804 230 33 -820 -626 35 520 204 306 332 -831 -807 644 326
-.076-.076-.078-.083-.088-.090-.092-.101-.101-.101-.119-.119-.124-.131

-643 122 -716 -617 201 211 -531 -832 -614 724 126 -729 -818 -615
-.146-.147-.149-.151-.155-.157-.158-.167-.170-.174-.175-.179-.184-.186

336 115 428 532 218 -703 39 -707 118 31 -608 -723 416 340
-.212-.217-.222-.222-.226-.227-.230-.238-.240-.273-.273-.273-.295-.298

```
 -732   32  425
-.370-.392-.392
        SEUIL INTERNE = 0.2397
        SEUIL CALCULE =   11.5 MPa
        SIGMA1-SIGMA3 =    48.0
        SIGMA2-SIGMA3 =    30.7
        SIGMA1d =          21.8
```

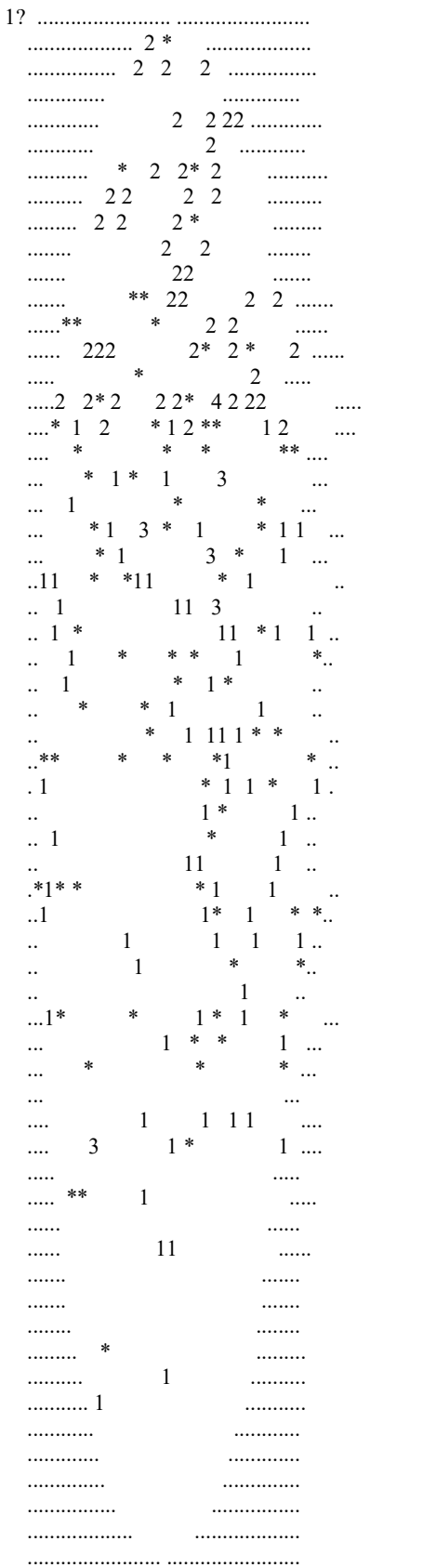

```
1   .2
    .1*
    . *1
    . *1
    . *      1
    . *       1
    .   *       1
    .   *          1
    .    *           1
    .    *            1
    .    *              1
    .       *              1
    .           *           1
    .             *              1
    .              *             1
    .                 *                    1
    .                      *                   1
    .                           *              1
    .                               *            1
    .                                 *           1
    .                                      *          1
    .                                         *          1
    .                                            *            1
    .                                             *              1
    .                                                 *              1
    .                                                     *           1
    .                                                       *           1
    .                                                          *         1
    .                                                             *          1
    .                                                                    *    1
    ..... .... .... .... .... .... .... .... .... .... .... .... .... ....*...1
    .                                                                        *
    .
    .
    .
```